



**Titre:** Concurrent, Integrated and Multicriteria Design Support for  
Title: Mechatronic Systems

**Auteur:** Abolfazl Mohebbi  
Author:

**Date:** 2017

**Type:** Mémoire ou thèse / Dissertation or Thesis

**Référence:** Mohebbi, A. (2017). Concurrent, Integrated and Multicriteria Design Support for  
Citation: Mechatronic Systems [Thèse de doctorat, École Polytechnique de Montréal].  
PolyPublie. <https://publications.polymtl.ca/2508/>

 **Document en libre accès dans PolyPublie**  
Open Access document in PolyPublie

**URL de PolyPublie:** <https://publications.polymtl.ca/2508/>  
PolyPublie URL:

**Directeurs de recherche:** Sofiane Achiche, & Luc Baron  
Advisors:

**Programme:** Génie mécanique  
Program:

UNIVERSITÉ DE MONTRÉAL

CONCURRENT, INTEGRATED AND MULTICRITERIA DESIGN SUPPORT FOR  
MECHATRONIC SYSTEMS

ABOLFAZL MOHEBBI

DÉPARTEMENT DE GÉNIE MÉCANIQUE  
ÉCOLE POLYTECHNIQUE DE MONTRÉAL

THÈSE PRÉSENTÉE EN VUE DE L'OBTENTION  
DU DIPLÔME DE PHILOSOPHIAE DOCTOR  
(GÉNIE MÉCANIQUE)

MARS 2017

UNIVERSITÉ DE MONTRÉAL

ÉCOLE POLYTECHNIQUE DE MONTRÉAL

Cette thèse intitulée :

CONCURRENT, INTEGRATED AND MULTICRITERIA DESIGN SUPPORT FOR  
MECHATRONIC SYSTEMS

présentée par : MOHEBBI Abolfazl

en vue de l'obtention du diplôme de : Philosophiae Doctor

a été dûment acceptée par le jury d'examen constitué de :

M. BALAZINSKI Marek, Docteur ès sciences, président

M. ACHICHE Sofiane, Ph. D., membre et directeur de recherche

M. BARON Luc, Ph. D., membre et codirecteur de recherche

M. GOURDEAU Richard, Ph. D., membre

M. KOKKOLARAS Michael, Ph. D., membre externe

## DEDICATION

*To my beloved family*



## ACKNOWLEDGEMENTS

I wish to express my sincere gratitude to my adviser, Prof. Sofiane Achiche for his confidence in me, his constant support, his invaluable patience, and his insightful ideas and guidance. I owe him a deep debt of gratitude for the space and atmosphere he provided that allowed me to develop ideas and to drive my research in a self-dependent way. In addition to being an adviser, he was truly a kind and supportive friend. I would also like to thank my co-adviser Prof. Luc Baron who stands amongst the kindest and most supportive professors I know.

I would like to thank Prof. Maxime Raison for his guidance and endless support. Even though he was not a member of my supervising committee, he has always motivated me and given me confidence in my research work.

I owe my academic success, if any, to all my teachers and professors and everyone who believed in me and encouraged me not only to learn a science but also to gain knowledge, to understand how to be a better human being. Listing names would not do justice. I thank all of them from Bushehr to Ahwaz, and from Isfahan to Montreal.

I am especially thankful to Saviz, Sara, Sadegh, Babak-Naghmeh, Majid, M. Keshmiri, Ali Ajdari and M. Haftanani for always being there for me and lighting up the time spent outside the academic work. I am also thankful to my friends Pouya, Hamidreza, Shahraad, Reza Moradi and Reza Farhadi for their kind companionship and their genuine warmth.

Finally, I would like to thank my parents, Fathieh and Abdollah, and my siblings, Sajjad and Fatemeh. They have been there for me all the time, giving me support and encouragement. They have been truly an unimaginable source of love and kindness.

## RÉSUMÉ

Les systèmes mécatroniques sont une combinaison coopérative de composantes mécaniques, électroniques, de contrôle et logiciels. Dans les dernières décennies, Ils ont trouvé diverses applications dans l'industrie et la vie quotidienne. En raison de leur aspect multi-physique, du nombre élevé de leurs composantes et des interconnexions dynamiques entre les différents domaines impliqués dans leur fonctionnement, les dispositifs mécatroniques sont souvent considérés comme hautement complexes ce qui rend la tâche de les concevoir très difficile pour les ingénieurs. Cette complexité inhérente a attiré l'attention de la communauté de recherche en conception, en particulier dans le but d'atteindre une conception optimale des systèmes multi-domaines. Ainsi, cette thèse, représente une recherche originale sur le développement d'un paradigme de conception systématique, intégrée et multi-objectifs pour remplacer l'approche de conception séquentielle traditionnelle qui tend à traiter les différents domaines de la mécatronique séparément.

Dans le but d'augmenter l'efficacité, la fiabilité, la facilité de contrôle et sa flexibilité, tout en réduisant la complexité et le coût effectif, ainsi que l'intégration systèmes, cette thèse présente de nouvelles approches pour la conception concurrente et optimale des systèmes mécatroniques aux stades de design conceptuel et détaillé. Les modèles mathématiques et les fondements qui soutiennent cette pensée sont présentés dans cette thèse. Les contributions des travaux de recherche de ce doctorat ont commencé par l'introduction d'un vecteur d'indices appelé le profile mécatronique multicritère (PMM) utilisé pour l'évaluation des concepts lors de la conception des systèmes mécatroniques. Les intégrales floues non linéaires de la théorie de décisions multicritères sont utilisées pour agréger les critères de conception et pour gérer les interactions possibles entre elles. Ensuite, une méthodologie de conception conceptuelle systématique est proposée et formulée.

Le soutien à l'intégration d'outils d'aide à la décision multicritère dans le processus de conception est un autre objectif de cette thèse où un certain nombre de cadres de travail sont proposés pour aider les ingénieurs concepteurs à évaluer l'importance de certains critères et des paramètres d'interaction. Ces cadres de travail ne s'appliquent pas uniquement l'évaluation de la conception et de la conception optimales, mais aussi à la détermination des possibles façons d'améliorer les concepts développés. Des méthodes basées sur l'exploitation de données ainsi que des algorithmes d'optimisation sémantique sont utilisées pour identifier les paramètres flous avec le peu d'information disponibles sur les différents choix de concepts et les préférences des concepteurs.

De plus, une approche multi-objectifs basée sur des approches de logique floue a été entreprise pour proposer et formuler une méthodologie pour le support à la conception détaillée. Un indice unifié d'évaluation de la performance a été introduit par le moyen d'intégrales de Choquet puis optimisé à l'aide d'un algorithme d'optimisation de type « particle swarm ». En utilisant la méthode proposée, tous les critères de conception et les objectifs de diverses disciplines et des sous-systèmes d'ingénierie peuvent être intégrés dans un seul indice de performance tout en considérant les interactions et les corrélations entre eux. Cette méthodologie de conception offre un point de vue intégré, concurrent et systématique à la conception mécatronique, qui diffère des approches de conception séquentielles non optimales.

Les méthodologies développées dans cette thèse de doctorat ont été validées, en les appliquant au processus de modélisation et de conception d'un système robotique et aussi un drone quadrotor guidé par la vision. Les deux systèmes sont considérés hautement complexes à concevoir incluant leurs sous-systèmes émanant de différents domaines d'ingénierie interconnectés avec divers objectifs opérationnels. Les résultats obtenus montrent que les méthodologies de conception développées ont produit des systèmes très performants en ce qui a trait à la performance du système et aussi au critère de conception.

## ABSTRACT

Mechatronic systems are a combination of cooperative mechanical, electronics, control and software components. They have found vast applications in industry and everyday life during past decades. Due to their multi-physical aspect, the high number of their components, and the dynamic inter-connections between the different domains involved, mechatronic devices are often considered to be highly complex which makes the design task very tedious and non-trivial. This inherent complexity, has attracted a great deal of attention in the research community, particularly in the context of optimal design of multi-domain systems. To this end, the present thesis represents an original investigation into the development of a systematic, integrated and multi-objective design paradigm to replace the traditional sequential design approach that tends to deal with the different domains separately.

With the aim of increasing efficiency, reliability, controllability and flexibility, while reducing complexity and effective cost, and finally facilitating system integration, this thesis presents new approaches towards concurrent and optimal design of mechatronic systems in conceptual and detailed design stages. The mathematical models and foundations which support this thinking are presented in the thesis. The contributions of our research work start with introducing an index vector called Mechatronic Multi-criteria Profile (MMP) used for concept evaluation in design of mechatronic systems. Nonlinear fuzzy integrals from multicriteria decision theory are utilized to aggregate design criteria and for handling possible interactions among them. Then, a systematic conceptual design methodology is proposed and formulated.

Supporting the incorporation of multicriteria decision making tools into the design process, is another focus of this work where a number of frameworks are proposed to help the designers with assessment of criteria importance and interaction parameters. These frameworks are not only applicable in optimal design and design evaluation procedures, but also for determining possible ways for design improvements. Both data-driven methods as well as semantic-based optimization algorithms are used to identify the fuzzy parameters with limited available information about the design alternatives and designer preferences.

Moreover, a fuzzy-based multi-objective approach has been undertaken for proposing and formulating a detailed design methodology. A unified performance evaluation index is introduced by the means of Choquet integrals and then optimized using a constrained particle swarm optimization (PSO) algorithm. Using the proposed fuzzy-based method, all the design criteria and objectives from various engineering disciplines and subsystems can be integrated in a single

performance index while considering the interactions and correlations among them. This design methodology offers an integrated, concurrent, and system-based viewpoint to mechatronic design, which deviates from the non-optimal sequential design approaches.

The methodologies developed in this research are validated by applying them to the modeling and design process of a robotic visual servoing system and also a vision-guided quadrotor drone as highly complex systems which include sub-systems from various interconnected domains with numerous operational objectives. The results show that the design methodologies used, produce systems with high efficiency with regards to both system performance and design criteria.

## TABLE OF CONTENTS

DEDICATION .....	III
ACKNOWLEDGEMENTS.....	IV
RÉSUMÉ.....	V
ABSTRACT .....	VII
TABLE OF CONTENTS .....	IX
LIST OF TABLES.....	XIV
LIST OF FIGURES .....	XVII
LIST OF ABBREVIATIONS .....	XX
LIST OF APPENDICES .....	XXII
CHAPTER 1    INTRODUCTION.....	1
1.1    Background Information and Problem Definition.....	1
1.2    Research Scope and Objectives .....	4
1.3    Manuscript Outline .....	6
CHAPTER 2    LITERATURE SURVEY .....	7
2.1    Mechatronic Design Challenges.....	7
2.1.1    Design Methods .....	7
2.1.2    Design Tools .....	9
2.1.3    Design Support and Decision Aid .....	10
2.1.4    Human Communication and Cooperation .....	11
2.1.5    Control Design Software.....	11
2.2    Available Solutions to Design Challenges .....	12
2.2.1    Design Methods .....	12
2.2.2    Design Tools .....	15

2.2.3	Optimization and Design Support.....	17
2.2.4	Human Communication and Cooperation .....	18
2.2.5	Control Software.....	18
CHAPTER 3 ARTICLE 1: MULTICRITERIA DECISION SUPPORT FOR CONCEPTUAL DESIGN OF MECHATRONIC SYSTEMS; A QUADROTOR DESIGN CASE STUDY.....		
3.1	Abstract .....	19
3.2	Introduction .....	19
3.3	Multicriteria Mechatronic Profile (MMP).....	22
3.3.1	Machine Intelligence.....	23
3.3.2	System Reliability.....	26
3.3.3	Design Complexity .....	27
3.3.4	Design Flexibility.....	28
3.3.5	Cost.....	28
3.4	Multi-Criteria Decision Support and Aggregation of Criteria .....	29
3.4.1	Choquet Integrals .....	30
3.4.2	Sugeno Fuzzy.....	31
3.4.3	Neural Networks.....	31
3.5	Case Study: Design of a Vision-Guided Quadrotor Drone .....	36
3.5.1	MMP Assessment .....	39
3.5.2	Aggregation of Criteria and Global Concept Scores .....	43
3.5.3	Choosing the Elite Concept and Comparison of Results .....	45
3.6	Discussion and Conclusion .....	48
CHAPTER 4 ARTICLE 2: A FUZZY-BASED FRAMEWORK TO SUPPORT CONCURRENT AND MULTICRITERIA DESIGN OF MECHATRONIC SYSTEMS.....		
4.1	Abstract .....	50
4.2	Introduction .....	50

4.3	Conceptual Design of Mechatronic Systems .....	53
4.3.1	Conceptual Design.....	53
4.3.2	Concept Evaluation.....	54
4.3.3	Mechatronic Multicriteria Profile (MMP).....	54
4.4	Fuzzy Decision Support and Aggregation.....	56
4.4.1	Criteria Aggregation.....	56
4.4.2	Fuzzy Measures and Choquet Integrals .....	56
4.5	Identification of Fuzzy Measures.....	60
4.5.1	Identification Using Sugeno $\lambda$ -measures .....	60
4.5.2	Identification Based on Learning Data .....	60
4.5.3	Identification Based on Fuzzy Measure Semantics and Learning Data .....	62
4.5.4	Identification Using a 2-Additive Model.....	63
4.6	Case Study: Conceptual Design of a Vision-Guided Quadrotor Drone.....	65
4.6.1	Identification Using Sugeno $\lambda$ -measures .....	67
4.6.2	Identification Based on Learning Data .....	68
4.6.3	Identification based on fuzzy measure semantics and learning data .....	70
4.6.4	Identification using a 2-Additive Model.....	72
4.7	Discussion and Comparison.....	75
4.8	Conclusion .....	76
CHAPTER 5      ARTICLE 3: DESIGN OF A VISION GUIDED MECHATRONIC QUADROTOR SYSTEM USING DESIGN FOR CONTROL METHODOLOGY .....		78
5.1	Abstract .....	78
5.2	Nomenclature.....	78
5.3	Introduction.....	79
5.4	System Modelling and Formulation .....	82
5.5	Controller Design.....	85



5.5.1	Motion Control .....	85
5.5.2	Visual Servoing Control .....	86
5.6	Integrated Design Strategy.....	88
5.7	DFC-Based Design Optimization.....	91
5.7.1	Iteration 1: Deign $XN$ Based on Non-RTBs, $YN$ :.....	92
5.7.2	Iteration 2: Deign $XR$ Based on RTBs, $YR$ : .....	93
5.7.3	Iteration 3: Redesign $XN$ to Improve Non-RTBs, $YN$ :.....	95
5.7.4	Iteration 4: Redesign $XR$ based on the modified Non-RTBs, $YN$ : .....	96
5.8	Conclusion .....	100
CHAPTER 6 ARTICLE 4: INTEGRATED AND CONCURRENT DETAILED DESIGN OF A MECHATRONIC QUADROTOR SYSTEM USING A FUZZY-BASED PARTICLE SWARM OPTIMIZATION .....		101
6.1	Abstract .....	101
6.2	Introduction .....	101
6.3	Particle Swarm optimization .....	105
6.3.1	Swarm Topology.....	106
6.3.2	PSO Algorithm.....	106
6.3.3	Constrained Optimization .....	107
6.4	Multicriteria Fuzzy Aggregation .....	108
6.5	Integrated Mechatronic Detailed Design Formulation.....	110
6.5.1	Cascade Fuzzy-based multidisciplinary objective function .....	110
6.5.2	Parameter Selection for PSO .....	112
6.5.3	Identification of Fuzzy Measures.....	112
6.6	Quadrotor System Modeling .....	113
6.6.1	Quadrotor Body and Structure .....	113
6.6.2	Quadrotor Dynamics .....	115

6.6.3	Rotor Dynamics.....	118
6.6.4	Aerodynamic Forces and Moments.....	119
6.6.5	Complete System Dynamics.....	120
6.7	Control System Design.....	121
6.7.1	Flight Motion Control System.....	122
6.7.2	Visual Servoing System (Vision-based Control).....	125
6.8	Detailed Design Objectives and Constraints.....	127
6.8.1	Structure and Body Design Objectives.....	127
6.8.2	Aerodynamics and Propulsion System Objectives.....	129
6.8.3	Control System Objectives.....	129
6.8.4	Visual Servoing System Objectives:.....	132
6.8.5	System-Level Objectives.....	133
6.9	Quadrotor Detailed Design Implementation - Optimization Results.....	134
6.10	Simulations and Discussion.....	140
6.11	Conclusion.....	146
CHAPTER 7	GENERAL DISCUSSION.....	147
7.1	Research Contributions.....	147
7.2	Computer Implementations.....	150
CHAPTER 8	CONCLUSION AND FUTURE WORK.....	151
8.1	Summary of the Thesis.....	151
8.2	Future Work.....	152
BIBLIOGRAPHY	.....	154
APPENDIX	.....	169

## LIST OF TABLES

Table 2-1: Most common challenges in mechatronic system design and related publications .....	8
Table 2-2: Summary of recent methods in concurrent and integrated mechatronic design .....	15
Table 2-3: Evaluation Summary of the languages and tools per mechatronic design process .....	17
Table 3-1: Fuzzy Interactions and Measurements .....	30
Table 3-2: Design alternatives .....	38
Table 3-3: Estimated design features for generated concepts .....	38
Table 3-4: Parameters required for assessing MIQ for two cases of PBVS and IBVS .....	40
Table 3-5: Mean time to failure (Hrs.) for the components used in the generated concepts .....	42
Table 3-6: Reliability scores for generated concepts .....	42
Table 3-7: Complexity values for design alternatives .....	42
Table 3-8: Flexibility values for design alternatives .....	43
Table 3-9: Cost factors for generated concepts .....	43
Table 3-10: Criteria interactions and the correlation measure .....	44
Table 3-11: 30 fuzzy measures for the case study of conceptual design of a Quadrotor drone with a visual servoing system .....	44
Table 3-12: MMP elements and global concept scores (GCS) for design alternatives .....	45
Table 3-13: Initial (IR, IL) and desired (DR, DL) location of feature points in pixel for Right and Left images .....	46
Table 4-1: Fuzzy Interactions and Measurements .....	57
Table 4-2: Design alternatives [136] .....	65
Table 4-3: Estimated design parameters for generated concepts [136] .....	66
Table 4-4: Concept Evaluations for design alternatives .....	66
Table 4-5: Fuzzy measures for conceptual design of a Quadrotor drone equipped with a visual servoing system .....	67
Table 4-6: Fuzzy measures identified using Sugeno $\lambda$ - measures .....	68

Table 4-7: Decision Maker's preferences on criteria relations.....	69
Table 4-8: Results for fuzzy measures identified using a learning set.....	70
Table 4-9: Linguistic representation of relative importance of criteria.....	70
Table 4-10: Linguistic representation of dependence between criteria .....	70
Table 4-11: Linguistic representation of support between criteria .....	71
Table 4-12: Decision maker's preferences as linear constraints.....	71
Table 4-13: Results for fuzzy measures identified using a learning set and fuzzy measure semantics .....	72
Table 4-14: Decision maker's preferences as linear constraints.....	73
Table 4-15: Fuzzy measures identified using a 2-additive model.....	74
Table 5-1: DFC-based design results for a vision-guided quadrotor system.....	96
Table 5-2. The step-response characteristics of the attitude and altitude control systems based on the results from iteration 2 and iteration 4. ....	98
Table 6-1: Fuzzy Interactions and Measurements .....	109
Table 6-2: Design Parameters .....	134
Table 6-3: PSO Parameters.....	135
Table 6-4: Penalty coefficients, $ai$ , for constrained PSO.....	136
Table 6-5: Results for fuzzy measures identified using $\lambda$ -method for the main subsystems .....	137
Table 6-6: Fuzzy measures identified for the structure subsystems .....	137
Table 6-7: Fuzzy measures identified for the control subsystems.....	137
Table 6-8: Fuzzy measures identified for the aerodynamics, visual servoing and system-level objectives.....	137
Table 6-10: Physical and control Specifications of an AR. Drone 2.....	139
Table 6-10: Optimization results for swarm size of $n = 100$ with maximum .....	139
Table 6-12: Optimization results for swarm size of $n = 500$ with maximum .....	139

Table 6-12: Design objective values for the PSO run with swarm size of $n = 100$ with maximum iterations of $Tmax = 200$ .....	140
Table 6-14: Design objective values for the PSO run with swarm size of $n = 500$ with maximum iterations of $Tmax = 1000$ .....	140

## LIST OF FIGURES

Figure 1-1 : The scope of mechatronic systems [1] .....	1
Figure 1-2: Model of Mechatronic design. (a) Traditional sequential design (b) Concurrent design adapted from [6] .....	4
Figure 3-1: Concept evaluation in design, adopted from [44] .....	24
Figure 3-2: Example of intelligent task graph (ITG).....	25
Figure 3-3: A fuzzy integral-based neural node where inputs are information sources and output is a fuzzy integral value.....	32
Figure 3-4: A fuzzy integral-based neural network structure with three hidden layers .....	32
Figure 3-5: The structure of the fuzzy integral-based neural network with one hidden layer .....	35
Figure 3-6: Conceptual Design of a Mechatronic System based on MMP and Global Concept Score (GCS).....	35
Figure 3-7: A Quadrotor drone in tracking and following mission using a visual servoing system. .....	36
Figure 3-8: An integrated visual servo control for a Quadrotor system .....	37
Figure 3-9: Parts and Subsystems for generation design concepts .....	37
Figure 3-10: ITG model for (a) a position-based visual servoing (PBVS) scheme and (b) an image- based visual servoing (IBVS) scheme for a quadrotor system. ....	39
Figure 3-11: (a) A simulation model of a Quadrotor drone with a visual servoing system. Image feature trajectories in (b) concept 4: Monocular IBVS with LQR controller, (c, d) concept 3: Stereo IBVS with PID controller. ....	47
Figure 3-12: Camera frame velocity in systems based on concept 4 (a) and concept 3 (b). ....	48
Figure 3-13: Image feature errors in systems based on concept 4 (a) and concept 3 (b). ....	48
Figure 4-1: Process of concept evaluation in design.....	54
Figure 4-2: Mechatronic Multicriteria Profile (MMP) and all sub-criteria.....	55
Figure 4-3: Graphical illustration of Choquet integral.....	57
Figure 4-4: Lattice of the coefficients of a fuzzy measure ( $n = 4$ ) .....	58

Figure 5-1: Quadrotor model coordinate system.....	82
Figure 5-2: UAV Quadrotor control structure consisting of attitude motion control and visual servoing control .....	85
Figure 5-3: Model of the parallel stereo vision system observing a 3D point .....	87
Figure 5-4: Process of concurrent Mechatronic system design adopted from [153] .....	89
Figure 5-5: The simulation model of the vision-guided Quadrotor system .....	94
Figure 5-6: The step-response of the attitude and altitude control systems based on the final system-level optimization results.....	97
Figure 5-7: Position tracking performances based on results from (a) iteration 2 and (b) iteration 4, and a comparative graph of paths for a complete motion. ....	99
Figure 5-8: Visual feature errors from (a) iteration 2 and (b) iteration 4. ....	100
Figure 6-1: Three most common neighborhood topologies used in particle swarm optimization .....	106
Figure 6-2: Cascade Choquet integral-based aggregation on subsystems objective functions.....	111
Figure 6-3: The inertial and body frames of the quadrotor system.....	114
Figure 6-4: Quadrotor body structure and corresponding masses in x-y plane.....	114
Figure 6-5: UAV Quadrotor control structure consisting of flight motion control and visual servoing system .....	121
Figure 6-6: Quadrotor control system for attitude and position .....	122
Figure 6-7: Quadrotor PID Controller .....	122
Figure 6-8: Open Loop Block Diagram .....	124
Figure 6-9: Quadrotor complete position, attitude and altitude control scheme .....	124
Figure 6-10: Model of the parallel stereo vision system observing a point in 3D space .....	126
Figure 6-11: Forces acting on quadrotor arm as a cantilever beam .....	128
Figure 6-12: Natural Frequency Modes of a Cantilever Beam [191].....	128
Figure 6-13: Step response properties of flight control system .....	132
Figure 6-14: The structure of AR. Drone 2 as the benchmark system for case study of the proposed detailed design process.....	134

Figure 6-15: Functional Dependency Tables (FDT) for: (a) System design objectives, (b) design constraints. ....	136
Figure 6-16: Quadrotor simulation model in test scenario where it tracks and intercepts a target .....	141
Figure 6-17: Step response results for attitude and altitude control system obtained from original AR. Drone.....	141
Figure 6-18: Step response results for attitude and altitude control system obtained from: (a) PSO optimization results with swarm size of $n = 100$ with maximum iterations of $Tmax = 200$ , (b) PSO optimization results with swarm size of $n = 500$ with maximum iterations of $Tmax = 1000$ . ....	142
Figure 6-18: Tracking error results for the visual servoing system obtained from: (a) PSO optimization results with swarm size of $n = 100$ with maximum iterations of $Tmax = 200$ , (b) PSO optimization results with swarm size of $n = 500$ with maximum iterations of $Tmax = 1000$ . ....	143
Figure 6-19: Image feature trajectories for the visual servoing system obtained from: (a, b) PSO optimization results with swarm size of $n = 100$ with maximum iterations of $Tmax = 200$ , (c, d) PSO optimization results with swarm size of $n = 500$ with maximum iterations of $Tmax = 1000$ . ....	144
Figure 6-20: Main frame translational velocity components during the object tracking process, obtained from: (a) PSO optimization results with swarm size of $n = 100$ with maximum iterations of $Tmax = 200$ , (b) PSO optimization results with swarm size of $n = 500$ with maximum iterations of $Tmax = 1000$ . ....	145
Figure 7-1: Proposed mechatronic design roadmap based on the research contributions and developments in various design phases.....	147
Figure 7-2: Research sub-objectives covered in this thesis.....	148



## LIST OF ABBREVIATIONS

RTB	Real Time Behaviour
Non-RTB	Non-Real Time Behaviour
RTP	Real Time Parameter
Non-RTP	Non-Real Time Parameter
SO	Sub-Objective
DFC	Design for Control
MDQ	Mechatronic Design Quotient
BG	Bond Graph
GP	Genetic Programming
FBS	Function-Behavior-State
MDI	Mechatronic Design Indicator
NLDOP	Nonlinear Dynamic Optimization Problem
UML	Unified Modeling Language
SysML	Systems Modeling Language
DEE	Design and Engineering Engine
MDO	Multidisciplinary Design Optimization
PIDO	Process Integration Design Optimization
LSC	Live Sequence Chart
RBP	Requirements-based Programming
MCDM	Multi Criteria Decision Making
MMP	Mechatronic Multicriteria Profile
MIQ	Machine Intelligence Quotient
DFG	Data Flow Graph
ITG	Intelligent Task Graph
FTA	Fault Tree Analysis
FMEA	Failure Modes and Effect Analysis
PN	Petri Net
DSM	Design Structure Matrix
ANN	Artificial Neural Network
FI	Fuzzy Integral

IBVS	Image-based Visual Servoing
PBVS	Position-based Visual Servoing
LQR	Linear Quadratic Regulator
DTM	Design Theory and Methodology
UAV	Unmanned Aerial Vehicle
UQH	Unmanned Quadrotor Helicopters
COG	Center of Gravity
PSO	Particle Swarm Optimization
FDT	Functional Dependency Table

## LIST OF APPENDICES

APPENDIX A IMPROVEMENTS ON CONCEPTUAL DESIGN OF MECHATRONIC SYSTEMS USING A FUZZY-BASED APPROACH.....	169
--	-----

## CHAPTER 1 INTRODUCTION

### 1.1 Background Information and Problem Definition

Mechatronic systems, as a combination of cooperative mechanical, electronics and software components with the aid of various control strategies (Figure 1-1), have led the engineering design into a new era by integrating the most advanced technologies with the best design schemes [1]. Design of a wide variety of products such as transportation systems, aircrafts, construction machines or even home appliances are now considered within the area of mechatronic systems. Mechatronic systems are often highly complex, because of the high number of their components, their multi-physical aspect and the couplings between the different engineering domains involved [2].

Generally, a systematic and multi-objective thinking method to mechatronics design is ideally needed due to the complexity of interactions between the subsystems. Design of mechatronic devices includes two major steps: conceptual design and detailed design. In the conceptual design phase, a complete and consistent listing of the requirements and behaviors is required as well as a thorough identification of critical parts of the solution that affects the overall performance. Then in detailed design phase, those candidate solutions that meet the requirements should be identified and provide the level of needed performance.

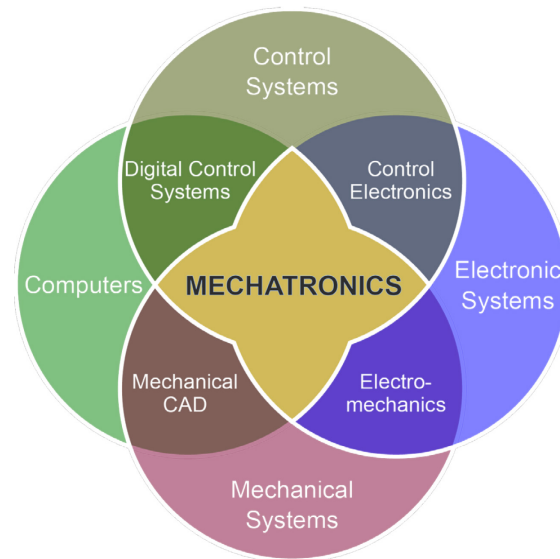


Figure 1-1 : The scope of mechatronic systems [1]

Designing a mechatronic product ideally needs an integrated and concurrent approach to achieve the following goals [3, 4]:

- Increased reliability;
- High controllability;
- Reduced complexity
- Better component matching;
- Increased efficiency;
- Proper cooperation with other systems;
- Increased flexibility
- Reduced effective cost;
- Facilitated system integration;

To achieve the above goals a concurrent and integrated design approach is ideally required. Although, due to lack of a systematic approach, design engineers in various industries still prefer to use traditional and sequential design methods.

Suh [5] suggested to define an engineering design process as a mapping from a requirement space consisting of behaviors, to a structural parameter space. To gain insight into the design of a mechatronic system, Li *et al.* [6] suggested dividing the requirement space into two subspaces which represent: Real-time behaviors (RTBs) and Non-real-time behaviors (Non-RTBs). Following this division of the requirements, system parameters in structural space can also be divided into two subspaces as: Real-time (or controllable) parameters (RTPs), and Nonreal-time (or uncontrollable) parameters (Non-RTPs). Here, “real-time” corresponds to parameters, specifications and behaviors that are changeable in a timely manner after the machine is built. Controller gains, accuracy and speed are some examples of RTPs and RTBs. On the other hand, “Non-real-time” parameters and specifications are the ones that can be hard to alter after the machine is made, either because it would be costly to change them or they are inherently unchangeable at this stage. Structural material, dimensions, weight, and workspace can be considered as Non-RTPs and Non-RTBs. Traditional methodologies for mechatronic systems design consisted of sequences of the real-time and non-real-time requirements rather than a concurrent design process (Figure 1-2a).

As a typical example in the design of traditional controllable machines, a robot manipulator can be pointed out. At the beginning of such a traditional design scenario, Non-RTPs are designed based on the Non-RTB specifications. This process itself includes designing the mechanical structure and then adding electrical components. The mechanical structure (e.g., configurations, dimensions, layout of actuators and sensors, etc.) is first determined based on the requirements in the Non-RTB space (e.g., robot workspaces, maximum payloads, etc.). Subsequently, RTPs (e.g., controller algorithm and parameters, signal conditioning) are determined based on RTB specifications (e.g., desired path, speed, accuracy, stability) to control the already established structure.

Recent progresses in control engineering and computer science have created a misconception in design community that the design of the structure and electrical hardware can be considered to be no longer the main design aspect in some cases and the inadequacies of the system mechanics could be compensated by some high performance state-of-the-art control schemes. One can easily criticize this thinking because a perfect control strategy may be very hard to achieve due to hardware limitations and dynamic interactions, regardless of the effort devoted to the design of the controller system. However, this does not imply at all that the performance of an electro-mechanical system cannot be improved by better control strategies. It is the design process “optimality” that is in doubt and question.

In a concurrent model for mechatronic systems design (Figure 1-2b), both RTBs and Non-RTBs should be considered simultaneously for realization of RTPs and Non-RTPs. In a common mechatronic system, the system performance which is the real-time and nonreal-time system behaviors (RTBs and Non-RTBs) explicitly relies on the design of its control algorithm and parameters (RTPs) and also the design of the mechanical structure (Non-RTPs). More specifically, the design specifications for controller and limitations should be considered in the design of the mechanical structure and in the considering the alternatives for the electrical hardware. In addition, unlike in a traditional design, controllability and programmability of RTPs should be considered as an opportunity to further improve the design after the machine is built.

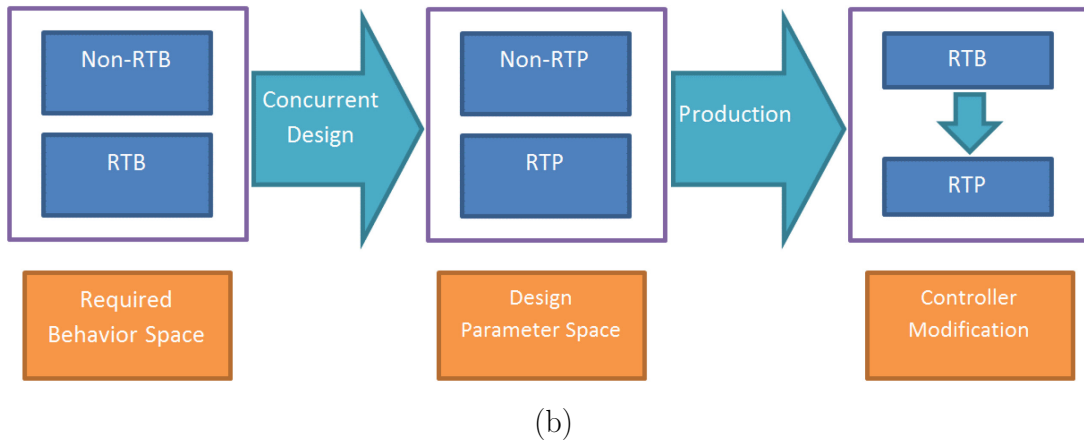
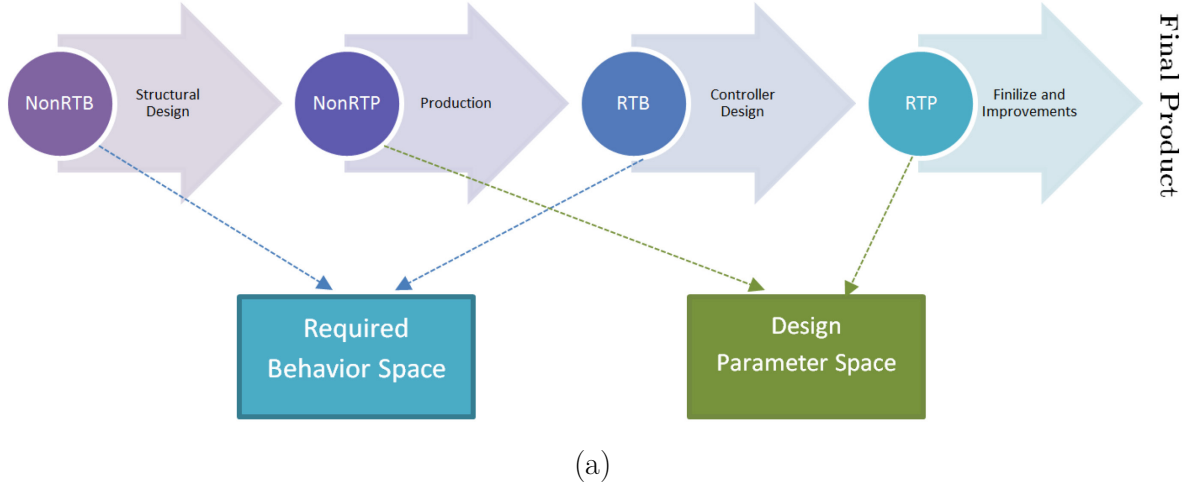


Figure 1-2: Model of Mechatronic design. (a) Traditional sequential design (b) Concurrent design adapted from [6]

## 1.2 Research Scope and Objectives

The importance of mechatronic systems in engineering has been increasing in past decades as they are able to perform very complex tasks with various applications. Design of mechatronic systems concerns the integration of several disciplines where mechanics are combined with electronics, control, software, hydraulics, aerodynamics, etc. This inherent complexity of product development and consequently its multi-domain integration, make it difficult for design engineers to understand mechatronics systems as one whole. Furthermore, being multi-criteria problematic, design of mechatronic systems tends to deal with Pareto decisions. Therefore, achieving optimal or near optimal design solutions is a very complex if not impossible task, especially without identification of the performance parameters involved and a good level of understanding of their co-influences. It is therefore vital to take into account interactions between system requirements.

Hence, this thesis aims at answering the following research question: How to systematically use design criteria and parameters as well as their interactions to formulate an integrated solution to evaluate and optimize mechatronic system designs?

In this research work, the **main objective** is therefore to develop a systematic, concurrent and integrated approach which will support the design of a wide range of mechatronic systems. From this objective, four sub-objectives emerge;

Although mechatronic systems design is commonly recognized to deal with an important issue in terms of finding the right criteria to evaluate and synthesize designs, there is still no systematic approach to support this. Thus, as an early research concentration, the first sub-objective (SO) of this work is:

**SO1:** Identify and quantify a set of most-common yet highly effective criteria for mechatronics design.

In early phases of design i.e. product architecture and conceptual design, a number of challenges are faced by designers with regards to the selection of system components and choosing between various schemes and approaches for software and control system developments. Due to the lack of a multi-criteria overview of the mechatronic systems design, designers usually choose the seemingly most available and feasible components fitting their design requirements. Although they merely fulfill a functional design, but not necessarily an optimal one. Therefore, the second sub-objective is:

**SO2:** Develop a decision support framework for conceptual design of mechatronic systems to properly define performance criteria and provide information about their co-influences and their collective effect on the design optimality.

After obtaining an “elite set” of the design alternatives and architectures from conceptual design, it is generally time to extend the multicriteria thinking from previous sub-objective to the preliminary and detailed design phases where the design engineers deal with numbers, values and parameters with regards to each subsystem and their corresponding design objectives. Hence, the third sub-objective is:

**SO3:** Develop a multicriteria design solution, flexible enough to be applicable to both preliminary and detailed design phases.

With the intention of helping the designers with incorporating the developed design supports and methodologies into their projects, a fourth sub-objective rises as follows:



**SO4:** Provide guidelines to facilitate the use of the decision analysis and optimization tools.

SO4 will ultimately help attain the right preferences and settings used in mathematical models of the design methodologies and system integrations.

It is important to note that the present thesis does not address the problem of developing a unified software platform capable of automated synthesis and evaluation for mechatronic system design, however the implemented models and functions are collected as a MATLAB toolbox to be published under a free license agreement. All the presented case studies are based on mathematical models of the physical components and their dynamic behavior. No experiments have been performed, but some of the models have been verified against data of commercially available products and components using computer simulations. Furthermore, to limit the scope of the present research, no major study, analysis and development have been carried out with regards to the optimization and decision making tools used in design methodologies.

### **1.3 Manuscript Outline**

A literature review on mechatronics design methodologies and challenges is presented in Chapter 2. In Chapter 3, the new Mechatronic Multi-criteria Profile (MMP) is introduced for the purpose of concept evaluation in mechatronic systems design and the assessment procedures for each of its elements are described. Moreover, three different methods for decision support and aggregation based on fuzzy sets in the presence of interacting criteria are also presented in this chapter along with a case study of conceptual design of a vision-guided quadrotor UAV. In Chapter 4, four methods for identification of fuzzy capacities and parameters used in multicriteria design are introduced and exemplified. Chapter 5 is dedicated to the study and analysis of the “Design-for-Control (DFC)” approach for preliminary design of mechatronic systems. A design case study on the same quadrotor system is also presented in this chapter to provide us with more insights about advantages and disadvantages of using the DFC approach. In Chapter 6, we discuss a method for detailed design where we have embedded fuzzy information into a particle swarm optimization process for the sake of incorporating multi-criteria and multi-objective design problems. The conclusion of this thesis and the proposed future works are presented in Chapter 7. The references cited in this thesis are sorted in the bibliography section.

## CHAPTER 2 LITERATURE SURVEY

The design of mechatronic systems is a direct result of intensive collaboration between engineers of the mechanical, electronic, control, and software domains in a design team which aims to attain product-related advantages, which are not feasible through mono-disciplinary efforts. The multidisciplinary nature of a mechatronic systems increases the complexity of the design task and requires special attention to product and design activities dependencies. In this chapter, a survey on the available literature is carried out to review the most common challenges faced by the designers during various phases of mechatronic design. We then explore the research efforts and standardized solutions/tools found to address these problems.

### 2.1 Mechatronic Design Challenges

In order to improve the development of solutions for mechatronic designers, identifying and understanding the challenges related to the design of mechatronic products is essential. Both academic and industrial sources have reported many challenges related to the design and development of mechatronic systems. Table 1-1 lists these challenges (from A to M) and the design stages they may appear in, and also the related work that have been performed to identify and/or solve the problems. By examining these challenges, five main types of challenges can be identified, which influence many of the problems in the development of mechatronic systems. These main categories are: 1) Design Methods, 2) Design Tools, 3) Design Support, 4) Human Factors, and 5) Control Software.

#### 2.1.1 Design Methods

During past decades, many endeavors has been carried out to ideally form a reliable and comprehensive design framework for mechatronic systems, but it can be inferred that this goal has not been achieved yet [7]. It has been reported that still in many industrial projects, traditional methods with a sequential flow of activities are the main engineering design guideline [8]. The sequential approaches separate the design operations in the sense that some design activities require the information resulted by the design of the other domains. These approaches have proven to be unsuitable due to their lack of flexibility, and their inefficiency towards a concurrent design which increases the cost and development time [4].

Table 2-1: Most common challenges in mechatronic system design and related publications

#	Type	Design Stages Challenges	Preliminary Conceptual	Detailed Design	Post Processing &	Related Work
A	Design Methods	Requirement handling and traceability				[7] [9] [10] [11] [12] [13]
B		Synchronizing the designs from different disciplines to attain concurrent engineering				[14] [15] [13, 16] [17]
C		System complexity as a generic problem				[14] [18] [12] [5] [19]
D		Exchange of design models and information between domains				[15] [20] [11] [21] [22]
E	Design Tools	Model consistency and interoperability				[23] [24]
F		Lack of tools and methods supporting multi-disciplinary design				[25] [26] [9] [24]
G		A lack of a common language to represent a concept and overall system design				[27] [9] [28]
H		Design Integration				[27] [25] [23] [26] [9] [29]
I	Design Supports	Early evaluation, testing and verification				[30, 31] [32- 34] [35, 36]
J		Support for decision making				[30, 31] [35, 36]
K		Difficulty in assessing the consequences of choosing between two alternatives				[37] [38] [30, 31]
L	Human Factors	Cooperative work, communication and interaction between engineers from different disciplines				[15]
M	Control Software	Design support for generation of a control software				[32] [24]
N		Lack of automation in control software design				[10]

In a concurrent approach, all phases of the life-cycle of the product are considered as early as possible in the design [39]. This is a challenging task when dealing with complex design situations, where strong interdependencies might have unpredicted effects on the overall system performance [6]. A number of research works have suggested to ideally build the system by assembling single-domain subsystems and by focusing more on the design of interfaces among them [15, 39]. Therefore, research on mechatronics should also focus on the interactions of the different engineering disciplines rather than only on the interactions between the subsystems that are being designed [15]. Moreover, a concurrent method should be ultimately utilized to deal with the interactions between designers and their designs since it facilitates early detection of possible problems.

### **2.1.2 Design Tools**

Nowadays, different tools are devoted to managing design data within the design disciplines. However, the lack of tools capable of integration and sharing the design data is still one of the main challenges in mechatronics design and development [40]. In a multidisciplinary design project, designers from different domains employ specialized tools. Examples are tools like SolidWorks [41] in the mechanical design domain, OrCad [42] in the electrical domain, and MATLAB [43] in the control domain. Furthermore, there are not many specialized tools that support the conceptual and preliminary stages of design and which are also capable of extension to the subsequent phases [20]. These domain-specific tools perform quite well within their own domain, but handling information from other domains is quite rare among them. Although, the tools used in design of the control systems and interfaces are usually more flexible as they use mathematical models, mostly as block diagrams or bond graphs, as modeling bases [23, 25].

Consequently, several problems towards system integration arise when using domain-specific tools in a multi-disciplinary design activity. For example, in mechanical design tools, the main focus is on the physical aspects of the product while providing abstract concepts and categorizing parts and elements based on other non-physical criteria are rarely applicable. Moreover, in control design tools, an abstract of the physical system is often used. Thus, it becomes difficult to find the explicit connection between all the system behavior and their corresponding physical actors. In electronic systems design tools, only predictions of electrical and logical behavior are supported, while the physical implementation of the control algorithm is often overlooked. Finally, in requirement management tools, most of the focus is on representing documented requirements

information. The inter-connection to other design domains is mainly made through reports, and it is the designer’s responsibility to connect such documents with the available design data.

### 2.1.3 Design Support and Decision Aid

The decisions of system designers immensely influence the evolving mechatronic product design concepts [26], thus, support for decision making is of high importance. During different stages of design, different questions are answered about the product at different levels of abstraction and detail. The resources being spent in finding effective answers to define how well and how efficiently decisions are being made. The main goal is ideally making better decisions as early as possible while utilizing less resources. Success in this requires support that based on predictions, provides a good comparison of what is gained or lost by making a certain design choices and alternatives.

Another considerable challenge in mechatronic design is towards design evaluation and interdisciplinary verification. The four classical verification methods are demonstration, test, inspection, and analysis [9]. Among these four methods, the first three require physical prototypes, while the latter requires mathematical models of the system and its interconnections. Developing appropriate models for analysis and a platform to verify various aspects of the system, including control system, is a place for additional challenges. In practice, specific models are developed to perform tests at different stages of design. Due to the use of domain-specific modeling tools, such models usually correspond to a specific point of view on the system. With the expected synergetic effects that characterize mechatronic systems, these separate views cannot capture the overall system behavior. Moreover, the analysis of different operation modes of the system, requires reconfigurable multi-domain models, which are seldom supported.

In early design activities, it is needed to select the system components and choose between alternatives for software and control strategies. This part of conceptual and preliminary design is usually known as choosing the “Elite Set” which includes a number of feasible yet efficient design alternatives. Without sufficient multi-criteria support, this practice always faces a number of problems and limitations [44]. In such cases, engineers tend to choose the first and the best components from what they see as available and feasible to meet their design requirements. Such decisions can optimistically lead to a functional design, but rarely to an optimal one. This problematic decision making generally occurs due to ill-defined performance criteria and lack of knowledge about the co-influences between criteria and the functionalities expected to be provided by neighbouring disciplines.

### 2.1.4 Human Communication and Cooperation

Human communication and cooperation is an important additional factor that influences the design integration of the mechatronic system. The issues within this challenge can be categorized as:

- Communicating the goals and design requirements and relating them to the chosen solutions.
- Decomposition of the requirements and to facilitate monitoring them throughout the design process.
- Building an information exchange platform to notify the designers about the influence of their solution on other parts.

All the mentioned issues strongly relate to the fact that there are currently very few methods and tools that support design activities from a system engineering point of view and facilitate the exchange of information between designers.

### 2.1.5 Control Design Software

Modern control system design tools such as MATLAB/Simulink [43], Maple [45] and LabView [46] provide means to translate control algorithms, in the form of block diagrams and state transition diagrams, to executable codes. The mentioned tools are just capable of transforming the model descriptions into control algorithms and codes. Generating codes from a block diagram or a logical and structural description from the Unified Modeling Language (UML) [47] is part of what is known as model-based software development. A limited number of industries use this approach for design of mechatronic systems and it is not a very common practice [40]. To reach a formal control description that can be transformed into codes and algorithms, the designer must define a control approach, and consider the implementation of functions for the signal measurements or filtering used for the control system outputs to the overall system. Once the control structure and strategy are chosen, design rules and optimization routines can be employed to determine the controller parameters, if the requirements are given in a suitable form. These requirements must be derived by the system experts first, as they are usually specified at a higher level of abstraction. There is still a considerable gap towards supporting and automating the control system design activities in the early stages of mechatronic design.

## 2.2 Available Solutions to Design Challenges

Many efforts from industries and researchers in academia have come up with methods and tools to deal with the challenges identified above. In this section, a group of these solution methods and tools are discussed.

### 2.2.1 Design Methods

As previously mentioned, the traditional design methodology in mechatronics usually decomposes the overall system into several sub-systems according to some practical considerations and a unique guideline is used for each design aspect, to design the system sequentially. This method does not consider couplings and inter-connections. When more than one criterion is required in the design process, which happens quite often, the decision making about the components and subsystems becomes very tedious. For complex and multi-disciplinary designs requiring a significant amount of time and optimality, an algorithm which directly leads to the best efficient solutions is needed.

Following the concurrent design concept, Zhang et al. [48] proposed an integrated approach for mechatronic design of a programmable closed-loop mechanism. They used an objective function to minimize the shaking force and moment and consequently to facilitate the design of the control system. As an improvement to this work, Li et al. [6] developed a concurrent design framework known as design for control (DFC). They stated that although control parameters could be changed after the machine is built, they should be designed simultaneously with the structural parameters to ensure system integration. To facilitate controller design, the reduction of the shaking forces and moments of the actuators, was the only objective considered in their method. Although they suggested an effective concurrent approach, but improving the system performance using changeability of the controller parameters was overlooked.

De Silva [49] discussed that in a sequential design approach for mechatronic systems, optimal design of subsystems does not necessarily provide the optimum overall configuration. He proposed to associate performance indices to the mechatronic subsystems within an indicator index, called “mechatronic design quotient (MDQ)” and maximizing this index after integrating all the subsystems. Following this method, Behbahani [50] proposed a formal methodology for design of mechatronic systems by using the concepts of mechatronic design quotient (MDQ), where links between design criteria have been taken into account by using fuzzy sets. The MDQ methodology was implemented in pilot projects and has proved to be efficient; however, measurement and

determination of criteria for design are more qualitative and no systematic assesment approach has been suggested. Aiming at performance evaluation in conceptual design, Ferreira et al. [51] proposed a neural networks-based decision support to recommend design solutions based on earlier successful designs. Similarly, Hammadi et al. [52] defined a multicriteria performance indicator as a neural network of radial basis functions for early stages of mechatronic design. However, both of these approaches did not include a proper modelling for correlation between objectives and also sub-domains. Furthermore, these endeavors did not support any extension to stages of detailed design.

Villarreal-Cervantes et al. [53] proposed a concurrent design methodology to formulate the mechatronic design problem of a parallel robot. They incorporated a nonlinear dynamic optimization problem where both kinematic and dynamic behaviors were considered to minimize a performance criterion. Their method avoids a recursive design approach and enables the designers to obtain a set of optimal parameters in only one design step. Despite the benefit of abstraction in the design process, their method did not include a systematic approach for design and also did not cover early stages of design.

Due to their explorative power and flexible design representation, evolutionary algorithms are widely used in design synthesis methods during the past decade. These algorithms are usually embedded into an optimization problems regarding certain design objectives. In an automated design framework proposed by Xu et al. [54], designs were generated according to various design objectives and constraints.

In order to automate the design generation of mechatronic systems, Seo et al. [36] proposed to combine bond graph (BG) modeling with Genetic Programming (GP). Even though their method has been successfully applied to the detailed design of a mechatronic system but it was more focused on the structural part of the design rather than control. Also, early stages of design were not supported in their approach. Similarly, Behbahani and de Silva [55, 56] have used GP and BG for identification of the topology and the parameter values of a mechatronic system while Hu et al. [57] have applied BG and GP for automated synthesis of mechatronic systems. Although, all the case studies presented were limited to time-driven systems. Since most mechanical systems involve both continuous and discrete dynamics, enabling the evolution of hybrid systems can result in increase of the design complexity.

Various authors have proposed using models that contain functional descriptions of systems, such as Function-Behavior-State (FBS) [10], Functional Representation [18] and MACE [18], to



track and improve choices made in early design phases. These models usually provide proper representations about the functions of the system as well as all the hardware and software components involved in each system functionality. In other approaches, functional flow and block diagrams are used where functions are modeled as transformation procedures of matter, energy, or information [13, 16]. The IDEF0 method [17] is an example of using functional flow diagrams, which provides a vast formalization. FunKey [58] method proposes allocating budgets of resources to the functions of a system to provide a good documentation of the architecting process and a means to compare product architectures. However not all the aspects and design criteria are considered within this approach. The implementation of these methods is also a challenging task. Furthermore, functional descriptions are mainly used to help the designers to identify related information, but not to classify or identify such information with the help of an automated system. Additionally, requirements information is not included in most of these methods. Suh et al. [5] presented an axiomatic design method, where they discussed that functional independence of the system components leads to an optimal design. To attain this, the method provides guidelines, namely, the axioms of independence and information, to compare and evaluate early design choices. They reported multiple situations where their method was successfully implemented and used [5]. Although, according to modern functionalities of mechatronic devices and products, a tight integration of subsystems is desirable, which is very hard to achieve through an approach based on functional independence.

The above discussions about the available design methodologies to support concurrent mechatronic design are summarized in Table 2-2.

Table 2-2: Summary of recent methods in concurrent and integrated mechatronic design

Type	Design Methods (Short Title)	Conceptual & Prelim.	Detailed Design	Post Proc. & Modification	Reference
Design Evaluation	A model for concept evaluation in design				(Moulianitis et al. [59])
	Mechatronic Design Quotient (MDQ)				(Behbahani [3])
	Neural networks for decision support in conceptual design				(Ferreira [60])
	Mechatronic Design Indicator (MDI)				(Hammadi, et al. [52])
Evolutionary Algorithms	Function-based design synthesis (Using Genetic Programming)				(Xu et al. [54])
	A unified and automated design method based on BG and GP				(Seo, et al. [36])
	Genetic prog. and BG for the identification of the topology				(De Silva [61])
	BG and GP for automated synthesis of mechatronic systems				(Jianjun et al. [57])
Design Optimization	Concurrent design optimization of structure and control				(Park [62])
	Integrated design of mechanical structure and control				(Zhang et al. [63])
	Design for Control (DFC)				(Li et al. [6])
	Nonlinear dynamic optimization problem (NLDOP)				(Villarreal et al. [53])

### 2.2.2 Design Tools

Citherlet et al. [21] stated that there are mainly four different approaches to multi-disciplinary tool integration for the design of mechatronic systems: stand-alone, interoperable, linked, and integrated programs. Stand-alone programs are not desirable, as the tools are unrelated and the flow of information is not always possible. Interoperable programs are able to exchange or share models. Coupled tools are able communicate at run-time. Due to the flexibility of their modeling functionalities, some tools used in the control systems domain have taken this third approach.

Finally, integrated programs facilitate work in different domains within a single tool. Numerous CAD tools, have chosen this approach and incorporated tools from other domains into their software suites. For example, the latest version of CATIA [19] also supports electronics system modeling, and supports embedded control code generation. The existing coupled and integrated programs predict the behavior of systems from a detail design viewpoint. However, establishment of a direct connection with information from earlier design stages is still missing.

Modelica [22] language possesses an advanced environment for modeling, simulation and prototyping of complex physical systems. It supports the exchange of simulation models and the development of simulation libraries. Modelica supports libraries of models and functions with design capabilities for multi-domain modeling, enabling the designers to combine electrical, mechanical, control, thermodynamics and hydraulics within a system. This tool is also capable of executing and analyzing design models through connecting Modelica models with external solvers.

The Unified Modeling Language (UML) is a standardized modeling language which originated from object oriented software engineering, and it is maintained by the Object Management Group (OMG)[28]. UML aims at describing and documenting systems, rather than simulating them. Thus, a new modeling language named Systems Modeling Language (SysML)[64] is produced which reuses a subset of UML functionalities and extends them to some new functionalities such as creating block diagrams and parametric diagrams. The SysML language is intended to model systems from a broad range of industry domains such as aerospace, automotive, energy or health care and mechatronics. A number of researchers have tried integrate the descriptive capabilities of SysML to other analysis and simulation tools [65].

MATLAB in combination with Simulink [43] is well established for technical computing, simulation and model based design in many engineering domains. Simulink is an extension of MATLAB, which allows user to create graphical models, without writing any code. In fact, Simulink has many different libraries, which cover different domains with physical modeling e.g. SimMechanics [66] toolbox, signal processing toolbox, rapid prototyping toolbox, etc. Using these toolboxes a strong co-simulation and design integration can take place in the MATLAB/Simulink environment as the basis for any mechatronic analysis. Simscape [67] is a tool for the design and simulation for multi-domain physical systems. The aim of Simscape is the modeling of systems as networks of physical components. It extends Simulink with libraries for modeling systems from mechanical, electrical, hydraulic, and other physical domains.

CORE [68] is another software which uses a model-based system engineering approach for system integration. This tool captures requirements through making models and functional decomposition and flows. The models provided by CORE can be related manually by the designers, outside the CORE tool where a framework based on SysML is available to integrate information from other modeling and simulation tools.

In support of multi-disciplinary design and optimization, a framework called the Design and Engineering Engine (DEE) has been developed by La Rocca [69]. DEE is a domain-independent tool suitable for the design of a variety of systems from multiple domains. Data sharing between the various tools is enabled by using an agent-based network [70].

For the languages and tools used in design a multidomain systems such as mechatronic devices, an evaluation is summarized in a Table 2-3 by considering some key characteristics relevant to the development and design process for mechatronics. The cells shaded in black indicate whether the tool or language is suited for the specified criteria while the cells shaded in grey represent partly suited and the blank cells represent non-suitability.

Table 2-3: Evaluation Summary of the languages and tools per mechatronic design process

#	Tool/Language	System Concept Design	Domain-Specific Detailed Design	Design Integration	Simulation and/or Verification
I	Modelica				
II	UML				
III	SysML				
IV	Matlab & Simulink				
V	Simscape				
VI	CAMeL-View				
VII	KIEF				
VIII	CORE				

### 2.2.3 Optimization and Design Support

To be able to optimize a multi-domain system, multidisciplinary design optimization (MDO) and process integration design optimization (PIDO) approaches are available [37, 71-73]. MDO is, as presented in [73], a methodology for the design of complex engineering systems that coherently exploits the synergism of mutually interacting phenomena. In other words, a MDO approach helps the process of design to decide what to change, and to what extent to change it, when everything influences everything else. In mechatronic design, optimizing domain-specific system performance indices require performing trade-off studies through multi-domain models. By finding the best

possible values for different properties through an optimization, the net objective or fitness function can be maximized. It is important for the designers to be able to make decisions in the right direction during all phases of product development. Thus, PIDO tools and an integration infrastructure are used concurrently to support the designers in taking the right actions.

#### **2.2.4 Human Communication and Cooperation**

In order to achieve an integrated design approach, it is of high importance to consider human factors and the communication between the people involved in the design of a system. Pahl et al. [74] have identified the communication and exchange of information between designers as one of the fundamental aspects of their systematic design approach. They mentioned methods like brainstorming and group evaluations to support the information exchange activities. They stated that these activities are helpful specifically in the conceptual phase. However, such methods cannot be appropriately extended to the later stages of design, because they have been intended to deal with less detailed information.

Unfortunately, despite the recognized importance of communication between design engineers and the exchange of information, there is still no formal tool supporting the design activity while considering the integrating of individual design contributions alongside an overview of the system and its goals.

#### **2.2.5 Control Software**

There are various commercial code generators available, both for unified environments such as Matlab/Simulink and also UML-based modeling tools such as SysML. Towards automation of the control design, requirements must be interpreted into control structure and logic in the early design phase. By using live sequence charts (LSC), it is possible to automatically derive control software logic and structure from requirements in the form of UML. To get from requirements to control software, a method based on requirements-based programming (RBP) is proposed by Rash et al. [75]. This method increases development productivity and the quality of the generated code by automatically performing verification of the software. A more functional connection between requirements and control software can be achieved using the functional block computer-aided design environment [60]. A prototyping tool can be used to design and analyze high-level control software components while generating run-time code for distributed control systems. Moreover, partial automation of the control development process is attainable through incorporation of pre-developed control codes from component-specific databases.

## CHAPTER 3 ARTICLE 1: MULTICRITERIA DECISION SUPPORT FOR CONCEPTUAL DESIGN OF MECHATRONIC SYSTEMS; A QUADROTOR DESIGN CASE STUDY

Abolfazl Mohebbi, Sofiane Achiche and Luc Baron

Submitted to *Springer Journal of Research in Engineering Design*, Jan. 2015

### 3.1 Abstract

Designing mechatronic systems is known to be both a very complex and tedious process due to the high number of system components, their multi-physical aspects, the couplings between the different domains involved in the product and the interacting design objectives. This inherent complexity calls for the crucial need of a systematic and multi-objective design thinking methodology to replace the often-used sequential design approach that tends to deal with the different domains and their corresponding design objectives separately leading to functional but not necessarily optimal designs. Thus, a new approach based on a multi-criteria profile for mechatronic systems is presented in this paper for the conceptual design stage. Additionally, in order to facilitate fitting the intuitive requirements for decision-making in the presence of interacting criteria, three different methods are proposed and compared using a case study of designing a vision-guided quadrotor drone system. These methods benefit from three different aggregation techniques such as Choquet integral, Sugeno integral and fuzzy-based neural network. It is shown that although the Sugeno fuzzy can be a useful aggregation function for decisions under uncertainty, but the approaches using Choquet fuzzy and fuzzy integral-based neural network seem to be more precise and reliable in a multi-criteria design problem where interaction between the objectives cannot be overlooked.

### 3.2 Introduction

Introduction of mechatronic systems was a direct result of an increased need for controlled and intelligent electromechanical systems with better performance, more flexibility and higher reliability capable of performing complex tasks. The process of designing a wide variety of products such as avionic systems, robots, transportation and construction machines or even home appliances

is now considered within the area of mechatronic systems design that requires coherent design activities between several disciplines such as mechanical, electrical, control and software engineering. The high number of their components, their multi-physical aspect and the couplings between the different disciplines involved, make the design task very tedious and complex which requires a significant amount of time [8, 76, 77]. Therefore, this inherent complexity and the dynamic couplings between subsystems, urges for a methodology to find the optimal design solutions and to replace the often-used sequential design approach that tends to deal with the different subsystems and domains (i.e. mechanical, electrical, software, fluid, thermal, etc.) separately. Moreover, a systematic and multi-objective design methodology is needed. The resulting products would eventually form a spatial integration and a functional interaction in components, modules, products and systems.

Design activities, including of mechatronic products, include three major phases: conceptual design, detailed design, and prototyping and improvements. Conceptual design is an early stage of design in which concepts are selected and employed to solve a given design problem and then a decision is made on how to interconnect these concepts into an appropriate system architecture [39]. Moreover, at this stage, a comprehensive and consistent listing of the requirements and behaviors is required as well as a thorough identification of critical parts of the solution that affects the overall performance. Rzevski [39] discusses conceptual design of mechatronic systems based on multi-agent technology. He argues that the best configuration of a design process is a network of autonomous, intelligent decision making units able to reach decisions through the process of negotiation. However, the given examples of systems designed by such methodology indicated the use of high number of sensory components and control agents as well as geometrically variable parts, which all together could elevate the cost of production and increase the risk of failure. Zivav & Reich [78] presented a comprehensive approach for generating optimal concepts in diverse disciplines. They suggested to decompose a complex problem into smaller sub-problems, to use highly simplified evaluations. In another effort [79] they defined a design robustness term as the stability of the optimal concept or configuration generated by the approach presented in [78] with respect to variations in many factors such as designers' subjective judgment, availability of the technology, organization context, and customers' preferences.

A number of problems and limitations are encountered when design is at its early stages, as it requires the selection of components and choosing between alternatives for software and control strategies [39, 44, 80]. This part of conceptual and preliminary design is usually known as choosing

the “Elite Set”. This practice creates challenges due to insufficient support of the multi-criteria nature of mechatronics systems design, which calls for decision support across various disciplines. In such cases, engineers tend to choose the first and the best components from what they see as available and feasible to meet their design requirements. Such decisions can often lead to a functional design, but rarely to an optimal one. This ill decision making generally occurs due to improperly-defined performance criteria and lack of knowledge about the co-influences between criteria and the functionality to be provided by neighbouring disciplines. Avigada & Moshaiov [81] presented an approach to support the selection of conceptual solutions for multi-objective problems. Their method involved performing a set-based comparison between concepts by considering both optimality and variability. Their method was consistent with the so-called Toyota set-based concurrent engineering process. Moulianitis et al. [44] proposed a methodology for decision making in conceptual mechatronic design based upon an evaluation index including three criteria: intelligence, flexibility, and complexity. Weight factors were manually applied to highlight the importance of each criterion. The formulation of the evaluation score has been presented based on t-norms [82] and averaging operators. However, the methodology does not consider interactions between criteria and a limited, discrete search space was considered. A producibility index vector has been proposed by Byun and Elsayed [83], in which both quality and cost requirements are considered. Their producibility index is defined as a measure of the desirability of a product, quality of process design and manufacturing costs. Based on this index, overall process capability is calculated using weighted geometric means. The main drawback of their work is that the design evaluation for various alternatives is achieved by direct comparison of every element of the index vector.

De Silva [49] stated that in a sequential design approach for mechatronic systems, optimal design of subsystems does not necessarily provide the optimum overall configuration. He proposed to associate performance indices to the mechatronic subsystems within an indicator, called “mechatronic design quotient (MDQ)” and maximizing this indicator after integrating all the subsystems. Based on this method, Behbahani [50] proposed a formal and systematic framework for design of a mechatronic system by using the concepts of mechatronic design quotient (MDQ) in a concurrent design approach, where correlations between design criteria have been taken into account by using fuzzy concepts to define them. MDQ was implemented in pilot projects [84], and was claimed to be efficient; however measurement and determination of criteria for design are very qualitative and no systematic measurement approach has been presented nor implemented. In a different approach, Janschek [85] proposed a method based on performance metrics defined as the



deviation of the measured criteria relative to a reference value. P-norm of the standard deviations of the  $p$  criteria were used to define the standard deviation of the overall mechatronic design. Correlations and interactions between objectives were also taken into account by calculating the covariance values between different criteria. For the same purpose of performance analysis in conceptual design, Ferreira et al. [51] proposed using feedforward multilayer perceptron neural networks as a decision support to recommend design solutions for engineering systems based on existing database of successful designs. They focused on reducing the complexity of the neural model from the designer's point of view. In order to measure the quality of the design prediction and to avoid misleading solutions an error index was also provided.

It can be understood that although a number of efforts focused on presenting supports for decision making in design, but there is still a need for a comprehensive approach that simultaneously considers a set of general main criteria for conceptual design of mechatronic products and also provides the necessary means to assess these criteria and aids the designers to decide among all generated alternatives. As the main contribution, this paper presents a systematic approach for supporting multi-objective and concurrent design of mechatronic systems in early stages of design. First and after a thorough literature study and analysis of the available research work on mechatronic system design, a vector of five main criteria and corresponding sub-criteria for conceptual design are identified and then the assessment methods for each one of them are explained and in some cases adapted to the case of designing a complex mechatronic system. This provides a unified framework for evaluation of design concepts for mechatronic systems. Consequently, in section 3.3, the new index vector- Mechatronic Multicriteria Profile (MMP), is introduced for the purpose of concept evaluation in mechatronic systems design. MMP can be determined numerically through mathematical measures by including sub-criteria and by reflecting an aggregated value for each main criterion. Section 3.4 is devoted to presenting and comparing three different methods for decision support and aggregation based on fuzzy sets in the presence of interacting criteria by incorporating Choquet integrals, Sugeno fuzzy and fuzzy-based neural networks. Finally, in section 3.5, the effectiveness of the proposed approach alongside the presented decision support methods is studied and compared by applying it to the conceptual design of a vision-guided quadrotor UAV.

### **3.3 Multicriteria Mechatronic Profile (MMP)**

One of the most challenging problems faced with regards to design of mechatronic systems is to find the right set of criteria to concurrently evaluate and synthesise the designs. Making design

decisions with multiple criteria, in general and for mechatronic systems in particular, is often performed using a Pareto approach. Achieving optimal solutions is a very complex if not impossible task without the identification of the performance parameters involved and the understanding of their co-influences. Optimal mechatronics design simultaneously requires a precise and systematic design evaluation stage. The lack of simultaneous consideration of objectives within various domains involved at the early design stage increases the need for iterations. This evaluation includes both comparison and decision making [86]. In other words, decision-making is achieved by selecting the “best” alternative by comparison. It is crucial to take into account both correlation between system requirements and also interactions between the multidisciplinary subsystems [4]. The goal of concept evaluation is to compare the generated concepts against the requirements and to select the best one for the detailed design and optimization stages. In a conceptual design stage and based on sets of design specifications and goals, candidate solutions are generated (Figure 3-1). In most of design projects, more than one candidate solutions is generated and evaluated in order to select the best one meeting the design objectives and constraints.

In order to form an integrated and systematic evaluation stage, the most important quantitative criteria have been identified to form an index vector of five normalized elements called Mechatronic Multi-criteria Profile (MMP) as follows:

$$MMP = [MIQ, RS, CX, FX, CT]^T \quad (3.1)$$

where MIQ is the machine intelligence quotient, RS is the reliability score, CX is the complexity, FX is the flexibility and CT is cost of manufacture and production. We also define  $m_i$  as the values for the members of MMP sorted in ascending order such that  $m_1 \leq m_2 \leq \dots \leq m_5$  and  $0 \leq m_i \leq 1$ .

### 3.3.1 Machine Intelligence

The term “Machine Intelligence Quotient (MIQ)” was firstly introduced by Bien [87] and Kim [88] as an index used to assess the intelligence of a control system in mechatronic machines. This index significantly differs from other well-known indices such as control performance, reliability, fault diagnosis capability, etc. Bien [87] also proposed two measurement methods: the ontological method and the phenomenological method. In Kim’s work [88] control performance, fault diagnosis capability and reliability were defined as the main factors in machine intelligence. The term MIQ used in the newly introduced MMP will be assessed based on a method presented by park et al. [89] in which the machine intelligence is divided into two components of control intelligence and

interface intelligence. Accordingly, the mechatronic system was modeled using an intelligent task graph (ITG). In the topics related to parallel processing and scheduling, the set of tasks and their data dependencies are usually described by Data Flow Graph (DFG). They modified the DFG from the viewpoint of intelligence and transformed it into the ITG, which is suitable for analyzing the machine intelligence. Furthermore, the intelligence required for interaction between the human operator and the machine is taken into account. Some examples were given by park *et al.* [89] for assessing expert systems for power plants to verify the proposed modeling and measuring procedures. Studying their examples shows that their approach has been more or less aligned with that specific line of application which can not necessarily contribute to a complex robotic mechatronic system.

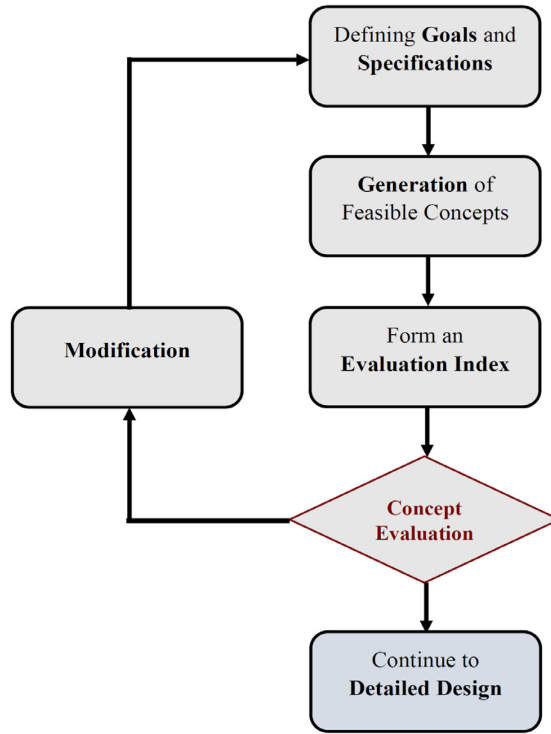


Figure 3-1: Concept evaluation in design, adopted from [44]

A number of research work have been dedicated to further adapt this method for specific applications [50, 90]. Here, we provide a modified approach to model and assess the MIQ for a robotic platform and at the end in section 3.5 we apply the method to a visual servoing system for quadrotor UAV. Figure 3-2 shows an example of the ITG in which the circles denote the tasks of control jobs and the directional arrows denote information flow from one task to another. With regards to an ITG, a task set  $T = \{T_1, T_2, \dots, T_n\}$  is the set of  $n$  tasks required to control events.  $\tau = \{\tau_1, \tau_2, \dots, \tau_n\}$  is a set of task intelligence costs, in which,  $\tau_i$  is a scalar representing the

intelligence required to execute  $T_i$ . Accordingly, in a data transfer matrix  $F$ ,  $f_{ij}$  is a scalar showing the data quantity transferred from task  $T_i$  to  $T_j$  such that:

$$F = \begin{pmatrix} 0 & f_{12} & f_{13} & \cdots & f_{1n} \\ f_{21} & 0 & f_{23} & \cdots & f_{2n} \\ f_{31} & f_{32} & 0 & \cdots & f_{3n} \\ \vdots & \vdots & \vdots & \ddots & \vdots \\ f_{n1} & f_{n2} & f_{n3} & \cdots & 0 \end{pmatrix} \quad (3.2)$$

Interface complexity is the complexity of transferring one unit of data between the operator and the machine using user interface devices such as: displays, keyboards, control switches, haptic devices and etc.  $c_{hm}$  is defined as the interface complexity of transferring data from the operator (user) to the machine. Accordingly,  $c_{mh}$  is defined as the interface complexity of transferring data from the machine to the user. Average Interface Complexity of a component-based system is calculated as follows:

$$c = \frac{1}{n} \sum_{i=1}^n (N_i + O_i), \quad (3.3)$$

where  $n$  is the number of all components and interface devices in the system and  $N_i$  and  $O_i$  are the number of incoming and outgoing interactions for every component. Interface intelligence cost  $f_{ij} \cdot c_{hm}$  and  $f_{ij} \cdot c_{mh}$  are the user intelligence amount required to communicate data with the machine, which is proportional to both data quantity and interface complexity.

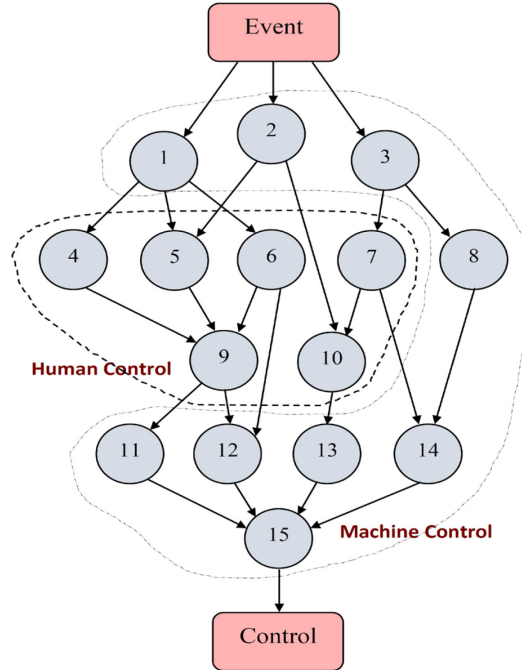


Figure 3-2: Example of intelligent task graph (ITG)

In a task allocation matrix,  $A$ ,  $a_{i1}$  is equal to 1, if the machine performs task  $T_i$ , and  $a_{i2}$  is equal to 1 if the human performs task  $T_i$ . If  $T_i$  cannot be assigned to either the machine or the human user,  $a_{i3}$  is equal to 1. Thus;

$$a_{i1} + a_{i2} + a_{i3} = 1. \quad (3.4)$$

For  $\forall i, 1 \leq i \leq n$ , the  $n$ -by-3 matrix  $A$  is defined as:

$$A = \begin{pmatrix} a_{11} & a_{12} & a_{13} \\ a_{21} & a_{22} & a_{23} \\ \vdots & \vdots & \vdots \\ a_{n1} & a_{n2} & a_{n3} \end{pmatrix}. \quad (3.5)$$

The control intelligence quotient or CIQ is calculated as the sum of all task intelligence costs:

$$CIQ = \sum_{i=1}^n a_{i1}\tau_i + \sum_{i=1}^n a_{i2}\tau_i \quad (3.6)$$

The human intelligence quotient (HIQ) is defined as the required intelligence quantity from the human for controlling plants and is calculated such that:

$$\begin{aligned} HIQ = & \left( \sum_{i=1}^n a_{i2}\tau_i \right) + \left( c_{mh} \sum_{i=1}^n \sum_{j=1}^n a_{i1}a_{j2}f_{ij} \right) \\ & + \left( c_{hm} \sum_{i=1}^n \sum_{j=1}^n a_{i2}a_{j1}f_{ij} \right) \end{aligned} \quad (3.7)$$

Finally, The MIQ can be calculated as follows:

$$MIQ = CIQ - HIQ. \quad (3.8)$$

### 3.3.2 System Reliability

System reliability assessment (SRA) has been addressed as an important issue of the design process of mechatronic systems in many research work [50, 91]. Reliability engineering mainly deals with analyzing the expected or actual reliability of a product, process or service, and identifying the actions to reduce failures or their malicious effects. To achieve this goal, all levels of design and production require a process of reliability engineering. A number of methods for reliability assessment have been developed, most of which estimate the system reliability using only the data of components [92]. The methods of fault tree analysis (FTA) and failure modes and effect analysis (FMEA) are the most popular tools for reliability assessment, while some other research have been established based upon using Petri nets (PN) for modeling of dynamic characteristics of complex mechatronic systems [50]. In order to avoid complexity, the dynamic effects for reliability

assessment can be neglected and for a multi-components system with no redundancy, the global reliability score (RS) can be expressed by:

$$RS = \prod_{i=1}^m (1 - p_i) \quad (3.9)$$

in which  $p_i$  is the failure probability of  $i^{th}$  component and  $m$  is the number of components in the mechatronic design concept.

### 3.3.3 Design Complexity

Due to the multi-disciplinary nature of mechatronic systems, the complexity of products themselves and also the complexity of product design and development are significantly increased. Using Design Structure Matrix (DSM) [93, 94] and Axiomatic Design (AD) [95] are two well-known techniques to deal with complexity. Despite design complexity being considered as one of the most important challenges faced by mechatronic designers, just a few work efforts have been carried out for quantitative assessment and estimation of complexity in a design procedure for mechatronic systems [96]. In the presented paper, the term “Complexity”, which was introduced earlier as a member of MMP, is defined by modifying and expanding the work presented in [44]. The sources of complexity are identified and represented as a vector of six elements as follows:

$$\Phi = [\phi_1, \phi_2, \phi_3, \phi_4, \phi_5, \phi_6]^T, \quad (3.10)$$

where  $\phi_1$  is the number of components as the first and most common source of complexity,  $\phi_2$  is the degree of architecture complexity (number of interconnections),  $\phi_3$  is the design complexity which is specified by the backtracks to the earlier stages (number of feedback loops in design process),  $\phi_4$  is the intrinsic multi-disciplinarily complexity (number of distinct knowledge bases),  $\phi_5$  is the control complexity (number of closed loops in all control strategies used in the system) and finally  $\phi_6$  is the extent of embedded software in product and depends on the degree of the system intelligence such that:

$$\phi_6 = 1 - \overline{MIQ} \quad (3.11)$$

These types of complexity sources mostly come from interactions among design parameters and physical phenomena, which sometimes unexpectedly, cause undesired matters that can result in design or system failures. After determination and normalization of  $\Phi$ , and by using a linear summation of weighted factors, the complexity value of the concept will be assessed as follows:

$$CX = \sum_{j=1}^6 w_j \bar{\phi}_j \quad (3.12)$$

where  $w_j$  are the assigned-by-designer weights associated to each complexity element.

### 3.3.4 Design Flexibility

Despite the traditional design approaches, which define a task and create a design for a specific situation, considering flexibility in design leads to producing adaptable systems. A vector of design flexibility for a mechatronic concept and its members can be presented as follows:

$$\Psi = [\psi_1, \psi_2, \psi_3, \psi_4, \psi_5]^T, \quad (3.13)$$

in which  $\psi_1$  is the component design flexibility (the number of alternative component design paths),  $\psi_2$  is the customization flexibility (the number of customization options for components),  $\psi_3$  is the number of choices for system architecture,  $\psi_4$  is the interface flexibility (the number of choices for user interface) and  $\psi_5$  is the control flexibility (the number of options for control algorithms). After determination and normalization of  $\Psi$ , the flexibility score for the corresponding concept can be calculated as:

$$FX = \sum_{j=1}^3 \rho_j \bar{\psi}_j, \quad (3.14)$$

From Equation (3.12) and Equation (3.14),  $w_j$  and  $\rho_j$  are the product-dependent weighting factors defined by the designer.

### 3.3.5 Cost

To achieve an efficient project cost control and management, an estimation of the total cost of a system in the early stages of design is necessary. Managing and reducing the cost of a system at the conceptual design stage is more effective than at the manufacturing and development stage. This will also help the designers to customize and modify the design during the early design stage, to achieve both performance and cost efficiency. According to a number of authors [97, 98] 70 to 80 percent of a product cost is determined during the early design stage. There are various methods for evaluating design and manufacturing costs of a system such as parametric, neural networks and feature-based methods. Among all, using artificial neural network (ANN) seems to be particularly effective for cost estimation of complex systems in which the relationships between cost and design variables cannot be expressed by simple mathematical expressions [99-101]. In this paper, the term “cost” (CT) in mechatronic multi-criteria profile (MMP) will be calculated such as:

$$CT = \sum_{i=1}^4 CT_i, \quad (3.15)$$

in which  $CT_1$  is the component costs as the summation of prices of all subsystems,  $CT_2$  is the development and manufacturing cost,  $CT_3$  is the integration cost and  $CT_4$  is the failure, repair and overhaul cost.

### 3.4 Multi-Criteria Decision Support and Aggregation of Criteria

After specifying quantitative values for all MMP criteria and corresponding subsets, an effective evaluation technique is needed for choosing among all possible conceptual choices. Thus, a global concept score (GCS) as a multi-criteria design evaluation index can be defined as follows in order to enable the designers to compare between the feasible generated design concepts;

$$GCS = S(m_1^*, m_2^*, \dots, m_n^*) \cdot \prod_{i=1}^m g(m_i), \quad (3.16)$$

where  $m_i$  is the value of the  $i^{th}$  criterion from MMP and  $m_i^*$  is the corresponding normalized score. For a criterion that the larger value is more desired (e.g. MIQ, flexibility and reliability), we have:

$$m_i^* = \frac{m_i}{\max(m_i)}, \quad (3.17)$$

and for a criterion that the smaller value is more desirable (e.g. cost and complexity), we can write:

$$m_j^* = \frac{1}{\left(\frac{m_j}{\max(m_j)}\right)} \quad (3.18)$$

Furthermore,  $S(.)$  represents an aggregation function, and  $g(m_i)$  indicates whether a design constraint has been met;

$$g(m_i) = \begin{cases} 1 & \text{constraint is met} \\ 0 & \text{constraint is not met} \end{cases} \quad (3.19)$$

There are a variety of research efforts in providing aggregation operators for decision analysis based on fuzzy set theory in the presence of dependant and interacting criteria [102, 103]. In this work, we consider and compare three different aggregation operators based on well-known Choquet and Sugeno fuzzy integrals and also a fuzzy-based multi-layer neural network to calculate the global concept score for each design concept.



### 3.4.1 Choquet Integrals

As the first aggregation technique, a nonlinear Choquet integral [104, 105] can be used to compute the global concept score for each feasible generated design concepts. Choquet integral provides a weighting factor for each criterion, and also for each subset of criteria. Using Choquet integrals is a very effective way to measure an expected utility when dealing with uncertainty, which is the case in design in general and mechatronic design in particular. Using this technique and by defining a weighting factor for each subset of criteria, the interactions between multiple objectives and criteria can be easily taken into account along with the designer's intuition. The weighting factor of a subset of criteria is represented by a fuzzy measure on the universe  $N$  satisfying the following fuzzy measures ( $\mu$ ) equations:

$$\mu(\phi) = 0, \quad \mu(N) = 1. \quad (3.20)$$

$$A \subseteq B \subseteq N \rightarrow \mu(A) \leq \mu(B). \quad (3.21)$$

where  $A$  and  $B$  represent the fuzzy sets. Table 3-1 shows the most common semantic interactions and the corresponding fuzzy measures.

Table 3-1: Fuzzy Interactions and Measurements

#	Description of Interaction	Fuzzy Measurement
I	Negative Correlation	$\mu(i, j) > \mu(i) + \mu(j)$
II	Positive Correlation	$\mu(i, j) < \mu(i) + \mu(j)$
III	Substitution	$\mu(T) < \begin{Bmatrix} \mu(T \cup i) \\ \mu(T \cup j) \end{Bmatrix} \approx \mu(T \cup i \cup j)$ $T \subseteq Y \setminus i, j$
IV	Veto Effect	$\mu(T) \approx 0$ if $T \subset Y, i \notin T$
V	Pass Effect	$\mu(T) \approx 1$ if $T \subset Y, i \in T$
VI	Complementarity	$\mu(T) \approx \begin{Bmatrix} \mu(T \cup i) \\ \mu(T \cup j) \end{Bmatrix} < \mu(T \cup i \cup j)$ $T \subseteq Y \setminus i, j$

Thus, GCS can be re-written as follows:

$$\begin{aligned}
 GCS &= C_{\mu}(m_1^*, m_2^*, \dots, m_n^*) \\
 &= \left( \sum_{i=1}^n \phi(\mu, i) m_i - \frac{1}{2} \sum_{\{i, j\} \subseteq N} I(\mu, ij) |m_i - m_j| \right) \cdot \prod_{i=1}^m g(m_i)
 \end{aligned} \quad (4)$$

where  $\phi(\mu, i)$  is the importance of criterion  $i$  and computed by the Shapley value ( $\phi$ ) [104], which is defined as:

$$\phi(\mu, i) = \sum_{T \subseteq N \setminus i} \frac{(n - t - 1)! t!}{n!} [\mu(T \cup i) - \mu(T)]. \quad (4.1)$$

From above,  $T$  is a subset of criteria. Furthermore  $I(\mu, ij)$  is the interaction index between criteria  $i$  and  $j$  and is defined as follows [104]:

$$I(\mu, ij) = \sum_{T \subseteq N \setminus i, j} \frac{(n - t - 2)! t!}{(n - 1)!} [\mu(T \cup ij) - \mu(T \cup i) - \mu(T \cup j) + \mu(T)]. \quad (4.2)$$

A Choquet fuzzy integral behaves like parameterized aggregator; it can cover the range between min and max of the input level by assigning the density values (fuzzy measures) appropriately. It is important to note that desired overall importance and the interaction indices need to be satisfied during identification of fuzzy measures.

### 3.4.2 Sugeno Fuzzy

Using a Sugeno fuzzy integral as a method of aggregation of interaction criteria can yield to a relative global concept score (GCS) as follows:

$$GCS = S_\mu(m_1^*, m_2^*, \dots, m_n^*) \cdot \prod_{i=1}^m g(m_i) = \bigvee_{i=1}^n [\overline{m}_i \wedge \mu(A_{(i)})] \cdot \prod_{i=1}^m g(m_i), \quad (4.3)$$

where  $(.)$  in  $A_{(i)}$  indicates a permutation on  $N$  such that  $m_1 \leq m_2 \leq \dots \leq m_n$ . Also,  $\wedge := \min$  and  $\vee := \max$ . Furthermore,  $A_{(i)} = \{(i), \dots, (n)\}$  and  $A_{(n+1)} = \emptyset$ .

### 3.4.3 Neural Networks

As the third technique, a Choquet integral-based neural network is presented to be used for the aggregation of criteria and fitting the intuitive requirements for decision-making in the presence of interacting criteria. These networks are highly flexible and their parameters are learned through training [106, 107]. The structure of a Choquet integral-based neural node and corresponding multi-layer network is illustrated in Figures 3-3 and 3-4, where the output is a Choquet integral value [108].

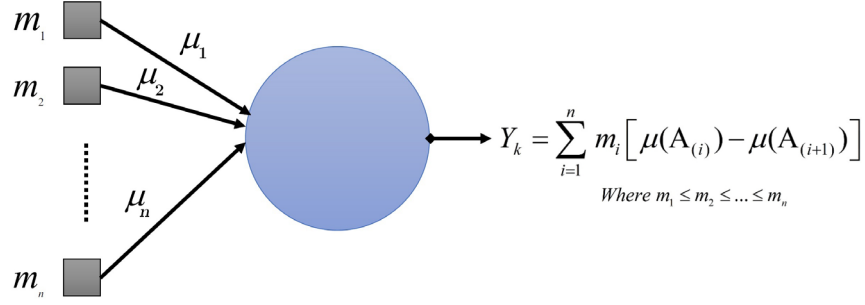


Figure 3-3: A fuzzy integral-based neural node where inputs are information sources and output is a fuzzy integral value.

In this new structure, each neuron is an operator of Choquet integral of  $m: N \rightarrow \mathbb{R}$  with respect to  $\mu$  such that;

$$Y_k = C_{\mu}^{NN}(m_1^*, m_2^*, \dots, m_n^*) = \sum_{i=1}^n m_i [\mu(A_{(i)}) - \mu(A_{(i+1)})], \quad (4.4)$$

where  $(.)$  indicates a permutation on  $N$  such that  $m_1 \leq m_2 \leq \dots \leq m_n$ . Also,  $A_{(i)} = \{(i), \dots, (n)\}$  and  $A_{(n+1)} = \phi$ .

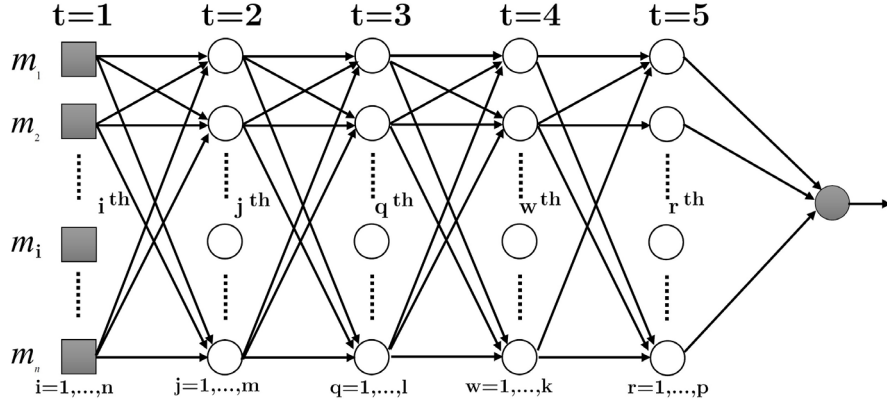


Figure 3-4: A fuzzy integral-based neural network structure with three hidden layers

In addition to Equations (3.20 - 3.21), the fuzzy measures used in Eq. (3.26) satisfy the following additional property where  $A \cap B = \phi$ :

$$\mu(A \cup B) = \mu(A) + \mu(B) + \xi \mu(A)\mu(B). \quad (4.5)$$

$\xi$  is the corrective coefficient where  $\xi > -1$  and satisfies the following equation:

$$\xi + 1 = \prod_{i=1}^n (1 + \xi \mu_i) \quad (4.6)$$

The value of  $\mu(A_{(i)})$  can be determined by a recursive solution of the following equations:

$$\mu(A_{(n)}) = \mu_n \quad (4.7)$$

$$\mu(A_{(i)}) = \mu_i + \mu(A_{(i+1)}) + \xi \mu_i \mu(A_{(i+1)}) \quad \text{for } 1 \leq i \leq n. \quad (4.8)$$

The proposed neural network is called a fully connected network such that the input layer projects onto a hidden layer of Choquet integral-based neurons and the output of hidden layers projects onto the output layer [109]. As illustrated before in Figures 3-4, in this network each neuron is represented by a set of linear synaptic links and a fuzzy integral function with respect to a certain fuzzy measure. The synaptic links of a neuron can be interpreted as the degree of importance of the respective input signals. In other words, in this network, a typical “directed link” originates at node  $i$  and ends at node  $k$ . It has an associated transfer function of Choquet fuzzy integral that specifies the manner in which the output value  $Y_k$  at node  $k$  depends on the input signal and the “synaptic” links. We assume that the training data for an output node consists of  $n$  sets of inputs:  $m_1^k, m_2^k, \dots, m_m^k$  and with  $q$  corresponding desired outputs:  $Y_1^k, Y_2^k, \dots, Y_m^k$ . The training process is achieved through the well-known backward-error propagation algorithm [110, 111]. With regards to a neural network, a supervised training, is a process in which a desired output value for each input pattern is presented. In other words, in supervised training, both the inputs and the outputs are provided. The network then processes the inputs and compares its resulting outputs against the desired outputs. Errors are then propagated back through the system, causing the system to adjust the measures, which control the network. Finally, the best set of fuzzy measures are determined for a node in such a way that the difference between the desired and actual fuzzy integral behavior is minimized. The error is represented as:

$$E = \sum_k E_k = \sum_k \sum_i (C_i^k - Y_i^k)^2 \quad (4.9)$$

where  $C_i^k$  is the Choquet fuzzy integral function of the  $k^{th}$  training input vector  $(m_1^k, m_2^k, \dots, m_m^k)$  with respect to fuzzy measures  $\mu$ . Using Eq. (3.26) we can write  $C_i^k$  as follows:

$$C_i^k = \sum_{j=1}^n m_j^k [\mu(A_{(i)}) - \mu(A_{(i+1)})] \quad (4.10)$$

Using Eq. (3-32) we can obtain:

$$C_i^k = \sum_{j=1}^n m_j^k \mu_{ij} \left( 1 + \xi^k \mu(A_{(i+1)}) \right), \quad i = 1, 2, \dots, q \quad (4.11)$$

where  $n$  is the number of the input nodes,  $q$  is the number of output nodes and we also have  $(m_1^k \leq m_2^k \leq \dots \leq m_m^k)$ .  $\mu_{ij}$  is the synaptic weight connecting input node  $j$  to fuzzy integral  $i$ . The network is then optimized by minimizing with respect to the synaptic weights (fuzzy measures)

of the network. Thus, we update the fuzzy measures,  $\mu_{ij}$  using the following equations based on gradient descent:

$$\mu_{ij}^* = \mu_{ij} - \gamma \cdot \frac{\partial E}{\partial \mu_{ij}}, \quad (4.12)$$

where  $\mu_{ij}^*$  is the new value for  $\mu_{ij}$  and for  $\partial E / \partial \mu_{ij}$  we have;

$$\frac{\partial E}{\partial \mu_{ij}} = 2 \sum_{k=1}^q (C_i^k - Y_i^k) \frac{\partial C_i^k}{\partial \mu_{ij}}, \quad (4.13)$$

where  $\partial C_i^k / \partial \mu_{ij}$  can be obtained from:

$$\frac{\partial C_i^k}{\partial \mu_{ij}} = \frac{\partial}{\partial \mu_{ij}} \left( \sum_{j=1}^n m_j^k \mu_{ij} \left( 1 + \xi^k \mu(A_{(i+1)}) \right) \right) \quad (4.14)$$

The choice of  $\gamma$ , as a suitable positive constant, is important and it determines the reliability and also time of convergence [112]. The learning process is repeated until the changes in  $\mu_{ij}$  are inferior to a specified small number. The training procedure can be extended to a multi-layer network where there are several nodes arranged in a hierarchical manner. In this case, the training data normally consists of input values at the first layer and the desired output at the last layer. Accordingly, it is possible to compute the fuzzy integral functions and their parameters. After defining the base of the decision making neural network, now we can intuitively build the structure of the fuzzy-based neural network for newly introduced MMP as illustrated in Figure 3-5. In the proposed structure, 56 densities should be identified through the training process and the initial values fed into the network are intuitively chosen. The corresponding global concept score can be calculated as follows:

$$GCS = C_{\mu}^{NN}(MMP^*) \cdot \prod_{i=1}^m g(m_i) \quad (4.15)$$

where  $MMP^*$  indicates that all input criteria and sub-criteria to the neural network contain normalized values and are between 0 and 1. After assessing global concept scores (GCS) for each design alternative based on three suggested approaches, the concept selection can be performed to choose the best available design concept and consequently, in a recursive manner, modifications can be applied to the selected concept and subsystems. Based on the requirements and objectives defined in the first stage, a more precise concept selection can be performed and after a few iterations the final decision for the conceptual design can be made. The procedure of conceptual design using the proposed methodology and based on the calculated global concept score is described in flowchart shown in Figure 3-6.

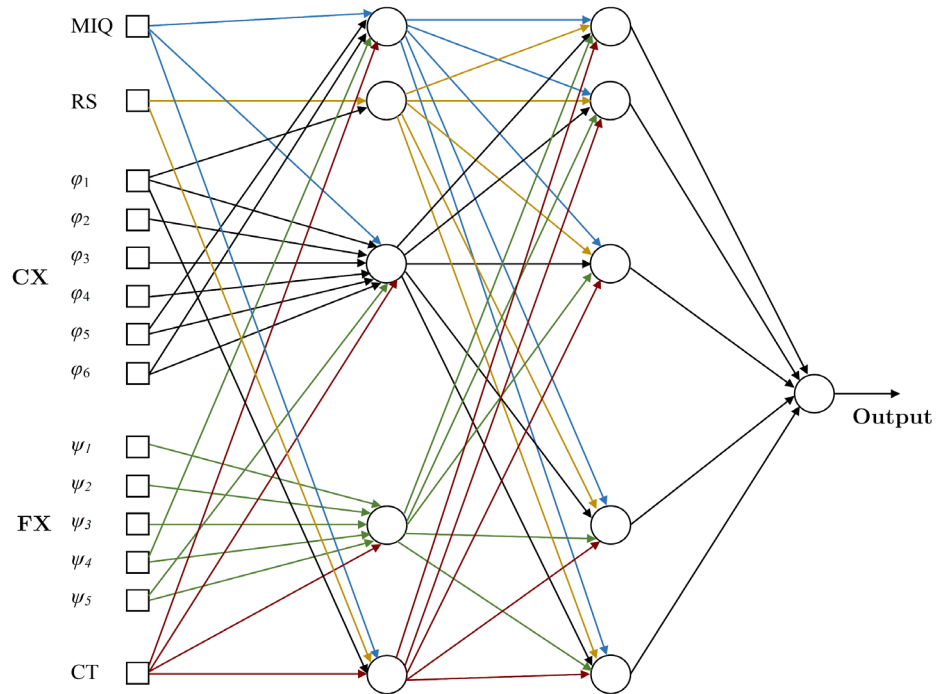


Figure 3-5: The structure of the fuzzy integral-based neural network with one hidden layer

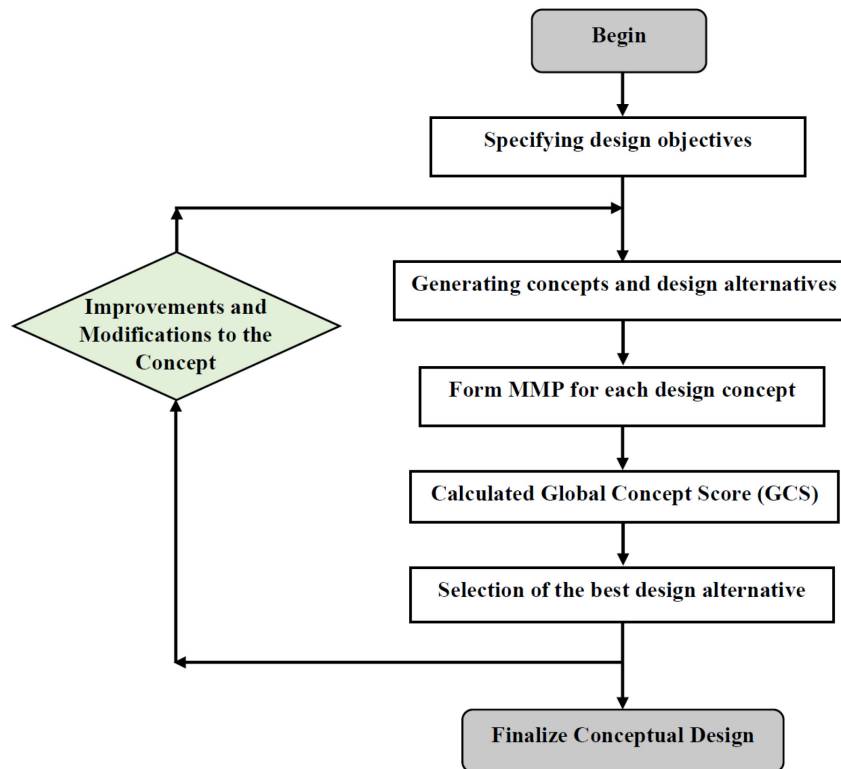


Figure 3-6: Conceptual Design of a Mechatronic System based on MMP and Global Concept Score (GCS)

### 3.5 Case Study: Design of a Vision-Guided Quadrotor Drone

Conceptual design is a crucial stage in a product design process. In order to find the best solution among a variety of possible configurations, it is less practical and efficient to search a complex design space in just one iteration. In conceptual design and based on different knowledge-bases involved, a complex design space is divided into several subspaces, which also correspond to conceptual alternatives. By performing a proper evaluation for all of these subspaces, the designer then is able to narrow down the search space to one or two of the subspaces.

Autonomous systems and robotic machineries have been increasingly employed in various industrial, urban and exploratory applications during the last decades. However, these types of systems are generally limited to operate in highly structured environments. Thus, integration of vision sensors with automatic systems and generally “visual servoing” systems helped solve this problem by producing non-contact and wide measurements of the working area for the machine [113]. As a case study of using mechatronic multi-criteria profile (MMP) for conceptual design of a mechatronic system, design of a Quadrotor drone along with a visual servoing system for tracking and following a moving target is presented here. As a mechatronic system, design of a Quadrotor drone can be considered as a non-trivial problem which involves a medium-level complexity and allows several alternatives in both structure and controller design. Figure 3-7 shows a schematic diagram of a Quadrotor utilizing a visual servoing system to track a target [114]. The integrated control system is also described in Figure 3-8. The objective here is to design a quadrotor with a visual servoing system which is capable of tracking and following a moving object  $x_k$  with the maximum velocity of 1 m/s, starting within 3 seconds after the object enters the vision system’s field of sight and also within the area of motion with dimensions of 3000mm×3000mm×1000mm.

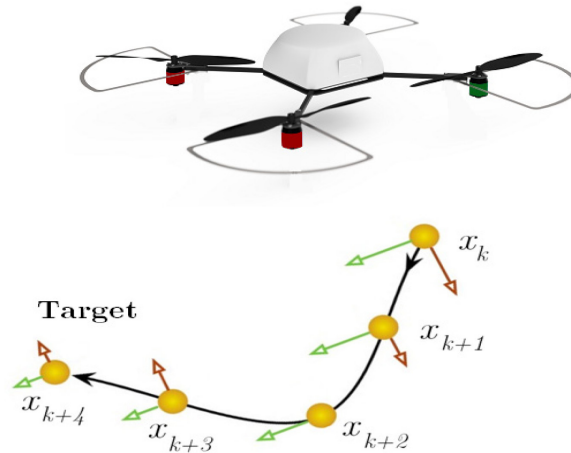


Figure 3-7: A Quadrotor drone in tracking and following mission using a visual servoing system.

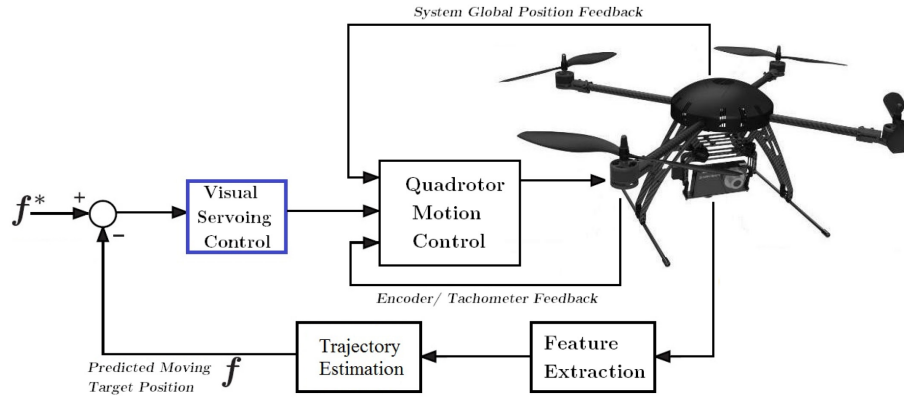


Figure 3-8: An integrated visual servo control for a Quadrotor system

Based on the defined objective(s), the concept selection and design should be performed upon deciding for the mechanical structure, actuators, position and velocity sensors, vision sensors, controllers, and battery as the most essential components of the system. After a careful identification of feasible subsystems and components by the designer, the generation of the design alternatives can be performed. The main responsibility of the decision-making task in conceptual design is to select between all possible alternatives and subsystems which better match the design objectives. Generation of design concepts and alternatives for a Quadrotor system is described in Figure 3-9. Based on the number of options for each subsystem (material, structure, actuator, battery, vision and position sensors, motion control and visual servoing system), we are able to generate 7,776 concepts but after a feasibility study and dependency modeling, just 972 concepts were considered as acceptable as some components are not compatible with others.

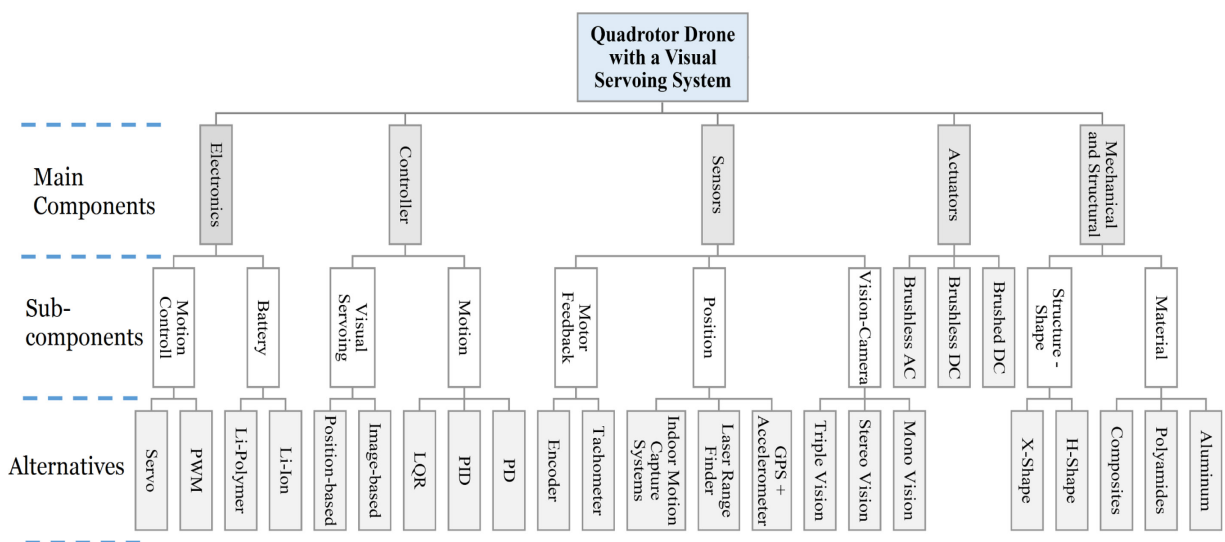


Figure 3-9: Parts and Subsystems for generation design concepts



In order to simplify the case study and based on feasibility in system integration, we have chosen four concepts to study the proposed design method. For example, a concept with three cameras should not use a position-based visual servoing controller. Based on the material used, the frame structure and subsystems selected for one specific concept, the total mass, required power, payload, maximum allowable inertia moment, force and bandwidth can be also easily estimated (Table 2). An approximation of the total cost can also be identified based on the components and manufacturing process. Table 3 briefly gives the results for the estimated values for proposed concepts.

Table 3-2: Design alternatives

	Concept 1	Concept 2	Concept 3	Concept 4
Frame Structure	X-shape	H-shape	X-shape	H-shape
Material	Aluminum	Aluminum	Polyamides	Polyamides
Motors	Brushed DC	Brushed DC	Brushless DC	Brushless AC
Motor Feedback	Encoder	Tachometer	Encoder	Tachometer
Visual Servo.	PBVS	PBVS	IBVS	IBVS
Camera Config.	Mono	Stereo	Stereo	Mono
Motion Control.	PID	LQR	PID	LQR
Position Sensor	GPS +Accel.	Motion capture	GPS +Accel.	GPS +Accel.
Battery	Li-ion	Li-Poly.	Li-ion	Li- Poly.

Table 3-3: Estimated design features for generated concepts

	Concept 1	Concept 2	Concept 3	Concept 4
Power (W)	450	500	350	400
Max Inertia Moment (kg.m <sup>2</sup> )	5E-3	5.2E-3	4E-3	4.5E-3
Bandwidth (Hz)	70	70	60	60
Payload (Kg)	0.5	0.5	0.6	0.6
Cost (unit)	0.8	1	0.7	0.7

### 3.5.1 MMP Assessment

#### 3.5.1.1 Machine Intelligence Quotient

In order to measure the machine intelligence quotient (MIQ) based on the proposed method in section 3.3.1, two ITG models for the quadrotor system with a position-based visual servoing (PBVS) and an image-based visual servoing (IBVS) are considered and depicted in Figure 3-10.

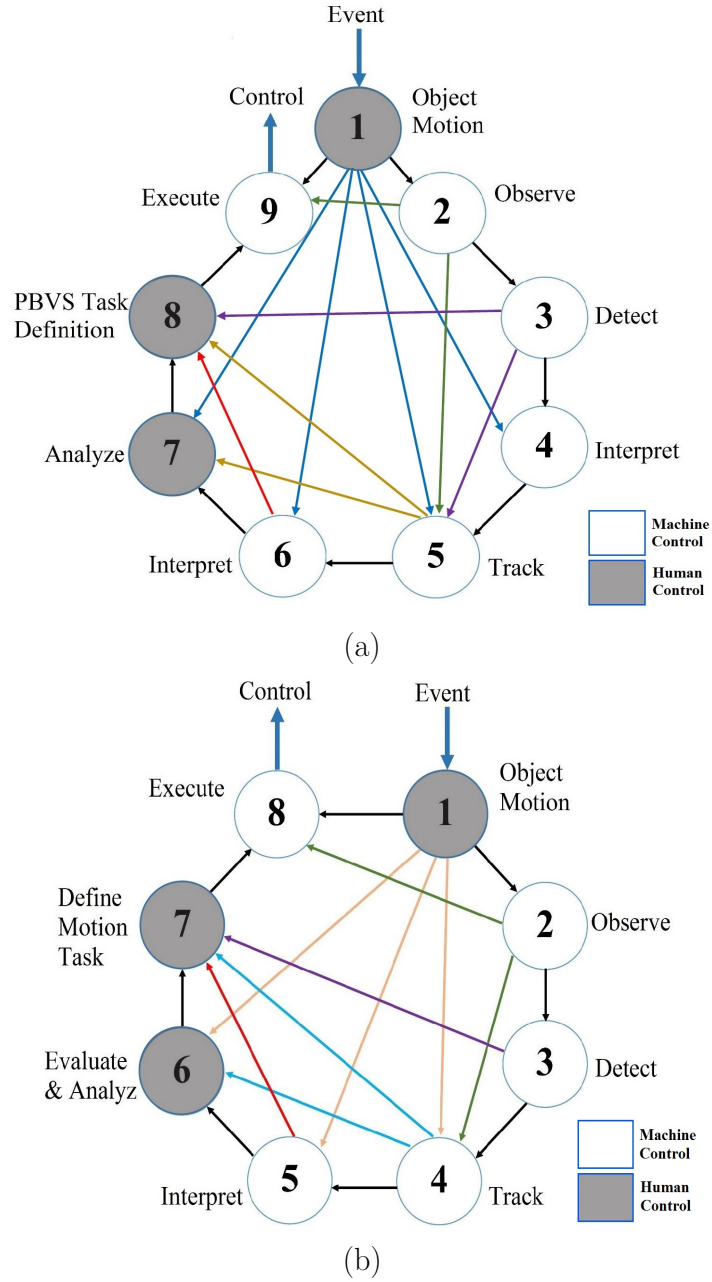


Figure 3-10: ITG model for (a) a position-based visual servoing (PBVS) scheme and (b) an image-based visual servoing (IBVS) scheme for a quadrotor system.

In order to measure the task intelligence costs, a counting agent was built in the computer simulation to measure the controllers' output data units per time (kb/hrs) and human interface input data per time for each task defined. Another unit was put in the simulations to count and accumulate data quantities (packets) transferred between subsystems, interface and controllers. The result would form the data transfer matrix,  $F$ . Task intelligence cost, data transfer quantity, and interface complexity for both cases are measured, scaled and listed in Table 3-4.

Table 3-4: Parameters required for assessing MIQ for two cases of PBVS and IBVS

PBVS	IBVS
$\tau_{pb} = \{\tau_1, \tau_2, \tau_3, \tau_4, \tau_5, \tau_6, \tau_7, \tau_8, \tau_9\}$ $= \{4, 6, 11, 10, 12, 10, 17, 10, 12\}$	$\tau_{pb} = \{\tau_1, \tau_2, \tau_3, \tau_4, \tau_5, \tau_6, \tau_7, \tau_8\}$ $= \{4, 6, 11, 12, 19, 18, 9, 12\}$
$F_{pb}$ $= \begin{bmatrix} 0 & 77 & 0 & 28 & 42 & 38 & 30 & 0 & 53 \\ 0 & 0 & 61 & 0 & 52 & 0 & 0 & 0 & 39 \\ 0 & 0 & 0 & 59 & 54 & 0 & 0 & 44 & 0 \\ 0 & 0 & 0 & 0 & 51 & 0 & 0 & 0 & 0 \\ 0 & 0 & 0 & 0 & 0 & 31 & 40 & 39 & 0 \\ 0 & 0 & 0 & 0 & 0 & 0 & 31 & 27 & 0 \\ 0 & 0 & 0 & 0 & 0 & 0 & 0 & 37 & 0 \\ 0 & 0 & 0 & 0 & 0 & 0 & 0 & 0 & 21 \\ 0 & 0 & 0 & 0 & 0 & 0 & 0 & 0 & 0 \end{bmatrix}$	$F_{ib}$ $= \begin{bmatrix} 0 & 77 & 0 & 42 & 38 & 32 & 0 & 53 \\ 0 & 0 & 61 & 52 & 0 & 0 & 0 & 37 \\ 0 & 0 & 0 & 59 & 0 & 0 & 47 & 0 \\ 0 & 0 & 0 & 0 & 53 & 39 & 34 & 0 \\ 0 & 0 & 0 & 0 & 0 & 43 & 40 & 0 \\ 0 & 0 & 0 & 0 & 0 & 0 & 40 & 0 \\ 0 & 0 & 0 & 0 & 0 & 0 & 0 & 34 \\ 0 & 0 & 0 & 0 & 0 & 0 & 0 & 0 \end{bmatrix}$
$c_{mh} = 0.07, c_{hm} = 0.08.$	$c_{mh} = 0.07, c_{hm} = 0.08.$
$A_{pb} = \begin{bmatrix} 0 & 1 & 0 \\ 1 & 0 & 0 \\ 1 & 0 & 0 \\ 1 & 0 & 0 \\ 1 & 0 & 0 \\ 1 & 0 & 0 \\ 0 & 1 & 0 \\ 0 & 1 & 0 \\ 1 & 0 & 0 \end{bmatrix}$	$A_{ib} = \begin{bmatrix} 0 & 1 & 0 \\ 1 & 0 & 0 \\ 1 & 0 & 0 \\ 1 & 0 & 0 \\ 1 & 0 & 0 \\ 0 & 1 & 0 \\ 0 & 1 & 0 \\ 1 & 0 & 0 \end{bmatrix}$

The MIQ for the case of using a PBVS approach can be calculated as follows through Equations (2.3 - 2.8).

$$\begin{aligned}
 CIQ &= \sum_{i=1}^n a_{i1}\tau_i + \sum_{i=1}^n a_{i2}\tau_i \\
 &= (\tau_2 + \tau_3 + \tau_4 + \tau_5 + \tau_6 + \tau_9) + (\tau_1 + \tau_7 + \tau_8) = 92
 \end{aligned} \tag{4.16}$$

$$\begin{aligned}
HIQ &= \left( \sum_{i=1}^n a_{i2} \tau_i \right) + \left( c_{mh} \sum_{i=1}^n \sum_{j=1}^n a_{i1} a_{j2} f_{ij} \right) \\
&\quad + \left( c_{hm} \sum_{i=1}^n \sum_{j=1}^n a_{i2} a_{j1} f_{ij} \right) \\
&= (\tau_1 + \tau_7 + \tau_8) + c_{mh}(f_{38} + f_{57} + f_{58} + f_{67} + f_{68}) \\
&\quad + c_{hm}(f_{12} + f_{14} + f_{15} + f_{16} + f_{17} + f_{19} + f_{89}) \\
&= 31 + (0.07)181 + (0.08)289 = 66.79.
\end{aligned} \tag{4.17}$$

$$MIQ_{pb} = CIQ_{pb} - HIQ_{pb} = 92 - 66.79 = 25.21. \tag{4.18}$$

The same procedure can be used to calculate the MIQ for the case of using an IBVS approach.

$$CIQ = \sum_{i=1}^n a_{i1} \tau_i + \sum_{i=1}^n a_{i2} \tau_i = (\tau_2 + \tau_3 + \tau_4 + \tau_5 + \tau_6) + (\tau_1 + \tau_6 + \tau_7) = 91 \tag{4.19}$$

$$\begin{aligned}
HIQ &= \left( \sum_{i=1}^n a_{i2} \tau_i \right) + \left( c_{mh} \sum_{i=1}^n \sum_{j=1}^n a_{i1} a_{j2} f_{ij} \right) + \left( c_{hm} \sum_{i=1}^n \sum_{j=1}^n a_{i2} a_{j1} f_{ij} \right) \\
&= (\tau_1 + \tau_6 + \tau_7) + c_{mh}(f_{46} + f_{56} + f_{37} + f_{47} + f_{57}) \\
&\quad + c_{hm}(f_{12} + f_{14} + f_{15} + f_{16} + f_{18} + f_{78}) \\
&= 25 + (0.07)203 + (0.08)276 = 61.29.
\end{aligned} \tag{4.20}$$

$$MIQ_{pb} = CIQ_{pb} - HIQ_{pb} = 91 - 61.29 = 29.71. \tag{4.21}$$

### 3.5.1.2 Reliability Score

The reliability scores for all the presented design alternatives can be calculated using Equation (3.9) and the components listed in Figure 3-9 and Table 3-2. As stated before, in the presented case study and in order to avoid complexity in assessing MMP for all the design concepts, the dynamic effects for reliability assessment has not been taken into account. The reliability of each concept has been determined based on the failure probability of their components. Although there is not a solid reference to address each component's failure rate, we managed to extract a number of values for sensors and actuators from various resources i.e. technical manuals, reports and experiment documentations [115-117] (Table 3-5). The failure probabilities were considered for a system under 100,000 hours of work. Based on information listed in Table 5, the reliability score for each concept can be calculated as shown in Table 3-6.

Table 3-5: Mean time to failure (Hrs.) for the components used in the generated concepts

Components	Motors	Motor Feedback	Position Sensor	Battery
Concept 1	Brushed	Encoder	GPS + Accel.	Li-ion
	3810	8230	2920	10540
Concept 2	Brushed	Tachometer	Motion Capture	Li-Poly
	3810	8900	1750	11780
Concept 3	Brushless	Encoder	GPS + Accel.	Li-ion
	5120	8230	2920	10540
Concept 4	Brushless	Tachometer	GPS + Accel.	Li-Poly
	5120	8900	2920	11780

Table 3-6: Reliability scores for generated concepts

	Concept 1	Concept 2	Concept 3	Concept 4
Reliability Score	RS <sub>1</sub> =0.86	RS <sub>2</sub> =0.91	RS <sub>3</sub> =0.93	RS <sub>4</sub> =1

### 3.5.1.3 Complexity Value

Based on the method proposed in Section 3.3.3, complexity values for all the design concepts can be determined. The values for each members of complexity vector and the final complexity score are shown in Table 3-7, where  $\Phi_i$  are the complexity scores and  $\bar{\Phi}_i$  are the normalized values for which  $0 \leq \bar{\Phi}_i \leq 1$  and for a concept with minimum complexity,  $\bar{\Phi}_i = 1$ . Furthermore  $w_j$ , are the weights associated to the complexity components, and considered to be equal to 0.17 for  $i = 1, \dots, 5$  and 0.15 for  $i = 6$ .

Table 3-7: Complexity values for design alternatives

Concept 1	Concept 2
$\Phi_1 = [24 \ 12 \ 5 \ 5 \ 3 \ 0.16]^T$	$\Phi_2 = [32 \ 16 \ 5 \ 6 \ 4 \ 0.16]^T$
$\bar{\Phi}_1 = [1 \ 1 \ 1 \ 1 \ 1 \ 0]^T$	$\Phi_2 = [0.75 \ 0.75 \ 0.83 \ 0.75 \ 0]^T$
$CX_1 = 0.850$	$CX_2 = 0.693$
Concept 3	Concept 4
$\Phi_3 = [25 \ 13 \ 5 \ 5 \ 4 \ 0]^T$	$\Phi_4 = [25 \ 14 \ 5 \ 6 \ 3 \ 0]^T$
$\bar{\Phi}_3 = [0.96 \ 0.92 \ 1 \ 1 \ 0.75 \ 1]^T$	$\bar{\Phi}_4 = [0.96 \ 0.86 \ 1 \ 0.83 \ 0.75 \ 1]^T$
$CX_3 = 0.937$	$CX_4 = 0.898$

### 3.5.1.4 Flexibility Value

The final results for flexibility assessment based on the proposed method in Section 3.3.4 are presented in Table 3-8, where  $\Psi_i$  are the flexibility scores and  $\bar{\Psi}_i$  are the normalized values which  $0 \leq \bar{\Psi}_i \leq 1$ .  $\rho_i = [0.3, 0.2, 0.1, 0.1, 0.3]$  are the weights associated to the flexibility components to assess the final flexibility score.  $\Psi_i$  are calculated based on the number of alternative component designs, the number of customization options for components, the number of choices for system architecture, user interface and also for control algorithms.

Table 3-8: Flexibility values for design alternatives

Concept 1	Concept 2
$\Psi_1 = [12 \ 18 \ 3 \ 4 \ 2]^T$	$\Psi_2 = [17 \ 18 \ 2 \ 4 \ 2]^T$
$\bar{\Psi}_1 = [0.705 \ 1 \ 1 \ 1 \ 1]^T$	$\bar{\Psi}_2 = [1 \ 1 \ 0.667 \ 1 \ 1]^T$
$FX_1 = 0.911$	$FX_2 = 0.967$
Concept 3	Concept 4
$\Psi_3 = [12 \ 18 \ 3 \ 4 \ 2]^T$	$\Psi_4 = [14 \ 15 \ 2 \ 4 \ 2]^T$
$\bar{\Psi}_3 = [0.705 \ 1 \ 1 \ 1 \ 1]^T$	$\bar{\Psi}_4 = [0.823 \ 0.833 \ 0.667 \ 1 \ 1]^T$
$FX_3 = 0.911$	$FX_4 = 0.880$

### 3.5.1.5 Overall Cost

According to Equation (3.15) and considering a set of standard and commonly used components, the cost factor for each concept can be calculated as shown in Table 3-9. For a concept with minimum total cost we have  $CT = 1$ .

Table 3-9: Cost factors for generated concepts

Concept 1	Concept 2	Concept 3	Concept 4
$CT_1 = 1$	$CT_2 = 0.78$	$CT_3 = 0.94$	$CT_4 = 0.91$

## 3.5.2 Aggregation of Criteria and Global Concept Scores

By taking into account the five design criteria as elements of MMP, one can conclude that  $2^5=32$  fuzzy measures should be specified to be used in Choquet and Sugeno aggregation functions. Equation (3.20) identifies two of these measures ( $\mu_\phi = 0$ ,  $\mu_{12345} = 1$ .) which leaves 30 measures to be specified. In the present case study, the fuzzy measures were obtained in an intuitive manner by the authors and a group of 30 researchers (all specialized in system design and mechatronics) through a questionnaire. This questionnaire collects the following information from various design point of views;

- The degree of importance for each of the mentioned 5 criteria in designing a good mechatronic product (i.e.  $\mu_i$ ,  $1 \leq i \leq 5$ ).
- The degree of correlation between each pair of criteria or the effect of increasing criterion  $i$  on criterion  $j$  (Table 3-10), i.e.  $\gamma_{ij}$ ,  $1 \leq i, j \leq 5$ , which specifies the fuzzy measures as follows;

$$\mu_{ij} = \mu_i + \mu_j - \gamma_{ij} \quad (4.22)$$

$$\mu_{ijk\dots} = \mu_i + \mu_j + \mu_k + \dots - (\max(|\gamma_{ij}|, 1 \leq i, j \leq 5) \cdot \text{sign}(\gamma_{ij})) \quad (4.23)$$

Table 3-10: Criteria interactions and the correlation measure

Interactions	Correlation Measure
Positive Correlation	$\gamma_{ij} > 0$
Negative Correlation	$\gamma_{ij} < 0$
No Correlation	$\gamma_{ij} = 0$

The starting point of the values could be first obtained by comparing the possible scenarios to what was found in literature [44, 84, 87, 92, 96]. The specified fuzzy measures used in the present case study are shown in Table 3-11.

Table 3-11: 30 fuzzy measures for the case study of conceptual design of a Quadrotor drone with a visual servoing system

$\mu_1 = 0.23$	$\mu_{12} = 0.45$	$\mu_{13} = 0.47$	$\mu_{14} = 0.34$	$\mu_{15} = 0.51$
$\mu_{123} = 0.61$	$\mu_2 = 0.29$	$\mu_{23} = 0.52$	$\mu_{24} = 0.42$	$\mu_{25} = 0.56$
$\mu_{124} = 0.60$	$\mu_{135} = 0.69$	$\mu_3 = 0.17$	$\mu_{34} = 0.35$	$\mu_{35} = 0.33$
$\mu_{125} = 0.67$	$\mu_{145} = 0.67$	$\mu_{245} = 0.73$	$\mu_4 = 0.16$	$\mu_{45} = 0.41$
$\mu_{134} = 0.63$	$\mu_{234} = 0.68$	$\mu_{345} = 0.49$	$\mu_{235} = 0.62$	$\mu_5 = 0.22$
$\mu_{1234} = 0.77$	$\mu_{1235} = 0.84$	$\mu_{1345} = 0.84$	$\mu_{2345} = 0.78$	$\mu_{1245} = 0.82$

Based on what was suggested for the structure of the fuzzy integral-based neural network (Figure 3-6), 56 weights have been identified (instead of  $2^{14}$  measures which corresponds to a case which all criteria and sub-criteria are considered in the same level and form a total of 14 criteria) and incorporated for the aggregation of criteria. Table 3-13 shows the results for the assessed MMP elements and global concept scores related to Choquet Sugeno and Neural network aggregations ( $GCS_C$ ,  $GCS_S$ ,  $GCS_{NN}$ ) for each generated concept and design alternatives for a Quadrotor system.

Table 3-12: MMP elements and global concept scores (GCS) for design alternatives

MMP Criterion	Concept 1	Concept 2	Concept 3	Concept 4
MIQ	0.84	0.84	1	1
RS	0.86	0.91	0.93	1
CX	0.85	0.69	0.93	0.89
FX	0.91	0.96	0.91	0.88
CT	1	0.78	0.94	0.91
<b>GCS<sub>C</sub></b>	<b>0.89</b>	<b>0.83</b>	<b>0.96</b>	<b>0.94</b>
<b>GCS<sub>S</sub></b>	<b>0.84</b>	<b>0.78</b>	<b>0.91</b>	<b>0.91</b>
<b>GCS<sub>NN</sub></b>	<b>0.87</b>	<b>0.82</b>	<b>0.93</b>	<b>0.92</b>

### 3.5.3 Choosing the Elite Concept and Comparison of Results

Based on the values indicated in Table 3-13 for global concept scores (GSC), one can conclude that based on a Choquet integral aggregator and also a neural network-based aggregator, the best selected concept corresponds to the third design alternative in which a stereo vision is used and the visual servoing scheme is an Image-based system (IBVS) with a PID controller. In this concept, Polyamide is selected as the structure material and an X-shape chassis along with brushless DC motors and encoders is used. The navigation system is based on a GPS and the energy source would be a Lithium-ion battery set. On the other hand, the Sugeno aggregator decides that the fourth concept is equally efficient for designing a Quadrotor drone system. In the fourth concept a monocular vision system is used and the visual servoing scheme is also an Image-based system (IBVS) with a LQR controller (Linear Quadratic Regulator). For the structure, an H-shape frame is selected and polyamide is chosen to be the main material for the chassis. Since brushless AC motors are suitable in this concept an inverter is also needed and the velocity of the shafts are determined using tachometers.

For the navigation, the same GPS and accelerometers are used and the energy source would be a Lithium-Polymer battery set. Based on the selected elements and subsystems listed in Table 3-2, and in order to validate the results for global concept score for each aggregation function and consequently the design decisions, a computer simulation of a visual servoing system on a Quadrotor drone has been performed. The models have been built for concept 3 and concept 4 as the best concepts with regards to their global concept scores. The physical parameters of the models were taken into account based on information from Table 3-3. Besides the actuator, sensor



and battery types, the difference between the selected concepts mostly concerns the camera configuration (Stereo vs. Mono) and motion controllers (PID vs. LQR).

Figures (3-11)-(3-13) show the simulation results for a visual servoing system designed based on concepts no.3 and no.4. The servoing task consists of coinciding four image feature to four desired predefined points in the image plane. The initial and desired configuration of the image features for each test are given in Table 3-14.

Table 3-13: Initial and desired location of feature points in pixel for Right and Left images

Features		Point 1 (x y)		Point 2 (x y)		Point 3 (x y)		Point 4 (x y)	
Initial Points	IR	279	726	279	864	415	853	415	719
	IL	281	712	281	851	415	839	415	705
Final Points	DR	312	492	312	892	712	892	712	492
	DL	312	452	312	852	712	852	712	452

As shown in Figure 3-12, the system designed based on concept 3 shows a relatively better performance than the one designed based on concept 4. In terms of feature trajectories, concept 3 has less oscillation, overshoot and unnecessary motion than concept 4 (Figure 3-12 b, c, d) and the system has a better convergence time (Figure 3-14 a, b), and with regards to the motion, the overall frame velocity components for the Quadrotor frame start at relatively smaller values (Figure 3-13 a, b) which effects the system reliability and total energy consumption. These results indicate that  $GCS_C$  and  $GCS_{NN}$  have performed a better job than  $GCS_S$  in suggesting the best conceptual design. Choquet integral as a nonlinear fuzzy integral is an effective way for decision-making in the presence of interacting criteria. The overall importance of a criterion and the interaction indices are carefully determined using the Shapely value (Equations 3.23-3.24). On the other hand, the Sugeno fuzzy integral, more or less performs as a kind of a weighted median. Therefore, it can be inferred that Sugeno integral produces a very conservative value for the global concept score for each design. Although, due to the consideration of weight of importance for different sets of criteria, this aggregation function can also be useful for decisions under uncertainty as well as for multi-criteria design problems. Due to the iterative nature and learning process in the neural network-based aggregation method, more reliable and precise values are achieved for the global concept scores. In a more complex design case where more feasible components and subsystems are involved, the elite set of the generated concepts includes larger numbers of design alternatives and the precision of the aggregation function comes in use to choose one final concept. More

importantly, in the neural network-based aggregation, not only the interactions between the main criteria are considered, but also the interactions between a specific sub-criterion of a criteria with another sub-criterion of a different criteria is considered and measured. This feature vastly increases the reliability of the aggregation results.

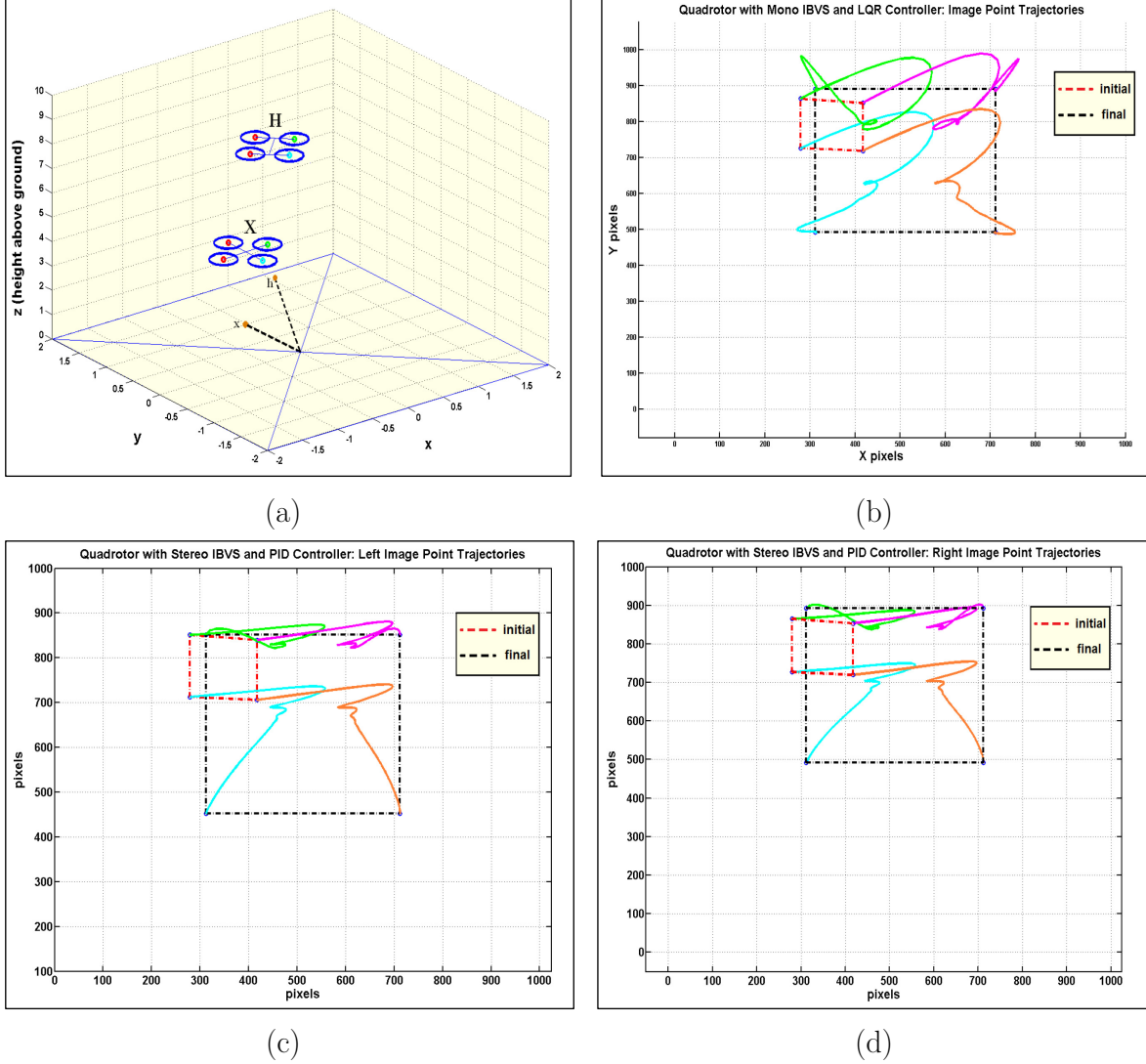


Figure 3-11: (a) A simulation model of a Quadrotor drone with a visual servoing system. Image feature trajectories in (b) concept 4: Monocular IBVS with LQR controller, (c, d) concept 3: Stereo IBVS with PID controller.

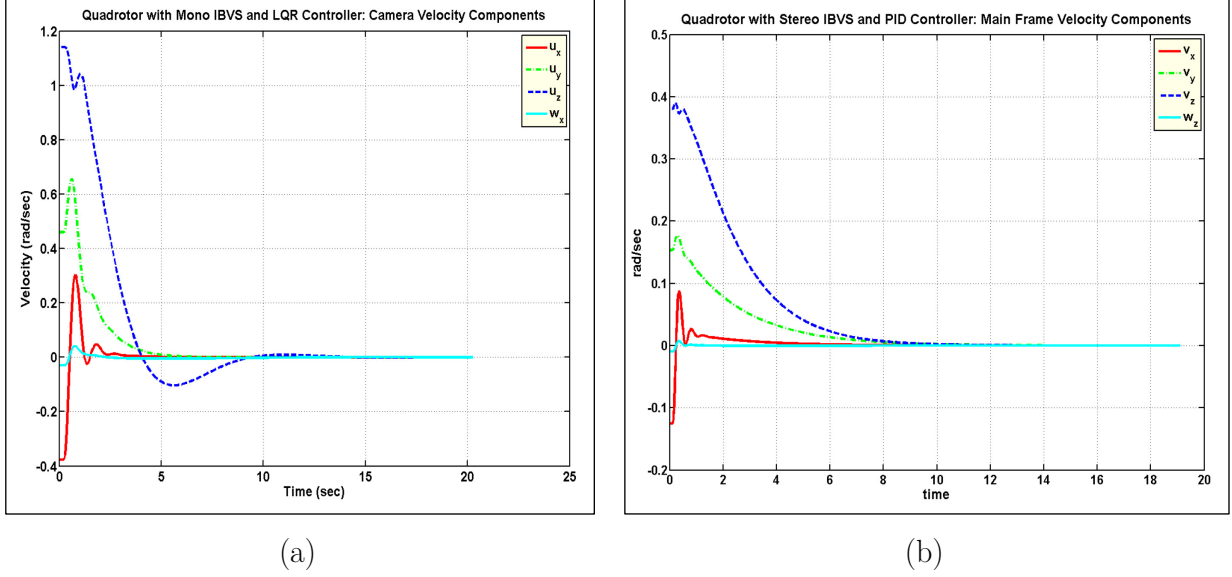


Figure 3-12: Camera frame velocity in systems based on concept 4 (a) and concept 3 (b).

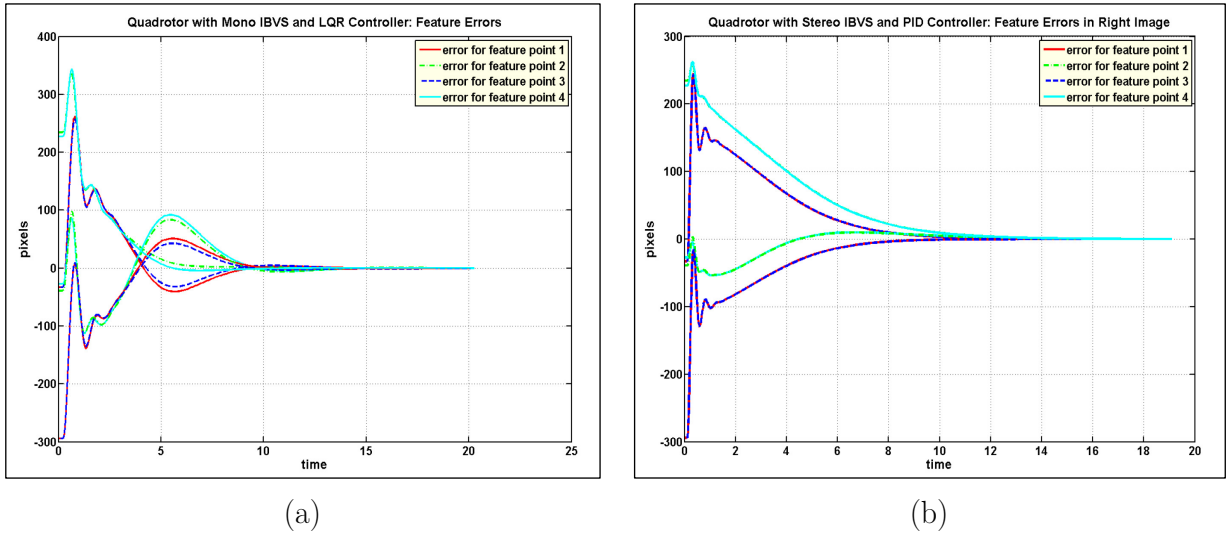


Figure 3-13: Image feature errors in systems based on concept 4 (a) and concept 3 (b).

### 3.6 Discussion and Conclusion

In this paper, a new multicriteria profile (MMP) has been introduced for concept evaluation in design of mechatronic systems and the assessment procedure has been thoroughly discussed. The MMP consists of five main design criteria such as intelligence, reliability, complexity, flexibility and cost and can be embedded in an automated design routine. Based on the assessed MMP for each concept and using various aggregation techniques, a global concept score (GCS) has been calculated to ease the procedure of concept evaluation, selection and modification. For the

aggregation of criteria, three functions have been introduced based on Choquet integral, Sugeno integral and a fuzzy integral-based neural network. Moreover, the proposed method has been applied to a case study of designing a Quadrotor drone system capable of tracking and following an object using a visual servoing system. At the end, the two selected concepts based on different aggregation functions have been tested and compared using a computer simulation of a visual servoing task. Besides the introduction of MMP and the methods of aggregation, the main contribution of this paper can be stated as providing a systematic approach to support generating and finding an optimal conceptual design of a mechatronic system in the presence of large number of interacting criteria. This approach can be used in an automated software platform along with a collaboration between the designers from various disciplines based on a guide line that the presented methodology has provided.

One of the limitation of the proposed approach is that there is a large number of fuzzy measures and also parameters used in criteria assessment. However, the presented approach can be used to build upon an interactive agent-enabled expert system (e.g. web-based) to gradually learn and optimize the measures for various occasions by clustering and analyzing the input data gathered for various design cases. This way, the precision of the fuzzy measures and consequently the multi-criteria design evaluation, can be improved by incorporating a wider and more correlated range of designers and industrial specialists. Consequently, after a period of time, the users will not be required to provide all the measures for each design case. Just providing their customization parameters and preferences would certainly suffice. Further studies should be also carried out towards the improvement of the methods of assessment for each criterion and sub-criterion and also validation of these methods specially in the cases of design complexity and flexibility.

## CHAPTER 4 ARTICLE 2: A FUZZY-BASED FRAMEWORK TO SUPPORT CONCURRENT AND MULTICRITERIA DESIGN OF MECHATRONIC SYSTEMS

Abolfazl Mohebbi, Sofiane Achiche and Luc Baron

Submitted to *Elsevier Journal of Engineering Applications of Artificial Intelligence*, Feb. 2017

### 4.1 Abstract

Designing a mechatronic system is a complex task since it deals with a high number of system components with multi-disciplinary nature in the presence of interacting design objectives. Currently, sequential design is widely used by designers in industries which deals with different domains and their corresponding design objectives separately leading to a functional but not necessarily an optimal result. Consequently, the need for a systematic and multi-objective design methodology arises. A new conceptual design approach based on a multi-criteria profile for mechatronic systems, has been previously presented by the authors which uses a series of nonlinear fuzzy-based aggregation functions to facilitate fitting the intuitive requirements for decision-making in the presence of interacting criteria. Choquet fuzzy integrals are one of the most expressive and reliable preference models used in decision theory for multicriteria decision making. They perform a weighted aggregation by the means of fuzzy measures assigning a weight to any coalition of criteria. This enables the designers to model importance and also interactions among criteria thus covering an important range of possible decision behaviours. However, specification of the fuzzy measures involves many parameters and is very difficult when only relying on designer's intuition. In this paper, we discuss four different methods of fuzzy measure identification tailored for a mechatronic design process and exemplified by a case study of conceptual design of a vision-guided quadrotor drone. The results obtained from each method are discussed at the end.

### 4.2 Introduction

Multidisciplinary systems that include synergetic integration of mechanical, electrical, electronic and software components, are known as Mechatronic Systems [2]. Because of the high number of the constituent components, the multi-physical aspect of the subsystems and the couplings between the different engineering disciplines involved, the design of mechatronic systems

can be rather complex and it requires an integrated and concurrent approach to obtain optimal solutions [118, 119]. The current design support efforts in industry general focus on the final phases of the design – the detailed design to improve the performance and meet design requirements [120]. Moreover, the traditional design approach is a sequential process where subsystems are designed separately in their separate domains neglecting their dynamical interactions with each other.

In a similar manner to other systems, design of mechatronic devices includes three major phases: conceptual design, detailed design, and prototyping and improvements. The present paper contributes towards a better concept evaluation process during the conceptual design phase. The goal of concept evaluation is to compare the generated concepts based on the design requirements and to select the best alternative for further device and then product development. Tomiyama et al. [121] presented a comprehensive description of the design theory and methodology (DTM) and an evaluation of its application in practical scenarios. Ullman [122] has analysed four concept evaluation methods. All of these methods provide qualitative frameworks to evaluate the candidate solutions. The results of these comparisons highly depend on the experience of the design engineer. Novice designers would make decisions easier if quantitative evaluation methods are available for them. To this effect, an evaluation index can be used to rank the generated feasible solutions and therefor more easily choose between design alternatives. Moulianitis et al. [59] introduced a mechatronic index that characterizes the mechatronic designs by their control performance, complexity and flexibility. The overall evaluation was formulated based on the averaging operators and weight factors were manually applied to highlight the importance of each criterion. They did not, however, consider the interactions between design criteria. Behbahani et al. [123] proposed a framework for design of mechatronic systems in which the performance requirements were represented by a mechatronic design quotient (MDQ). Correlations between design criteria have been taken into account by using fuzzy functions. MDQ was implemented in a number of case studies [124], and was claimed to be efficient; however, the assessment of criteria was very qualitative and no systematic measurement approach has been presented nor implemented, which puts the burden on the engineering designers.

Mohebhi et al. [77] presented a new approach based on their newly introduced multi-criteria mechatronic profile (MMP) for the conceptual design stage. The MMP included five main elements of machine intelligence, reliability, flexibility, complexity and cost, while each main criterion has a number of sub-criteria. In order to facilitate fitting the intuitive requirements for decision-making in the presence of interacting criteria, three different criteria aggregation methods were proposed

and inspected using a case study of designing a vision-guided quadrotor drone and also a robotic visual servoing system. These methods benefit from three different aggregation techniques namely: Choquet integral, Sugeno integral [119] and a fuzzy-based neural network [125]. These techniques proved to be more precise and reliable in multi-criteria design problems where interaction between the objectives cannot, and should not, be overlooked. The Choquet integral is one of the most expressive preference models used in decision theory. It performs a weighted aggregation of criteria using a capacity function assigning a weight to any coalition of criteria. This enables the expression of both positive and negative interactions and covering an important range of possible decision dilemmas, which is generally ignored in other multicriteria decision making (MCDM) methods [102, 126]. A 2-additive Choquet integral has been used in [119], which only uses relatively simple quadratic complexity and enables the modeling of interaction between pairs of criteria.

Despite the modelling capabilities, the specification of the fuzzy measures has been always a place for various challenges which makes the practical use of such aggregation techniques difficult. While the definition of a simple weighted sum operator with  $n$  criteria requires  $n - 1$  parameters, the definition of the Choquet integral with  $n$  criteria requires setting of  $2^n - 2$  capacities (measures), which can become quickly unmanageable even for low values of  $n$  and even for an expert who can assess the coefficients on the basis of semantical considerations. Most of previous works on capacity specification for Choquet integral-based decision analysis, consider a static preference database as input (learning set), and focuses on the determination of a set of measures that best fits the available preferences [127]. For example, a quadratic error between Choquet values and target utility values prescribed by the decision maker (DM) can be minimized on a sample of reference alternatives [128]. Generally, questions are asked to the decision maker and the information obtained is represented as linear constraints over the set of parameters. An optimization problem is then solved in order to find a set of parameters which minimizes the error according to the information given by the decision maker [129]. In [130] it is supposed that an expert is able to tell the relative importance of criteria and identify the type of interaction between them, if any. These relations can be expressed as a partial ranking of the alternatives on a global basis; partial ranking of the criteria, partial ranking of interaction indices and also the type of interaction between some pairs of criteria. These approaches differ with respect to the optimization objective function and the preferential information they require as input. Two major problems of the aforementioned approaches are the lack of transparency on how the measures are made, the lack of robustness and the lack of reproducibility [131]. Another alternative seems to be appropriate

when using an optimization algorithm alongside a minimal intuitive determination by the decision maker. These approaches take advantage of the lattice structure of the coefficients [132].

While most of these methods are developed within a pure mathematical framework, some others were reflected in a limited number of applications such as computer vision, pattern recognition, software engineering and website design. To our knowledge, none of the developed approaches are applied to a multidisciplinary engineering design problem with multiple design objectives. In this paper, we will explore various approaches of fuzzy measure identification applied to a conceptual design problem for a mechatronic system. A Choquet integral aggregation was previously used by the authors for multicriteria design evaluation in [119] where the measures were determined intuitively by the authors and a group of 30 researchers (all specialized in system design and mechatronics) through a questionnaire. The presented paper is organized as follows: Section 4.3 gives a brief overview to the conceptual design of mechatronic systems and the previously developed methodology based on Mechatronic Multicriteria Profile (MMP) as a design evaluation index. A fuzzy decision support and the Choquet aggregation technique are described in Section 4.4 alongside the necessary definitions on fuzzy measures and integrals, illustrated with some properties. Section 4.5 describes four different algorithms for elicitation and identification of fuzzy measures with their philosophy, while Section 4.6 reports the results of a case study to incorporate and compare all the design evaluation attempts. Finally, Section 4.7 discusses the concluding remarks of the presented research.

## **4.3 Conceptual Design of Mechatronic Systems**

### **4.3.1 Conceptual Design**

Conceptual design is an early stage of design in which the designers generally choose amongst the concepts that fulfil the design requirements and then decide how to interconnect these concepts into system architectures. Usually, at the beginning of every conceptual design process, a large number of candidate concepts exist for a given design problem. Consequently, a considerable amount of uncertainty arises about which of these solutions will be best fitted to the given requirements and objectives. This is more evident when the designer must meet highly dynamic and interconnected design requirements. It is crucial to abandon the traditional end-to-end and sequential design process and to consider all aspects of a design problem concurrently. This is particularly necessary for multi-disciplinary systems such as mechatronic systems where



mechanical, control, electronic and software components interact and a high-quality design cannot be achieved without simultaneously considering all domains [39].

### 4.3.2 Concept Evaluation

All useful. To achieve more optimal mechatronics designs, one requires a systematic evaluation approach to choose amongst the candidate design solutions. This evaluation includes both comparison and decision making [133]. In other words, decision-making is achieved by selecting the “best” alternatives by comparison. It is crucial to take into account both correlation between system requirements and also interactions between the multidisciplinary subsystems. The candidate solutions are generated based on a series of design specifications, candidate solutions are generated. The goal of concept evaluation is to compare the generated concepts against the requirements and to select the best one for the detailed design and optimization stages. This process is illustrated in Figure 4-1.

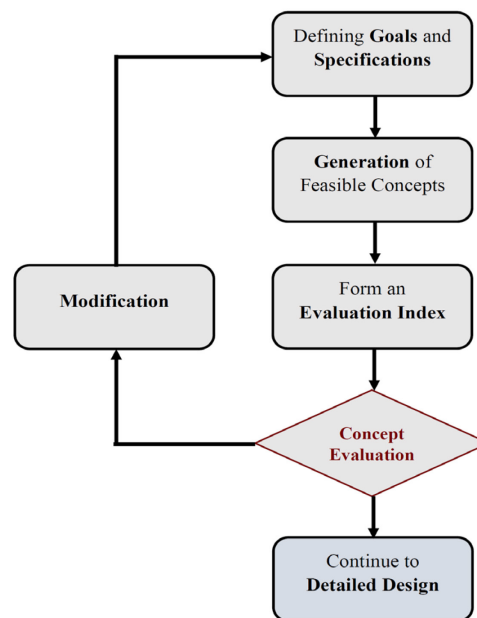


Figure 4-1: Process of concept evaluation in design

### 4.3.3 Mechatronic Multicriteria Profile (MMP)

One important challenge faced during conceptual design is to find the right set of criteria to concurrently evaluate and synthesize the designs. Generally, making design decisions with multiple criteria is often performed using a Pareto approach. Without the identification of the system performance parameters and the full understanding of their co-influences, it is unrealistic to expect achieving optimal solutions. In order to form an integrated and systematic evaluation approach,

the most important criteria and their related sub-criteria have been quantified by the authors in [77] to form an index vector of five normalized elements called Mechatronic Multicriteria Profile (MMP) as follows:

$$MMP = [MIQ, RS, CX, FX, CT]^T \quad (5.1)$$

where MIQ is the machine intelligence quotient, RS is the reliability score, CX is the design complexity, FX is the flexibility and CT is cost of manufacture and production. Figure 4-2 describes the MMP with all corresponding sub-criteria. MMP will be used in this paper. We also define  $m_i$  as the criteria values for the elements of MMP sorted in ascending order such that  $m_1 \leq m_2 \leq \dots \leq m_n$  and  $0 \leq m_i \leq 1$ . After determination and normalization of each sub-criterion, and by using a linear summation of weighted factors, the value of each main criterion will be assessed as follows:

$$m_i = \sum_{j=1}^n w_j \bar{\phi}_i \quad (5.2)$$

where  $\bar{\phi}_i$  is the calculated value for each criterion,  $n$  is the total number of sub-criteria, and  $w_j$  are the assigned-by-designer weights associated to each sub-criterion.

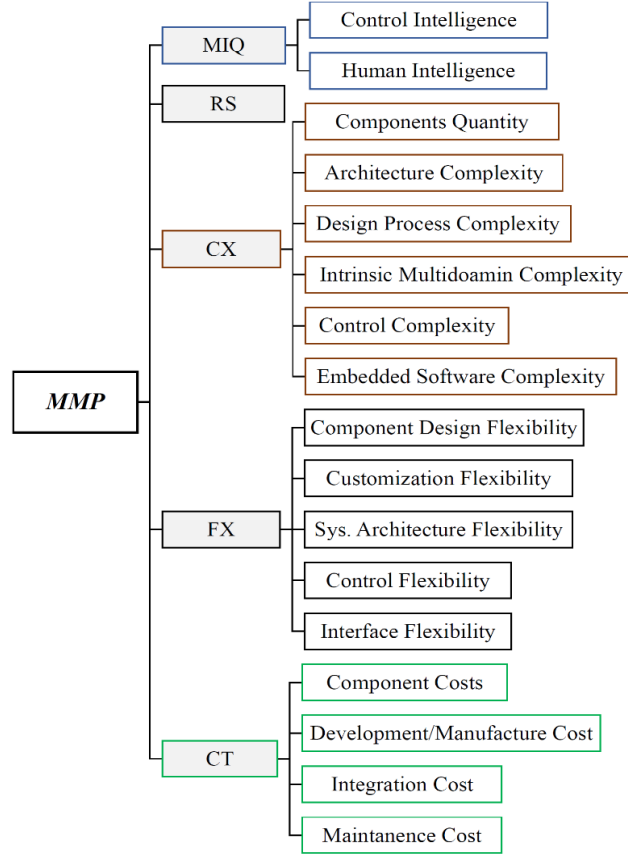


Figure 4-2: Mechatronic Multicriteria Profile (MMP) and all sub-criteria

## 4.4 Fuzzy Decision Support and Aggregation

### 4.4.1 Criteria Aggregation

The problem of aggregating criteria functions to form overall decision functions is of considerable importance in many disciplines. A primary factor in the determination of the structure of such aggregation functions is the relationship between the criteria involved. Choquet integral is a nonlinear fuzzy integral that has been successfully used for the aggregation of criteria in the presence of interactions. For mechatronics design and after quantifying all MMP elements and corresponding subsets, an effective comparison algorithm is needed. A global concept score (GCS) as a multi-criteria evaluation index can be defined in order to enable the designers to compare between the feasible generated design concepts. GCS can be expressed as follows:

$$GCS = S(m_1^*, m_2^*, \dots, m_n^*) \cdot \prod_{i=1}^m g(m_i), \quad (5.3)$$

where  $m_i^*$  are the normalized criteria values,  $S(\cdot)$  represents an aggregation function which, in this paper, is the Choquet integral, and  $g(m_i)$  indicates whether a design constraint has been met (binary value).

### 4.4.2 Fuzzy Measures and Choquet Integrals

Choquet integral provides a weighting factor for each criterion, and also for each subset of criteria. Using Choquet integrals is a very effective way to measure an expected utility when dealing with uncertainty, which is the case in design in general and mechatronics design in particular. Using this technique and by defining a weighting factor for each subset of criteria, the interactions between multiple objectives and criteria can be easily taken into account. To help a better understanding of the proposed solution, we will state some definitions in the following paragraphs.

**Definition 1:** The weighting factor of a subset of criteria is represented by a fuzzy measure on the universe  $N$  satisfying the following fuzzy measure ( $\mu$ ) equations:

$$\mu(\phi) = 0, \quad \mu(N) = 1. \quad (5.4)$$

$$A \subseteq B \subseteq N \rightarrow \mu(A) \leq \mu(B). \quad (5.5)$$

where  $A$  and  $B$  represent the fuzzy sets [134]. Eq. 4 represents the boundary conditions for fuzzy measures while Eq. 5 is also called the monotonicity property of fuzzy measures.

**Definition 2:** Let  $\mu$  be a fuzzy measure on vector  $X$ , whose  $n$  elements are denoted by  $x_1, x_2, \dots, x_n$ . The discrete Choquet integral of a function  $f: X \rightarrow \mathbb{R}^+$  with respect to  $\mu$  is defined by:

$$C_\mu(f) = \sum_{i=1}^n (f(x_i) - f(x_{i-1})) \mu(A_{(i)}), \quad (5.6)$$

where indices have been permuted so that  $0 \leq f(x_1) \leq f(x_2) \leq \dots \leq f(x_n)$  and  $A_{(i)} = \{(i), \dots, (n)\}$ , and  $A_{(n+1)} = \emptyset$  while  $f(x_0) = 0$ . Figure 4-3 gives a graphical illustration of Choquet integral while Table 4-1 shows the most common semantic interactions among criteria pairs and the corresponding fuzzy measures.

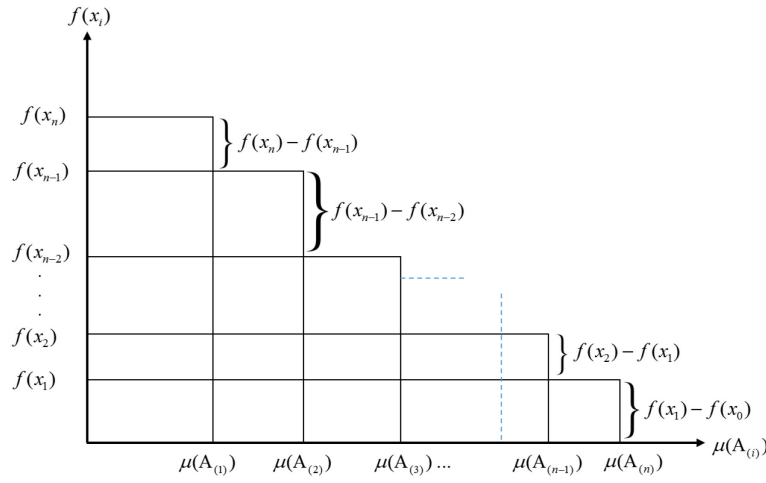


Figure 4-3: Graphical illustration of Choquet integral

Table 4-1: Fuzzy Interactions and Measurements

#	Description of Interaction	Fuzzy Measurement
I	Negative Correlation	$\mu(i, j) > \mu(i) + \mu(j)$
II	Positive Correlation	$\mu(i, j) < \mu(i) + \mu(j)$
III	Substitution	$\mu(T) < \begin{cases} \mu(T \cup i) \\ \mu(T \cup j) \end{cases} = \mu(T \cup i \cup j)$
IV	Veto Effect	$\mu(T) \approx 0$ if $T \subset Y, i \notin T$
V	Pass Effect	$\mu(T) \approx 1$ if $T \subset Y, i \in T$
VI	Complementarity	$\mu(T) = \begin{cases} \mu(T \cup i) \\ \mu(T \cup j) \end{cases} < \mu(T \cup i \cup j)$

A lattice representation can be used for describing fuzzy measures in the case of a finite number of criteria. Figure 4-4 gives an illustration when  $n = 4$ . Please note that for simplicity we use  $\mu_{ij}$  instead of  $\mu(\{i, j\})$ .

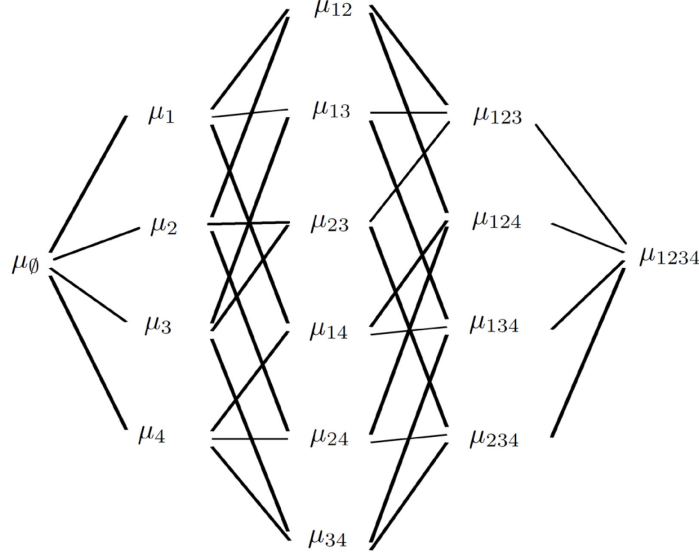


Figure 4-4: Lattice of the coefficients of a fuzzy measure ( $n = 4$ )

**Definition 3:** Let  $\mu$  be a set function on  $X$ . The Möbius transform of  $\mu$  is a set function on  $X$  defined by:

$$m(A) = \sum_{B \subset A} (-1)^{|A/B|} \mu(B), \quad \forall A \subset X. \quad (5.7)$$

This transformation is invertible such that:

$$\mu(A) = \sum_{B \subset A} m(B), \quad \forall A \subset X. \quad (5.8)$$

**Definition 4:** A fuzzy measure  $\mu$  is said to be *k-order additive* if its Möbius transform  $m(A) = 0$  for any  $A$  such that  $|A| > k$  and there exists at least one subset  $A$  of  $X$  of exactly  $k$  elements such that  $m(A) \neq 0$ . Thus, *k-additive* measures can be represented by a limited set of coefficients at most  $\sum_{i=1}^k \binom{n}{i}$ . Accordingly,  $\mu$  is said to be **2-additive** if its Möbius transform  $m$  satisfies the following:

$$\forall T \in 2^N, m(T) = 0 \text{ if } |T| > 2. \quad (5.9)$$

$$\forall T \in 2^N, \text{ such that } |B| = 2 \text{ and } m(T) \neq 0. \quad (5.10)$$

The basic quantity for defining interaction seems to be:  $a_{ij} = \mu_{ij} - \mu_i - \mu_j$ . But it is important to examine what happens when  $i$  and  $j$  are added to coalitions  $T$  e.g.  $\{i, j, k\}$ .

**Definition 5:** Let  $\mu$  be a fuzzy measure. The interaction index  $I(\mu, ij)$  for any pair of criteria  $i$  and  $j$  is defined as follows [104]:

$$I(\mu, ij) = \sum_{T \subseteq N \setminus \{i, j\}} \frac{(n-t-2)! t!}{(n-1)!} [\mu(T \cup ij) - \mu(T \cup i) - \mu(T \cup j) + \mu(T)]. \quad (5.11)$$

where  $T$  is a subset of criteria. The interaction index ranges in  $[-1, 1]$ .

**Definition 6:** The importance index  $\phi(\mu, i)$  for a criterion  $i$  is computed by the Shapley value  $(\phi)$  [104], which is defined as:

$$\phi(\mu, i) = \sum_{T \subseteq N \setminus \{i\}} \frac{(n-t-1)! t!}{n!} [\mu(T \cup i) - \mu(T)]. \quad (5.12)$$

The Shapley value ranges between  $[0, 1]$  and represents a true sharing of the total amount  $\mu(N)$ , since:

$$\sum_{i=1}^n \phi(\mu, i) = \mu(N) = 1. \quad (5.13)$$

It is convenient to scale these values by a factor  $n$ , so that an importance index greater than 1 indicates an attribute more important than the average.

**Lemma:** If the coefficients  $\mu(\{i\})$  and  $\mu(\{i, j\})$  are given for all  $i, j \in N$ , then the necessary and sufficient conditions that  $\mu$  is a 2-additive measure are:

$$\sum_{\{i, j\} \subseteq N} \mu(\{i, j\}) - (n-2) \sum_{i \in N} \mu(\{i\}) = 1 \quad (\text{Normality}) \quad (5.14)$$

$$\mu(\{i\}) \geq 0, \forall i \in N \quad (\text{Non-negativity}) \quad (5.15)$$

$$\forall A \subseteq N, |A| \geq 2, \forall k \in A,$$

$$\sum_{i \in A \setminus \{k\}} (\mu(\{i, k\}) - \mu(\{i\})) \geq (|A| - 2) \mu(\{k\}) \quad (\text{Monotonicity}) \quad (5.16)$$

The expression of the 2-additive Choquet is:

$$C_\mu(f) = \sum_{i=1}^n \phi(\mu, i) f(x_i) - \frac{1}{2} \sum_{\{i, j\} \subseteq N} I(\mu, ij) |f(x_i) - f(x_j)| \quad (5.17)$$

Here,  $I(\mu, ij) = 0$  means criteria  $i$  and  $j$  are independent while  $I(\mu, ij) > 0$  means there is a complementary among  $i$  and  $j$  and that for the decision maker, both criteria have to be satisfactory in order to get a satisfactory alternative. If  $I(\mu, ij) < 0$  then there is a substitutability or redundancy among  $i$  and  $j$ . This means that for the decision maker, the satisfaction of one of the

two criteria is sufficient to have a satisfactory alternative. It is worthy to note that a *positive correlation* leads to a *negative interaction* index, and vice versa. The fuzzy measures should be specified in such a way that the desired overall importance and the interaction indices are satisfied.

## 4.5 Identification of Fuzzy Measures

We now address the problem of identification of  $(2^n - 2)$  fuzzy measures,  $\mu$ , taking into account the monotonicity relations between the coefficients and the preferences specified by requirements and the decision makers. Four different approaches are essentially discussed here;

### 4.5.1 Identification Using Sugeno $\lambda$ -measures

As the number of criteria,  $n$ , grows specifications of the fuzzy measures using aforementioned methods become more and more difficult. Sugeno [134] created a way to automatically generate the entire lattice based on just the  $\mu_i$  densities, thus  $(2^n - 2 - n)$  values. The Sugeno  $\lambda$ —fuzzy measure has the following additional property: If  $A, B \in \Omega$  and  $A \cap B = \emptyset$ ,

$$\mu(A \cup B) = \mu(A) + \mu(B) + \lambda\mu(A)\mu(B). \quad (5.18)$$

It is proven that a unique  $\lambda$  can be found by solving the following equation:

$$\lambda + 1 = \prod_{i=1}^n (1 + \lambda\mu_i), \quad -1 < \lambda < \infty, \lambda \neq 0 \quad (5.19)$$

where  $\mu_i = \mu \{x_i\}$ . Thus, the  $n$  densities determine the  $2^n$  values of a Sugeno measure. There are three cases with regards to the singleton measures;

$$\text{If } \sum_{i=1}^n \mu_i > \mu(N) \text{ then, } -1 < \lambda < \infty. \quad (5.20)$$

$$\text{If } \sum_{i=1}^n \mu_i = \mu(N) \text{ then, } \lambda = 0. \quad (5.21)$$

$$\text{If } \sum_{i=1}^n \mu_i < \mu(N) \text{ then, } \lambda > 0. \quad (5.22)$$

### 4.5.2 Identification Based on Learning Data

Having a set of learning data in hand, the parameters of a Choquet integral model can be identified by minimizing an error criterion. Suppose that  $(f_k, y_k)$ ,  $k = 1, 2, \dots, l$  are learning data where  $f_k = [f^k(x_1), \dots, f^k(x_n)]^T$  is a  $n$ -dimensional input vector, containing the degrees of satisfaction of alternative (concept)  $k$  with respect to criteria 1 to  $n$ , and  $y_k$  is the global evaluation of object  $k$  (not necessarily an aggregated value). There must be at least  $l = \frac{n!}{[(\frac{n}{2})!]^2}$  (when  $n$  is even)

or  $l = \frac{n!}{[\frac{n-1}{2}]![\frac{n+1}{2}]!}$  (when  $n$  is odd) sets of learning data [135]. Then, one can try to identify the best fuzzy measure  $\mu^*$  so that the squared error criterion (E) is minimized [102].

$$E^2 = \sum_{k=1}^l [C_\mu(f^k(x_1), \dots, f^k(x_n)) - y_k]^2 \quad (5.23)$$

Under a quadratic program form, we have:

$$\min \left( E^2 = \left( \frac{1}{2} \mathbf{u}^t \mathbf{D} \mathbf{u} + \mathbf{c}^t \mathbf{u} \right) \right) \quad (5.24)$$

where  $\mathbf{u}$  is a  $(2^n - 2)$  dimensional vector containing all the coefficients of the fuzzy measure  $\mu$ , except for  $\mu_\emptyset = 0$  and  $\mu_N = 1$ , as follows:

$$\mathbf{u} = [\mu_i, [\mu_{ij}], [\mu_{ijk}], [\mu_{ijkl}], \dots]^T \quad (5.25)$$

It is important to note that the components of  $\mathbf{u}$  are not independent of each other because fuzzy measures must satisfy a set of monotonicity relations. Moreover,  $\mathbf{D}$  is a symmetric  $(2^n - 2)$  dimensional matrix, and  $\mathbf{c}$  is a  $(2^n - 2)$  dimensional vector. The first set of constraints contains the measures monotonicity constraints described as follows:

$$\mathbf{A} \mathbf{u} + \mathbf{b} \leq 0 \quad (5.26)$$

where, matrix  $\mathbf{A}$  is a  $n(2^{n-1} - 1) \times (2^n - 2)$  dimensional matrix and  $\mathbf{b}$  is a  $n(2^{n-1} - 1)$  vector defined by:

$$\mathbf{b} = [0, \dots, 0, \underbrace{-1, \dots, -1}_n]^T. \quad (5.27)$$

More precisely for Eq. 18 we have:

$$C_\mu(f_k) = \mathbf{c}_k^t \cdot \mathbf{u} + f^k(x_1), \quad (5.28)$$

where  $\mathbf{c}_k$  is a  $(2^n - 2)$  dimensional vector containing the differences  $f(x_i) - f(x_{i-1})$ ,  $i = 2, \dots, n$ , so that there are at most  $(n - 1)$  non-zero terms in it, which are all positive. Accordingly, we attain:

$$\mathbf{c} = 2 \sum_{k=1}^l (f^k(x_1) - y_k) \mathbf{c}_k. \quad (5.29)$$

Additionally,  $\mathbf{D}_k$  is a  $(2^n - 2)$  dimensional square matrix where:

$$\mathbf{D} = 2 \sum_{k=1}^l \mathbf{D}_k = 2 \sum_{k=1}^l \mathbf{c}_k \mathbf{c}_k^T. \quad (5.30)$$

Thus, we can rewrite the program in Eq. (4.24) as:



$$\min \left( E^2 = 2 \sum_{k=1}^l \mathbf{u}^T \mathbf{c}_k \mathbf{c}_k^T \mathbf{u} + 2 \sum_{k=1}^l \mathbf{c}_k^T \cdot \mathbf{u} (f^k(x_1) - y_k) \right) \quad (5.31)$$

Subj. to:  $\mathbf{A}\mathbf{u} + \mathbf{b} \leq 0$

Since  $\mathbf{u}^T \mathbf{D} \mathbf{u}$  consists of a sum of squares, thus for all  $\mathbf{u} \geq 0$ ,  $\mathbf{u}^T \mathbf{D} \mathbf{u} \geq 0$  and  $\mathbf{D}$  is positive semidefinite. The above quadratic program has a unique (global) minimum since the criterion to be minimized is convex. This solution can be a point or a convex set in  $[0, 1]^{2n-2}$ . This program can be solved by any standard method of quadratic optimization, although matrix  $\mathbf{D}$  may be ill-conditioned ( $rank < 2^n - 2$ ) since based on the definition of vector  $\mathbf{c}_k$ , matrix  $\mathbf{D}$  contains columns and rows of zeroes. Obviously, this effect will disappear if the number of training data increases. Now, we can take into account the decision maker's (DM) preferences with regards to importance of criteria and interactions among criterion pairs as constraint relations;

$$\mu(A \cup i) - \mu(A) \geq 0, \quad \forall i \in N, \forall A \in N \setminus i \quad (5.32)$$

$$C_\mu(f) - C_\mu(\hat{f}) \geq \delta_C \quad (5.33)$$

$$\phi(\mu, i) - \phi(\mu, j) \geq \delta_\phi \quad (5.34)$$

$$\text{Constraints on } I(\mu, ij) \quad (5.35)$$

### 4.5.3 Identification Based on Fuzzy Measure Semantics and Learning Data

In order to reduce the complexity and provide better guidelines for identification of measures, the combination of semantical considerations with learning data can lead to a more efficient algorithm. With this approach the objective would be to minimize the distance to the additive equi-distributed fuzzy measure defined by  $\mu_j = 1/n$ . Consequently, instead of trying to minimize the sum of the squared errors between model output and data, we try to minimize the distance to the additive equi-distributed measure set  $\mathbf{u}_0$ . Thus, we can have the following quadratic form:

$$\text{Min } J = \frac{1}{2} (\mathbf{u} - \mathbf{u}_0)^T (\mathbf{u} - \mathbf{u}_0) \quad (5.36)$$

$$\text{Subj. to: } \mathbf{A}\mathbf{u} + \mathbf{b} \leq 0$$

Here, training data are no longer in the objective function, but are used as the second set of constraints;

$$y_k - \delta_k \leq \mathbf{c}_k^t \cdot \mathbf{u} + f(x_1) \leq y_k + \delta_k \quad (5.37)$$

Moreover, the decision maker needs to express some preferences as the relative importance of the criteria and on their mutual interactions, such that:

$$\mu(A) \leq \eta\mu(B) \quad (5.38)$$

$$\mu(A \cup B) = \mu(A) + \lambda\mu(B) \quad (5.39)$$

where  $\mu(A) \geq \mu(B)$  and  $\eta$  defines the degree of relative importance of A with respect to B. For the interactions between criteria A and B,  $\lambda \in [0, 1]$  and A and B are fully dependent when  $\lambda = 0$ , and independent when  $\lambda = 1$ . Support (synergy) between A and B can be modeled by:

$$\mu(A \cup B) = \mu(A) + \mu(B) + \gamma(1 - \mu(A) - \mu(B)) \quad (5.40)$$

where  $\gamma$  specifies the level of support between criteria pairs. All these constraints based on the decision maker's preferences can be used to modify the initial monotonicity constraint by adding to the initial **A** and **b** and form a new constraint as:

$$\mathbf{A}'\mathbf{u} + \mathbf{b}' \leq 0 \quad (5.41)$$

#### 4.5.4 Identification Using a 2-Additive Model

For a combination of more than two criteria, the different meanings of the interaction index and the corresponding fuzzy measure is not so clear for the decision maker. Namely the interpretation of  $\mu(S)$  and  $a(S)$  is not straightforward where for a couple of criteria,  $i$  and  $j$ , we have  $a(i, j) = \mu_{ij} - \mu_i - \mu_j$  and  $a(i) = \mu_i$ . To overcome this problem, one can use the concept of  $k$ -order fuzzy measure proposed by [126]. Such a fuzzy measure is called  $k$ -order since it represents a  $k$ -order approximation of its polynomial expression. Here we discuss the 2-order case, which seems to have most practical applications, since it permits to model interaction between criteria while remaining very simple. For a 2-order fuzzy measure we have:

$$\mu(S) = \sum_{i \in S} a(i) + \sum_{\{i, j\} \subseteq S} a(i, j), \quad \forall S \subseteq N. \quad (5.42)$$

Moreover, for the interaction index we have:

$$I(i, j) = a(i, j) \quad (5.43)$$

$$I(S) = 0, \forall S \subseteq N, |S| > 2. \quad (5.44)$$

$$\phi_i = \mu_i + \frac{1}{2} \sum_{k \in N \setminus i} I_{ik}. \quad (5.45)$$

While the information needed to form the above equations can be directly provided by the decision maker in an intuitive manner, there is also another way to attain them by just providing relative information for importance and interactions. In order to use the 2-additive model to

identify the capacities we assume that the decision maker is able to tell the relative importance of criteria, and the kind of interaction between them. Accordingly, the information provided by decision maker can be summarized as follows:

- A table of scores for  $n$  criteria of  $m$  alternatives.
- A ranking of  $m$  alternatives and a ranking of  $n$  criteria importance  $\phi_i$ .
- A ranking of interaction indices and the sign of some interactions  $(i, j)$  : positive, null, negative (translating synergy, independence or redundancy).

All the above information can be formulated as linear equalities or inequalities. Accordingly, the identification problem as well can be translated into a linear program [130]. It is obvious that the quality of input information vastly affects the solution set. The program can be described by taking into account the relations in Equation (4.42 - 4.45) as follows:

$$\max z = \epsilon \quad (\epsilon > 0) \quad (5.46)$$

Subject to:

$C_\mu(a) - C_\mu(b) \geq \delta + \epsilon$	- Alternative $a$ is preferred over $b$
$-\delta \leq C_\mu(a) - C_\mu(b) \leq \delta$	- Alternative $a$ and $b$ has almost the same preference.
$\phi_i - \phi_j \geq \epsilon$	- Criteria $i$ is more important than $j$
$\phi_i = \phi_j$	- Criteria $i$ and $j$ have the same importance.
$I(i, j) - I(k, l) \geq \epsilon$	- Interaction between criteria $i$ and $j$ is bigger than the interaction between criteria $k$ and $l$ .
$(i, j) = I(k, l)$	- Interaction between criteria $i$ and $j$ is equal to the interaction between $k$ and $l$ .
$I(i, j) \geq \epsilon$ , if $I(i, j) > 0$	
$I(i, j) \leq \epsilon$ , if $I(i, j) < 0$	- The sign of interactions between criteria $i$ and $j$ .
$I(i, j) = \epsilon$ , if $I(i, j) = 0$	
$\sum_i \phi(i) = 1, \phi(i) \geq 0,$	
$\phi(i) + \sum_{j \in N \setminus i} I(i, j) \geq 0.$	- Boundary and monotonicity conditions

Here,  $C_\mu(a)$  represents the unknown global score for alternative (a) and  $\delta$  represents the threshold level that should be reached by the difference between global scores to consider that one alternative should be significantly preferred to another alternative. Here, the objective function of the linear program to be maximized is the value of the positive slack variable.

#### 4.6 Case Study: Conceptual Design of a Vision-Guided Quadrotor Drone

Recently, the quadrotors are being deployed as highly maneuverable aerial robots which have the ability of easy hover, take off, fly, and land in small and remote areas [136]. Recent technological advances in energy storage devices, sensors, actuators and information processing have boosted the development of Unmanned Aerial Vehicle (UAV) platforms with significant capabilities. Unmanned Quadrotor Helicopters (UQH) are excellent examples of highly coupled mechatronic systems where the disciplines of aerodynamics, structures and materials, flight mechanics and control are acting upon each other in a typical flight condition. Moreover, the integration of vision sensors with robots has helped solve the limitation of operating in non-structured environments [137].

Here, the discussed fuzzy measure identification methods are utilized in a conceptual design process using multicriteria mechatronic profile (MMP) for a vision-guided quadrotor UAV. From our previous work [138], we have chosen four concepts to study the proposed design method. Table 4-2 shows the design alternative and the corresponding sub-systems and components. Based on the material used, the frame structure and subsystems selected for one specific concept, the total mass, required power, payload, maximum allowable inertia moment, force and bandwidth can be also easily estimated. An approximation of the total cost can also be calculated based on the components and manufacturing process. Table 4-3 briefly gives the results for the estimated values for proposed concepts.

Table 4-2: Design alternatives [138]

	Concept I	Concept II	Concept III	Concept IV
Frame Structure	X-shape	H-shape	X-shape	H-shape
Material	AL.	AL.	Poly.	Poly.
Motors	Brushed DC	Brushed DC	Brushless DC	Brushless AC
Motor Encoder	Optical	Magnetic	Optical	Magnetic
Visual Servo.	PBVS	PBVS	IBVS	IBVS
Camera Config.	Mono	Stereo	Stereo	Mono
Motion Control.	PID	LQR	PID	LQR
Position Sensor	GPS +Accel.	Motion Cam.	GPS +Accel.	GPS +Accel.
Battery	Li-ion	Li-Poly.	Li-ion	Li- Poly.

Table 4-3: Estimated design parameters for generated concepts [138]

	Concept I	Concept II	Concept III	Concept IV
Power (W)	450	500	350	400
Max Inertia Moment (kg.m <sup>2</sup> )	5E-3	5.2E-3	4E-3	4.5E-3
Bandwidth (Hz)	70	70	60	60
Payload (Kg)	0.5	0.5	0.6	0.6
Cost (unit) (normal.)	0.8	1	0.7	0.7

Ultimately, by using a set of intuitive Choquet fuzzy measures the evaluations for all concepts and corresponding design criteria are listed in Table 4-4. For more information about criteria assessment and measurements please refer to our previous work [119, 138]. The fuzzy measures used in the previous study were obtained in an intuitive manner by the authors and a group of 30 researchers (all specialized in system design and mechatronics) through a questionnaire. This questionnaire collects the following information from various design point of views; The degree of importance for each of the mentioned five criteria in designing a good mechatronic product, and the degree of correlation between each pair of criteria or the effect of increasing criterion  $i$  on criterion  $j$ . These measures are shown in Table 4-5.

Table 4-4: Concept Evaluations for design alternatives

MMP	Concept I	Concept II	Concept III	Concept IV
MIQ	0.84	0.84	1	1
RS	0.86	0.91	0.93	1
CX	0.85	0.69	0.93	0.89
FX	0.91	0.96	0.91	0.88
CT	1	0.78	0.94	0.91
<b>GCS<sub><math>\mu</math></sub></b>	0.89	0.83	0.96	0.94

Table 4-5: Fuzzy measures for conceptual design of a Quadrotor drone equipped with a visual servoing system

$\mu_1$ = 0.23	$\mu_{12}$ = 0.45	$\mu_{13}$ = 0.47	$\mu_{14}$ = 0.34	$\mu_{15}$ = 0.51
$\mu_{123}$ = 0.61	$\mu_2$ = 0.29	$\mu_{23}$ = 0.52	$\mu_{24}$ = 0.42	$\mu_{25}$ = 0.56
$\mu_{124}$ = 0.60	$\mu_{135}$ = 0.69	$\mu_3$ = 0.17	$\mu_{34}$ = 0.35	$\mu_{35}$ = 0.33
$\mu_{125}$ = 0.67	$\mu_{145}$ = 0.67	$\mu_{245}$ = 0.73	$\mu_4$ = 0.16	$\mu_{45}$ = 0.41
$\mu_{134}$ = 0.63	$\mu_{234}$ = 0.68	$\mu_{345}$ = 0.49	$\mu_{235}$ = 0.62	$\mu_5$ = 0.22
$\mu_{1234}$ = 0.77	$\mu_{1235}$ = 0.84	$\mu_{1345}$ = 0.84	$\mu_{2345}$ = 0.78	$\mu_{1245}$ = 0.82

$$\Phi = [\phi_1, \phi_2, \phi_3, \phi_4, \phi_5] = [0.2085, 0.2612, 0.1598, 0.1431, 0.2020]. \quad (5.47)$$

We remind that in order to calculate a Choquet integral and its corresponding measures, a permutation on the criteria values should be initially performed in such a way that  $0 \leq f(x_1) \leq f(x_2) \leq \dots \leq f(x_n)$ . Although, throughout our case study and in order to avoid any confusion, we reshape the outputs for measures and also importance indices at the end of the identification algorithm so that the following order always persists:

$$\Phi = [\phi_1, \phi_2, \phi_3, \phi_4, \phi_5] = [\phi_{MIQ}, \phi_{RS}, \phi_{CX}, \phi_{FX}, \phi_{CT}]. \quad (5.48)$$

#### 4.6.1 Identification Using Sugeno $\lambda$ -measures

Based on Equations (4.18) and (4.19) for five criteria illustrated in Table 4-4 we have:

$$\lambda + 1 = (\lambda\mu_1 + 1)(\lambda\mu_2 + 1)(\lambda\mu_3 + 1)(\lambda\mu_4 + 1)(\lambda\mu_5 + 1) \quad (5.49)$$

$$-1 < \lambda < \infty, \quad \lambda \neq 0. \quad (5.50)$$

where for  $\mu_i$  we use the values from Table 4-5. The solution of the above equation yields  $\lambda = 0.0255$  and consequently, we attain the results for fuzzy measures as listed in Table 4-6.

Table 4-6: Fuzzy measures identified using Sugeno  $\lambda$ - measures

$\mu_1$ = 0.22	$\mu_{12}$ = 0.4613	$\mu_{13}$ = 0.3910	$\mu_{14}$ = 0.3809	$\mu_{15}$ = 0.4211
$\mu_{123}$ = 0.6333	$\mu_2$ = 0.24	$\mu_{23}$ = 0.4110	$\mu_{24}$ = 0.4010	$\mu_{25}$ = 0.4412
$\mu_{124}$ = 0.6232	$\mu_{135}$ = 0.5930	$\mu_3$ = 0.17	$\mu_{34}$ = 0.3307	$\mu_{35}$ = 0.3709
$\mu_{125}$ = 0.6637	$\mu_{145}$ = 0.5828	$\mu_{245}$ = 0.6030	$\mu_4$ = 0.16	$\mu_{45}$ = 0.3608
$\mu_{134}$ = 0.5526	$\mu_{234}$ = 0.5727	$\mu_{345}$ = 0.5324	$\mu_{235}$ = 0.6131	$\mu_5$ = 0.20
$\mu_{1234}$ = 0.7959	$\mu_{1235}$ = 0.8366	$\mu_{1345}$ = 0.7554	$\mu_{2345}$ = 0.7756	$\mu_{1245}$ = 0.8264

The fuzzy measures obtained by the Sugeno  $\lambda$  – method yield the following importance indices:

$$\Phi = [\phi_1, \phi_2, \phi_3, \phi_4, \phi_5] = [0.2221, 0.2422, 0.1718, 0.1617, 0.2020]. \quad (5.51)$$

#### 4.6.2 Identification Based on Learning Data

As mentioned before, in order to identify the fuzzy measures, it is possible to employ a “learning set”—a number of objects whose assessment is manually performed by the decision maker (DM). According to [135], the minimum number of data set we need to solve the squared error minimization program (4.24) is equal to:

$$l = \frac{n!}{\left[\frac{n-1}{2}\right]! \left[\frac{n+1}{2}\right]!} = \frac{5!}{\left[\frac{5-1}{2}\right]! \left[\frac{5+1}{2}\right]!} = 10. \quad (5.52)$$

Accordingly, we need provide 10 sets of criteria evaluation and corresponding global concept scores. The vector of variables contains the 30 fuzzy measures and as for the monotonicity constrains described in Equation (4.26) we have the following matrices:

$$\mathbf{A}_{[75 \times 30]}, \mathbf{u}_{[30 \times 1]}, \mathbf{b} = \left[ 0, \dots, 0, \underbrace{-1, \dots, -1}_5 \right]_{[75 \times 1]}^T, \quad (5.53)$$

in which we describe all 75 monotonicity relations such as:

$$\begin{aligned} \mu_1 &\leq \mu_{12}, \dots, \mu_5 \leq \mu_{45}, \\ \mu_{12} &\leq \mu_{123}, \dots, \mu_{45} \leq \mu_{345}, \\ \mu_{123} &\leq \mu_{1234}, \dots, \mu_{345} \leq \mu_{2345}, \\ \mu_{1234} &\leq 1, \dots, \mu_{2345} \leq 1. \end{aligned} \quad (5.54)$$

In order to form the objective function from Equation (4.24) we also need to form the matrix  $\mathbf{D}$  and vector  $\mathbf{c}$  which have the following format:

$$\mathbf{D}_{[30 \times 30]}, \mathbf{c}_{[30 \times 1]}, \mathbf{c}_k_{[30 \times 1]}$$

$$\mathbf{c} = 2 \sum_{k=1}^{10} (f^k(x_1) - y_k) \mathbf{c}_k, \quad (5.55)$$

$$\mathbf{D} = 2 \sum_{k=1}^{10} \mathbf{D}_k = 2 \sum_{k=1}^{10} \mathbf{c}_k \mathbf{c}_k^T. \quad (5.56)$$

in which  $\mathbf{c}_k$  is a 30- dimensional vector containing the differences  $f(x_i) - f(x_{i-1})$ ,  $i = 2, \dots, 5$  so that there are at most 4 non-zero terms in it, which are all positive. Consequently, we get:

$$\begin{aligned} \mathbf{c}_k(5) &= f^k(x_5) - f^k(x_4), \\ \mathbf{c}_k(15) &= f^k(x_4) - f^k(x_3), \\ \mathbf{c}_k(25) &= f^k(x_3) - f^k(x_2), \\ \mathbf{c}_k(30) &= f^k(x_2) - f^k(x_1), \\ \mathbf{c}_k(i) &= 0, \quad (\forall i \neq 5, 15, 25, 30) \end{aligned} \quad (5.57)$$

Finally, the decision maker's preferences can be taken into account using the constraints listed in Table 4-7.

Table 4-7: Decision Maker's preferences on criteria relations	
Maximum separation of alternatives:	
$C_\mu(f) - C_\mu(f') \geq \delta_c \quad (\delta_c = 0.05)$	
Preferences on the importance of criteria:	
$\phi_2 - \phi_1 \geq \epsilon$	$\phi_2 - \phi_5 \geq \epsilon$
$\phi_1 - \phi_3 \geq \epsilon$	$\phi_5 - \phi_3 \geq \epsilon$
$\phi_1 - \phi_4 \geq \epsilon$	$\phi_5 - \phi_4 \geq \epsilon$
$\phi_2 - \phi_3 \geq \epsilon$	$\phi_1 = \phi_5$
$\phi_2 - \phi_4 \geq \epsilon$	$\phi_3 = \phi_4$
Preferences on the interactions between criteria pairs	
$I(1,5) - I(1,3) \geq \epsilon$	$I(4,5) - I(3,4) \geq \epsilon$
$I(2,5) - I(2,3) \geq \epsilon$	$I(2,4) = I(3,4)$
$I(1,3) - I(2,4) \geq \epsilon$	$I(1,4) = I(3,5)$

The above problem will be solved here using MATLAB quadratic programming from the optimization toolbox and the method of “interior-point-convex”. Table 4-9 shows the resulting values for the fuzzy measures.



Table 4-8: Results for fuzzy measures identified using a learning set

$\mu_1$ = 0.3292	$\mu_{12}$ = 0.4502	$\mu_{13}$ = 0.6366	$\mu_{14}$ = 0.2985	$\mu_{15}$ = 0.6416
$\mu_{123}$ = 0.7983	$\mu_2$ = 0.2829	$\mu_{23}$ = 0.5137	$\mu_{24}$ = 0.5615	$\mu_{25}$ = 0.5332
$\mu_{124}$ = 0.4398	$\mu_{135}$ = 0.7296	$\mu_3$ = 0.1901	$\mu_{34}$ = 0.4698	$\mu_{35}$ = 0.1789
$\mu_{125}$ = 0.8048	$\mu_{145}$ = 0.6610	$\mu_{245}$ = 0.8620	$\mu_4$ = 0.2584	$\mu_{45}$ = 0.5167
$\mu_{134}$ = 0.6273	$\mu_{234}$ = 0.8137	$\mu_{345}$ = 0.5088	$\mu_{235}$ = 0.5446	$\mu_5$ = 0.2082
$\mu_{1234}$ = 0.8093	$\mu_{1235}$ = 0.9334	$\mu_{1345}$ = 0.8093	$\mu_{2345}$ = 0.8093	$\mu_{1245}$ = 0.8444

The above results will lead to the following importance indices:

$$\Phi = [\phi_1, \phi_2, \phi_3, \phi_4, \phi_5] = [0.2145, 0.2535, 0.1701, 0.1597, 0.1967]. \quad (5.58)$$

#### 4.6.3 Identification based on fuzzy measure semantics and learning data

In order to use Equations (4.38-4.39) for modeling the relations between criteria pairs, we define the proper linguistics as described in the following Tables.

Table 4-9: Linguistic representation of relative importance of criteria

Relative Importance	Value
Same level	$0.9 \leq \eta \leq 1.1$
$A$ is a little more important than $B$	$1.1 \leq \eta \leq 1.3$
$A$ is more important than $B$	$1.3 \leq \eta \leq 1.7$
$A$ is quite more important than $B$	$1.7 \leq \eta \leq 1.9$

Table 4-10: Linguistic representation of dependence between criteria

Criteria Dependence	Value
Highly dependent	$\lambda = 0.0$
Dependent	$0.0 \leq \lambda \leq 0.5$
A little dependent	$0.5 \leq \lambda \leq 1.0$
Independent	$\lambda = 1.0$

Table 4-11: Linguistic representation of support between criteria

Criteria Synergy	Value
High support	$\gamma = 1.0$
Support	$0.5 \leq \gamma \leq 1.0$
A little support	$0.0 \leq \gamma \leq 0.5$

This linguistics in addition to the monotonicity conditions are translated into the following constraints as the decision maker's preferences:

Table 4-12: Decision maker's preferences as linear constraints

Relative Importance of criteria	
$\mu_2 \leq 1.3\mu_1$	$0.9\mu_4 \leq \mu_3 \leq 1.1\mu_4$
$\mu_1 \leq 1.3\mu_4$	$0.9\mu_3 \leq \mu_5 \leq 1.1\mu_3$
$\mu_2 \leq 1.7\mu_4$	$0.9\mu_5 \leq \mu_1 \leq 1.1\mu_5$
$\mu_2 \leq 1.7\mu_3$	$0.9\mu_5 \leq \mu_1 \leq 1.1\mu_5$
Dependence between criteria pairs	
$\mu_2 + 0.5\mu_3 \leq \mu_{23} \leq \mu_2 + \mu_3$	$\mu_3 + 0.8\mu_4 \leq \mu_{34} \leq \mu_3 + \mu_4$
$\mu_2 + 0.5\mu_4 \leq \mu_{24} \leq \mu_2 + \mu_4$	$\mu_4 + 0.5\mu_5 \leq \mu_{45} \leq \mu_4 + \mu_5$
$\mu_2 + 0.5\mu_5 \leq \mu_{25} \leq \mu_2 + \mu_5$	
Synergy between criteria pairs	
$\mu_1 + \mu_4 + 0.3(1 - \mu_1 - \mu_4) \leq \mu_{14} \leq \mu_1 + \mu_4 + 0.7(1 - \mu_1 - \mu_4)$	
$\mu_3 + \mu_5 + 0.3(1 - \mu_3 - \mu_5) \leq \mu_{35} \leq \mu_3 + \mu_5 + 0.7(1 - \mu_3 - \mu_5)$	
$\mu_1 + \mu_2 \leq \mu_{12} \leq \mu_1 + \mu_2 + 0.3(1 - \mu_1 - \mu_2)$	

This approach can also include an interactive dialogue between DM and the fuzzy measure identifying system. Solutions are presented to the decision maker, who can refine them by specifying or modifying the relative importance and interaction between criteria if he is not satisfied with the solution. As an example here, we use the concept evaluation data from our previous work. As for the additive equi-distributed singleton fuzzy measures we have:

$$M_0 = [0.2 \ 0.2 \ 0.2 \ 0.2 \ 0.2], \quad (5.59)$$

Moreover, we use the 10 training data sets from the previous section to form the following second set of constraints based on Equation (4.37) with  $\delta_k = 0.35$ ;

$$\begin{aligned}
0.54 &\leq c_1^T \mathbf{u} + 0.84 \leq 1.24, & 0.47 &\leq c_6^T \mathbf{u} + 0.64 \leq 1.17, \\
0.48 &\leq c_2^T \mathbf{u} + 0.69 \leq 1.18, & 0.19 &\leq c_7^T \mathbf{u} + 0.45 \leq 0.89, \\
0.61 &\leq c_3^T \mathbf{u} + 0.91 \leq 1.31, & 0.53 &\leq c_8^T \mathbf{u} + 0.75 \leq 1.23, \\
0.59 &\leq c_4^T \mathbf{u} + 0.88 \leq 1.29, & 0.58 &\leq c_9^T \mathbf{u} + 0.85 \leq 1.28, \\
0.44 &\leq c_5^T \mathbf{u} + 0.72 \leq 1.14, & 0.07 &\leq c_{10}^T \mathbf{u} + 0.35 \leq 0.77.
\end{aligned} \tag{5.60}$$

where  $c_k^T$  is a  $[1 \times 30]$  vector and can be calculated from Eq. (4.37), while for  $\mathbf{u}$  we have:

$$\mathbf{u}_{[30 \times 1]} = [\mu_i, [\mu_{ij}], [\mu_{ijk}], [\mu_{ijkl...}], \dots]^T. \tag{5.61}$$

By combining all the constraints in Eq. (4.60), Table 4-13 and also the monotonicity constraints, we can formulate a new linear constraint as  $\mathbf{A}'\mathbf{u} + \mathbf{b}' \leq 0$  and solve the quadratic program in Equation (4.36). Again, by using MATLAB quadratic programming and the interior-point-convex algorithm we attain the following results:

Table 4-13: Results for fuzzy measures identified using a learning set and fuzzy measure semantics

$\mu_1$ = 0.3243	$\mu_{12}$ = 0.4860	$\mu_{13}$ = 0.6160	$\mu_{14}$ = 0.2441	$\mu_{15}$ = 0.6318
$\mu_{123}$ = 0.8198	$\mu_2$ = 0.2615	$\mu_{23}$ = 0.4741	$\mu_{24}$ = 0.5514	$\mu_{25}$ = 0.5090
$\mu_{124}$ = 0.4258	$\mu_{135}$ = 0.7174	$\mu_3$ = 0.1705	$\mu_{34}$ = 0.4618	$\mu_{35}$ = 0.1748
$\mu_{125}$ = 0.8307	$\mu_{145}$ = 0.6068	$\mu_{245}$ = 0.8540	$\mu_4$ = 0.2700	$\mu_{45}$ = 0.5354
$\mu_{134}$ = 0.5572	$\mu_{234}$ = 0.7854	$\mu_{345}$ = 0.5212	$\mu_{235}$ = 0.5446	$\mu_5$ = 0.2104
$\mu_{1234}$ = 0.7810	$\mu_{1235}$ = 0.9584	$\mu_{1345}$ = 0.7810	$\mu_{2345}$ = 0.7810	$\mu_{1245}$ = 0.8255

Accordingly, we get the following Shapley values:

$$\Phi = [\phi_1, \phi_2, \phi_3, \phi_4, \phi_5] = [0.2085, 0.2612, 0.1598, 0.1431, 0.2020]. \tag{5.62}$$

#### 4.6.4 Identification using a 2-Additive Model

From the linear program presented in Eq. (4.46), we can create a negative null form minimization with the following format:

$$\min_{\mathbf{I}} -\epsilon \quad (\epsilon > 0) \tag{5.63}$$

$$\text{Subject to: } \mathbf{A} \cdot \mathbf{I} \leq \mathbf{b}. \tag{5.64}$$

where the decision maker's preferences are formulated in Table 4-14 based on the constraints described in Equation (4.46) as:

Table 4-14: Decision maker's preferences as linear constraints	
Preferences on alternatives:	
$C_\mu(I) - C_\mu(II) \geq \delta + \epsilon$	$C_\mu(III) - C_\mu(II) \geq \delta + \epsilon$
$C_\mu(III) - C_\mu(I) \geq \delta + \epsilon$	$C_\mu(IV) - C_\mu(II) \geq \delta + \epsilon$
$C_\mu(IV) - C_\mu(I) \geq \delta + \epsilon$	$-\delta \leq C_\mu(III) - C_\mu(IV) \leq \delta$
Preferences on the importance of criteria	
$\phi_2 - \phi_1 \geq \epsilon$	$\phi_2 - \phi_5 \geq \epsilon$
$\phi_1 - \phi_3 \geq \epsilon$	$\phi_5 - \phi_3 \geq \epsilon$
$\phi_1 - \phi_4 \geq \epsilon$	$\phi_5 - \phi_4 \geq \epsilon$
$\phi_2 - \phi_3 \geq \epsilon$	$\phi_1 = \phi_5$
$\phi_2 - \phi_4 \geq \epsilon$	$\phi_3 = \phi_4$
Preferences on the interactions between criteria pairs	
$I(1,5) - I(1,3) \geq \epsilon$	$I(4,5) - I(3,4) \geq \epsilon$
$I(2,5) - I(2,3) \geq \epsilon$	$I(2,4) = I(3,4)$
$I(1,3) - I(2,4) \geq \epsilon$	$I(1,4) = I(3,5)$
The sign of interactions between criteria pairs	
$I(1,2) \leq -\epsilon$	$I(2,3) \geq \epsilon$
$I(1,4) \leq -\epsilon$	$I(2,4) \geq \epsilon$
$I(3,5) \leq -\epsilon$	$I(2,5) \geq \epsilon$
$I(1,3) \geq \epsilon$	$I(3,4) \geq \epsilon$
$I(1,5) \geq \epsilon$	$I(4,5) \geq \epsilon$
Boundary and monotonicity conditions	
$\sum_i \phi(i) = 1, \phi(i) \geq 0 \quad \text{and} \quad \phi(i) + \sum_{j \in N \setminus i} I(i, j) \geq 0$	

The preferences used in this example are inferred from the intuitive information provided by a group of 30 mechatronics experts through a questionnaire. This information merely discusses the preferences not the actual values for concept scores, interactions or importances. This problem has an optimal variable of  $I^*$  with an optimal value of  $\epsilon^*$ . In this case,  $I^* = [I(i, j)]^*$  is a vector of solutions for the constrained satisfaction problem. We can reshape this vector and describe it as the following symmetric matrix:

$$I = \begin{bmatrix} \phi_1 & I_{12} & I_{13} & I_{14} & I_{15} \\ I_{21} & \phi_2 & I_{23} & I_{24} & I_{25} \\ I_{31} & I_{32} & \phi_3 & I_{34} & I_{35} \\ I_{41} & I_{42} & I_{43} & \phi_4 & I_{45} \\ I_{51} & I_{52} & I_{53} & I_{54} & \phi_5 \end{bmatrix}, \quad (5.65)$$

where  $\mathbf{I}(i, i) = \phi_i$ .

By solving the problem using the MATLAB linear programming solver and the least squares algorithm, we get the following results:

$$I = \begin{bmatrix} 0.2232 & -0.1018 & 0.1082 & -0.2931 & 0.1121 \\ -0.1018 & 0.2481 & 0.0472 & 0.0213 & 0.0394 \\ 0.1082 & 0.0472 & 0.1662 & 0.0189 & -0.2023 \\ -0.2931 & 0.0213 & 0.0189 & 0.1691 & 0.0476 \\ 0.1121 & 0.0394 & -0.2023 & 0.0476 & 0.2002 \end{bmatrix} \quad (5.66)$$

which yields the following lattice of fuzzy measures:

Table 4-15: Fuzzy measures identified using a 2-additive model

$\mu_1$ = 0.3105	$\mu_{12}$ = 0.4537	$\mu_{13}$ = 0.5989	$\mu_{14}$ = 0.2892	$\mu_{15}$ = 0.6244
$\mu_{123}$ = 0.7893	$\mu_2$ = 0.2450	$\mu_{23}$ = 0.4724	$\mu_{24}$ = 0.5381	$\mu_{25}$ = 0.4863
$\mu_{124}$ = 0.4537	$\mu_{135}$ = 0.7105	$\mu_3$ = 0.1802	$\mu_{34}$ = 0.4708	$\mu_{35}$ = 0.1797
$\mu_{125}$ = 0.8070	$\mu_{145}$ = 0.6507	$\mu_{245}$ = 0.8269	$\mu_4$ = 0.2717	$\mu_{45}$ = 0.5212
$\mu_{134}$ = 0.5965	$\mu_{234}$ = 0.7844	$\mu_{345}$ = 0.5180	$\mu_{235}$ = 0.5113	$\mu_5$ = 0.2018
$\mu_{1234}$ = 0.8082	$\mu_{1235}$ = 0.9403	$\mu_{1345}$ = 0.8082	$\mu_{2345}$ = 0.8082	$\mu_{1245}$ = 0.8546

Here, the importance indices are:

$$\Phi = [\phi_1, \phi_2, \phi_3, \phi_4, \phi_5] = [0.2232, 0.2481, 0.1662, 0.1691, 0.2002]. \quad (5.67)$$

We chose the value of  $\delta$  to be equal to 0.05 which means there should be at least a difference of 5% between the global scores of the concepts. This method consists of maximizing the difference in overall scores among alternatives. if the decision maker prefers alternative (a) over alternative (b), then this should be reflected in the model by two sufficiently different and unequal outputs.

## 4.7 Discussion and Comparison

Sugeno measures are among the most widely used fuzzy measures [139]. Using  $\lambda$ -measures is an abstract and efficient way when there is not enough information about decision maker preferences or the order of preference on alternatives or interaction and importance indices. It can rapidly generate the entire lattice of fuzzy measures based on just the singleton densities. Although, not all expert reasoning can be described by these measures and guessing the  $\mu_i$  values intuitively is not a trivial process. In that case, this method can be also regarded as an optimization problem with all the preferences as constraints. Further information can be found in [140] since a complete identification process on  $\lambda$ - measures was not in the scope of this paper.

The identification based on learning data which uses minimization of the squared error, needs only a global score, which can be provided by a ranking of the acts through a suitable mechanism. Besides the fuzzy measure, the output also provides an estimation of the model error. One important advantage of using this method is that having a proper optimization solver, it always provides a solution, which fits the given global scores. Moreover, the method does not need any information on the decision strategy (importance and interaction). It is perfectly suitable for identifying a hidden decision behaviour. Although it may temper with the concept rankings provided by the decision maker.

In the identification based on combined fuzzy semantics and learning data, we need a ranking of the acts, not necessarily the global scores, a ranking on the importance of the criteria, and possibly some information on the interactions. There is no notion of model error in this approach in a sense that either there is a solution satisfying the constraints, or there is not. This method only requires an ordinal information on the alternative, and more importantly does not violate the ranking provided by the decision maker. Although, the method ideally needs some information on the decision strategy. For example, one may use the method without any information on constraints but only the ranking of the relations. This makes the space of feasible solutions very big that the solution chosen may not have a real interpretation in terms of decision strategy. This method is more suitable when we need to define or build a decision strategy in terms of importance and interaction.

The problem of finding 2-additive fuzzy measures has been formalized with the help of a linear program. It is obvious that the more the input information is poor, the more the solution set is big. Hence, it is desirable that the information is as complete as possible. However, if this information contains incoherencies then the solution set could be empty. It is important to note

that, in practice, finding a solution to this optimization problem does not necessarily end the identification process. If the results are not completely in accordance with the decision maker's reasoning, the initial preferences can be supplied with additional constraints and a new identification is performed. Such an incremental process is carried out until a satisfactory model is found. The most important property of this method is that the global scores are not needed as the input data. Moreover, there is no need to provide any information regarding the value of importance or interaction indices. However, using the least squares algorithm, this method does not necessarily give a unique solution. Moreover, the solution can be sometimes considered as too extreme.

## 4.8 Conclusion

Mechatronic systems are seen as a combination of cooperative mechanical, electronics and software components aided by various control strategies. They are often highly complex, because of the high number of their components, their multi-physical aspect and the couplings between the different engineering domains involved which complexifies the design task. Therefore, in order to achieve a better design process as well as a better final product more efficiently, these couplings need to be considered in the early stages of the design process. The concept of Mechatronic Multicriteria Profile (MMP) has been previously introduced to facilitate fitting the intuitive requirements for decision-making in the presence of interacting criteria in conceptual design. The MMP includes five main elements: machine intelligence, reliability, flexibility, complexity and cost. Each main criterion has a number of sub-criteria. The design process using MMP includes a fuzzy aggregation function based on Choquet fuzzy integrals which can efficiently model the interdependencies between a subset of criteria. Although, the main difficulty of the Choquet method is the identification of its fuzzy measures which exponentially increase by the number of design objectives. The objective of this study was to provide a framework to support the designers with identification of fuzzy measures based on various available information and the design preferences. We discussed four different methods of fuzzy measure identification applied to a case study of conceptual design of a vision-guided quadrotor drone. These methods include using a Sugeno fuzzy model, 2-additive measures, a learning data set and fuzzy semantics. The results obtained from each method have been presented in the case study section and finally, a discussion on each method and their applications was carried out.

From the implementation and results we infer that in the case that there is not enough information about the design preferences or the interaction and importance of coalitions of criteria,

using Sugeno  $\lambda$ -measures can be an abstract and efficient way. When only the relative global scores on each design alternative are available, the identification based on learning data is shown to be effective since this method does not need any information on importance and interaction indices. The data sets can be obtained from previous design cases or from an available data-base. This suggests an interesting subject of future work where an implementation of a web-based integrated platform connecting various design projects would be explored. In the absence of the global scores, the method combining the fuzzy measure semantics and learning data can be used. This method calls only for an ordinal information on the alternatives and their importance of the criteria. Moreover, using a 2-additive model, the global scores are not needed as the input data and there is no need to provide any information regarding the value of importance or interaction indices. However, the results are very sensitive to the coherence of the input information.



## CHAPTER 5 ARTICLE 3: DESIGN OF A VISION GUIDED MECHATRONIC QUADROTOR SYSTEM USING DESIGN FOR CONTROL METHODOLOGY

Abolfazl Mohebbi, Sofiane Achiche and Luc Baron

Published in *Transactions of the Canadian Society for Mechanical Engineering*, Vol. 40, 2016

### 5.1 Abstract

Designing mechatronic systems is known to be both a very complex and tedious process. This complexity is due to the high number of system components, their multi-physical aspects, the couplings between different engineering domains and the interacting and/or conflicting design objectives. Due to this inherent complexity and the dynamic coupling between subsystems of mechatronic systems, a systematic and multi-objective design approach is needed to replace the traditionally used sequential design methods. The traditional approaches usually lead to functional but non-optimal designs solutions. In this paper, and based on an integrated and concurrent design approach called “Design-for-Control” (DFC), a quadrotor UAV equipped with a stereo visual servoing system is used as a case study. After presenting the dynamics and the control model of the Quadrotor UAV and its visual servoing system, the design process has been performed in four iterations and as expected, the control performance of the system has been significantly improved after finishing the final design iteration.

### 5.2 Nomenclature

Symbol	Description	Unit	Symbol	Description	Unit
$x, y, z$	Absolute CoG position	$m$	$R_m$	Motor internal resistance	$\Omega m$
$\phi, \theta, \psi$	Euler angles	$rad$	$L_m$	Motor inductance	$H$
$m$	Overall mass	$kg$	$\eta$	Motor time-constant	—
$l$	Arm length	$m$	$r$	Gearbox reduction ratio	—
$\Omega_i$	speed of propeller-i	$rad/s$	$\gamma$	Gearbox efficiency	—
$\omega_m$	Motors angular speed	$rad/s$	$b_t$	Propeller Thrust factor	$N \cdot s^2$
$\tau_m$	Motors torque	$N \cdot m$	$d$	Propeller Drag factor	$N \cdot m \cdot s^2$

$\tau_d$	Motor load	$N.m$	$k_p$	Proportional control gain	—
$T_i$	Thrust of rotor - $i$	$N$	$k_d$	Derivative control gain	—
$I_{xx}$	Inertia moment- $x$ axis	$kg.m^2$	$k_i$	Integral control gain	—
$I_{yy}$	Inertia moment- $y$ axis	$kg.m^2$	$k_e$	Back-EMF constant	$rad/V.s$
$I_{zz}$	Inertia moment- $z$ axis	$kg.m^2$	$k_m$	Torque constant	$N.m/Amp$
$J_r$	Rotor inertia	$kg.m^2$	$f$	Camera focal length	$m$
$J_m$	Motor inertia	$kg.m^2$	$b$	cameras distance	$m$
$J_t$	Total rotor inertia	$kg.m^2$	$\lambda$	Visual servo control gain	—

### 5.3 Introduction

The domain of Mechatronic systems deals with an interactive and synergistic application of mechanics, electronics, controls, and computer engineering in the integrated design and development of electromechanical products. A multidisciplinary approach is ideally needed for the tasks of modeling, design, development, optimization and implementation of a mechatronic system.

Due to the large number of couplings and dynamic interdependencies occurring between elements and components, coming from different engineering domains with different physical natures; the design of Mechatronic systems is considered to be a highly complex task on various levels [4, 8, 118, 120]. Therefore, in order to achieve a better design process as well as a better final product more efficiently, these couplings need to be considered in the early stages of the design process [77, 119, 141]. The main difficulty in the process of designing Mechatronic systems is that it requires a system perspective during all stages of the design process in such a way that system interactions can be considered at all times, as a comprehensive system modeling is required. Design of a large number of modern mechatronic systems can be mapped into at least three aspects of structure or machine body, control system, and task [142]. This design process has been traditionally performed in a sequential manner where the design of the structure is carried out first and then the control system design is carried out. In such a sequential design process, once a mechatronic machine is developed, the mechanical structure can be hardly altered and all the mechanical parameters are therefore time-invariant.

A number of research efforts have demonstrated that compared to systems designed by a traditional sequential approach, designing the structure and control in a concurrent process, considerably improves the system performance and efficiency [63, 143-147]. Accordingly, on the one hand the mechanical system design can contribute to the controller design and on the other

hand, the behavior of the control system can be studied to further improve the mechanical design to ideally improve the whole system performance. Integrated and concurrent design methodologies have been proposed over a number of works to optimally relate the mechanical and control components of mechatronic systems [148, 149]. In [148], various approaches towards design of control systems for mechatronic products are explored to overcome the mechanical limitations. In [149], a concurrent structure-control redesign approach has been proposed to find the minimum positioning time of an underactuated robot manipulator, by considering a synergetic combination between the structural parameters and a specific control algorithm.

Due to their non-convex nature, many difficulties arise when solving optimization problems which simultaneously involve structural and control variables and parameters. Thus, despite the advances in optimal control design, optimal integrated Mechatronic system design is still an open and challenging research area. The other difficulty faced when seeking an optimal integrated design of Mechatronic systems, is the problem of modeling multidisciplinary systems that includes all the interconnections, and interactions between the subsystems and the design parameters over several engineering domains.

Toward the objective of optimal integrated design of Mechatronic systems, several investigations have been done in the past decade. In [150], authors focused on the control system design for direct-drive manipulators performing high-speed trajectory control applications. They stated that the control algorithm could be simplified by using parallel drive mechanism in order to get invariant inertia and decoupled dynamics. First they introduced a concept for simplification and decoupling of system dynamics. Then, a simple procedure for control system design was presented. Although their method of design was case-specific. In [151], a method to reduce the control effort and increase the dynamic performance of an actively controlled space structure is presented. With another application, a method of a mass-redistribution has been utilized in [152], to improve the motion tracking performance of manipulators. In this study, the structure of a robot arm was reduced into equivalent point masses thus the gravitational term in the dynamic model has been eliminated. Then, a simple control strategy was used and satisfactory trajectory tracking results were reported. In [63] the control performance of a closed-chain machine has been improved by incorporating a PD control scheme along with a design approach of shaking force/shaking moment balancing. In all the above-mentioned design studies, the mechanical structure of the system is usually determined in advance without considering the future aspects of the controller design. Therefore a “perfect” control action may become far from practice, due to

limitations imposed by the poorly designed mechanical structure, even if much effort has been made on the design of advanced controllers.

A more general concept called Design for Control (DFC) was proposed in [153] where the design of the mechanical structure has been simplified as much as possible in such way that the dynamic modeling of the system is facilitated and as it is less complex. Thus, a better overall control performance has been achieved. In this method, the physical understanding of the overall system is fully explored with the aim of simplification of the controller design as well as the execution of the control algorithm with the least hardware-in-the-loop restrictions. In [146, 154, 155], three specific design methods for machine body were proposed for the DFC approach based on considering invariant potential energy, invariant generalized inertia and partially invariant generalized inertia in order to perform a re-design and simplify the system dynamics in just one iteration. The results from all three dynamics derivation methods, were also compared. In these studies, although the design integration takes place in a single step, less effort was focused on design of the control system. Furthermore, the optimality of the results for structure-control design is in doubt. In [149], a concurrent design approach is proposed to find the minimum positioning time of an underactuated two-link manipulator where a synergetic combination between the structural parameters and a control law has been considered. In their approach, the concurrent redesign process was formulated as a dynamic optimization problem, in which the structural and control parameters are considered as independent variables. Although the optimality is more or less ensured in this study, a high computational load was reported for design of a simple electromechanical system.

In this paper, the DFC is used to design a complex mechatronic system composed of a vision-guided UAV quadrotor. In terms of system dynamics, a quadrotor is an underactuated system with six degrees of freedom and four inputs which is inherently unstable and difficult to control. Thus, the design and control of this nonlinear system is a challenge from both practical and theoretical point of views [156-159]. Integrating the sensors, actuators and intelligence into a lightweight vertically flying system with a decent operation time is not a trivial task to achieve. Designing an autonomous quadrotor is basically a complex task since it requires dealing with numerous design parameters that are originated from various engineering disciplines and subsystems and more importantly they are closely interdependent. Taking a decision about all these parameters requires a clear integrated methodology. Moreover, in order to enable the system with autonomous capabilities, a visual feedback control strategy will be used which extensively

increases the parameters of the system that need to be optimized hence increasing the overall complexity of the design task. The remaining of this paper is organized as follows; Section 5.4 recalls the dynamic model and formulations of a small quadrotor system. In Section 5.5, the control system design is presented. A formulation for the image-based stereo visual servoing system is also presented in this section. In Section 5.6, the DFC-based integrated design strategy is introduced while in section 5.7 this method is utilized to optimize the integrated design of the quadrotor system. This section also includes validations with computer simulations. Finally, the concluding remarks are discussed in section 5.8.

#### 5.4 System Modelling and Formulation

The design of quadrotor systems is a highly complex task since various engineering domains and their affecting factors e.g. aerodynamics, mechanics, control and intelligence should be included in the design and optimization process. The model of the quadrotor should consider all the important effects such as aerodynamic, inertial counter torques, friction, gyroscopic and gravitational effects. Therefore, in this paper, Euler- Lagrange formalism and DC motor equations were used to model the Quadrotor system. The dynamic model developed in this section is derived based on the following simplifying assumptions;

- The structure of the system is supposed to be rigid and symmetric.
- The thrust and drag affecting the system are considered to be proportional to the square of propellers speed [160].
- The origin of the body fixed frame and the center of gravity (COG) are located at the same position.

Figure 5-1 illustrates the coordinate system for the quadrotor model in which  $W$  is the fixed world coordinate frame and  $B$  is the body fixed frame. The space orientation is also given by a rotation matrix  $R$  from frame  $B$  to  $W$ , where  $R \in SO3$ .

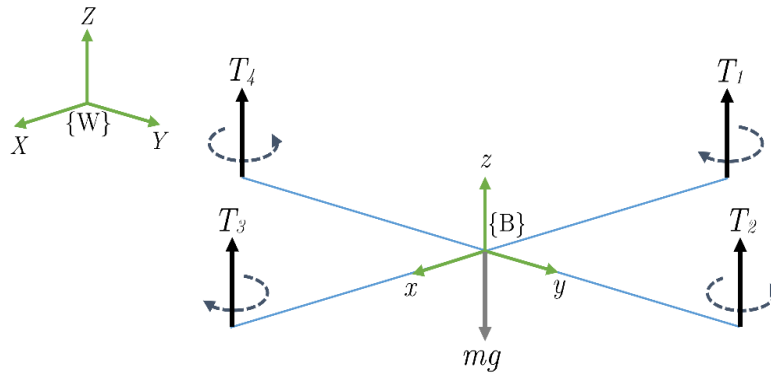


Figure 5-1: Quadrotor model coordinate system

For any point expressed in the fixed world coordinate frame, we can write (with, C:cos, S:sin);

$$\begin{cases} r_X = (C\psi C\theta)x + (C\psi S\theta S\phi - S\psi C\phi)y + (C\psi S\theta C\phi + S\psi S\phi)z \\ r_Y = (S\psi C\theta)x + (S\psi S\theta S\phi + C\psi C\phi)y + (S\psi S\theta C\phi - C\psi S\phi)z \\ r_Z = (-S\theta)x + (C\theta S\phi)y + (C\theta C\phi)z \end{cases} \quad (6.1)$$

The corresponding velocities are obtained by differentiation of Eq. (5.1). The squared magnitude of the velocity for any point can be given by:

$$\nu^2 = \nu_X^2 + \nu_Y^2 + \nu_Z^2 \quad (6.2)$$

From equation Eq. (5.2), and by assuming the inertia matrix to be diagonal, the kinetic energy expression can be written as follows:

$$T = \frac{1}{2}I_{xx}(\dot{\phi} - \dot{\psi}S\theta)^2 + \frac{1}{2}I_{yy}(\dot{\theta}C\phi + \dot{\psi}S\phi C\theta)^2 + \frac{1}{2}I_{zz}(\dot{\theta}S\phi - \dot{\psi}C\phi)^2 \quad (6.3)$$

Moreover, for the potential energy  $U$  and with regards to the fixed frame, we can write:

$$U = \int x dm(x)(-gS\theta) + \int y dm(y)(gS\phi C\theta) + \int z dm(z)(gC\phi C\theta) \quad (6.4)$$

Using the Lagrangian function and the derived formula for the equations of motion we have:

$$L = T - U, \quad Q_i = \frac{d}{dt} \left( \frac{\partial L}{\partial \dot{q}_i} \right) - \frac{\partial L}{\partial q_i} \quad (6.5)$$

where  $q_i$  are the generalized coordinates and  $Q_i$  are the generalized forces. Moreover, the non-conservative torques acting on the system result, firstly from the action of the thrust difference of each pair. Thus;

$$\begin{aligned} \tau_x &= b_t l (\Omega_4^2 - \Omega_2^2) \\ \tau_y &= b_t l (\Omega_3^2 - \Omega_1^2) \\ \tau_z &= d(\Omega_2^2 + \Omega_4^2 - \Omega_1^2 - \Omega_3^2) \end{aligned} \quad (6.6)$$

where the  $\Omega_i$  are angular speed of  $i^{th}$  propeller. From the gyroscopic effects resulting from the propellers rotation we have the following torques:

$$\begin{aligned} \tau'_x &= J_r w_y (\Omega_1 + \Omega_3 - \Omega_2 - \Omega_4) \\ \tau'_y &= J_r w_x (\Omega_2 + \Omega_4 - \Omega_1 - \Omega_3) \end{aligned} \quad (6.7)$$

where  $w_x, w_y$  are the vectors of body rotational speeds which are approximated by the derivatives of Euler angles. Consequently, The quadrotor dynamic model describing respectively the roll, pitch and yaw rotations contains three terms which are the gyroscopic effect resulting from the rigid

body rotation, the gyroscopic effect resulting from the propeller rotation coupled with the body rotation and finally the actuators action. Applying the small angles approximation, we obtain the following:

$$\begin{cases} \ddot{\phi} = \frac{J_r \dot{\theta} (\Omega_1 + \Omega_3 - \Omega_2 - \Omega_4)}{I_{xx}} + \frac{(I_{yy} - I_{zz})}{I_{xx}} \dot{\theta} \dot{\psi} + \frac{b_t l (\Omega_4^2 - \Omega_2^2)}{I_{xx}} \\ \ddot{\theta} = \frac{J_r \dot{\phi} (\Omega_1 + \Omega_3 - \Omega_2 - \Omega_4)}{I_{xx}} + \frac{(I_{yy} - I_{zz})}{I_{xx}} \dot{\phi} \dot{\psi} + \frac{b_t l (\Omega_4^2 - \Omega_2^2)}{I_{xx}} \\ \ddot{\psi} = \frac{-d(\Omega_2^2 + \Omega_4^2 - \Omega_1^2 - \Omega_3^2)}{I_{zz}} + \frac{(I_{xx} - I_{yy})}{I_{zz}} \dot{\phi} \dot{\theta} \end{cases} \quad (6.8)$$

Using a Newton dynamics formulations, we can also achieve:

$$\begin{cases} \ddot{x} = \frac{U_1}{m} (S\psi S\phi + C\psi S\theta C\phi) \\ \ddot{y} = \frac{U_1}{m} (-C\psi S\phi + S\psi S\theta C\phi) \\ \ddot{z} = -g + \frac{U_1}{m} (C\theta C\phi) \end{cases} \quad (6.9)$$

where  $U_i$  are the system inputs as;

$$\begin{aligned} U_1 &= b_t \sum_{i=1}^4 \Omega_i^2, \\ U_2 &= b_t (\Omega_4^2 - \Omega_2^2), \\ U_3 &= b_t (\Omega_3^2 - \Omega_1^2), \\ U_4 &= d(\Omega_2^2 + \Omega_4^2 - \Omega_1^2 - \Omega_3^2), \\ \Omega &= \Omega_1 + \Omega_3 - \Omega_2 - \Omega_4. \end{aligned} \quad (6.10)$$

The rotors are considered to be driven by DC-motors with the following well established equations:

$$\begin{cases} L_m \frac{di}{dt} = u - Ri - k_e w_m \\ J_m \frac{dw_m}{dt} = \tau_m - \tau_d \end{cases}, \quad (6.11)$$

where  $u$  is the input voltage. Using a small motor with a very low inductance, the second order DC-motor dynamics may be approximated by the following equation:

$$J_m \frac{dw_m}{dt} = -\frac{k_m^2}{R} w_m - \tau_d + \frac{k_m}{R} u. \quad (6.12)$$

Now, by considering the propeller and the gearbox models, the above equation becomes:

$$\dot{w}_m = -\frac{1}{\eta}w_m - \frac{d}{\gamma r^3 J_t}w_m^2 + \frac{1}{k_m \eta}u, \quad (6.13)$$

where  $\eta = RJ_t/k_m^2$  is the motor time-constant. Now, by linearizing the above equation around an operation point  $\dot{w}_0$  we achieve:

$$\dot{w} = -Aw_m + Bu + C \quad (6.14)$$

where:

$$A = \left( \frac{1}{\eta} + \frac{2dw_0}{\gamma r^3 J_t} \right), \quad B = \left( \frac{1}{k_m \eta} \right), \quad C = \left( \frac{dw_0^2}{\gamma r^3 J_t} \right) \quad (6.15)$$

## 5.5 Controller Design

The control system of the proposed quadrotor UAV, consists of two components of motion control system and visual servoing (vision-based control) system. The cooperative configuration of these control systems is illustrated in a single control structure in Figure 5-2.

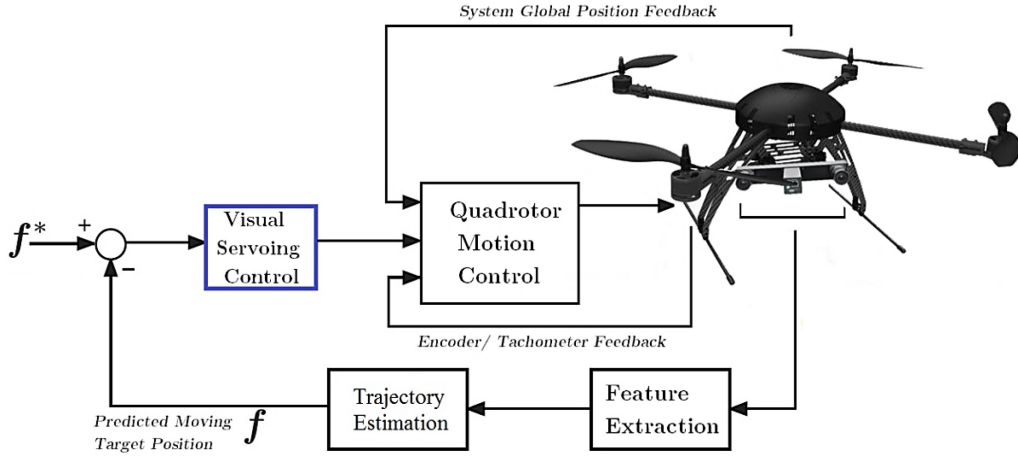


Figure 5-2: UAV Quadrotor control structure consisting of attitude motion control and visual servoing control

### 5.5.1 Motion Control

In this paper a PID controller is proposed for appropriate position control of the quadrotor. The dynamic model of the system, contains two gyroscopic effects. The influence of these effects in the present case and by considering a near-hover situation is less important than the motor's model. In order to design a PID controller for this system, one can neglect these gyroscopic effects and thus remove the cross couplings between body and propellers. The following equations have been derived by simplification of the system dynamics formulation:



$$\ddot{\phi} = \frac{lU_2}{I_{xx}}, \quad \ddot{\theta} = \frac{lU_3}{I_{yy}}, \quad \ddot{\psi} = \frac{U_4}{I_{zz}} \quad (6.16)$$

The transfer functions of quadrotor attitude plant (i.e. roll, pitch and yaw) can be obtained separately as follows:

$$\frac{\phi(s)}{U_2(s)} = \frac{l}{I_{xx}s^2}, \quad \frac{\theta(s)}{U_3(s)} = \frac{l}{I_{yy}s^2}, \quad \frac{\psi(s)}{U_4(s)} = \frac{1}{I_{zz}s^2}. \quad (6.17)$$

The error signals can be also introduced based on the difference between the current states and desired angles as:

$$e_\phi = \phi_d - \phi, \quad e_\theta = \theta_d - \theta, \quad e_\psi = \psi_d - \psi. \quad (6.18)$$

The system can be also described by using the motor inputs in Laplace domain, as:

$$\phi(s) = \frac{B^2lb}{s^2(s+A)^2I_{xx}}(\Omega_4^2(s) - \Omega_2^2(s)) \quad (6.19)$$

$$\theta(s) = \frac{B^2l}{s^2(s+A)^2I_{yy}}(\Omega_3^2(s) - \Omega_1^2(s)) \quad (6.20)$$

$$\psi(s) = \frac{B^2d}{s^2(s+A)^2I_{zz}}(\Omega_4^2(s) + \Omega_2^2(s) - \Omega_3^2(s) - \Omega_1^2(s)) \quad (6.21)$$

where  $A$  and  $B$  are the coefficients of the linearized rotor dynamics from equation 14. The output of a PID controller, which is also the input to the system control plant (e.g.  $\phi(s)$ ), in the time domain is as follows:

$$u_i(t) = k_p e_i(t) + k_i \int e_i(t) dt + k_d \frac{de_i(t)}{dt} \quad (6.22)$$

The transfer function of a PID controller is found by taking the Laplace transform of the last equation;

$$PID = G_C(s) = \left( k_p + \frac{k_i}{s} + k_d s \right) = \frac{k_d s^2 + k_p s + k_i}{s} \quad (6.23)$$

### 5.5.2 Visual Servoing Control

In general, it can be stated that in an image-based visual servoing system, the goal of vision-based control scheme is to minimize the error defined as:

$$e(t) = s - s^*, \quad (6.24)$$

where  $s$  and  $s^*$  are the vectors of current and desired image features. In the case of a traditional proportional controller, the input to the robot controller  $u_c$  is designed by letting  $\dot{e} = -\lambda e$ :

$$u_c = -\lambda J_e^+ e, \quad (6.25)$$

where  $J_e$  is the image interaction matrix which relates the time variation of error  $e$  and the camera velocity and  $J_e^+$  is the Moore-Penrose pseudo-inverse of the interaction matrix.  $\lambda$  is the proportional gain for the visual controller. In the case of moving image features we have;

$$u_c = J_e^+ \left( -\lambda e - \frac{\partial e}{\partial t} \right), \quad (6.26)$$

where the term  $\partial e / \partial t$  represents the time variation of  $e$  caused by the target motion which is considered to have a constant velocity. In our case we assume that the vision system is composed of a stereo vision system with two parallel cameras which are perpendicular to the baseline [114, 161]. The focal points of two cameras are apart at distance  $b/2$  with respect to origin of sensor frame  $C$  on the baseline which means the origin of the camera frame, is in the center of these points. Focal distance of both cameras is  $f$  so the image planes and corresponding frames for left and right cameras are located with the distance  $f$  from the focal points and orthogonal to the optical axis. We assign  $L$  and  $R$  as the frames of the left and right images. Figure 3 illustrates the case where both cameras observe a 3D point  ${}^C P$ . Using the image interaction matrices for the left and right cameras the stereo image interaction matrix,  $J_{st}$ , can be calculated as:

$$J_{st} = \begin{pmatrix} J_l & .^l M_C \\ J_r & .^r M_C \end{pmatrix} \quad (6.27)$$

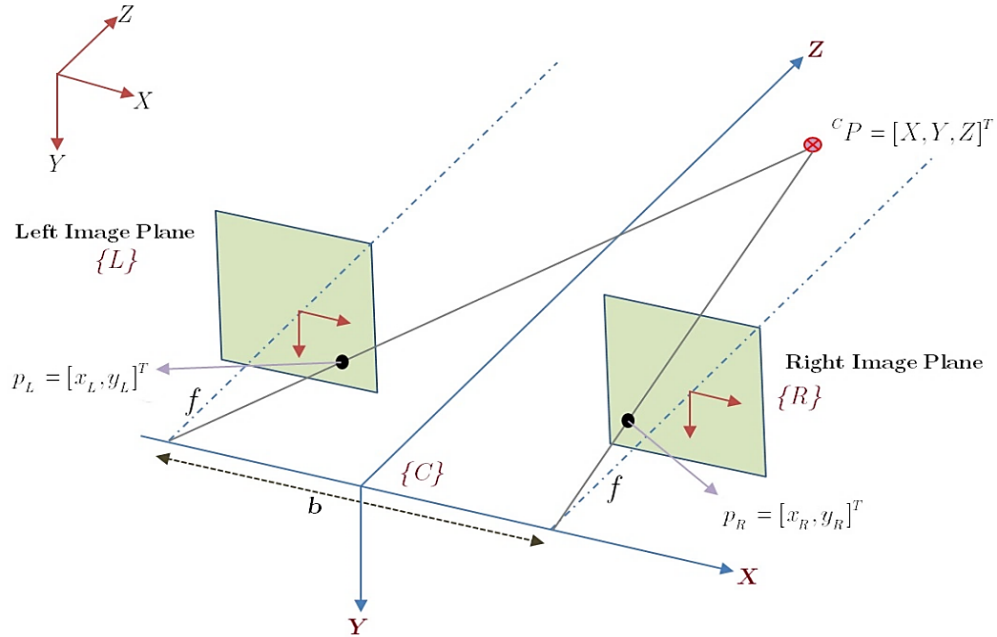


Figure 5-3: Model of the parallel stereo vision system observing a 3D point

The image interaction matrix for each camera is calculated as:

$$J_i = \begin{bmatrix} -\frac{1}{Z_i} & 0 & \frac{x_i}{Z_i} & x_i y_i & -(1 + x_i^2) & y_i \\ 0 & -\frac{1}{Z_i} & \frac{y_i}{Z_i} & 1 + x_i^2 & -x_i y_i & -x_i \end{bmatrix} \quad (6.28)$$

The stereo feature vector is defined as  $s = [x_l, y_l, x_r, y_r]^T$  where  $p_l = [x_l, y_l]^T$ ,  $p_r = [x_r, y_r]^T$  are the normalized image coordinates of the 3D point, observed by the left and right cameras respectively. A perspective camera model can be used to project observed point into left and right image planes. Thus, the following equations hold for 3D coordinates of the observed point:

$$(X, Y, Z) = \left( \frac{b x_l + x_r}{2 x_l - x_r}, \frac{b y_l}{x_l - x_r}, \frac{b}{x_l - x_r} \right) \quad (6.29)$$

## 5.6 Integrated Design Strategy

An engineering design process can be parametrically defined as a mapping from a requirement space consisting of behaviors to a structural parameter space [5]. To gain insight into the design of a mechatronic system, Li et al. [153] suggested dividing the requirement space into two subspaces which represent (this formalism is adopted in this paper):

- 1) Real-time behaviors (RTBs) and
- 2) Non-realtime behaviors (Non-RTBs)

Following this division of the requirements, system parameters in structural space can also be divided into two subspaces as follows:

- 1) Real-time (or controllable) parameters (RTPs) and
- 2) Nonreal-time (or uncontrollable) parameters (Non-RTPs)

From above, “real-time” means parameters, specifications, constraints and behaviors that may change with time after the machine is built. Controller gains, accuracy and speed are some examples of RTPs and RTBs. On the other hand, Nonreal-time parameters, constraints and specifications are the ones that can be hardly changed after the machine is built, because it would be costly to change them. Structural material, dimensions, weight, and workspace can be considered as Non-RTPs and Non-RTBs. Traditional methodologies for mechatronic systems design consisted of sequences of the real-time and non-real-time requirements rather than a concurrent design process. At the beginning of such a traditional design scenario, Non-RTPs are designed based on the Non-RTB specifications. This process itself includes designing the

mechanical structure and then adding electrical components. The mechanical structure (e.g., configurations, dimensions, layout of actuators and sensors, etc.) is first determined based on the requirements in the Non-RTB space (e.g., workspaces, maximum payloads, etc.). Subsequently, RTPs (e.g., controller algorithm and parameters, signal conditioning) are determined based on RTB specifications (e.g., desired trajectory, speed, stability, etc.) to control the already established structure. Due to recent advancements in control and computer engineering one may conclude that the design of the imperfections and inadequacies in structure and hardware of a Mechatronic system can be compensated by some state-of-the-art control schemes. This thinking can be easily criticized because a perfect control response may be hardly achieved due to hardware limitations and dynamic interactions, regardless of the effort devoted to the design of the control system. Although it can be observed in several cases that the performance of a Mechatronic system can be improved by using better control strategies, but reaching design process “optimality” is in serious doubt. In a concurrent model for mechatronic systems design (Figure 5-4), both RTBs and Non-RTBs should be considered simultaneously for realization of RTPs and Non-RTPs. In a Mechatronic system, the system performance, which is the real-time and nonreal-time system behaviors (RTBs and Non-RTBs), explicitly relies on the design of its control algorithm and parameters (RTPs) and also the design of the mechanical structure (Non-RTPs). More specifically, the design specifications for controller and limitations should be considered in the design of the mechanical structure and in the considering the alternatives for the electrical hardware. In addition, unlike in a traditional design, controllability and programmability of RTPs should be considered as an opportunity to further improve the design after the machine is built.

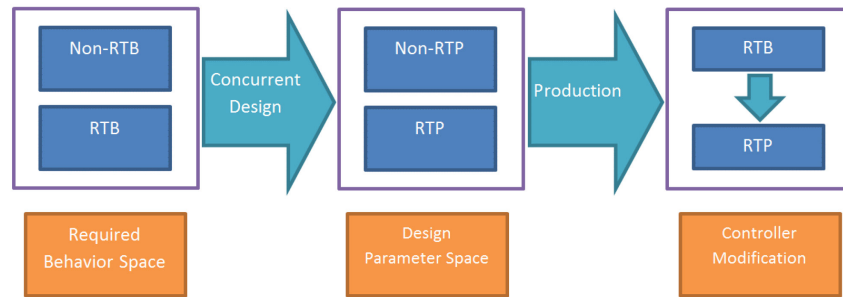


Figure 5-4: Process of concurrent Mechatronic system design adopted from [153]

Let  $X_R$  and  $X_N$  be RTP and Non-RTP design vectors. We also assume there exists  $n$  RTPs and  $m$  Non-RTPs, that is  $X_R \subset R^n$ , and  $X_N \subset R^m$ , where the total number of design parameters is  $q = m + n$ . Respectively, the determination of design parameters is subject to a set of constraints produced by the behavior requirements. Thus, let  $Y_R$  and  $Y_N$  denote  $u$ -RTB and

$v$ —NonRTB requirements which sums to  $p = u + v$  as the total number of variables in the requirement space. Thus,  $Y_R \subset R^u$ , and  $Y_N \subset R^v$ . Assuming  $Y = [Y_R, Y_N]$ , the performance error can be defined as  $E = Y - Y_d$ , where  $Y_d$  is the vector of desired behaviors. Accordingly, let  $S_{min}$  and  $S_{max}$  denote the design requirements associated with a particular design problem, where “min” and “max” indicate the performance indices of the requirements to be minimized and maximized, respectively. Finally, let  $P$  denote the system actuation power. A mechatronic system design problem can be described using the following mathematical models for objectives and constraints [153]:

$$E = \min \sum_{i=1}^p \alpha_i |E_R|_i + \xi_i |E_N|_i \quad (6.30)$$

$$P = \min \sum_{i=1}^{DOF} \beta_i p_i, \quad (6.31)$$

$$S_{min} = \min \sum_{i=1}^{q1} \lambda_i |S_{min}|_i, \quad (6.32)$$

$$S_{min} = \max \sum_{i=1}^{q2} \rho_i |S_{max}|_i, \quad (6.33)$$

$$I = E + P + S_{min} + S_{max}, \quad (6.34)$$

where  $\alpha_i, \xi_i, \beta_i, \lambda_i$ , and  $\rho_i$  are weighting factors determined by the designer,  $p_i$  is the power generated by each actuator in the system and  $q_1$  and  $q_2$  are the number of the design parameters associated with the minimized and maximized requirements. To optimize the overall design performance, a performance index ( $I$ ) is introduced to integrate are introduced individual objectives in one equation. The equality and inequality constraints can be respectively expressed by:

$$Y_R^E = f_R^E(X_R, X_N), \quad (6.35)$$

$$Y_N^E = f_N^E(X_N),$$

$$Y_{R,low} < f_R^I(X_R, X_N) < Y_{R,up} \quad (6.36)$$

$$Y_{N,low} < f_N^I(X_N) < Y_{N,up}$$

where the superscript “ $I$ ” indicates the inequality constraints and the superscript “ $E$ ” indicates the equality constraints. From the above design constraints it can be observed that, for a Mechatronic system, the system dynamic performance (RTBs or  $Y_R$ ) depends on both the control parameters (RTPs or  $X_R$ ) and the mechanical structure behaviors (NonRTPs or  $Y_N$ ). As stated

before, the essence of DFC method is to design the mechanical structure ( $X_N$ ) in an effort to achieve a simple dynamic model for the ease of designing the control system ( $X_R$ ), to ideally achieve an optimal system dynamic performance ( $Y_R$ ). In a simulation-based iterative integrated design strategy,  $X_N$  is first set for a mechanical structure based on the desired behaviors and requirements (associated with  $Y_N$  directly yet  $Y_R$  indirectly). This step can be expressed as:

$$Y_1 = f_1(X_N). \quad (6.37)$$

Then having  $X_R$  determined, the dynamic performance  $Y_2$  is obtained (based on  $Y_R$  explicitly and  $Y_N$  implicitly). This step can be expressed as:

$$Y_2 = f_2(Y_1, X_R). \quad (6.38)$$

Next,  $Y_N$  will be configured by comparing the desired behaviors with the measured ones. If the result is not satisfactory, then  $X_R$  is modified to improve the control performance. Thus, we have:

$$Y_3 = f_3(Y_2, X_N). \quad (6.39)$$

If the control performance  $Y_3$  does not satisfy the requirements,  $X_R$  is varied again to attain an improved performance. This step can be formulated as:

$$Y_4 = f_4(Y_3, X_R). \quad (6.40)$$

For an algorithmic implementation, the iterations can be formulated as:

$$\begin{cases} Y_{2i-1} = f_{2i-1}(Y_{2i-2}, X_N) \\ Y_{2i} = f_{2i}(Y_{2i-1}, X_R) \end{cases}, \quad i = 1, 2, \dots, k. \quad (6.41)$$

The design procedure iterates until a final design on  $X_R$  is found that enables the system to achieve a satisfactory performance. When an analytical system dynamic model is obtainable, the iterative design process described before can be carried out via a simulation process.  $X_N$  can be further changed towards various directions along the solution-search path. It is quite possible to find a solution to the optimal design problem with the fewest constraints. Having the dynamics model,  $X_N$  can be varied until a simpler dynamic model can be achieved which results in facilitating the procedure of the control system design.

## 5.7 DFC-Based Design Optimization

Using the Design-for-Control (DFC) approach, an integrated design of a vision-guided quadrotor UAV is detailed in this section. Before starting the design process, first we need to define parameters and behaviors. The first column of Table 5-1 classifies all the RTPs and Non-RTPs,

as the design parameters in the process of designing a vision-guided quadrotor drone with a PID attitude control system. After identifying all the parameters and behaviors, the integrated design approach can be divided in 4 iterations as follows:

### 5.7.1 Iteration 1: Deign $X_N$ Based on Non-RTBs, $Y_N$ :

The first step is to determine  $X_N$ , the mechanical structure parameters, so that the specified Non-RTBs,  $Y_N$ , are satisfied. As the first requirement and based on a series of commercial benchmarks, the quadrotor is subjected to the following physical constraints;

$$0.2 \leq l \leq 0.4 \text{ (m)} \quad (6.42)$$

$$m_t \geq 0.4 \text{ (kg)} \quad (6.43)$$

$$0.006 \leq I_{xx}, I_{yy} \leq 0.01 \text{ (kg.m}^2\text{)} \quad (6.44)$$

$$0.01 \leq I_{zz} \leq 0.03 \text{ (kg.m}^2\text{)} \quad (6.45)$$

where the inertia moments can be calculated from a simple physical model of the quadrotor where it consists of two rods as the arms, one disk at center and four concentrated mass at the end of each arm.

One of the major physical limitations of a quadrotor is the propeller's rotational speed which is constrained by the motor saturation speed. This saturation speed of the propellers should be approximately 41% higher than the hovering speed [162]. The propeller's rotational speed in hovering condition can be found by solving equations 8-10 for equilibrium point:

$$\Omega_H = \left( \frac{mg}{4b_t} \right)^{\frac{1}{2}} \quad (6.46)$$

Thus, having the condition of  $\Omega_i \leq 350 \text{ (rad/s)}$  based on some frequently used brushless motors and also the propellers' trust factor of  $b_t = 3.15e - 5$ , we can achieve an allowable total mass and payload capacity:

$$m \leq \frac{4b_t\Omega_{i,max}^2}{g(1.41)^2} = 0.791 \text{ (kg)} \quad (6.47)$$

Having the aforementioned Non-RTB constraints the first set of Non-RTPs can be calculated as the starting point of the optimization problem. The design result of  $X_N$  is given in the first column of Table 5-1.

### 5.7.2 Iteration 2: Design $X_R$ Based on RTBs, $Y_R$ :

Once the initial design of the mechanical structure is completed, the motion controller and visual servoing system must be designed carefully such that the required dynamic and visual performances are satisfied. Thus, the design objective is to minimize the performance index over the entire range of motion:

$$I_R = E_R^Q + E_R^C + P, \quad (6.48)$$

$$E_R^Q = \min \left( \alpha_1 \int_0^{t_f} ((X(t) - X_d)^2 + (Y(t) - Y_d)^2 + (Z(t) - Z_d)^2) dt \right. \\ \left. + \alpha_2 \int_0^{t_f} ((\dot{X}(t) - \dot{X}_d)^2 + (\dot{Y}(t) - \dot{Y}_d)^2 + (\dot{Z}(t) - \dot{Z}_d)^2) dt \right) \quad (6.49)$$

$$E_R^C = \min \left( \alpha_3 \int_0^{t_f} (s(t) - s^*)^2 dt \right) \quad (6.50)$$

$$P = \min \left( \beta \int_0^{t_f} |T_i(t)| dt \right) \quad (6.51)$$

where  $E_R^Q$  is the minimum performance error for position and velocity tracking and  $E_R^C$  is the minimum performance error for the visual servoing system.  $P$  signifies the driving torque generated by the motion control, and  $\alpha_i, \beta$  are the weighting factors to be determined. Accordingly, and again based on frequently used commercial benchmark parameter, the following RTB constraints (control inputs) are imposed on the controller design:

$$0 \leq \sum T_i \leq 2mg \quad (6.52)$$

$$|\phi| \leq 0.6 \text{ rad} \quad (6.53)$$

$$|\theta| \leq 0.6 \text{ rad} \quad (6.54)$$

$$0 \leq \psi \leq 0.01 \text{ rad} \quad (6.55)$$

For translational speed and descend rate we also have:

$$|\dot{z}| \leq 5 \text{ m. s}^{-1} \quad (6.56)$$

$$|\dot{x}| \leq 10 \text{ m. s}^{-1} \quad (6.57)$$

$$|\dot{y}| \leq 10 \text{ m. s}^{-1} \quad (6.58)$$



The target object which is being tracked by the vision system is moving along a circle path on  $x - y$  plane with the radius of 4 meters and the quadrotor is required to follow the target with the height of 2 meters with respect to target. The target object is travelling with the speed of  $10 \text{ m/s}$  along the circular path and the quadrotor is not allowed to have a translational speed more than the object. In order to simplify the problem no minimum time-trajectory is given. The control design problem is solved using MATLAB optimization toolbox. To ensure each performance characteristic (i.e.  $E_R^Q$ ,  $E_R^C$  and  $P$ ) contributes properly to the performance index in an equivalent magnitude, the weighting factors are selected to be  $\alpha_1 = 1.0$ ,  $\alpha_2 = 0.1$ ,  $\alpha_3 = 0.5$ ,  $\beta = 0.005$ . The design result of  $X_R$  is given in the second column of Table 5-1. The simulation model built in SIMULINK to reflect the design process results is shown in Figure 5-5.

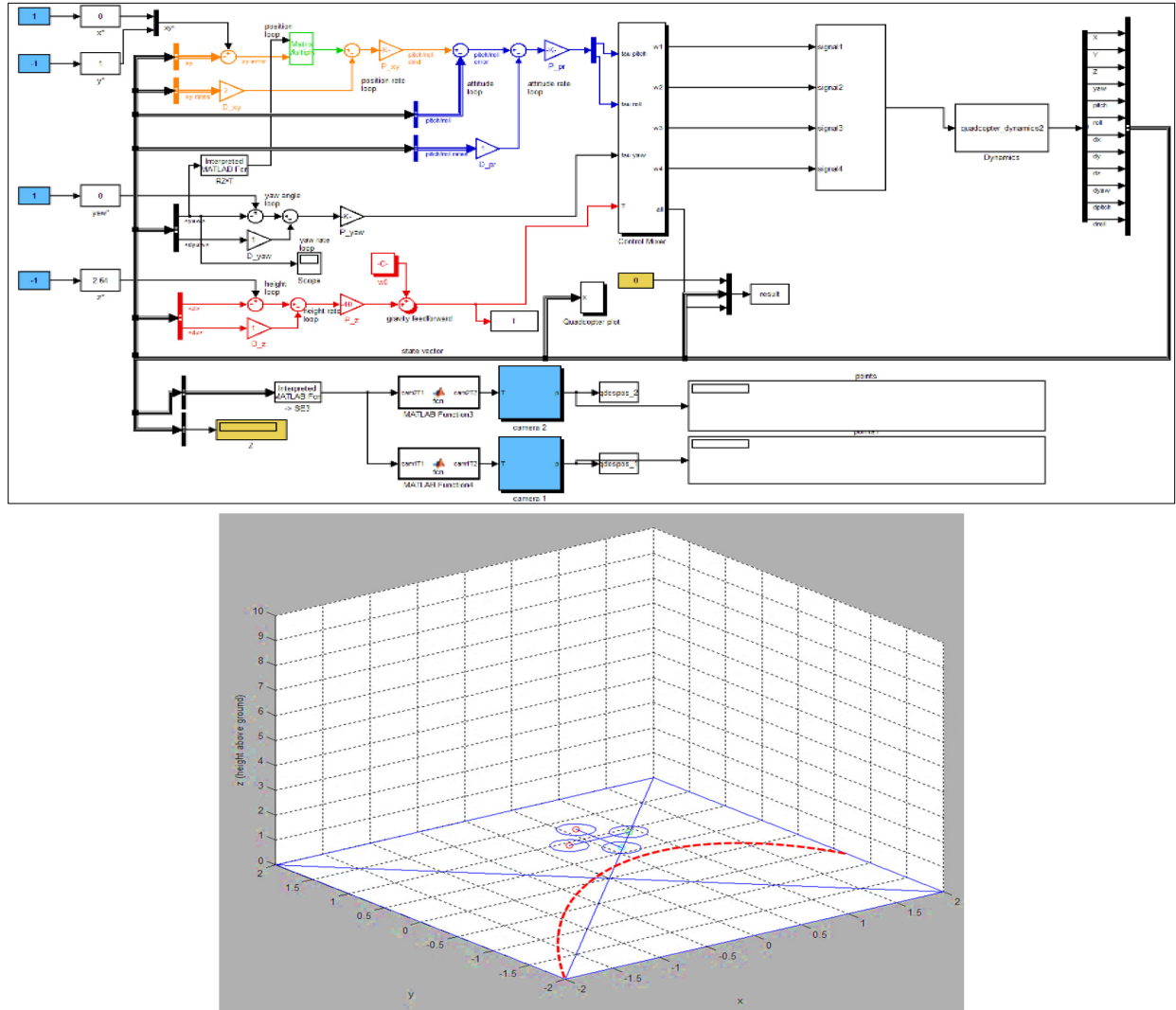


Figure 5-5: The simulation model of the vision-guided Quadrotor system

Using the control gains as a result from the aforementioned optimization solution, the tracking performances for both motion and vision-based control are comparatively displayed in Figures 6 and 7 and as it can be observed some undesired performance appears in the position tracking and the visual features error are also not quite satisfactory. Hence an extra iteration is needed.

### 5.7.3 Iteration 3: Redesign $X_N$ to Improve Non-RTBs, $Y_N$ :

In the third iteration the NonRTPs,  $X_N$ , will be modified with the aim of simplifying the system dynamic model so that the controller design on  $X_R$  can be facilitated. In this redesign, the following stability constraints are used for the modification of  $X_N$  [163]. These stem from the stability constraints in the hovering position.

The longitudinal dynamics of a quadrotor system can be considered as the dominant dynamics of the vehicle [164]. Around hovering position, the motion is largely decoupled in each axis. If the geometry of the system can be considered as symmetric, the important attitude dynamics can be described by a single equation. The natural stability of these dynamics is important to be analysed to provide insight into the best airframe geometry for controllability of the system [163]. From the basic dynamic equations for a quadcopter with translational and rotational motion in only  $x$  and  $\theta$ , and equal speeds on all rotors, the stability derivative equation is [164]:

$$\begin{vmatrix} -ms + \frac{\partial x}{\partial \dot{x}} & \frac{\partial x}{\partial \dot{\theta}}s - mg \\ \frac{\partial \theta}{\partial \dot{x}} & -I_{yy}s^2 + \frac{\partial \theta}{\partial \dot{\theta}} \end{vmatrix} \begin{vmatrix} \dot{x} \\ \dot{\theta} \end{vmatrix} = 0, \quad (6.59)$$

where  $s$  is the Laplace transform of the differential operator. Applying the Routh-Hurwitz stability criterion, the first column of the stability parameters table is needed to be all strictly positive. Thus;

$$\left( \frac{1}{m} \frac{\partial x}{\partial \dot{x}} + \frac{1}{I_{yy}} \frac{\partial \theta}{\partial \dot{\theta}} \right) > 0 \quad (6.60)$$

$$\left( \frac{g}{I_{yy}} \frac{\partial \theta}{\partial \dot{x}} \right) > 0 \quad (6.61)$$

Furthermore, the dynamic model can be finally simplified as:

$$\begin{cases} I_{xx}\ddot{\phi} = \dot{\theta}\dot{\psi}(I_{yy} - I_{zz}) \\ I_{yy}\ddot{\theta} = \dot{\phi}\dot{\psi}(I_{zz} - I_{xx}) \\ I_{zz}\ddot{\psi} = \dot{\phi}\dot{\theta}(I_{xx} - I_{yy}) \end{cases} \quad (6.62)$$

The redesigned values of  $X_N$  are now given in the third column of Table 5-1.

#### 5.7.4 Iteration 4: Redesign $X_R$ based on the modified Non-RTBs, $Y_N$ :

After redesigning the Non-RTPs,  $X_N$ , the visual servoing and motion control algorithms are again applied for the path and trajectory tracking of the target object. In this iteration, the design objective, constraints, and variables are the same as those in Iteration 2. The design result of control gains,  $X_R$ , is given in the fourth column of Table 5-1, which is the same as the control gains used in Iteration 3. The step response graphs based on the provided optimization solutions after the second and fourth iterations for altitude and attitude control systems are shown in Figure 5-6. A comparative table is also presented (Table 5-2) describing the performances of the altitude and attitude control systems.

The new visual tracking performances are also displayed in Figures 7 and 8. Compared with the results of Iteration 2, it can be observed that the position tracking performance has been enhanced and the performance with regards to visual features errors has also shown better convergence characteristics. From the simulation measurements for iterations 2 and 4, the convergence time was reduced from 3.7 sec to 1.35 sec, while the maximum tracking error decreased from 346 pixels to 288 pixels. Less oscillations were also reported for the tracking performance of iteration 4.

Table 5-1: DFC-based design results for a vision-guided quadrotor system

Non-RTPs, $X_N$	Descriptions	Iteration 1	Iteration 2	Iteration 3	Iteration 4
$l$	Arm length ( $m$ )	0.25	/	0.28	/
$m$	Total mass ( $kg$ )	0.65	/	0.72	/
$I_{xx}$	Inertia moments on $x$ ( $kg.m^2$ )	0.009	/	0.0076	/
$I_{yy}$	Inertia moments on $y$ ( $kg.m^2$ )	0.008	/	0.0076	/
$I_{zz}$	Inertia moments on $z$ ( $kg.m^2$ )	0.017	/	0.0152	/
$b$	Distance between cameras ( $m$ )	0.15	/	0.1	/
RTPs, $X_R$					
$k_p$	Proportional control gain	/	1.5	/	1.3
$k_i$	Integral control gain	/	1.0	/	0.8
$k_d$	Derivative control gain	/	0.6	/	0.4
$\lambda$	Visual servoing gain	/	0.5	/	0.35

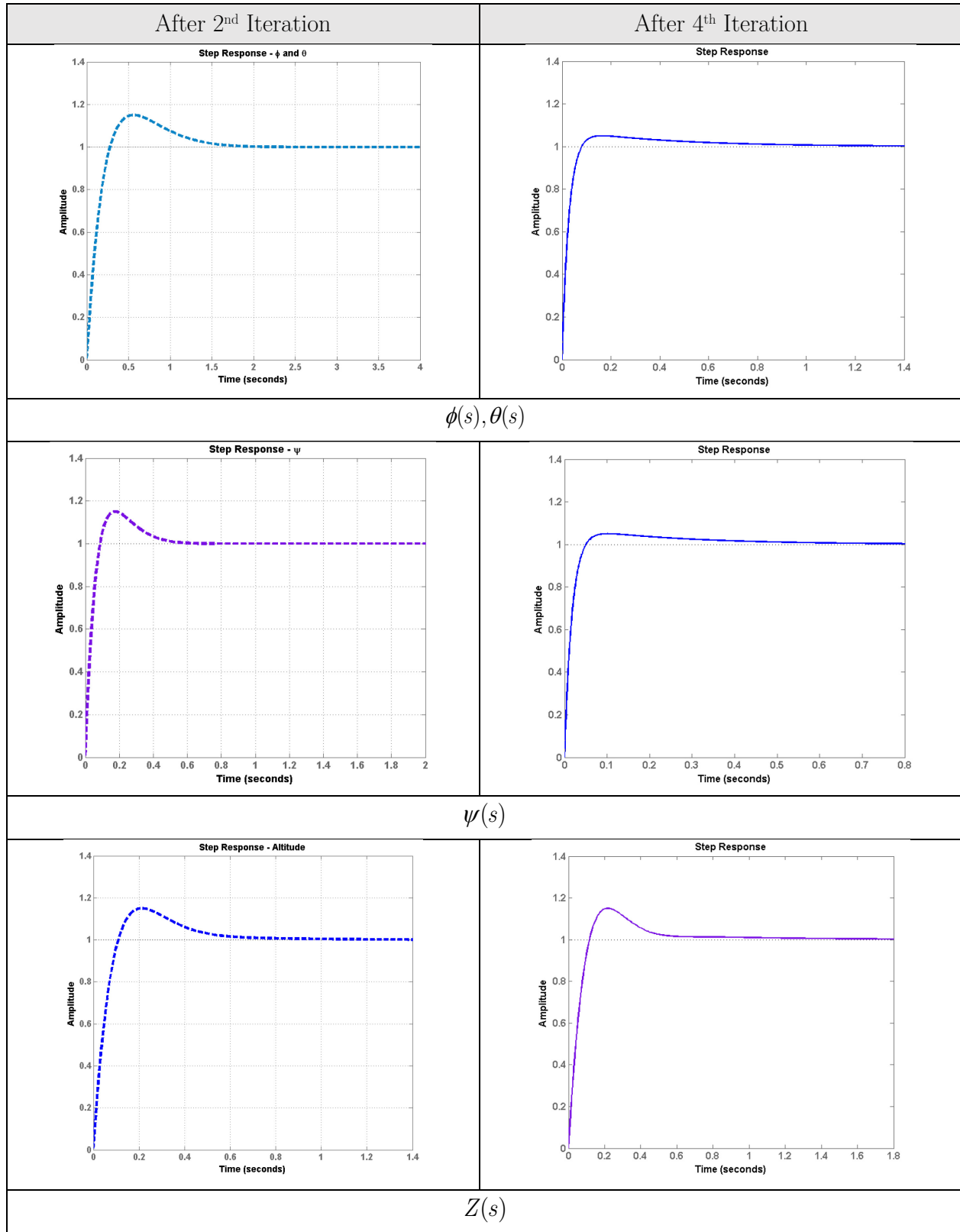


Figure 5-6: The step-response of the attitude and altitude control systems based on the final system-level optimization results

Table 5-2: The step-response characteristics of the attitude and altitude control systems based on the results from iteration 2 and iteration 4.

	Controller	Max. Overshoot %	Rise-time (sec)	Settling-time (sec)
<b>Iteration #2</b>	$\phi(s), \theta(s)$	17%	0.25	1.5
	$\psi(s)$	18%	0.1	0.42
	$Z(s)$	18%	0.1	0.46
<b>Iteration #4</b>	$\phi(s), \theta(s)$	7%	0.1	0.7
	$\psi(s)$	7%	0.06	0.37
	$Z(s)$	18%	0.1	0.5

It can be observed that after only four iterations, the obtained design variables are quite satisfactory and elevate the performance of the proposed system. Which in our case, and considering the assumptions made, shows that the DFC does help in terms of integrated design of a complex mechatronic system. However, the complexity of our systems lies within its behavior and not the number of components, as in our opinion the results obtained here will only hold for systems with small number of components and consequently design variables and parameters.

Using the DFC method for more complex mechanisms in terms of behavior and number of component as well as complex control systems would be very hard to implement in the way the DFC methodology is built. The difficulty stems from the fact that it requires for the designer to set a too large of a number of constants and this will definitely cause the design process to need much more iterations, not taking into accounts the new constraints which will be introduced to the optimization process. This will call for some additional efforts to establish guidelines for choosing those constants and more importantly, a faster and even more “integrated” approach, as future efforts.

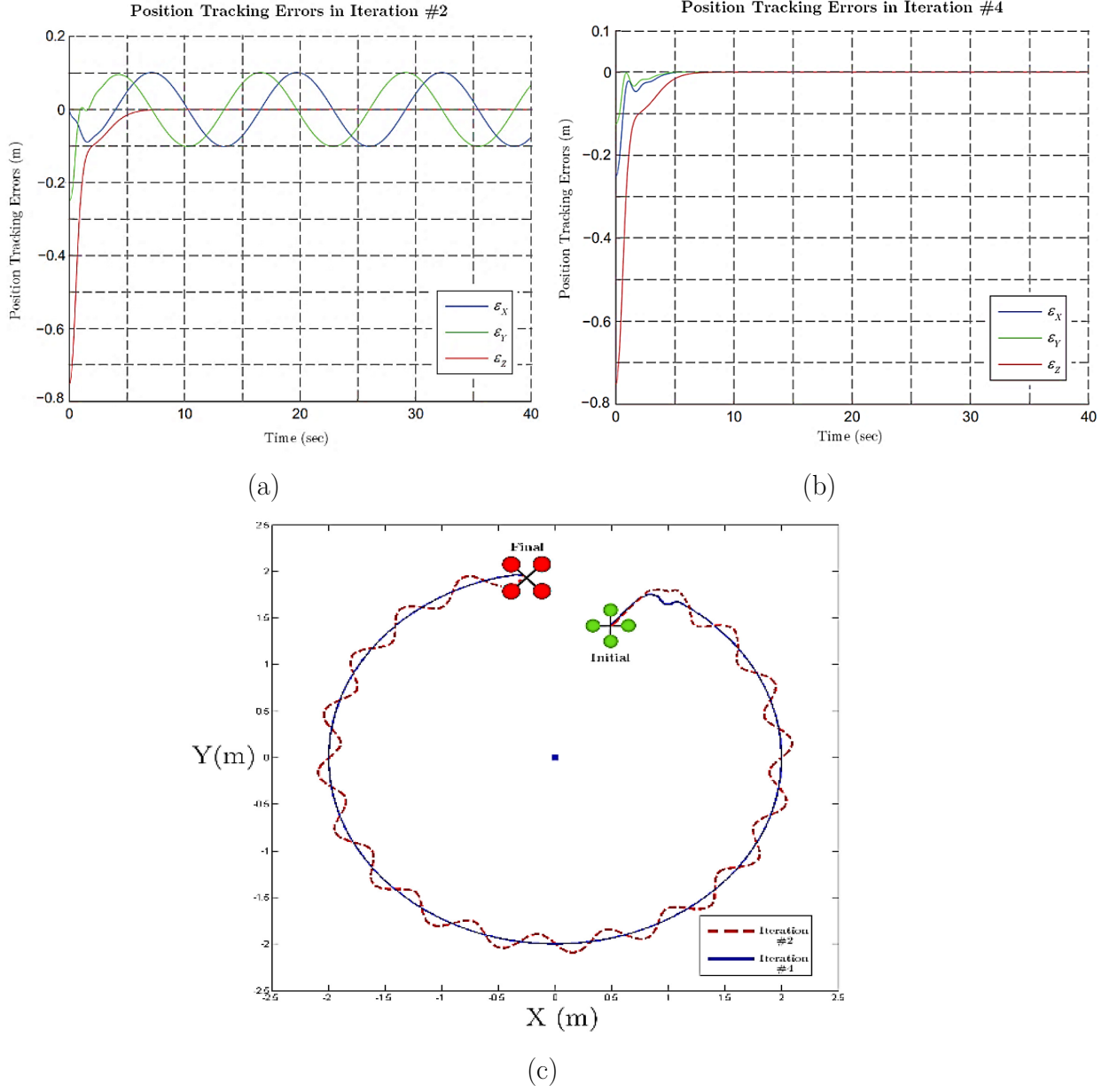


Figure 5-7: Position tracking performances based on results from (a) iteration 2 and (b) iteration 4, and a comparative graph of paths for a complete motion.

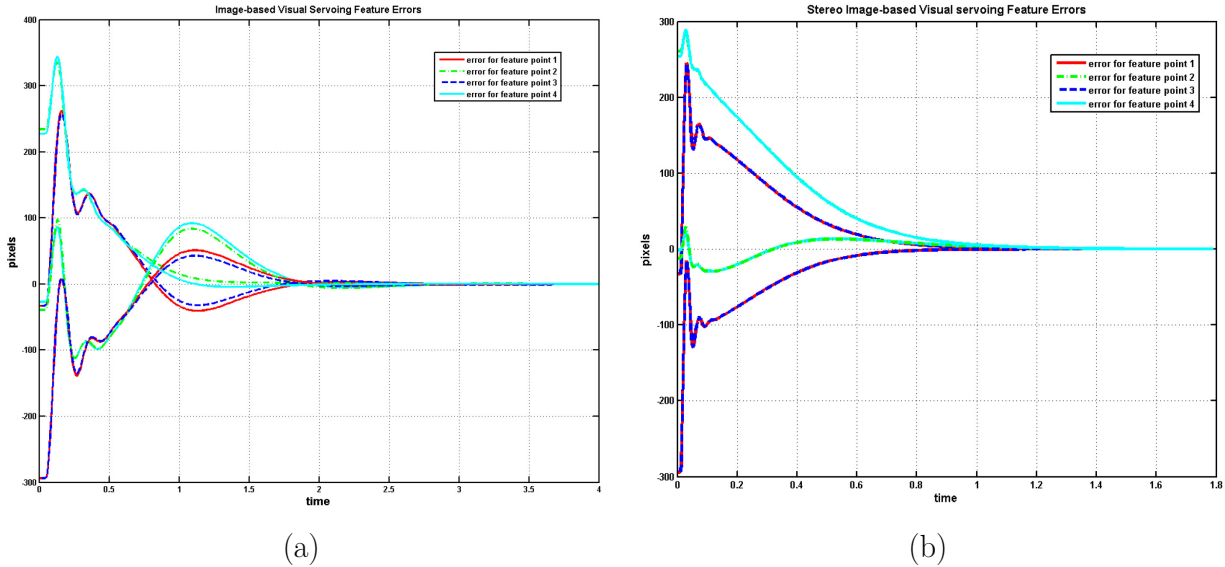


Figure 5-8: Visual feature errors from (a) iteration 2 and (b) iteration 4.

## 5.8 Conclusion

In this paper, the problem of integrated and concurrent design of a vision-guided quadrotor UAV has been studied using the Design-for-Control methodology that has never been applied to a system which combines both the control strategy and the mechanical design. We used the DFC considering the design of a mechatronic system as a mapping from a requirement space to a structure space. The mechatronic design concept is therefore interpreted as an integrated design framework that considers both real-time and non-real-time requirements simultaneously and configures both real-time and non-real-time parameters (design variables) concurrently.

Having discussed the design approach, the concurrent design of both mechanical and control structures of a vision-guided quadrotor system has been accomplished in an iterative manner and after finalizing the last iterations, desired performances with regards to both control systems, i.e. motion control and visual servoing, have been achieved. However, for systems with larger number of components and more complex control systems, additional efforts to establish guidelines for choosing the design optimization constants, hence a more “integrated” approach is still required. This approach would need to lighten the burden of the designer in terms of choosing a too large number of parameters and weights, as these decisions can vary from one designer to another. Furthermore, a need to consider the complexity of the process itself (e.g. number of design loop-backs) needs to be considered in the optimisation process.

## CHAPTER 6 ARTICLE 4: INTEGRATED AND CONCURRENT DETAILED DESIGN OF A MECHATRONIC QUADROTOR SYSTEM USING A FUZZY-BASED PARTICLE SWARM OPTIMIZATION

Abolfazl Mohebbi, Luc Baron, Sofiane Achiche

Submitted to the *IEEE Transaction on Automation Science and Engineering*, Feb. 2017

### 6.1 Abstract

Mechatronics Design is complex by nature as it involves a large number of couplings and interdependencies between subsystems and components alongside a variety of sometimes contradicting objectives and design constraints. Mechatronics design activity requires a cross disciplinary and multi-objective thinking. In this paper, a fuzzy-based approach for the modelling of a unified performance evaluation index in the detailed design phase is presented. This index acts as a multidisciplinary objective function aggregating all the design criteria and requirements from various disciplines and subsystems while taking into account the interactions and correlations among the objectives. Then this function is optimized using a particle swarm optimization algorithm alongside all the constraints facing each subsystem. As an application, the mechatronics design of a vision-guided quadrotor unmanned aerial vehicle is carried out to demonstrate the effectiveness of the proposed method. Thus, a thorough modeling of system dynamics, structure, aerodynamics, flight control and visual servoing system is carried out to provide the designer with all necessary design variables and requirements. The final results and related computer simulations, show the effectiveness of the proposed method to find solutions for an optimal mechatronic design.

### 6.2 Introduction

Mechatronic systems are multidisciplinary products, incorporating an interactive and synergistic application of various domains such as mechanics, electronics, controls, and computer engineering. Due to the large number of couplings and dynamic interdependences between subsystems and components, the design of mechatronic systems is considered to be a challenging and complex task, which requires a cross disciplinary design thinking [118, 120]. The traditional mechatronic design methodologies tend to separate the overall system into several sub-systems, and then design each subsystem sequentially passing forward the results from one subsystem to



another until a final set of design parameters is achieved [165]. Such approach can often lead to a functional design, but rarely to an optimal one. This calls for a more systematic and multi-objective design approach to mechatronics [77]. More precisely, a concurrent and integrated design is needed to achieve products with more efficiency, reliability and flexibility and on the other hand, with less complexity and at lower costs [4].

A number of research efforts have demonstrated that designing the structure and control concurrently, considerably improves the system performance and efficiency [63, 142, 148, 149]. They have explored various approaches towards design of control systems for mechatronic devices to overcome the mechanical limitations. Their work was based on the fact that the mechanical system design can contribute to the controller design and on the other hand, the behavior of the control system can improve the mechanical design for improved global performance. Although, in most of these efforts, the mechanical structures of the system were usually determined in advance without considering the future aspects of the controller design. Therefore, a perfect control action may be far from practical concerns, due to limitations imposed by the poorly designed mechanical structure, even if much effort has been made on the design of advanced controllers. A more general approach called “Design for Control” (DFC) was proposed in [153] where the design of the mechanical structure has been simplified as much as possible in such a way that the dynamic modeling of the system is facilitated and as it is less complex. Thus, a better overall control performance has been achieved. In this method the physical understanding of the overall system is fully explored with the aim of simplification of the controller design as well as the execution of the control algorithm with the less hardware-in-the-loop restrictions. It could be observed that after a few iterations, the obtained design variables using DFC approach were quite satisfactory and elevate the performance of the proposed system. Although, implementing this method for more complex mechanisms in terms of behavior and number of component as well as complex control systems would be very hard and complicated [166].

Complicated design of a mixed system can be treated as an optimization problem by using a proper evaluation function. Due to their non-convex nature, many difficulties arise when solving optimization problems involving various structural and control parameters. Thus, despite the advances in optimal control system design, optimal integrated mechatronic system design is still an open research area. Most of existing multidisciplinary design frameworks utilize gradient-based solvers as an optimization driver for all the disciplines. Although, due to the extensive increase in computational powers of modern computers and also the ability of using large numbers of parallel

processors, using non-gradient based and probabilistic search algorithms have attracted much interest in recent years. This class of algorithms typically require many more function evaluations than comparable gradient-based algorithms, but in return they provide the designers with several attractive characteristics. They are usually easy to implement they do not require continuity of response functions, and they are better suited to finding global or near-global solutions. Numerous research works have reported using multidisciplinary approaches alongside evolutionary and stochastic algorithms for designing and optimizing mechatronic systems. Affi et al. [167] presented a genetic algorithm-based method for design and optimization of the geometry and dynamic behaviors of a four-bar mechatronic system. Hammadi et al. [168] proposed a new methodology for optimizing mechatronic systems based on multi-agent technology. They decomposed the design process to three design agents and coordinated the local optimizations towards these agents. Behbahani et al. [124] presented a methodology for detailed mechatronic design based on a multicriteria index and also using a niching genetic algorithm.

Particle Swarm Optimization (PSO) is a recent addition to non-gradient-based stochastic and population-based optimization algorithms which was first introduced by Kennedy and Eberhart [169] in 1995. This method is based on a simplified social model that is closely tied to swarming theory and inspired by the social and cognitive behaviors of a flock of birds or school of fish seeking for food. In the birds' flock analogy, each bird makes use of its own memory, as well as knowledge gained by the flock as a whole, to efficiently adapt to its environment. PSO is a zero-order, non-calculus-based (gradient-free) method which can solve discontinuous, multi-modal, non-convex problems. Thus, it is a suitable tool to support engineering design problems. Many research works have reported that despite the computational cost, using PSO has shown considerable improvements in results and performance compared to other non-gradient-based algorithms [170-172]. Although the PSO algorithm has been applied to a wide range of engineering and design problems in the literature, few multidisciplinary applications are known [173]. In this paper, a multiobjective PSO is used and tailored for a constrained multi-disciplinary design problem.

Mechatronics design tends to deal with Pareto analysis and decisions. Achieving optimal solutions is not possible without identification of the performance parameters involved and understanding of their co-influences. The lack of simultaneous consideration of objectives within various domains, increases the need for more design iterations. Moreover, modeling all sub-systems and their interconnections, and at the same time modeling interactions between the design criteria over several engineering domains is not a trivial task. Mohebbi et al. [77] presented a new approach

based on their multi-criteria mechatronic profile (MMP) for the conceptual design stage. The MMP included five main elements: machine intelligence, reliability, flexibility, complexity and cost while each main criterion has a number of sub-criteria. In order to facilitate the design process and supporting decision making in the presence of interacting criteria, they used fuzzy integrals [119, 125] which are proven to be precise and reliable in a multi-criteria problem in the presence of interaction between the objectives. The Choquet integral is one of the most expressive preference models used in decision theory. It performs a weighted aggregation of criteria using a capacity function assigning a weight to any coalition of criteria. This enables the expression of positive and negative interactions and covering an important range of possible decision behaviors, which is generally ignored in other MCDM methods [102, 126].

In this work, we propose a novel Cascade Fuzzy-based multidisciplinary objective function which aggregates all the design criteria and requirements from various disciplines and subsystems involved. Using the proposed method, we are able to provide a multi-objective design index to be optimized using a particle swarm optimization (PSO) algorithm during the course of the detailed design process and simultaneously model the interdependences and interactions among the criteria to be considered. We validate our method to design a complex mechatronic system composed of a vision-guided quadrotor UAV. In terms of system dynamics, a quadrotor is an underactuated system with six degrees of freedom and four inputs which is inherently unstable and difficult to control. Thus, the design and control of this nonlinear system is a challenge from both practical and theoretical point of views [156-159]. This makes of it an excellent case to formulate a multidisciplinary design problem. Integrating the sensors, actuators and intelligence into a lightweight vertically flying system with a suitable operation time is not a trivial task to achieve as one needs to deal with numerous interdependent design parameters originating from various engineering disciplines. Making a decision about all these parameters requires a clear integrated methodology. Moreover, in order to enable the system with autonomous capabilities, a visual feedback control strategy i.e. visual servoing, will be used. This increases the number of requirements and objectives hence increasing the overall design task complexity.

The rest of this paper is organized as follows; Section 6.3 gives a brief description about the PSO algorithm and also incorporating design constraints in the optimization process using a penalty function. Section 6.4 introduces the Choquet integrals and the fuzzy-based multi-criteria aggregation while section 6.5 formulates the proposed integrated detailed design for mechatronic systems and the process of identifying the necessary parameters towards the optimization

algorithm and also modeling the interaction among objectives. Section 6.6 presents the quadrotor system modeling considering various engineering aspects involved. In Section 6.7, the control system design consisting of the flight motion controller and visual servoing system is discussed and also a formulation for an image-based stereo visual servoing system is presented. Section 6.8 includes the performance requirements for designing each subsystem and also constraints acting upon each of them. The results for the detailed design from the optimization process are presented and discussed in Section 6.9 while Section 6.10 shows the outcomes as a computer simulation and compares the performance of the system against a benchmark product. Finally, the concluding remarks are discussed in section 6.11.

### 6.3 Particle Swarm optimization

Particle Swarm Optimization (PSO) is heuristic optimization method generally used to find an optimal solution in a complex search space inspired by the collective intelligence of swarms of biological populations such as bird flocks, insects, etc. [169, 174]. Similar to genetic algorithms (GAs), it is a population-based method, in which the state of algorithm is represented by a population, which is iteratively modified until a termination criterion is satisfied. In PSO algorithms, the population  $P = \{p_1, \dots, p_n\}$  of the feasible solutions is often called a “swarm”. The feasible solutions  $p_1, \dots, p_n$  are called “particles”. The PSO method views the set  $R^d$  of feasible solutions as a space in which the particles move. Each particle is defined as a vector of its position and velocity, searching the space for a solution by modifying the trajectories of individual vectors. The particles are attracted stochastically towards a better position considering their personal best position and global best position. PSO is both easy and fast to implement because of its simple and intuitive structure [175]. Unlike GAs, PSOs do not change the population from generation to generation but they iteratively update the positions of the members of the population (i.e., particles). PSOs have no notion of the “survival of the fittest”. On the other hand, similarly to GAs, the members of the population interact or influence each other [176]. In PSO, the objective function can be non-differentiable as only the values of this function are used. The method can be applied to optimization problems of large dimensions, often producing quality solutions more rapidly than alternative methods.

### 6.3.1 Swarm Topology

Each particle  $p_i$  has its neighborhood  $N_i$  which is a subset of  $P$ . The structure of neighborhoods is called the “swarm topology”, which can be represented by a graph. Most popular topologies include fully connected topology, star topology, ring topology, etc. [177] (Figure 6-1).

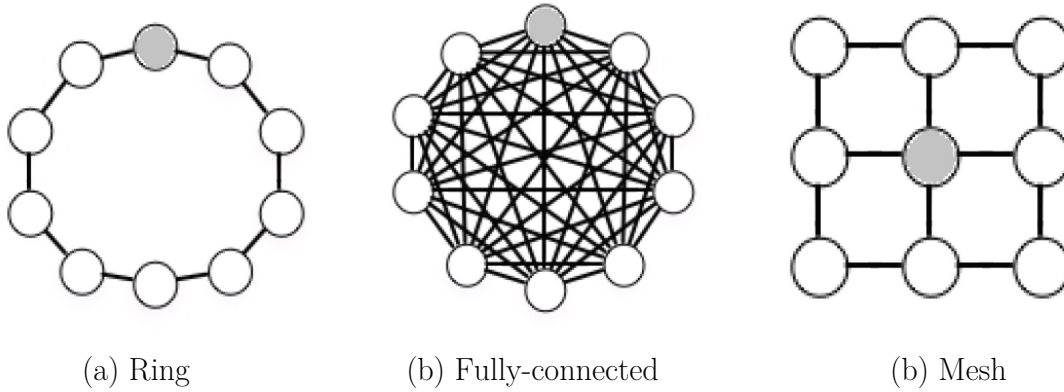


Figure 6-1: Three most common neighborhood topologies used in particle swarm optimization

### 6.3.2 PSO Algorithm

Each particle  $i$ , at iteration  $t$  has a set of characteristics as follows:

- Position,  $x_i^t$  (a  $d$ -dimensional vector),
- Last (historically) best position,  $p_i^t$ ,
- Last best position of the neighboring particles,  $l_i^t$ ,
- Speed  $v_i^t$ , which it is the step size between  $x_i^t$  and  $x_i^{t+1}$ .

In a  $d$ -dimensional search space,  $x_i^t = (x_{i,1}, \dots, x_{i,d})^t$  and  $v_i^t = (v_{i,1}, \dots, v_{i,d})^t$ . For a fully connected topology,  $l_i^t$  is the last best known position of the entire swarm. At the beginning of the algorithm, the particle positions are randomly initialized, and the velocity vectors are set to zero or randomly generated for each particle. For each swarm movement (iteration), each particle matches the velocity of its nearest neighbor to provide synchrony. Random changes in velocities are also added in each iteration to provide variation in motion and life-like appearance. After initialization, the objective function value of each particle at iteration  $t$  is evaluated such that

$$f(x_i^t): R^d \rightarrow \mathbb{R}$$

After fitness evaluation, the velocity and position of each particle are updated as follows:

$$v_i^{t+1} = w^t v_i^t + \zeta_1 u_i^{1,t} (p_i^t - x_i^t) + \zeta_2 u_i^{2,t} (l_i^t - x_i^t) \quad (7.1)$$

$$x_i^{t+1} = x_i^t + v_i^{t+1} \quad (7.2)$$

where  $w^t$  is the inertia weight or damping factor usually decreasing from around 0.9 to around 0.4 during the computation,  $\zeta_1$  and  $\zeta_2$  are acceleration coefficients usually between 0 and 4, and  $u_i^{1,t}$  and  $u_i^{2,t}$  are random real values uniformly distributed in  $[0, 1]$ . New random values are generated for each particle and generation. The first part of the velocity update equation is called “inertia”, the second part is the “cognitive (personal)” component, and the third one is the “social (neighborhood)” component. The algorithm is terminated after a given number of iterations, or once the fitness function values of the particles are close enough in some sense. Overall pseudo code of PSO is described in Algorithm I.

---

**Algorithm I - Particle Swarm Optimization**

---

- 1) Initialize swarm.
  - 2) Update swarm.
    - for** each particle **do**
      - Evaluate the objective function  $f(\vec{x})$ .
    - end for**
    - for** each particle **do**
      - Update  $l_i^t$ .
      - Update  $p_i^t$ .
      - Update  $v_i^t$  and  $x_i^t$ .
    - end for**
  - 3) Repeat.
- 

### 6.3.3 Constrained Optimization

In constrained optimization, solutions must satisfy a number of constraints, which either restrict the parameter values to certain intervals or define dependencies among them. Formally, the negative null form of a constrained optimization is defined as follows:

$$\min_x f(\vec{x}; p) \tag{7.3}$$

Subjected to:

$$g_i(\vec{x}) \leq 0, \quad i = 1, \dots, p \text{ (inequality constraint)} \tag{7.4}$$

$$h_i(\vec{x}) = 0, \quad i = 1, \dots, p \text{ (equality constraint)} \tag{7.5}$$

$$lb_k \leq x_k \leq ub_k, \quad k = 1, \dots, n \text{ (variable bounds)} \tag{7.6}$$

In which  $\vec{x}$  is the  $d$ -dimensional vector of design variables and  $\vec{p}$  is the vector of design parameters which will not be varied during the optimization process. The objective function  $f(\vec{x})$  maps the  $n$ -dimensional parameter space  $\mathbb{V} = [lb_1, ub_1] \times [lb_2, ub_2] \times \dots \times [lb_n, ub_n] \subseteq \mathbb{R}^n$  to  $\mathbb{R}$ .

The feasible region  $\mathbb{F} \subseteq \mathbb{R}^n$  is given by the intersection of  $\mathbb{V}$  with the equality and inequality constraints. The goal is to find a global optimal solution  $\vec{x}^* \in \mathbb{F}$  for which;

$$\forall \vec{x} \in \mathbb{F}: f(\vec{x}^*) \leq f(\vec{x}).$$

The use of a penalty function is one of the most common approaches to deal with constraints in evolutionary computation [178]. If a minimization problem is assumed, the objective function  $f(\vec{x})$  is modified to  $f_{pso}(\vec{x})$  such as:

$$f_{pso}(\vec{x}) = f(\vec{x}) + \sum_{i=1}^p a_i \max\{0, g_i(\vec{x})\}^\alpha + \sum_{j=1}^q b_j |h_j(\vec{x})|^\beta \quad (7.7)$$

where  $\alpha, \beta$ , and the penalty coefficients  $a_i$  and  $b_i > 0$  are user-defined parameters, which must be selected carefully. In case of very low penalty coefficients, the population might explore infeasible space while when chosen too high, the particles are distracted from the boundaries and might be unable to locate disconnected feasible regions. Besides being statically defined at the beginning of the optimization and used throughout the run, the penalty coefficients can be “dynamically” adapted during the process.

## 6.4 Multicriteria Fuzzy Aggregation

In order to incorporate all the objectives and design criteria into one objective function that will be minimized using a PSO approach, an aggregation operator should be used. A linear combination or a weighted sum is widely used for multi-objective optimizations. In this paper, the fuzzy measures are employed to represent designer’s degree of importance allocated to each criterion and also to the interactions among them. Furthermore, a global evaluation is calculated by the Choquet fuzzy integral. The fuzzy measures and fuzzy integral are briefly described in this section. Choquet integral provides a weighting factor for each criterion, and also for each subset of criteria. Using Choquet integrals is a very effective way to measure an expected utility when dealing with uncertainty, which is the case in design in general and mechatronics design in particular. Using this technique and by defining a weighting factor for each subset of criteria, the interactions between multiple objectives and criteria can be easily taken into account.

The weighting factor of a subset of criteria is represented by a fuzzy measure on the universe  $N$  satisfying the following fuzzy measure ( $\mu$ ) equations:

$$\mu(\emptyset) = 0, \quad \mu(N) = 1. \quad (7.8)$$

$$\emptyset \subseteq A \subseteq B \subseteq N \rightarrow 0 \leq \mu(A) \leq \mu(B) \leq 1, \quad (7.9)$$

where  $A$  and  $B$  represent the fuzzy sets [134]. Eq. 8 represents the boundary conditions for fuzzy measures while Eq. 9 is also called the monotonicity property of fuzzy measures.

Let  $\mu$  be a fuzzy measure on  $X$ , whose elements are denoted  $x_1, x_2, \dots, x_n$  here. The discrete Choquet integral of a function  $f: X \rightarrow \mathbb{R}^+$  with respect to  $\mu$  is defined by:

$$C_\mu(f) = \sum_{i=1}^n (f(x_i) - f(x_{i-1}))\mu(A_{(i)}), \quad (7.10)$$

where indices have been permuted so that  $0 \leq f(x_1) \leq f(x_2) \leq \dots \leq f(x_n)$  and  $A_{(i)} = \{(i), \dots, (n)\}$ , and  $A_{(n+1)} = \emptyset$  while  $f(x_0) = 0$ . Table 6-1 shows the most common semantic interactions among criteria pairs and the corresponding fuzzy measures.

Table 6-1: Fuzzy Interactions and Measurements

#	Description of Interaction	Fuzzy Measurement
I	Negative Correlation	$\mu(i, j) > \mu(i) + \mu(j)$
II	Positive Correlation	$\mu(i, j) < \mu(i) + \mu(j)$
III	Substitution	$\mu(T) < \begin{cases} \mu(T \cup i) \\ \mu(T \cup j) \end{cases} = \mu(T \cup i \cup j)$ $T \subseteq Y \setminus i, j$
IV	Veto Effect	$\mu(T) \approx 0$ if $T \subset Y, i \notin T$
V	Pass Effect	$\mu(T) \approx 1$ if $T \subset Y, i \in T$
VI	Complementarity	$\mu(T) = \begin{cases} \mu(T \cup i) \\ \mu(T \cup j) \end{cases} < \mu(T \cup i \cup j)$ $T \subseteq Y \setminus i, j$

The main difficulty in using Choquet integrals is the identification of the  $(2^n - 2)$  coefficients of fuzzy measures. Intuitive notions expressed in Table I can be used as a guide here. The overall importance of a criterion is not solely determined by the value of  $\mu(i)$  since  $\sum_{i=1}^n \mu(i)$  is not necessarily equal to one. Another useful concept is the overall importance index of a criterion, computed by the Shapley value, which is defined as [104]:

$$\phi(\mu, i) = \sum_{T \subseteq N \setminus i} \frac{(n - t - 1)! t!}{n!} [\mu(T \cup i) - \mu(T)]. \quad (7.11)$$

The Shapley value ranges between  $[0, 1]$  and represents a true sharing of the total amount  $\mu(N)$ , since:

$$\sum_{i=1}^n \phi(\mu, i) = \mu(N) = 1. \quad (7.12)$$



It is convenient to scale these values by a factor  $n$ , so that an importance index greater than 1 indicates an attribute more important than the average. Moreover, The interaction index  $I(\mu, ij)$  for any pair of criteria  $i$  and  $j$  is defined as follows [104]:

$$I(\mu, ij) = \sum_{T \subseteq N \setminus \{i, j\}} \frac{(n - t - 2)! t!}{(n - 1)!} [\mu(T \cup ij) - \mu(T \cup i) - \mu(T \cup j) + \mu(T)], \quad (7.13)$$

where  $T$  is a subset of criteria. The interaction index ranges in  $[-1, 1]$ . Using the Shapely value for criteria importance and also the interaction index, the Choquet integral can be expressed as:

$$C_\mu(f) = \sum_{i=1}^n \phi(\mu, i) f(x_i) - \frac{1}{2} \sum_{\{i, j\} \subseteq N} I(\mu, ij) |f(x_i) - f(x_j)| \quad (7.14)$$

Here,  $I(\mu, ij) = 0$  means criteria  $i$  and  $j$  are independent while  $I(\mu, ij) > 0$  means there is a complementary among  $i$  and  $j$  and that for the decision maker, both criteria have to be satisfactory in order to get a satisfactory alternative. If  $I(\mu, ij) < 0$  then there is a substitutability or redundancy among  $i$  and  $j$ . This means that for the decision maker, the satisfaction of one of the two criteria is sufficient to have a satisfactory alternative. It is worthy to note that a *positive correlation* leads to a *negative interaction index*, and vice versa. The fuzzy measures should be specified in such a way that the desired overall importance and the interaction indices are satisfied.

## 6.5 Integrated Mechatronic Detailed Design Formulation

The process of detailed design of a mechatronic system can be ideally formulated in a multi-objective multidisciplinary design optimization problem in which the design objectives of all subsystems are considered alongside the corresponding constraints. For example, for a UAV system we can assume that we have various objectives for all the subsystems such that  $S_i(\vec{x})$ , ( $i = 1, \dots, n_1$ ) represents the design objectives for Structural subsystem,  $C_i(\vec{x})$ , ( $i = 1, \dots, n_2$ ) for the control system,  $A_i(\vec{x})$ , ( $i = 1, \dots, n_3$ ) for the aerodynamics design requirements,  $V_i(\vec{x})$ , ( $i = 1, \dots, n_4$ ) for the visual servoing (vision) system and finally  $O_i(\vec{x})$ , ( $i = 1, \dots, n_5$ ) for the overall system-level design objectives. Moreover,  $g_i(\vec{x})$  and  $h_i(\vec{x})$  are inequality and equality constraints for all the aforementioned subsystems.

### 6.5.1 Cascade Fuzzy-based multidisciplinary objective function

In order to provide the optimization algorithm with an interactive objective function which includes all the design requirements from various disciplines involved, we propose a cascade Choquet integral-based aggregation to take into account all the interactions amongst design

objectives and also their relative importance in the design process. Figure 6-2 illustrates the proposed aggregation approach. In this approach, the fuzzy measures are used to model the interactions among all objectives in a subsystem (i.e. structure, control, aerodynamics, ...) such that:

$$f_S^\mu(\vec{x}) = C_\mu \left( S_1(\vec{x}), S_2(\vec{x}), \dots, S_{n_1}(\vec{x}) \right) \quad (7.15)$$

$$f_C^\mu(\vec{x}) = C_\mu \left( C_1(\vec{x}), C_2(\vec{x}), \dots, C_{n_2}(\vec{x}) \right) \quad (7.16)$$

$$f_A^\mu(\vec{x}) = C_\mu \left( A_1(\vec{x}), A_2(\vec{x}), \dots, A_{n_3}(\vec{x}) \right) \quad (7.17)$$

$$f_V^\mu(\vec{x}) = C_\mu \left( V_1(\vec{x}), V_2(\vec{x}), \dots, V_{n_4}(\vec{x}) \right) \quad (7.18)$$

$$f_O^\mu(\vec{x}) = C_\mu \left( O_1(\vec{x}), O_2(\vec{x}), \dots, O_{n_5}(\vec{x}) \right) \quad (7.19)$$

Finally, the multiobjective PSO optimization problem can be formulized as follows:

$$\begin{aligned} \min_{\vec{x}} f_{pso}(\vec{x}) = & C_\mu(f_s(\vec{x}), f_c(\vec{x}), f_A(\vec{x}), f_V(\vec{x}), f_O(\vec{x})) \\ & + \sum_{i=1}^p a_i \max\{0, g_i(\vec{x})\}^\alpha + \sum_{j=1}^q b_j |h_j(\vec{x})|^\beta. \end{aligned} \quad (7.20)$$

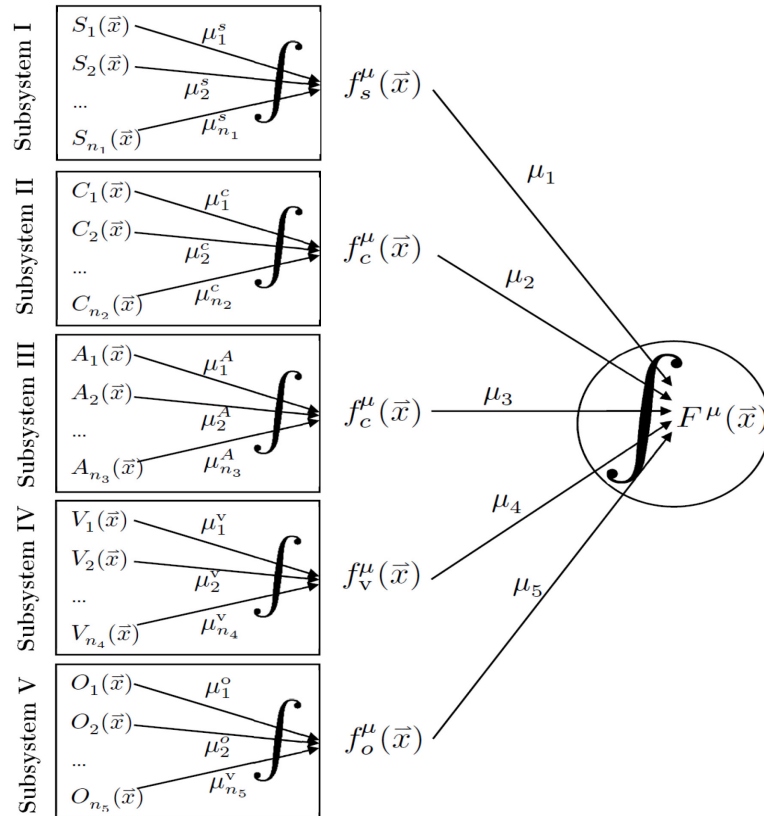


Figure 6-2: Cascade Choquet integral-based aggregation on subsystems objective functions

### 6.5.2 Parameter Selection for PSO

During the implementation of the PSO algorithm, many considerations are required to facilitate the prevention of swarm explosion and divergence. These considerations include selecting acceleration coefficients,  $\zeta_i$ , limiting the maximum velocity and choosing inertia weight  $w^t$ .

The velocity of the particles is a stochastic variable. Therefore, it creates an uncontrolled trajectory to follow wider cycles in the problem [179]. The upper and lower limits of the velocity are defined as follows to avoid this problem [180]:

$$\begin{aligned} \text{If } v_{i,d} > v_{max} \text{ then } v_{i,d} &= v_{max} \\ \text{If } v_{i,d} < -v_{max} \text{ then } v_{i,d} &= -v_{max} \end{aligned}$$

If velocity  $v_{max}$  is very large, then there is a possibility to move beyond the solution space. On the other hand, if it is too small, then the movement of the particles is limited. Therefore, an optimal solution may not be obtained. According to the problem characteristics, the value of  $v_{max}$  is selected empirically. H. Fan [181] proposed a maximum velocity to ensure that the uniform velocity throughout the all dimensions:

$$v_{max} = (x_{max} - x_{min})/N_{int}, \quad (7.21)$$

where  $x_{max}$  and  $x_{min}$  are the maximum and minimum values of the particle positions found so far, and  $N_{int}$  is the number of intervals. Acceleration of  $p_i$  and  $l_i$  are controlled by the acceleration coefficients  $\zeta_i$ . The larger values of these coefficients may diverge the particles, and small values may limit movement. Ozcan et al. [182] concluded that the trajectory of the particle goes to infinity when  $\zeta_i > 4$ . They suggested that a good starting acceleration coefficients are  $\zeta_1 = \zeta_2 = 2$ . Although the acceleration coefficients and maximum velocities may be well defined, but the particles might diverge, which is called the “swarm explosion”. Using inertia weights is a method to control the explosion of the swarm [183]. This weight is usually decreasing from around 0.9 to 0.4 during the computation.

### 6.5.3 Identification of Fuzzy Measures

There exist a variety of methods for identifying  $(2^n - 2)$  fuzzy measures which later on will be used in a Choquet integral for aggregating interactive criteria or objectives [102, 130]. The designer can intuitively choose the fuzzy measures or use a systematic approach to calculate them. Among all the data-driven or explicit calculation methods [131, 184], here we use Sugeno’s method [134] in which he created a way to automatically generate the entire lattice of fuzzy measures based on

just the  $\mu_i$  densities, thus  $(2^n - 2 - n)$  values. The Sugeno  $\lambda$ -fuzzy measure has the following additional property: If  $A, B \in \Omega$  and  $A \cap B = \emptyset$ ,

$$\mu(A \cup B) = \mu(A) + \mu(B) + \lambda\mu(A)\mu(B). \quad (7.22)$$

It is proven that a unique  $\lambda$  can be found by solving the following equation:

$$\lambda + 1 = \prod_{i=1}^n (1 + \lambda\mu_i), \quad -1 < \lambda < \infty, \lambda \neq 0 \quad (7.23)$$

where  $\mu_i = \mu\{x_i\}$ . Thus, the  $n$  densities determine the  $2^n$  values of a Sugeno measure. There are three cases with regards to the singleton measures  $\mu_i$ ;

If  $\sum_{i=1}^n \mu_i > \mu(N)$  then,  $-1 < \lambda < \infty$ .

If  $\sum_{i=1}^n \mu_i = \mu(N)$  then,  $\lambda = 0$ . (7.24)

If  $\sum_{i=1}^n \mu_i < \mu(N)$  then,  $\lambda > 0$ .

## 6.6 Quadrotor System Modeling

The modeling of a quadrotor system, requires careful considerations from various engineering aspects involved and their affecting factors such as aerodynamic, inertial counter torques, frictions, gyroscopic and gravitational effects. The quadcopter structure is presented in Figure 6-3 including the corresponding angular velocities, torques and forces created by the four rotors.

### 6.6.1 Quadrotor Body and Structure

The quadrotor mass consists of separate parts such as the mass of the battery, motors, propellers, frames, electronic devices and the payload. Figure 6-4 shows a schematic of the quadrotor body. The mass of the battery, motors and propellers can be found in the provided datasheets, while the mass of electronic devices is considered as a part of the payload.

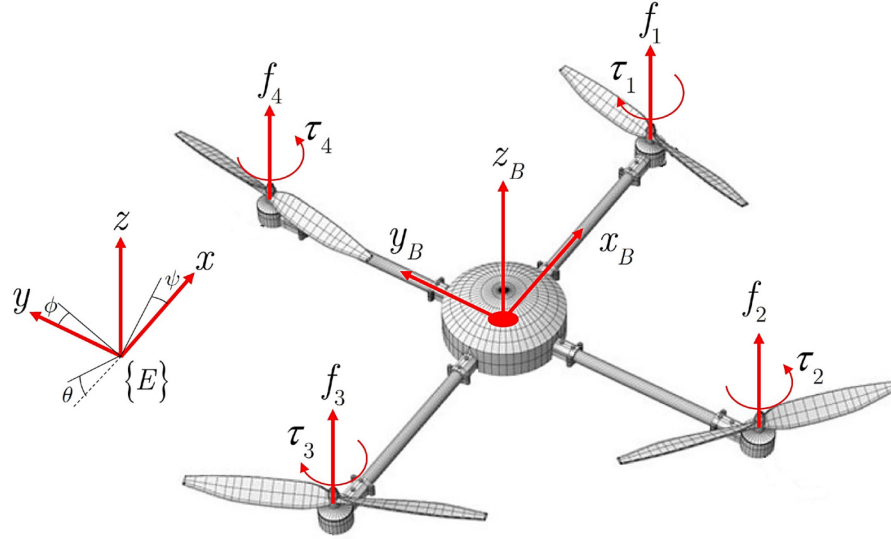


Figure 6-3: The inertial and body frames of the quadrotor system

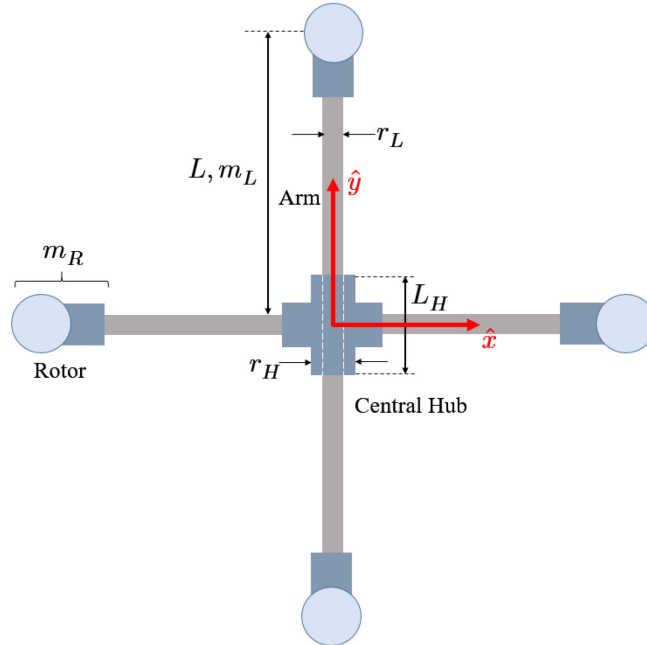


Figure 6-4: Quadrotor body structure and corresponding masses in x-y plane

The quadrotor's body mass can be calculated as:

$$m_{body} = 4m_R + 4m_L + 2m_H + m_{bat} \quad (7.25)$$

in which,  $m_R$  is the accumulated rotor, actuator and propellers mass,  $m_L$  is the quadrotor arm mass,  $m_H$  is the mass of the central hub and  $m_{bat}$  is the battery mass depicted in Figure 4. The total mass can be calculated as the sum of the body mass and payload,  $m_{PL}$  as follows:

$$m = m_{body} + m_{PL} \quad (7.26)$$

The arm and central hub masses can be calculated using the density of the carbon fiber tube,  $\rho_{cf}$ , which is the main material used in the design of the structure;

$$m_L = \pi r_L^2 L \rho_{cf} \quad (7.27)$$

$$m_H = \pi(r_H^2 - r_L^2)L_H \rho_{cf} \quad (7.28)$$

By assuming a structure's perfect symmetry between the x- and y-axis, we can conclude that the moments about each of these axes are numerically equivalent. In order to simplify the system modeling, the rotor mass is considered to be a point mass at the end of the arm and the central hub and arms are assumed to be consisted of intersecting rods. Any additional components such as electronic and control circuits are considered as a mass in the center of gravity and not affecting the inertia. Consequently, the inertia equations for the quadrotor body can be approximated as follows:

$$I_{xx} = I_{yy} = \frac{1}{3}m_L L^2 + \frac{1}{2}m_L r_L^2 + \frac{1}{3}m_H L_H^2 + \frac{1}{2}m_H(r_H^2 - r_L^2) + 2m_R L^2, \quad (7.29)$$

$$I_{zz} = \frac{2}{3}m_L L^2 + \frac{2}{3}m_H L_H^2 + 4m_R L^2, \quad (7.30)$$

where  $m_L$  and  $m_H$  are calculated using the Equations (27-28).

### 6.6.2 Quadrotor Dynamics

Throughout this paper, Euler-Lagrange formulation and DC motor equations are used to model the quadrotor system dynamics. The dynamic model developed in this section is derived based on the following simplifying assumptions:

- The origin of the body frame is in the center of mass of the quadrotor.
- The structure of the system is supposed to be rigid and symmetric.
- The thrust and drag affecting the system are proportional to the square of propellers speed [185].

The origin of the body fixed frame and the centre of gravity (COG) are located at the same position. The absolute linear position of the quadrotor is defined in the frame  $x, y, z$  with  $\xi$ . The attitude, i.e. the angular position, is defined with three Euler angles  $\eta$  where  $\phi, \theta, \psi$  are Roll, Pitch and Yaw angles respectively. Vector  $q$  contains the linear and angular position vectors.

$$\xi = [x, y, z]^T, \quad \eta = [\phi, \theta, \psi]^T, \quad q = [\xi, \eta]^T. \quad (7.31)$$

In the body frame, the linear velocities are determined by  $V$  and the angular velocities by  $\nu$  :

$$V_B = [v_x, v_y, v_z]^T, \quad \nu = [p, q, r]^T \quad (7.32)$$

The rotational transformation matrix between world frame  $E$  and body frame  $B$  is (with,  $C$ :  $\cos$ ,  $S$ :  $\sin$ );

$$R_{EB} = R_\psi R_\theta R_\phi = \begin{bmatrix} C_\psi C_\theta & -S_\psi C_\theta + C_\psi S_\theta S_\phi & S_\psi S_\theta + C_\psi S_\theta C_\phi \\ S_\psi C_\theta & -C_\psi C_\theta + S_\psi S_\theta S_\phi & -C_\psi S_\theta + S_\psi S_\theta C_\phi \\ -S_\theta & S_\phi C_\theta & C_\phi C_\theta \end{bmatrix}. \quad (7.33)$$

This rotation matrix is orthogonal thus  $R^{-1} = R^T$  which is the rotation matrix from the world frame to the body frame. The transformation matrix for angular velocities from the world frame to the body frame is  $R_\eta$  for which we have:

$$\nu = R_\eta \dot{\eta}, \quad \begin{bmatrix} p \\ q \\ r \end{bmatrix} = \begin{bmatrix} 1 & 0 & -S_\theta \\ 0 & C_\phi & C_\theta S_\phi \\ 0 & -S_\phi & C_\theta C_\phi \end{bmatrix} \begin{bmatrix} \dot{\phi} \\ \dot{\theta} \\ \dot{\psi} \end{bmatrix}, \quad (7.34)$$

$$\dot{\eta} = R_\eta^{-1} \nu, \quad \begin{bmatrix} \dot{\phi} \\ \dot{\theta} \\ \dot{\psi} \end{bmatrix} = \begin{bmatrix} 1 & S_\phi T_\theta & C_\phi T_\theta \\ 0 & C_\phi & -S_\phi \\ 0 & S_\phi / C_\theta & C_\phi / C_\theta \end{bmatrix} \begin{bmatrix} p \\ q \\ r \end{bmatrix}, \quad (7.35)$$

with  $T_\theta = \tan(\theta)$ .

The quadcopter is assumed to have symmetric structure with the four arms aligned with the body  $x$ - and  $y$ -axes. Thus, the inertia matrix is diagonal as:

$$I = \begin{bmatrix} I_{xx} & 0 & 0 \\ 0 & I_{yy} & 0 \\ 0 & 0 & I_{zz} \end{bmatrix}, \quad I_{xx} = I_{yy}. \quad (7.36)$$

The angular velocity of rotor  $i$ , denoted with  $w_i$ , creates force  $f_i$  in the direction of the rotor axis. The angular velocity and acceleration of the rotor also create torque  $\tau_{M_i}$  around the rotor axis as:

$$f_i = b_t w_i^2, \quad (7.37)$$

$$\tau_{M_i} = d w_i^2 + J_{rot} \dot{w}_i, \quad (7.38)$$

in which the Thrust factor is  $b_t$ , the drag factor is  $d$  and the total inertia moment of the rotor is  $J_{rot}$ . Usually the effect of  $\dot{w}_i$  is considered small and thus it is omitted.

The combined forces of rotors create thrust  $T$  in the direction of the body  $z$ -axis. Torque  $\tau_B$  consists of the torques in the direction of the body frame angles.

$$T = \sum_{i=1}^4 f_i = b_t \sum_{i=1}^4 w_i^2, \quad \mathbf{T}^B = [0, 0, T]^T, \quad (7.39)$$

$$\tau_B = \begin{bmatrix} \tau_\phi \\ \tau_\theta \\ \tau_\psi \end{bmatrix} = \begin{bmatrix} Lb_t(-w_2^2 + w_4^2) \\ Lb_t(-w_1^2 + w_3^2) \\ d(w_2^2 + w_4^2 - w_1^2 - w_3^2) \end{bmatrix}, \quad (7.40)$$

in which  $L$  is the arm length which is measured as the distance between the rotor and the center of mass of the quadrotor.

Using the Euler-Lagrange formulation for equations of motion we have:

$$L(q, \dot{q}) = T_\xi + T_\eta - U, \quad (7.41)$$

$$T_\xi = \left(\frac{1}{2}\right) m \dot{\xi}^T \dot{\xi}, \quad (7.42)$$

$$T_\eta = \left(\frac{1}{2}\right) \nu^T I \nu, \quad (7.43)$$

$$U = mgz, \quad (7.44)$$

$$\begin{bmatrix} f \\ \tau \end{bmatrix} = \frac{d}{dt} \left( \frac{\partial L}{\partial \dot{q}} \right) - \frac{\partial L}{\partial q}. \quad (7.45)$$

The rotational energy  $T_\eta$  can be expressed in the inertial frame using a Jacobian matrix from  $\nu$  to  $\dot{\eta}$  such that:

$$J(\eta) = R_\eta^T I R_\eta \quad (7.46)$$

$$T_\eta = \left(\frac{1}{2}\right) \dot{\eta}^T J(\eta) \dot{\eta}. \quad (7.47)$$

The linear external force is the total thrust of the rotors and The external angular force is the torques of the rotors. Thus:

$$f = R_{EB} \mathbf{T}^B = m\ddot{\xi} + mg[0, 0, 1]^T, \quad (7.48)$$

$$\tau = \tau_B = J\ddot{\eta} + \frac{d}{dt} J\dot{\eta} - \left(\frac{1}{2}\right) \frac{\partial}{\partial \eta} (\dot{\eta}^T J(\eta) \dot{\eta}) = J\ddot{\eta} + C(\eta, \dot{\eta})\dot{\eta}, \quad (7.49)$$

where the matrix  $C$  is the Coriolis term, containing the gyroscopic and centripetal effects. Accordingly, we get:

$$C(\eta, \dot{\eta}) = \begin{bmatrix} C_{11} & C_{12} & C_{13} \\ C_{21} & C_{22} & C_{23} \\ C_{31} & C_{32} & C_{33} \end{bmatrix}, \quad (7.50)$$

$$C_{11} = 0,$$

$$C_{12} = (I_{yy} - I_{zz}) \left( \dot{\theta} C_\phi S_\phi + \dot{\psi} (S_\phi^2 C_\theta - C_\phi^2 C_\theta) \right) - I_{xx} \dot{\psi} C_\theta,$$



$$\begin{aligned}
C_{13} &= (I_{zz} - I_{yy})(\dot{\psi}C_\phi S_\phi C_\theta^2), \\
C_{21} &= (I_{zz} - I_{yy})\left(\dot{\theta}C_\phi S_\phi + \dot{\psi}(S_\phi C_\theta - C_\phi^2 C_\theta)\right) + I_{xx}\dot{\psi}C_\theta, \\
C_{22} &= (I_{zz} - I_{yy})(\dot{\phi}C_\phi S_\phi), \\
C_{23} &= -I_{xx}\dot{\psi}S_\theta C_\theta + I_{yy}\dot{\psi}S_\phi^2 C_\theta S_\theta + I_{zz}\dot{\psi}C_\phi^2 C_\theta S_\theta, \\
C_{31} &= (I_{yy} - I_{zz})(\dot{\psi}C_\phi S_\phi C_\theta^2) - I_{xx}\dot{\theta}C_\theta, \\
C_{32} &= (I_{zz} - I_{yy})(\dot{\theta}C_\phi S_\phi S_\theta + \dot{\phi}S_\phi^2 C_\theta - \dot{\phi}C_\phi^2 C_\theta) + I_{xx}\dot{\psi}S_\theta C_\theta - I_{yy}\dot{\psi}S_\phi^2 C_\theta S_\theta - I_{zz}\dot{\psi}C_\phi^2 C_\theta S_\theta, \\
C_{33} &= (I_{yy} - I_{zz})\dot{\phi}C_\phi S_\phi C_\theta^2 - I_{yy}\dot{\theta}S_\phi^2 C_\theta S_\theta - I_{zz}\dot{\theta}C_\phi^2 C_\theta S_\theta + I_{xx}\dot{\theta}S_\theta C_\theta.
\end{aligned}$$

From Equation (7.49) we can get:

$$\ddot{\eta} = J^{-1}(\tau_B - C(\eta, \dot{\eta})\dot{\eta}). \quad (7.51)$$

The derived dynamic model for the quadrotor describing the roll, pitch and yaw rotations contains three terms which are the gyroscopic effect resulting from the rigid body rotation, the gyroscopic effect resulting from the propeller rotation coupled with the body rotation and finally the actuators action. Applying the small angles approximation, we obtain the following:

$$\begin{cases} \ddot{\phi} = \frac{J_r \dot{\theta}(w_1 + w_3 - w_2 - w_4)}{I_{xx}} + \frac{(I_{yy} - I_{zz})}{I_{xx}} \dot{\theta} \dot{\psi} + \frac{b_t L (w_4^2 - w_2^2)}{I_{xx}} \\ \ddot{\theta} = \frac{J_r \dot{\phi}(w_1 + w_3 - w_2 - w_4)}{I_{yy}} + \frac{(I_{yy} - I_{zz})}{I_{yy}} \dot{\phi} \dot{\psi} + \frac{b_t L (w_3^2 - w_1^2)}{I_{yy}} \\ \ddot{\psi} = \frac{-d(w_4^2 + w_2^2 - w_1^2 - w_3^2)}{I_{zz}} + \frac{(I_{xx} - I_{yy})}{I_{zz}} \dot{\phi} \dot{\theta} \end{cases} \quad (7.52)$$

From Equation (7.48) we can attain:

$$\begin{bmatrix} \ddot{x} \\ \ddot{y} \\ \ddot{z} \end{bmatrix} = -g \begin{bmatrix} 0 \\ 0 \\ 1 \end{bmatrix} + \frac{T}{m} \begin{bmatrix} S_\psi S_\phi + C_\psi S_\theta C_\phi \\ -C_\psi S_\phi + S_\psi S_\theta C_\phi \\ C_\theta C_\phi \end{bmatrix}, \quad (7.53)$$

where  $T = b_t \sum_{i=1}^4 w_i^2$ .

### 6.6.3 Rotor Dynamics

The rotors are considered to be driven by DC-motors with the well-known equations:

$$\begin{cases} L_m \frac{di}{dt} = u - Ri - k_e w_m \\ J_m \frac{dw_m}{dt} = \tau_m - \tau_d \end{cases}, \quad (7.54)$$

where  $u$  is the motor input,  $w_m$  is the motor angular rate,  $I$  is motor current,  $R$  is the motor internal resistance,  $k_e$  is the motor electrical constant and  $\tau_m$  and  $\tau_d$  are motor torque and load respectively. Using a small motor with a very low inductance, the second order DC-motor dynamics may be approximated by the following equation:

$$J_m \frac{dw_m}{dt} = -\frac{k_m^2}{R} w_m - \tau_d + \frac{k_m}{R} u. \quad (7.55)$$

where  $k_m$  is the motor torque constant and  $J_m$  is the motor inertia. Now, by considering the propeller and the gearbox models, the above equation becomes:

$$\dot{w}_m = -\frac{1}{\eta} w_m - \frac{d}{\gamma r^3 J_t} w_m^2 + \frac{1}{k_m \eta} u, \quad (7.56)$$

where  $\eta = RJ_{rot}/k_m^2$  is the motor time constant and  $J_{rot}$  is the rotor total inertia. Now, by linearizing the above equation around an operation point  $w_0$  and considering a gearbox efficiency of  $\gamma$ , we achieve:

$$\dot{w} = -Aw_m + Bu + C \quad (7.57)$$

where,

$$A = \left( \frac{1}{\eta} + \frac{2dw_0}{\gamma r^3 J_{rot}} \right), \quad B = \left( \frac{1}{k_m \eta} \right), \quad C = \left( \frac{dw_0^2}{\gamma r^3 J_{rot}} \right) \quad (7.58)$$

#### 6.6.4 Aerodynamic Forces and Moments

The aerodynamic forces and moments used here are derived by G. Fay [186] using a combination of momentum and blade element theory [187]. For the ‘‘Thrust Force’’ we have:

$$f_i = C_T \rho_a A_p (w_i r_{rot})^2, \quad (7.59)$$

in which  $C_T$  is thrust coefficient,  $\rho_a$  is air density,  $A_p$  is propeller disk area and  $r_{rot}$  is the rotor radius. Thrust coefficient is not constant for any velocity, but the variations are so small they are usually neglected. This force is the result of the vertical forces acting on all the blade elements. Furthermore, for thrust coefficient we have:

$$\frac{C_T}{\sigma a} = \left( \frac{1}{6} + \frac{1}{4} \chi^2 \right) \theta_0 - (1 + \chi^2) \frac{\theta_s}{8} - \frac{1}{4} \lambda, \quad (7.60)$$

where  $\sigma$  is the solidity ratio,  $a$  is lift slope,  $\chi$  is the rotor advance ratio,  $\theta_0$  is pitch of incidence,  $\theta_s$  is pitch of twist and finally,  $\lambda$  is inflow ratio.

From the horizontal forces acting on all the blade elements we calculate the “Hub Force” as:

$$H_i = C_H \rho_a A_p (w_i r_{rot})^2, \quad (7.61)$$

in which  $C_H$  is hub force coefficient and is calculated using the following equation.

$$\frac{C_H}{\sigma a} = \left( \frac{1}{4} \chi^2 \bar{C}_D \right) + \frac{1}{4} \lambda \chi \left( \theta_0 - \frac{\theta_s}{2} \right), \quad (7.62)$$

where  $\bar{C}_D$  is the drag coefficient at 70% radial station.

“Drag Moment” is a moment about the rotor shaft caused by the aerodynamic forces acting on the blade elements. The horizontal forces acting on the rotor are multiplied by the moment arm and integrated over the rotor. Drag moment determines the power required to spin the rotor.

$$D = C_D \rho_a A_p w_i^2 r_{rot}^3, \quad (7.63)$$

where  $C_D$  is the drag coefficient for which we have:

$$\frac{C_D}{\sigma a} = \frac{1}{8a} (1 + \chi^2) \bar{C}_D - \lambda \left( \frac{\theta_0}{6} - \frac{\theta_s}{8} - \frac{\lambda}{4} \right). \quad (7.64)$$

The “Propeller’s Rolling Moment” exists in forward flight when the advancing blade is producing more lift than the retreating one. It is the integration over the entire rotor of the lift of each section acting at a given radius.

$$M_i = C_M \rho_a A_p w_i^2 r_{rot}^3, \quad (7.65)$$

where  $C_M$  is the rolling moment coefficient for which we get:

$$\frac{C_M}{\sigma a} = -\chi \left( \frac{\theta_0}{6} - \frac{\theta_s}{8} - \frac{\lambda}{8} \right). \quad (7.66)$$

### 6.6.5 Complete System Dynamics

The complete quadrotor’s equations of motion taking into account all the aforementioned forces and moments can be expressed as follow:

$$\begin{aligned} I_{xx} \ddot{\phi} = & J_r \dot{\theta} (w_1 + w_3 - w_2 - w_4) + (I_{yy} - I_{zz}) \dot{\theta} \dot{\psi} + b_t L (w_4^2 - w_2^2) \\ & - h \sum H_{yi} + \sum (-1)^{i+1} M_{xi}, \end{aligned} \quad (7.67)$$

$$\begin{aligned}
I_{yy}\ddot{\theta} &= J_r\dot{\theta}(w_1 + w_3 - w_2 - w_4) + (I_{yy} - I_{zz})\dot{\theta}\dot{\psi} + b_t L (w_3^2 - w_1^2) \\
&\quad + h \sum H_{xi} + \sum (-1)^{i+1} + M_{yi}, \\
I_{zz}\ddot{\psi} &= -d(w_4^2 + w_2^2 - w_1^2 - w_3^2) + (I_{xx} - I_{yy})\dot{\phi}\dot{\theta} + L(H_{x2} - H_{x4}) \\
&\quad + L(H_{y3} - H_{y1}) + \sum (-1)^i D_i. \\
m\ddot{x} &= (S_\psi S_\phi + C_\psi S_\theta C_\phi) \left( b_t \sum_{i=1}^4 w_i^2 \right) - \sum H_{xi}, \\
m\ddot{y} &= (-C_\psi S_\phi + S_\psi S_\theta C_\phi) \left( b_t \sum_{i=1}^4 w_i^2 \right) - \sum H_{yi}, \\
m\ddot{z} &= mg - (C_\theta C_\phi) \left( b_t \sum_{i=1}^4 w_i^2 \right).
\end{aligned}$$

## 6.7 Control System Design

The control system of the proposed quadrotor system is considered to be composed of two components of motion control system and visual servoing (vision-based control) system. Basically, the vision system is needed for the quadrotor to track and follow a moving target. The cooperative configuration of these control systems is illustrated in a single control structure presented in Figure 5-6.

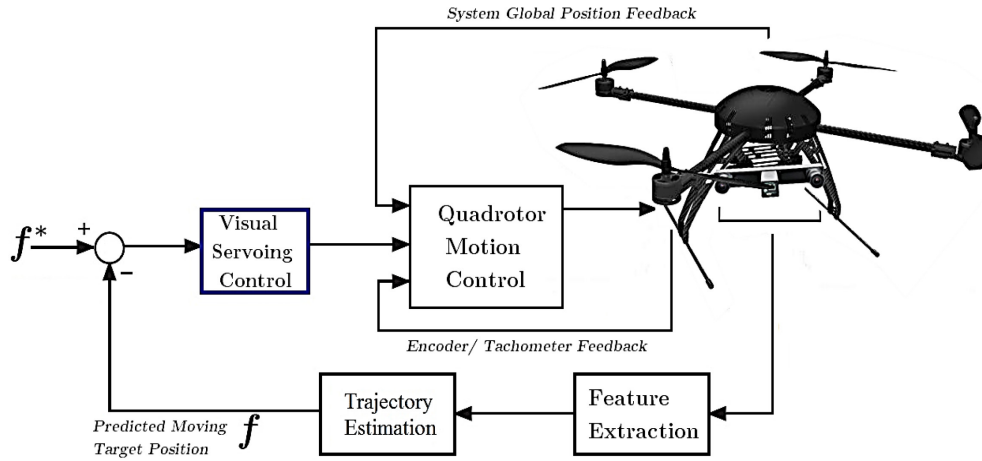


Figure 6-5: UAV Quadrotor control structure consisting of flight motion control and visual servoing system

### 6.7.1 Flight Motion Control System

In order to enable a quadrotor to follow a predefined trajectory, a full control of attitude  $(\phi, \theta, \psi)$ , altitude  $z$  and position  $x, y$  of the system is necessary. Accordingly, to control the attitude of the quadrotor system, a PID controller will be used in this paper. PID control is a benchmark control scheme and has shown good performance with low complexity. From a practical point of view, PID controllers are the simplest scheme and can be designed quickly. This control technique has already been investigated in many efforts [188, 189] to stabilize the attitude of the quadrotor. In order to successfully design this controller, the model is needed to be linearized around the hover situation (equilibrium point). Hence, the gyroscopic effects are sometimes neglected in the controller design [190]. Position control can be also implemented using a PID controller design which actuates the vehicle's roll and pitch angles as control inputs. Tilting the vehicle in any direction causes a component of the thrust vector to point in that direction. In other words, commanding pitch and roll is directly equal to enforcing accelerations in the X-Y plane. For that reason, in this paper we solely try to control the attitude of the quadrotor. The couplings between the control of attitude and position is illustrated in Figure 6-6. while Figure 6-7 shows the schematic of the PID controller.

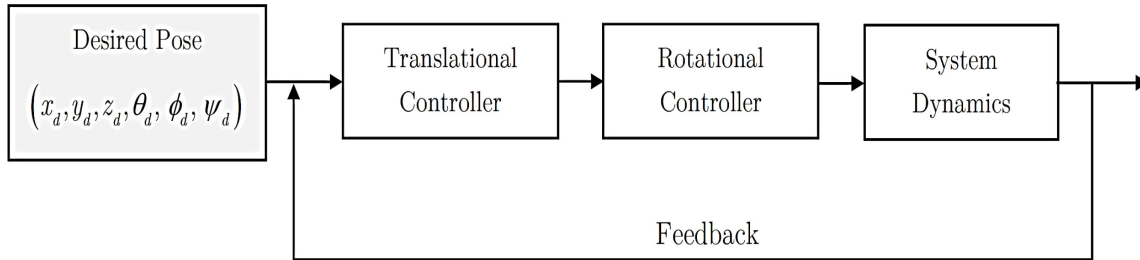


Figure 6-6: Quadrotor control system for attitude and position

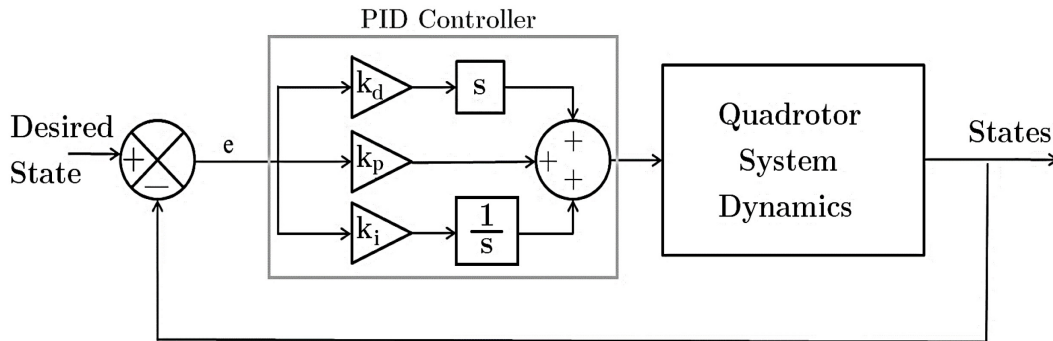


Figure 6-7: Quadrotor PID Controller

The dynamic model of the system, contains gyroscopic effects. By assuming a near-hover situation, the influence of these effects is less important than the actuator's model. Moreover, we can describe the system input vector based on rotors angular rates  $\omega_i$  as follows:

$$U = [U_1, U_2, U_3, U_4], \quad (7.68)$$

where;

$$U_1 = b_t \sum_{i=1}^4 w_i^2, \quad (7.69)$$

$$U_2 = b_t(w_4^2 - w_2^2), \quad (7.70)$$

$$U_3 = b_t(w_3^2 - w_1^2), \quad (7.71)$$

$$U_4 = d(w_2^2 + w_4^2 - w_1^2 - w_3^2) \quad (7.72)$$

$$\Omega = w_1 + w_3 - w_2 - w_4 \quad (7.73)$$

These Equations for control inputs can be re-arranged in a matrix format as:

$$\begin{bmatrix} U_1 \\ U_2 \\ U_3 \\ U_4 \end{bmatrix} = \begin{bmatrix} b_t & b_t & b_t & b_t \\ 0 & -b_t & 0 & b_t \\ b_t & 0 & -b_t & 0 \\ d & -d & d & -d \end{bmatrix} \begin{bmatrix} w_1^2 \\ w_2^2 \\ w_3^2 \\ w_4^2 \end{bmatrix}. \quad (7.74)$$

If the rotor velocities are needed to be calculated from the control inputs, the following equation can be acquired by inverting the matrix in above Equation;

$$\begin{bmatrix} w_1^2 \\ w_2^2 \\ w_3^2 \\ w_4^2 \end{bmatrix} = \begin{bmatrix} \frac{1}{4b_t} & 0 & \frac{1}{2b_t} & \frac{1}{4d} \\ \frac{1}{4b_t} & -\frac{1}{2b_t} & 0 & -\frac{1}{4d} \\ \frac{1}{4b_t} & 0 & -\frac{1}{2b_t} & \frac{1}{4d} \\ \frac{1}{4b_t} & \frac{1}{2b_t} & 0 & -\frac{1}{4d} \end{bmatrix} \begin{bmatrix} U_1 \\ U_2 \\ U_3 \\ U_4 \end{bmatrix}. \quad (7.75)$$

Based on the control inputs, rotor dynamics described in Equations (57-58) and also rotor velocities, the overall open-loop system can be described as Figure 6-8.

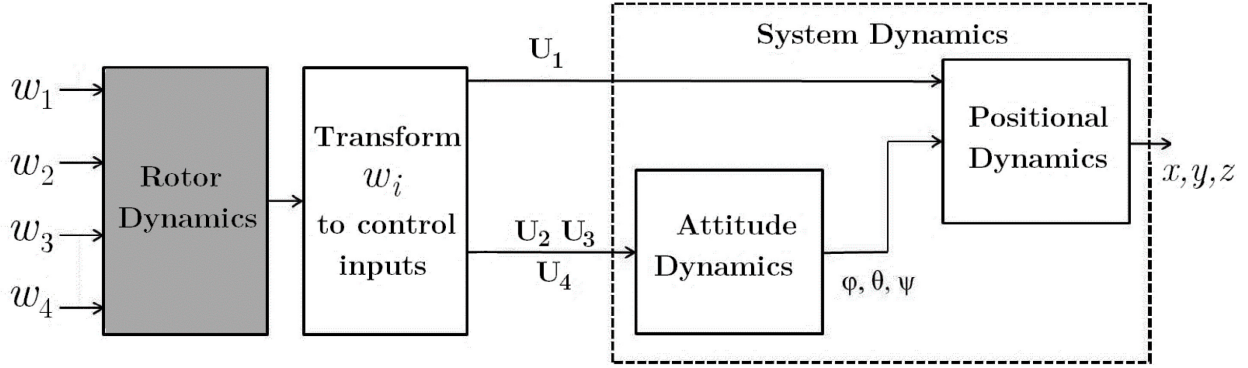


Figure 6-8: Open Loop Block Diagram

By taking into account the rotor dynamics and also system inputs, a complete quadrotor PID control scheme is illustrated in Figure 6-9.

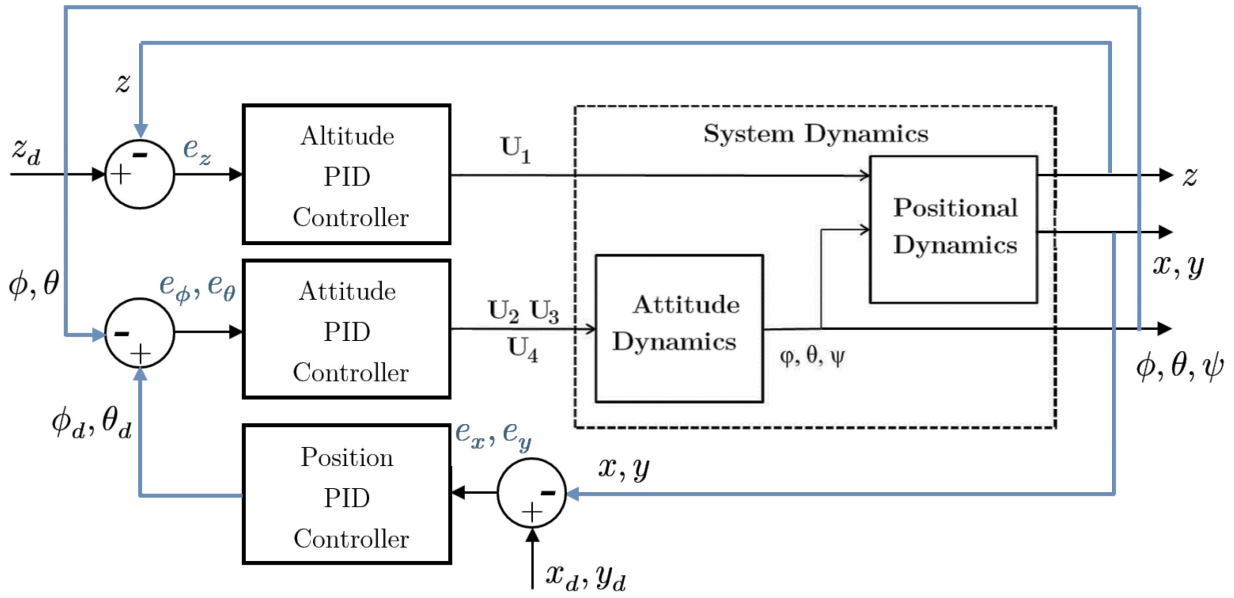


Figure 6-9: Quadrotor complete position, attitude and altitude control scheme

Based on the described control plant in Figure 6-9, PID controllers can be used to generate the control inputs as follows:

$$U_1 = k_{pz}e_z(t) + k_{iz}\int_0^t e_z(\tau)d\tau + k_{dz}\frac{de_z(t)}{dt}, \quad (7.76)$$

$$U_1 = k_{p\phi}e_\phi(t) + k_{i\phi}\int_0^t e_\phi(\tau)d\tau + k_{d\phi}\frac{de_\phi(t)}{dt}, \quad (7.77)$$

$$U_1 = k_{p\theta}e_\theta(t) + k_{i\theta} \int_0^t e_\theta(\tau)d\tau + k_{d\theta} \frac{de_\theta(t)}{dt}, \quad (7.78)$$

$$U_1 = k_{p\psi}e_\psi(t) + k_{i\psi} \int_0^t e_\psi(\tau)d\tau + k_{d\psi} \frac{de_\psi(t)}{dt}, \quad (7.79)$$

### 6.7.2 Visual Servoing System (Vision-based Control)

Using an image-based visual servoing system, the goal of the control problem can be stated as minimizing the error defined as:

$$e_v(t) = s - s^*, \quad (7.80)$$

where  $s$  and  $s^*$  are the vectors of current and desired image features. These features may include detected edges on the target object, colored markers, image moments, etc. In our case, three colored markers (red circle, blue triangle, green square) on the target object are considered as image features which can be extracted using a basic shape/color detection image processing algorithm. In the case of a traditional proportional controller, and by assuming that the camera is mounted on the robot central hub as depicted in Figure 6-5, the input of the visual servoing controller  $u_c$  is designed by letting  $\dot{e}_v = -\lambda e_v$ :

$$u_c = -\lambda_v J_e^+ e_v, \quad (7.81)$$

where  $\mathbf{J}_e$  is the image interaction matrix which relates the time variation of error  $e$  and the camera velocity  $u_c$  and  $\mathbf{J}_e^+$  is the Moore-Penrose pseudo-inverse of the interaction matrix.  $\lambda_v$  is the proportional gain for the visual servoing controller. In the case of moving (non-stationary) image features we have:

$$u_c = J_e^+ \left( -\lambda_v e_v - \frac{\partial e_v}{\partial t} \right), \quad (7.82)$$

where the term  $\partial e_v / \partial t$  represents the time variation of the error caused by the target motion which is considered to have a constant velocity. In our case we assume that the vision system is composed of a stereo camera system with two parallel lenses perpendicular to the baseline [114, 161]. The focal points of two cameras are apart at distance  $b/2$  with respect to origin of sensor frame  $\{C\}$  on the baseline which means the origin of the camera frame, is in the centre of these points. Focal distance of both cameras is  $f_c$  so the image planes and corresponding frames for left and right cameras are located at the distance  $f_c$  from the focal points and orthogonal to the optical axis. We assign  $\{L\}$  and  $\{R\}$  as the frames of the left and right images. Figure 6-10 illustrates the case where both cameras observe a 3D point  ${}^C P$ . Using the image interaction



matrices for the left and right cameras, the stereo image interaction matrix,  $\mathbf{J}_{st}$ , can be calculated as:

$$\mathbf{J}_{st} = \begin{pmatrix} \mathbf{J}_l & \mathbf{J}_r \\ \mathbf{J}_l & \mathbf{J}_r \end{pmatrix} \begin{pmatrix} \mathbf{M}_C \\ \mathbf{M}_C \end{pmatrix} \quad (7.83)$$

The image interaction matrix for each camera is calculated by:

$$\mathbf{J}_i = \begin{bmatrix} -\frac{1}{Z_i} & 0 & \frac{x_i}{Z_i} & x_i y_i & -(1 + x_i^2) & y_i \\ 0 & -\frac{1}{Z_i} & \frac{y_i}{Z_i} & 1 + x_i^2 & -x_i y_i & -x_i \end{bmatrix} \quad (7.84)$$

The stereo feature vector is defined as  $\mathbf{s} = [x_l, y_l; x_r, y_r]^T$  where  $p_l = [x_l, y_l]$ ,  $p_r = [x_r, y_r]^T$  are the normalized image coordinates of the 3D point, observed by the left and right cameras respectively. A perspective camera model using the focal distance,  $f_c$ , can be used to project observed point into left and right image planes. Thus, the following equations hold for 3D coordinates of the observed point:

$$(X, Y, Z) = \left( \frac{b x_l + x_r}{2 x_l - x_r} \quad \frac{b y_l}{x_l - x_r} \quad \frac{b}{x_l - x_r} \right) \quad (7.85)$$

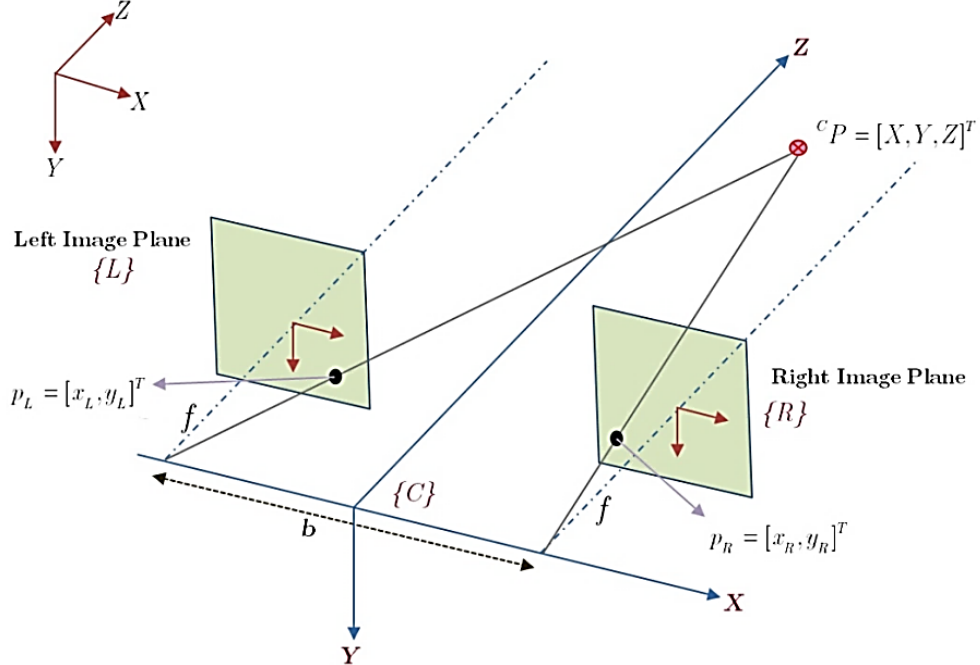


Figure 6-10: Model of the parallel stereo vision system observing a point in 3D space

## 6.8 Detailed Design Objectives and Constraints

In this section, we discuss the requirements for designing each subsystem including objectives representing the performance of the system towards a certain requirement and also constraints acting upon each design variable. Throughout this section,  $\tilde{x}$  is a subset of all design variables  $\mathbf{x}$ . We also provide a table of values for the parameters considered in objectives and constraints of each subsystem.

### 6.8.1 Structure and Body Design Objectives

As the first requirement and based on a series of commercial benchmarks and flight specifications, the quadrotor is subjected to the following physical constraints:

$$g_{1,2}(\tilde{x}): 0.15 \leq L \leq 0.25 \text{ (m)} \quad (7.86)$$

$$g_{3,4}(\tilde{x}): 0.4 \leq L \leq 0.6 \text{ (kg)} \quad (7.87)$$

$$g_{5-8}(\tilde{x}): 0.0025 \leq I_{xx}, I_{yy} \leq 0.0050 \text{ (kg.m}^2\text{)} \quad (7.88)$$

$$g_{9,10}(\tilde{x}): 0.0045 \leq I_{zz} \leq 0.0090 \text{ (kg.m}^2\text{)} \quad (7.89)$$

The first design objectives towards the body and structure of the quadrotor is to maximize the payload and minimize the body weight. We define the payload to be the maximal weight the quadcopter can take at its mass center while hovering. Formulating in negative standard form for minimization, we can write the above objectives as follows using Equations (25-28):

$$S_1(\tilde{x}) = -m_{PL} \quad (7.90)$$

$$S_2(\tilde{x}) = m_{body} \quad (7.91)$$

With regards to the structural strength, we can assume that each arm of the quadrotor behaves as a cantilever beam where the motor thrust and rotor weight act on the tips as depicted in Figure 6-11. Accordingly, we can define an objective function,  $S_2$ , and also a constraint based on the beam's deflection and maximum allowable bending stress as follows:

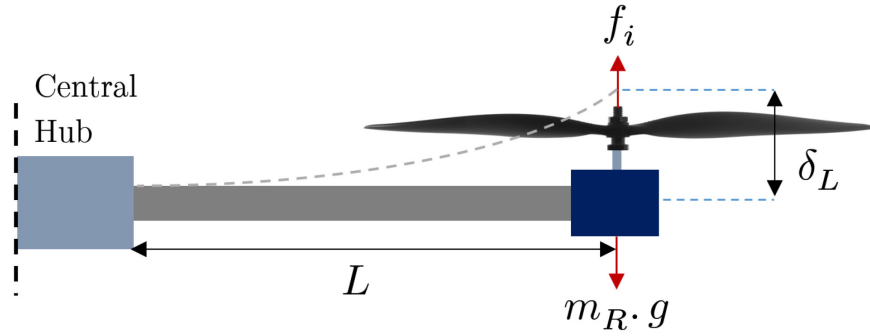


Figure 6-11: Forces acting on quadrotor arm as a cantilever beam

$$S_3(\tilde{x}) = \delta_L = \frac{(f_i - m_R g)L^3}{3EI} \quad (7.92)$$

$$g_{11}(\tilde{x}) : \sigma = \frac{(f_i - m_R g)Lr_L}{I} \leq \frac{1}{SF} \sigma_t \quad (7.93)$$

where the area moment of the rod is equal to  $I = \pi r_L^4/4$ ,  $E$  is the elastic modulus,  $\sigma_t$  is the tensile strength of carbon fiber and  $SF$  is the safety factor.

Also, the rod can fail due to resonance when the natural frequency of the rod matches the frequency of the motor. Hence the rod should be designed in such a way that the natural frequency of the rod is considerably different than the frequency of the motor. The natural frequency of the cantilever beam is given as:

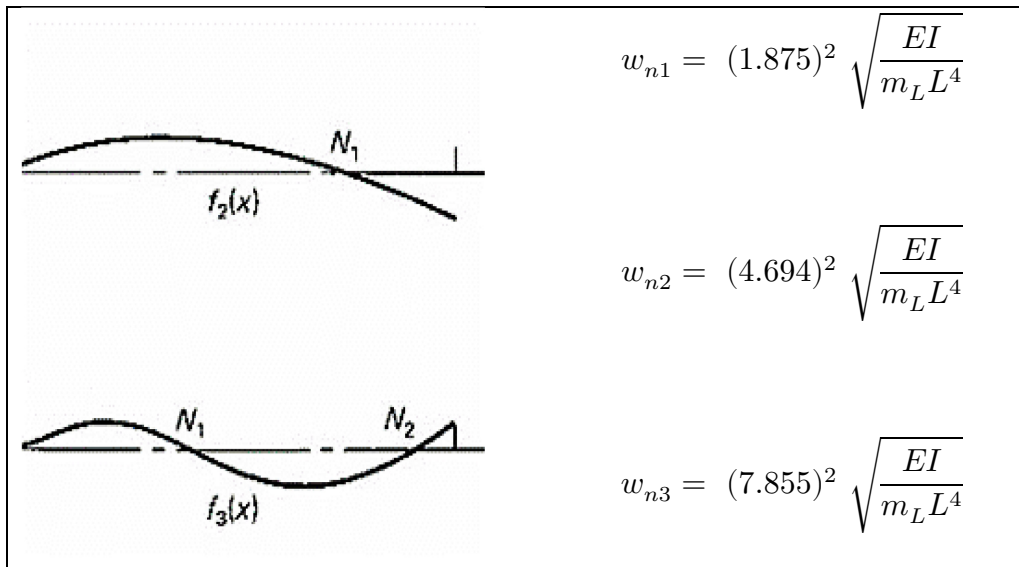


Figure 6-12: Natural Frequency Modes of a Cantilever Beam [191]

Thus, we get the following constraints for the rotor frequencies with regards to the arm's natural frequency:

$$g_{12}(\tilde{x}): |w_i - w_{n1}| \geq \delta_w \quad (7.94)$$

$$g_{13}(\tilde{x}): |w_i - w_{n2}| \geq \delta_w \quad (7.95)$$

$$g_{14}(\tilde{x}): |w_i - w_{n3}| \geq \delta_w \quad (7.96)$$

where  $\delta_w$  is the minimal difference between the rotor frequency and the natural frequency of the arm and is considered to be equal to 30 *rad/s*.

### 6.8.2 Aerodynamics and Propulsion System Objectives

The “propulsion cost factor” describes the cost in power of each gram lifted. The cost factor is an indicator that helps the design process by directly looking at the power spent for each gram of system's total mass. Thus, the cost factor  $C_{prop}$  can be used as a design objective to be minimized:

$$A_1(\tilde{x}) = C_{prop} = \frac{P_e}{\frac{f_i}{g} - m_R} \left[ \frac{W}{gr} \right] \quad (7.97)$$

in which  $P_e$  is electrical power from the battery,  $f_i$  is thrust force and  $m_R$  is the rotor (and propulsion system) mass. Moreover, the “propulsion quality index” describes the quality of mass lifting and indicates whether the system somehow is being disturbed while lifting. This index is necessary to take into account the notions of actuator bandwidth and thrust/weight ratio. This index can be formulated as an objective function to be minimized:

$$A_2(\tilde{x}) = Q_{prop} = \frac{B_{prop}\beta}{wC_{prop}} [Hz.gr/Rad.W] \quad (7.98)$$

where  $B_{prop}$  is the propulsion system bandwidth and  $\beta$  is the thrust/weight ratio.

### 6.8.3 Control System Objectives

The optimization problem for the proposed PID flight controller, can be formulated to achieve the controller gains to optimize some particular control performance functions in the presence of physical, stability and control constraints. For the flight control system, we consider four sets of PID controller gain for altitude ( $z$ ) and attitude control ( $\phi, \theta, \psi$ ). Thus, we have 12 design variables for this subsystem as:

$$K = [k_{pz}, k_{iz}, k_{dz}, k_{p\phi}, k_{i\phi}, k_{d\phi}, k_{p\theta}, k_{i\theta}, k_{d\theta}, k_{p\psi}, k_{i\psi}, k_{d\psi}]^T = [K_z, K_\phi, K_\theta, K_\psi]^T$$

Accordingly, we consider the controller gains to be all non-negative values. Moreover, in order to avoid sudden shocks and abrupt motion, we consider an upper bound of 4 for every gain;

$$g_{15-27}(\tilde{x}): K = [K_z, K_\phi, K_\theta, K_\psi]^T > 0. \quad (7.99)$$

Having the rotor dynamics in Equations (57-58) and using the motor inputs in Laplace domain, we can achieve the following transfer functions for the attitude control system:

$$G_\phi(s) = \frac{\phi(s)}{U_2(s)} = \frac{B^2 L}{s^2(s+A)^2 I_{xx}}, \quad (7.100)$$

$$G_\theta(s) = \frac{\theta(s)}{U_2(s)} = \frac{B^2 L}{s^2(s+A)^2 I_{yy}}, \quad (7.101)$$

$$G_\psi(s) = \frac{\psi(s)}{U_2(s)} = \frac{B^2}{s^2(s+A)^2 I_{zz}}, \quad (7.102)$$

where  $A$  and  $B$  are the coefficients of the linearized rotor dynamics from Equation (58). Moreover, the transfer function for any of the PID controllers is found by taking the Laplace transform of the Equations (76-79):

$$C(s) = \left( k_p + \frac{k_i}{s} + k_d s \right) = \frac{k_d s^2 + k_p s + k_i}{s} \quad (7.103)$$

Now, we can obtain the transfer function of the closed-loop system for each  $\phi, \theta$  and  $\psi$  as follows:

$$T_{\phi, \theta, \psi}(s) = \frac{C_{\phi, \theta, \psi}(s) G_{\phi, \theta, \psi}(s)}{1 + C_{\phi, \theta, \psi}(s) G_{\phi, \theta, \psi}(s)} \quad (7.104)$$

Now by using the Routh-Hurwitz stability criterion we can get the following constraints on the attitude flight control variables:

$$g_{28-31}(\tilde{x}): K_d < \frac{2A^3}{\Gamma} \quad (7.105)$$

$$g_{32-35}(\tilde{x}): 2A^3 K_d - \Gamma K_d^2 - 4A^2 K_p + 2A K_i > 0 \quad (7.106)$$

$$\begin{aligned} g_{36-39}(\tilde{x}): \Gamma^3 \left( 1 - \frac{1}{2A} \right) K_i K_d^2 - 2A \Gamma^3 K_p K_d^2 + 2A^2 \Gamma^2 (1 - A) K_i K_d + 8A^2 \Gamma^2 K_i K_p \\ + 4A^4 \Gamma^2 K_d K_p - 2A^5 \Gamma K_i - 2A \Gamma^2 K_i^2 - 8A^3 \Gamma^2 K_p^2 > 0 \end{aligned} \quad (7.107)$$

where  $K_p = [K_{p\phi}, K_{p\theta}, K_{p\psi}]$ ,  $K_i = [K_{i\phi}, K_{i\theta}, K_{i\psi}]$ ,  $K_d = [K_{d\phi}, K_{d\theta}, K_{d\psi}]$ , and  $\Gamma = [\Gamma_\phi, \Gamma_\theta, \Gamma_\psi]$  for which  $\Gamma_\phi = \frac{B^2 L}{I_{xx}}$ ,  $\Gamma_\theta = \frac{B^2 L}{I_{yy}}$  and  $\Gamma_\psi = \frac{B^2}{I_{zz}}$ .

Moreover, based on frequently used commercial benchmark parameters for a gentle and non-aerobatic flight, the following constraints for control inputs are imposed on the controller design:

$$g_{40-41}(\tilde{x}): |\phi| \leq 40 \text{ deg} \quad (7.108)$$

$$g_{42-43}(\tilde{x}): |\theta| \leq 40 \text{ deg} \quad (7.109)$$

$$g_{44-45}(\tilde{x}): 0 \leq \psi \leq 10 \text{ deg} \quad (7.110)$$

For translational speed and descend rate we also have:

$$g_{46-47}(\tilde{x}): |\dot{z}| \leq 1 \text{ ms}^{-1} \quad (7.111)$$

$$g_{48-49}(\tilde{x}): |\dot{x}| \leq 2 \text{ ms}^{-1} \quad (7.112)$$

$$g_{50-51}(\tilde{x}): |\dot{y}| \leq 2 \text{ ms}^{-1} \quad (7.113)$$

One of the major physical limitations of a quadrotor is the propeller's rotational speed which is constrained by the motor saturation speed. This saturation speed of the propellers should be approximately 41% higher than the hovering speed [162]. The propeller's rotational speed in hovering condition can be found by solving Equations (67-73) for equilibrium point:

$$w_H = \left( \frac{mg}{4b_t} \right)^{\frac{1}{2}} \quad (7.114)$$

Consequently, each rotor speed should agree with the following constraint:

$$g_{52}(\tilde{x}): w_i \leq 0.41 \left( \frac{mg}{4b_t} \right)^{\frac{1}{2}} \quad (7.115)$$

Finally, we formulate the goals of the flight control systems as optimization objective functions. The first control objective can be defined as minimizing a linear combination of the settling times for altitude and attitude control systems, where the settling time,  $T_s$  is the time required by the response to reach and steady within specified range of 2% to 5% of its final value. The same form of objective is also considered for the system's rise time,  $T_r$  and maximum overshoot,  $M_P$ . Thus, we have:

$$C_1(\tilde{x}) = \alpha_{s1} T_{s\phi}(\tilde{x}) + \alpha_{s2} T_{s\theta}(\tilde{x}) + \alpha_{s3} T_{s\psi}(\tilde{x}) + \alpha_{s4} T_{sz}(\tilde{x}), \quad (7.116)$$

$$C_2(\tilde{x}) = \alpha_{r1} T_{r\phi}(\tilde{x}) + \alpha_{r2} T_{r\theta}(\tilde{x}) + \alpha_{r3} T_{r\psi}(\tilde{x}) + \alpha_{r4} T_{rz}(\tilde{x}), \quad (7.117)$$

$$C_3(\tilde{x}) = \alpha_{P1} T_{P\phi}(\tilde{x}) + \alpha_{P2} T_{P\theta}(\tilde{x}) + \alpha_{P3} T_{P\psi}(\tilde{x}) + \alpha_{P4} T_{Pz}(\tilde{x}), \quad (7.118)$$

where  $\alpha_{si}$ ,  $\alpha_{ri}$  and  $\alpha_{Pi}$  are the objective function coefficients defined by the designer for settling time, rise time and maximum overshoot respectively. Figure 6-13 illustrates the properties accompanied with an example of the initial and desired control system responses.

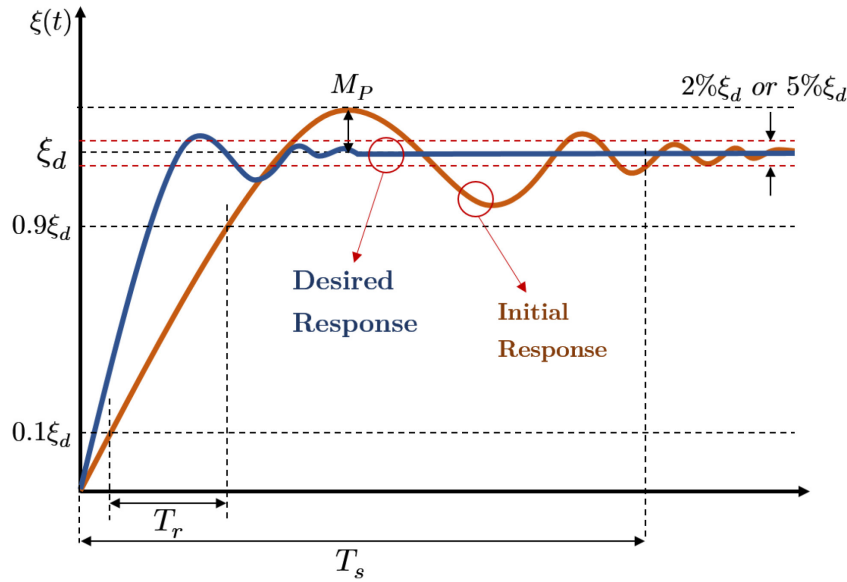


Figure 6-13: Step response properties of flight control system

Additional constraints imposed on the flight control systems are with respect to the system's phase margin and gain margin to guarantee performance and robustness as follows:

$$g_{53}(\tilde{x}): GM(\tilde{x}) > 6dB \quad (7.119)$$

$$g_{54}(\tilde{x}): PM(\tilde{x}) > 45 \text{ deg.} \quad (7.120)$$

#### 6.8.4 Visual Servoing System Objectives:

Towards designing the visual servoing system, the first objective is to minimize an index of the feature error. Here, we use integral squared error (ISE) as follows:

$$V_1(\tilde{x}) = ISE^v = \int_0^{t_f} (s(t) - s^*)^2 dt. \quad (7.121)$$

The overshoot and settling time in reaching the desired image feature positions are also indices which should be minimized for the visual servoing system. Thus, we have:

$$V_2(\tilde{x}) = M_P^{VS}(\tilde{x}). \quad (7.122)$$

One structural constraint imposed on the physics of the visual servoing system is the distance between the focal points of the cameras in the stereo vision system,  $b$ :

$$g_{55-56}(\tilde{x}): 5 \leq b \leq 20 \text{ cm} \quad (7.123)$$

### 6.8.5 System-Level Objectives

From a system-level perspective, various performance indices can be considered as the objective functions to be optimized. Here, we consider two energy-related measures to express the system behavior. First, we try to solve for a set of system design variables which minimizes the consumed energy by four rotors. This can be described as a summation of the rotor speeds during all instances of flight. Accordingly, we have:

$$O_1(\tilde{x}) = \int_0^{t_f} \sum_i w_i dt, \quad (7.124)$$

where  $t_f$  is the flight time.

Moreover, the operational time is an indicator that describes the endurance of the system in a flight. A common formulation of the operational time is described below as a measure we would like to maximize:

$$O_2(\tilde{x}) = -t_{op}(\tilde{x}) = -\frac{m_{bat}C_{bat}}{P_e} [sec] \quad (7.125)$$

where  $m_{bat}$  is the battery mass and  $C_{bat}$  is the battery capacity.

By using the adapted system model and making some simplifications it is possible to analyze the longitudinal dynamic stability of the system for near-hover conditions where the motion of the system is largely decoupled in each axis [192]. Due to the assumed symmetry of the quadrotors, the important attitude dynamics can be described by a single equation. Here, an analysis on the natural stability of system dynamics is presented to provide additional system-level constraints. The necessary simplifying assumptions are:

- The advance ratio  $\chi$  is small.
- The motion is constrained to pitch ( $\theta$ ) and translation  $x$ .
- The blade flapping angles are small.
- The same thrust is applied to each motor.

The system differential equations in terms of stability derivatives in  $x$  and  $\theta$  are [192, 193]:

$$m\ddot{x} + \frac{\partial x}{\partial \dot{x}} \dot{x} + \frac{\partial x}{\partial \theta} \theta - mg\theta = 0, \quad (7.126)$$

$$\frac{\partial M}{\partial \dot{x}} \dot{x} - I_{yy} \dot{\theta} + \frac{\partial M}{\partial \theta} \theta = 0, \quad (7.127)$$



where  $M$  is the pitch moment. Using Routh's Discriminant ( $R.D.$ ), the stability of the system can be assessed for varying physical parameters. The characteristic equation is given by the polynomial in the form of  $As^3 + Bs^2 + Cs + D = 0$ :

$$s^3 - \left( \frac{1}{m} \frac{\partial x}{\partial \dot{x}} + \frac{1}{I_{yy}} \frac{\partial M}{\partial \theta} \right) s^2 + \left( \frac{g}{I_{yy}} \frac{\partial M}{\partial \dot{x}} \right) = 0 \quad (7.128)$$

The stability derivatives can be presented as system-level design constraints:

$$g_{57}(\tilde{x}): \left( \frac{1}{m} \frac{\partial x}{\partial \dot{x}} + \frac{1}{I_{yy}} \frac{\partial M}{\partial \theta} \right) > 0, \quad (7.129)$$

$$g_{58}(\tilde{x}): \left( \frac{g}{I_{yy}} \frac{\partial M}{\partial \dot{x}} \right) > 0. \quad (7.130)$$

## 6.9 Quadrotor Detailed Design Implementation - Optimization Results

In this section, we describe the proposed process of detailed design for a test case of redesigning a commercial quadrotor UAV known as AR. Drone. Figure 6-14 shows the structure of this benchmark system. In the beginning, we need to specify the design variables for which we are willing to search the design space, and also the design parameters which are assumed constant during the process. Equation (131-132) present a list of design variables and parameters while Table 6-2 lists the design parameters with their corresponding values and units which are partially adopted from [194-196].

$$\begin{aligned} \mathbf{x} &= [x_1, x_2, \dots, x_{12}]^T = [r_L, L, r_H, L_H, I_{xx}, I_{yy}, I_{zz}, b, \lambda_v, K_p, K_i, K_d]^T, \\ \mathbf{p} &= [m_R, m_{bat}, \rho_{cf}, b_t, d, J_m, k_m, k_e, R, \gamma, r_{rot}, A_p, \rho_a, \\ &\quad C_T, C_H, C_D, C_M, f_c, E, SF, \sigma_t, \beta, C_{bat}]^T. \end{aligned}$$



Figure 6-14: The structure of AR. Drone 2 as the benchmark system for case study of the proposed detailed design process

Table 6-2: Design Parameters

Param.	Values(Unit)	Param.	Values(Unit)
$m_R$	53.3 ( $g$ )	$C_T$	0.0031
$m_{bat}$	119 ( $g$ )	$C_H$	$0.8e - 3$
$\rho_{cf}$	540 ( $kg/m^3$ )	$C_D$	$0.5e - 3$
$b_t$	$2.89e - 5$ ( $N.S^2$ )	$C_M$	$0.242e - 3$
$d$	$6.1e - 7$ ( $N.m.S^2$ )	$f_c$	0.004 ( $m$ )
$J_{rot}$	$2.0295e - 5$ ( $kg.m^2$ )	$E$	40 ( $GPa$ )
$k_m$	1.3014	$SF$	2
$k_e$	1.481	$\sigma_t$	600 ( $MPa$ )
$\gamma$	80%	$\max P_e$	40.3 ( $W$ )
$r_{rot}$	$99e - 3$ ( $m$ )	$R$	0.6029 ( $\Omega$ )
$A_p$	0.037 ( $m^2$ )	$\beta$	1.5
$\rho_a$	1.225 ( $kg/m^3$ )	$C_{bat}$	1500 ( $mA/H$ )

Since we are dealing with highly coupled and interdependent subsystems, specifying the common variables between each design objective and constraint from various domains helps us understand our mechatronic system as a whole. Figure 6-15 describes these couplings through functional dependency tables (FDT) for objectives and constraints separately.

Now, it is essential to specify our implementation parameters of the optimization algorithm described in Section 6.5 and Equations (6.1-6.7). Table 6-3 shows the best constrained PSO parameters used in the proposed detailed design methodology, while Table 6-4 shows the constrained handling penalty coefficients described in Equation (6.7) for different groups of design constraint functions.

Table 6-3: PSO Parameters

Parameter	Value	Description
$w^t$	0.9 $\rightarrow$ 0.4	Inertia weight
$\zeta_1, \zeta_2$	1.6, 1.8	Acceleration coefficients
$u_i^{1,t}, u_i^{2,t}$	varied	Random real values uniformly distributed in $[0, 1]$
$\alpha$	1.2	Constraint handling coefficient

$x_i$	$x_1$	$x_2$	$x_3$	$x_4$	$x_5$	$x_6$	$x_7$	$x_8$	$x_9$	$x_{10}$	$x_{11}$	$x_{12}$
Obj.	$r_L$	$L$	$r_H$	$L_H$	$I_{xx}$	$I_{yy}$	$I_{zz}$	$b$	$\lambda_v$	$K_p$	$K_i$	$K_d$
$S_1(\tilde{x})$												
$S_2(\tilde{x})$												
$S_3(\tilde{x})$												
$C_1(\tilde{x})$												
$C_2(\tilde{x})$												
$C_3(\tilde{x})$												
$A_1(\tilde{x})$												
$A_2(\tilde{x})$												
$V_1(\tilde{x})$												
$V_2(\tilde{x})$												
$O_1(\tilde{x})$												
$O_2(\tilde{x})$												

(a)

$x_i$	$x_1$	$x_2$	$x_3$	$x_4$	$x_5$	$x_6$	$x_7$	$x_8$	$x_9$	$x_{10}$	$x_{11}$	$x_{12}$
Constr.	$r_L$	$L$	$r_H$	$L_H$	$I_{xx}$	$I_{yy}$	$I_{zz}$	$b$	$\lambda_v$	$K_p$	$K_i$	$K_d$
$g_{1-10}(\tilde{x})$												
$g_{11-14}(\tilde{x})$												
$g_{15-27}(\tilde{x})$												
$g_{28-39}(\tilde{x})$												
$g_{40-52}(\tilde{x})$												
$g_{53-54}(\tilde{x})$												
$g_{55-56}(\tilde{x})$												
$g_{57-58}(\tilde{x})$												

(b)

Figure 6-15: Functional Dependency Tables (FDT) for: (a) System design objectives, (b) design constraints.

Table 6-4: Penalty coefficients,  $a_i$ , for constrained PSO

Constraint Function	Group and Subsystem	Penalty Coefficient
$g_1 - g_{10}$	Structure and Body	1.5
$g_{11} - g_{14}$	Structure and Body	0.9
$g_{15} - g_{27}$	Flight Control System	1
$g_{28} - g_{39}$	Flight Control System	1.1
$g_{40} - g_{51}$	Flight Control System	0.9
$g_{52} - g_{54}$	Flight Control System	1
$g_{55} - g_{56}$	Visual Servoing System	1
$g_{57} - g_{58}$	Dynamic Stability	0.5

Moreover, to model the interactions and relative importance of criteria involved in the detailed design, we also need to specify the fuzzy measures and indices based on the method described in Section 6.5. The mechanism of assigning the fuzzy measures to each criterion and sub-criterion from various domains has been depicted in Figure 6-2. Table 6-5 shows the results for identification of fuzzy measures based on Sugeno  $\lambda$ -method where:

$$[\mu_{structure}, \mu_{control}, \mu_{aero}, \mu_{visual}, \mu_{syslevel}] = [\mu_1, \mu_2, \mu_3, \mu_4, \mu_5] .$$

Table 6-5: Results for fuzzy measures identified using  $\lambda$ -method for the main subsystems

$\mu_1 = 0.22$	$\mu_{12} = 0.452$	$\mu_{13} = 0.374$	$\mu_{14} = 0.403$	$\mu_{15} = 0.471$
$\mu_{123} = 0.600$	$\mu_2 = 0.24$	$\mu_{23} = 0.394$	$\mu_{24} = 0.423$	$\mu_{25} = 0.490$
$\mu_{124} = 0.628$	$\mu_{135} = 0.619$	$\mu_3 = 0.16$	$\mu_{34} = 0.345$	$\mu_{35} = 0.413$
$\mu_{125} = 0.693$	$\mu_{145} = 0.646$	$\mu_{245} = 0.665$	$\mu_4 = 0.19$	$\mu_{45} = 0.442$
$\mu_{134} = 0.553$	$\mu_{234} = 0.7854$	$\mu_{345} = 0.591$	$\mu_{235} = 0.637$	$\mu_5 = 0.26$
$\mu_{1234} = 0.772$	$\mu_{1235} = 0.835$	$\mu_{1345} = 0.790$	$\mu_{2345} = 0.808$	$\mu_{1245} = 0.862$

Moreover, Tables 6-8 present the fuzzy measures for the objective functions within every subsystem.

Table 6-6: Fuzzy measures identified for the structure subsystems

$\mu_1^s$ = 0.30	$\mu_2^s$ = 0.45	$\mu_3^s$ = 0.28
$\mu_{12}^s$ = 0.738	$\mu_{13}^s$ = 0.572	$\mu_{23}^s$ = 0.7189

Table 6-7: Fuzzy measures identified for the control subsystems

$\mu_1^c$ = 0.40	$\mu_2^c$ = 0.30	$\mu_3^c$ = 0.35
$\mu_{12}^c$ = 0.683	$\mu_{13}^c$ = 0.731	$\mu_{23}^c$ = 0.635

Table 6-8: Fuzzy measures identified for the aerodynamics, visual servoing and system-level objectives

$\mu_1^a$ = 0.55	$\mu_2^a$ = 0.47	$\mu_{12}^a$ = 1
$\mu_1^v$ = 0.55	$\mu_2^v$ = 0.50	$\mu_{12}^v$ = 1
$\mu_1^o$ = 0.70	$\mu_2^o$ = 0.33	$\mu_{12}^o$ = 1

Based on the fuzzy measures obtained by the identification algorithm, we attain the resulting interaction and importance indices based on Equations (11-12). These indices are shown in Equation (133-138).

$$I = \begin{bmatrix} \phi_1 & I_{12} & I_{13} & I_{14} & I_{15} \\ I_{21} & \phi_2 & I_{23} & I_{24} & I_{25} \\ I_{31} & I_{32} & \phi_3 & I_{34} & I_{35} \\ I_{41} & I_{42} & I_{43} & \phi_4 & I_{45} \\ I_{51} & I_{52} & I_{53} & I_{54} & \phi_5 \end{bmatrix} \quad (7.133)$$

$$= \begin{bmatrix} 0.206 & -0.0078 & -0.0050 & -0.0061 & 0.0085 \\ -0.0078 & 0.224 & -0.0055 & -0.0067 & 0.0093 \\ -0.0050 & -0.0055 & 0.149 & -0.0042 & 0.0060 \\ -0.0061 & -0.0067 & -0.0042 & 0.177 & 0.0073 \\ 0.0085 & 0.0093 & -0.0060 & 0.0073 & 0.244 \end{bmatrix}$$

$$I^s = \begin{bmatrix} \phi_1^s & I_{12}^s & I_{13}^s \\ I_{21}^s & \phi_2^s & I_{23}^s \\ I_{31}^s & I_{32}^s & \phi_3^s \end{bmatrix} = \begin{bmatrix} 0.2905 & 0.0117 & -0.0072 \\ 0.0117 & 0.4386 & -0.0109 \\ -0.0072 & -0.0109 & 0.2709 \end{bmatrix} \quad (7.134)$$

$$I^c = \begin{bmatrix} \phi_1^c & I_{12}^c & I_{13}^c \\ I_{21}^c & \phi_2^c & I_{23}^c \\ I_{31}^c & I_{32}^c & \phi_3^c \end{bmatrix} = \begin{bmatrix} 0.3822 & -0.0163 & -0.0191 \\ -0.0163 & 0.2846 & -0.0142 \\ -0.0191 & -0.0142 & 0.3332 \end{bmatrix} \quad (7.135)$$

$$I^a = \begin{bmatrix} \phi_1^a & I_{12}^a \\ I_{21}^a & \phi_1^a \end{bmatrix} = \begin{bmatrix} 0.54 & -0.02 \\ -0.02 & 0.46 \end{bmatrix} \quad (7.136)$$

$$I^v = \begin{bmatrix} \phi_1^v & I_{12}^v \\ I_{21}^v & \phi_1^v \end{bmatrix} = \begin{bmatrix} 0.525 & -0.05 \\ -0.05 & 0.475 \end{bmatrix} \quad (7.137)$$

$$I^o = \begin{bmatrix} \phi_1^o & I_{12}^o \\ I_{21}^o & \phi_1^o \end{bmatrix} = \begin{bmatrix} 0.685 & -0.03 \\ -0.03 & 0.315 \end{bmatrix} \quad (7.138)$$

Using the parameters described in Tables 6-3:8 and Equations (6.133:138), the proposed PSO algorithm for detailed design has been executed using MATLAB Optimization and Global Optimization toolboxes and a multiobjective PSO implementation (MOPSO) by Coello et al. [197]. The optimization process has been carried out for a fully connected swarm topology while the swarm size and maximum number of iterations have been varied. While Table 9 shows the original specifications of the AR. Drone 2, Tables 6-10:11 present the results from the proposed detailed design algorithm with different configurations of PSO algorithm. Please note that the controller gains are  $K_p = [k_{p\phi}, k_{p\theta}, k_{p\psi}, k_{pz}]$ ,  $K_i = [k_{i\phi}, k_{i\theta}, k_{i\psi}, k_{iz}]$  and  $K_d = [k_{d\phi}, k_{d\theta}, k_{d\psi}, k_{dz}]$ .

Table 6-9: Physical and control Specifications of an AR. Drone 2

Param.	Values(Unit)	Param.	Values(Unit)
$m_{body}$	432.0 ( $g$ )	$m_{PL}$	131 ( $g$ )
$L$	0.1785 ( $m$ )	$K_p$	[3.2, 3.1, 4.1, 8.3]
$I_{xx}$	$2.233e - 3(kg.m^2)$	$K_i$	[0.6, 0.7, 1.7, 3.1]
$I_{yy}$	$2.988e - 3(kg.m^2)$	$K_d$	[1.4, 1.4, 1.5, 2.2]
$I_{zz}$	$4.834e - 3(kg.m^2)$	$t_{op}$	706 ( $sec$ )

Table 6-10: Optimization results for swarm size of  $n = 100$  with maximum iterations of  $T_{max} = 200$ .

Param.	Values(Unit)	Param.	Values(Unit)
$m_{body}$	407.1 ( $g$ )	$m_{PL}$	179 ( $g$ )
$L$	0.1809 ( $m$ )	$b$	0.12 ( $m$ )
$r_L$	0.01046 ( $m$ )	$\lambda_v$	0.599
$L_H$	0.03412 ( $m$ )	$K_p$	[3.04, 3.04, 4.42, 7.91]
$r_H$	0.01263 ( $m$ )	$K_i$	[0.41, 0.41, 0.93, 2.3]
$I_{xx}$	$3.803e - 3(kg.m^2)$	$K_d$	[1.1, 1.1, 1.75, 3.1]
$I_{yy}$	$3.803e - 3(kg.m^2)$	$t_{op}$	719 ( $sec$ )
$I_{zz}$	$7.631e - 3(kg.m^2)$		

Table 6-11: Optimization results for swarm size of  $n = 500$  with iterations of  $T_{max} = 1000$ .

Param.	Values(Unit)	Param.	Values(Unit)
$m_{body}$	415.1 ( $g$ )	$m_{PL}$	191 ( $g$ )
$L$	0.1582 ( $m$ )	$b$	0.102 ( $m$ )
$r_L$	0.00955 ( $m$ )	$\lambda_v$	0.410
$L_H$	0.03002 ( $m$ )	$K_p$	[3.7, 3.7, 5.5, 8.1]
$r_H$	0.01205 ( $m$ )	$K_i$	[0.24, 0.24, 0.44, 1.07]
$I_{xx}$	$2.187e - 3(kg.m^2)$	$K_d$	[0.93, 0.93, 1.57, 3.82]
$I_{yy}$	$2.187e - 3(kg.m^2)$	$t_{op}$	710 ( $sec$ )
$I_{zz}$	$4.549e - 3(kg.m^2)$		

With each described PSO configurations, Tables 6-12:13 show the values for the design objectives and also the final normalized value of the overall objective function. It is worth to note that we have considered  $\alpha_s = [0.3, 0.3, 0.2, 0.2]$ ,  $\alpha_r = [0.3, 0.3, 0.2, 0.2]$  and  $\alpha_P =$

$[0.27, 0.27, 0.27, 0.19]$  as the objective function coefficients for the settling time, rise time and maximum overshoot respectively.

Table 6-12: Design objective values for the PSO run with swarm size of  $n = 100$  with maximum iterations of  $T_{max} = 200$ .

Design Objective	Function Value	Design Objective	Function Value
$S_1(\tilde{x})$	0.179	$C_1(\tilde{x})$	0.788
$S_2(\tilde{x})$	0.4071	$C_2(\tilde{x})$	0.0231
$S_3(\tilde{x})$	0.00081	$C_3(\tilde{x})$	0.17
$A_1(\tilde{x})$	0.07563	$O_1(\tilde{x})$	18433
$A_2(\tilde{x})$	5.1753	$O_2(\tilde{x})$	719
Overall Objective Function $f_{pso}(\vec{x})$ :			0.68119

Table 6-13: Design objective values for the PSO run with swarm size of  $n = 500$  with maximum iterations of  $T_{max} = 1000$ .

Design Objective	Function Value	Design Objective	Function Value
$S_1(\tilde{x})$	0.191	$C_1(\tilde{x})$	0.612
$S_2(\tilde{x})$	0.4151	$C_2(\tilde{x})$	0.0166
$S_3(\tilde{x})$	0.00093	$C_3(\tilde{x})$	0.07
$A_1(\tilde{x})$	0.07291	$O_1(\tilde{x})$	18110
$A_2(\tilde{x})$	5.1648	$O_2(\tilde{x})$	710
Overall Objective Function $f_{pso}(\vec{x})$ :			0.73218

## 6.10 Simulations and Discussion

In order to visualize the results achieved from the optimization algorithm and to observe the effectiveness of the obtained systems variables, we have built a simulation model based on the derived mathematical model for the overall system and each subsystem. Then, we used SIMULINK to integrate all the subsystems and test the integrated final model in performing a specific task. The test scenario for the quadrotor was to start the flight in the altitude of  $z = 7.0$  ( $m$ ), detect and track a moving target on the ground, follow it for a distance of  $5$  ( $m$ ) with a maximum velocity of  $0.5$  ( $m.s^{-1}$ ) while maintaining the altitude of  $z = 4$  ( $m$ ) and finally approach and intercept it on the ground. The target is specified using four feature points to be tracible with the visual servoing system. Figure 16 describes the test scenario in the simulation model.

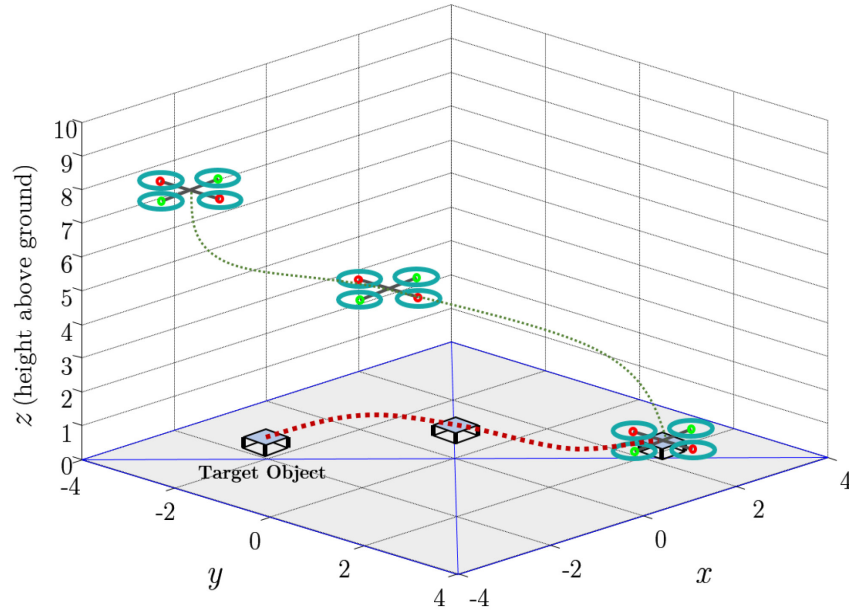


Figure 6-16: Quadrotor simulation model in test scenario where it tracks and intercepts a target

Figures 6-17 shows the step response of the original AR. Drone compared to the ones obtained by using the optimization results for attitude and altitude control systems. Moreover, Figure 6-18 shows the tracking error results for the visual servoing system while Figure 6-19 illustrates the image feature trajectories during the interception sequence. Finally, Figure 6-20 shows the body velocity screws during the visual tracking and interception.

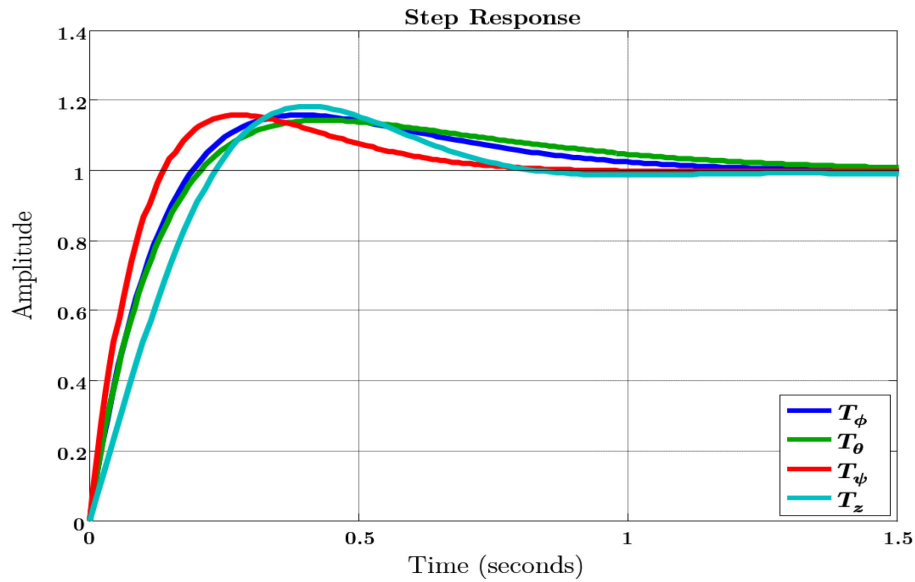
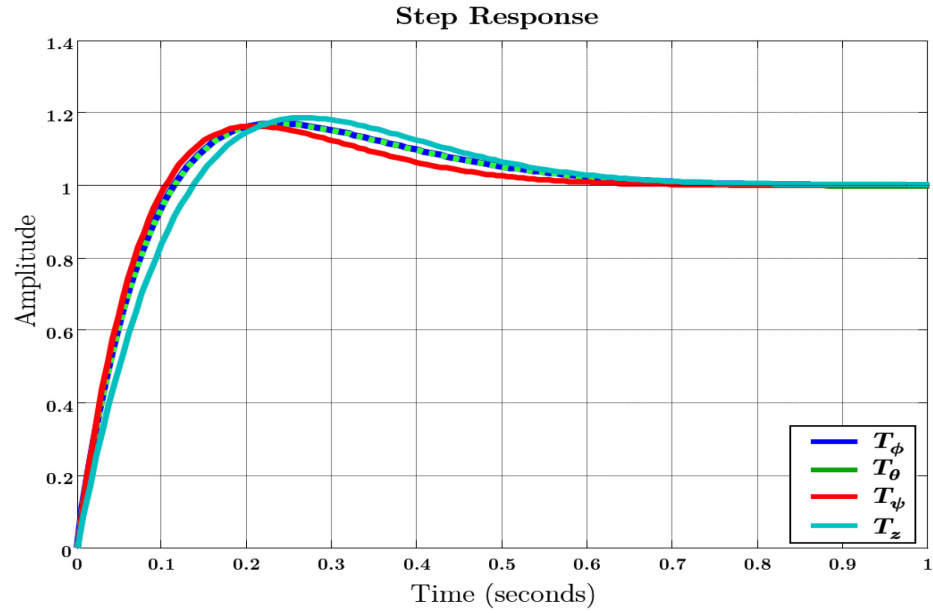
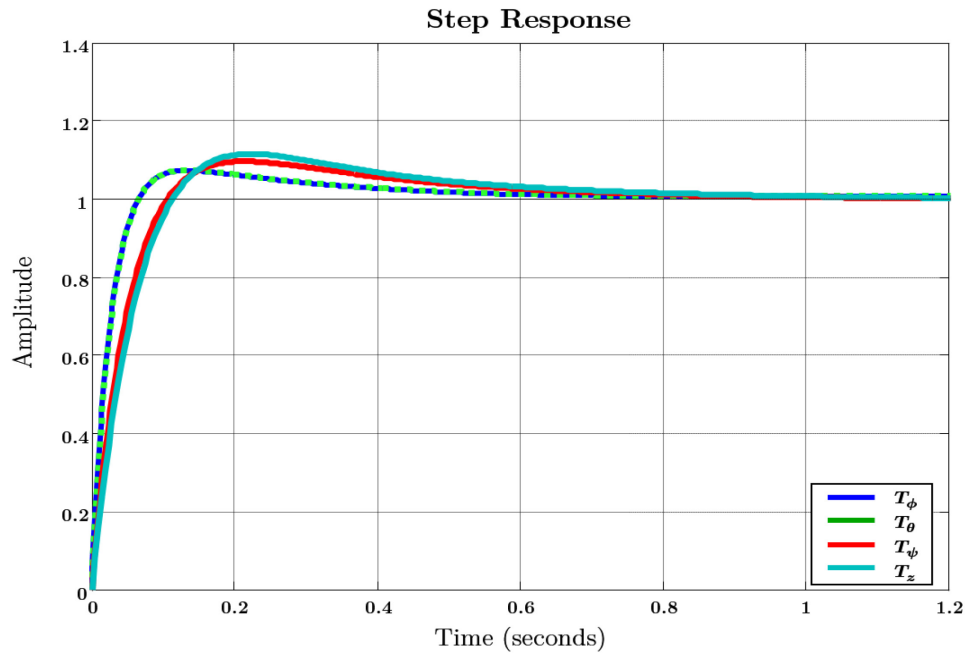


Figure 6-17: Step response results for attitude and altitude control system obtained from original AR. Drone





(a)



(b)

Figure 6-18: Step response results for attitude and altitude control system obtained from: (a) PSO optimization results with swarm size of  $n = 100$  with maximum iterations of  $T_{max} = 200$ , (b) PSO optimization results with swarm size of  $n = 500$  with maximum iterations of  $T_{max} = 1000$ .

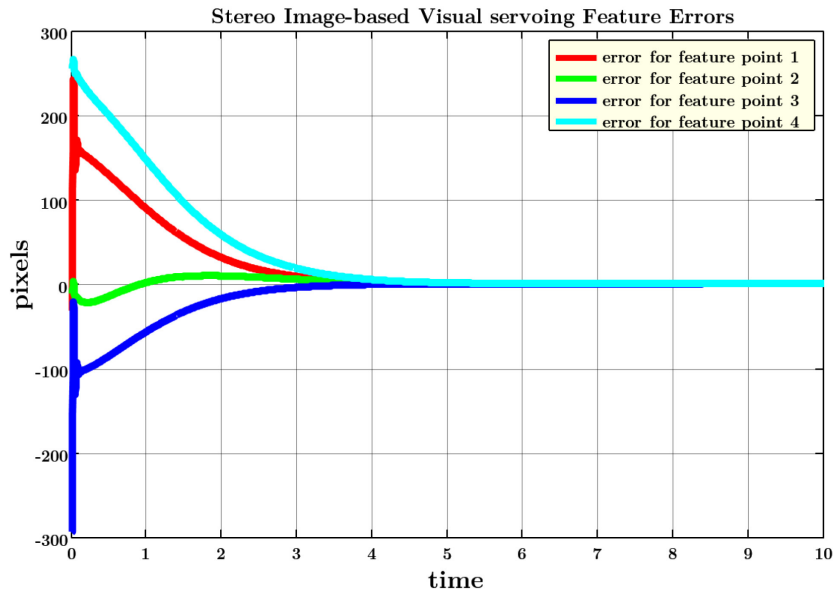
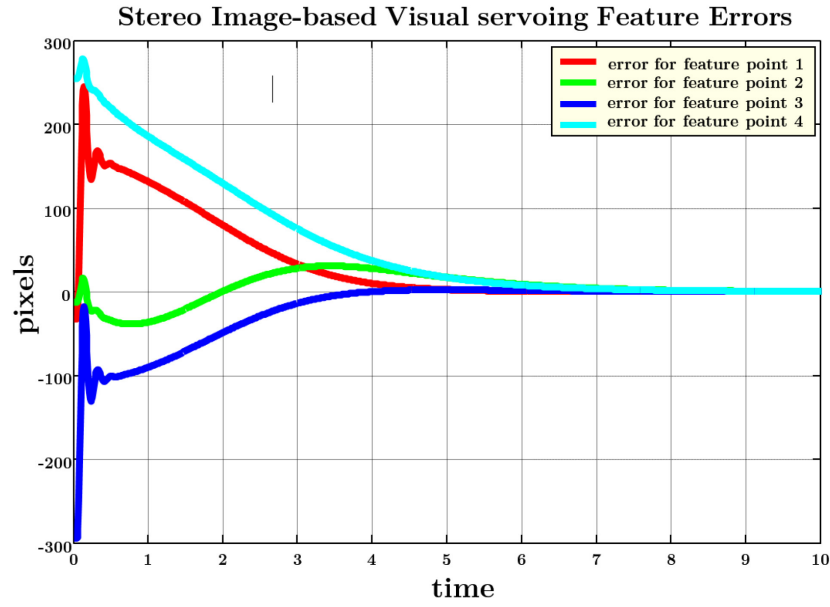
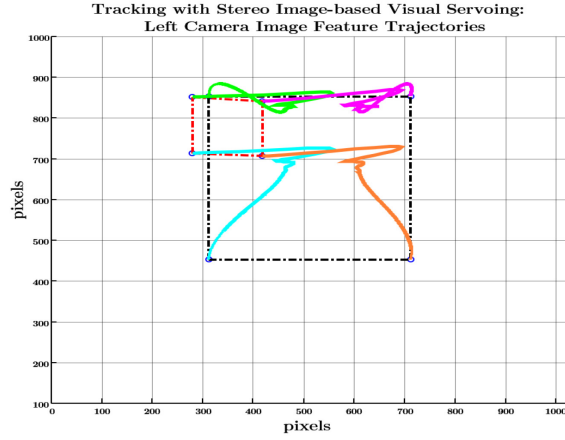
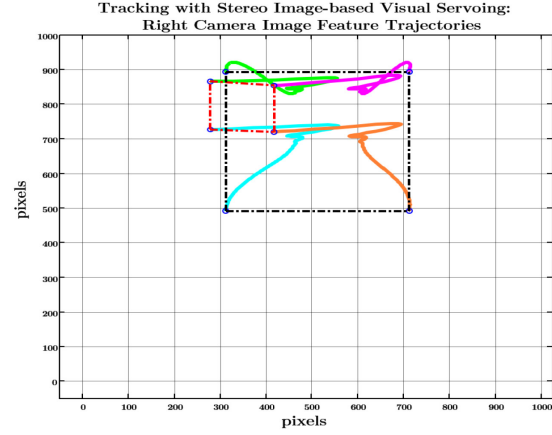


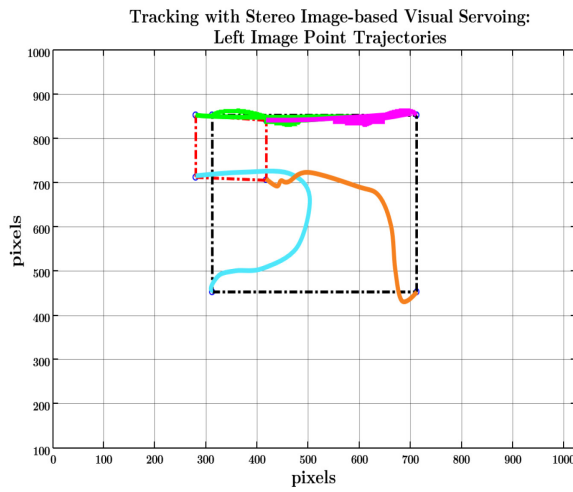
Figure 6-19: Tracking error results for the visual servoing system obtained from: (a) PSO optimization results with swarm size of  $n = 100$  with maximum iterations of  $T_{max} = 200$ , (b) PSO optimization results with swarm size of  $n = 500$  with maximum iterations of  $T_{max} = 1000$ .



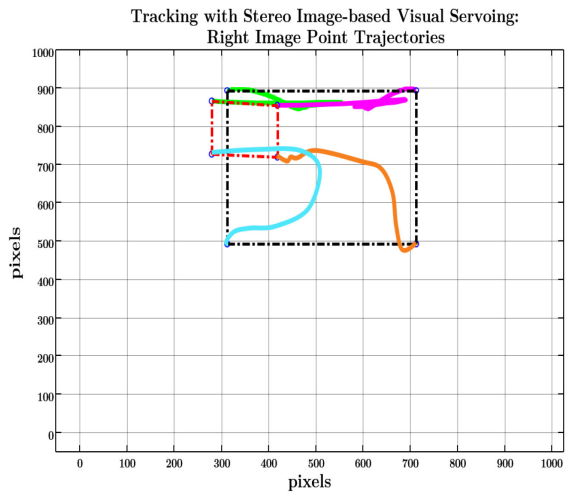
(a)



(b)

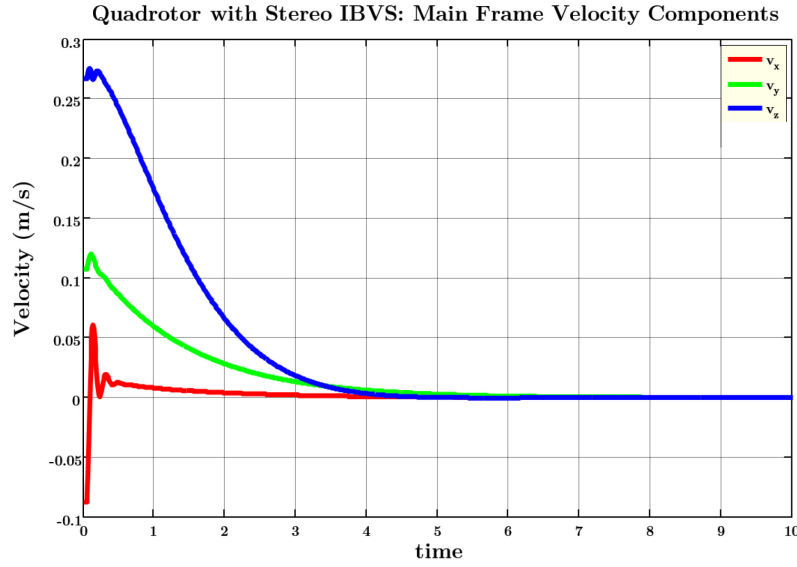


(c)

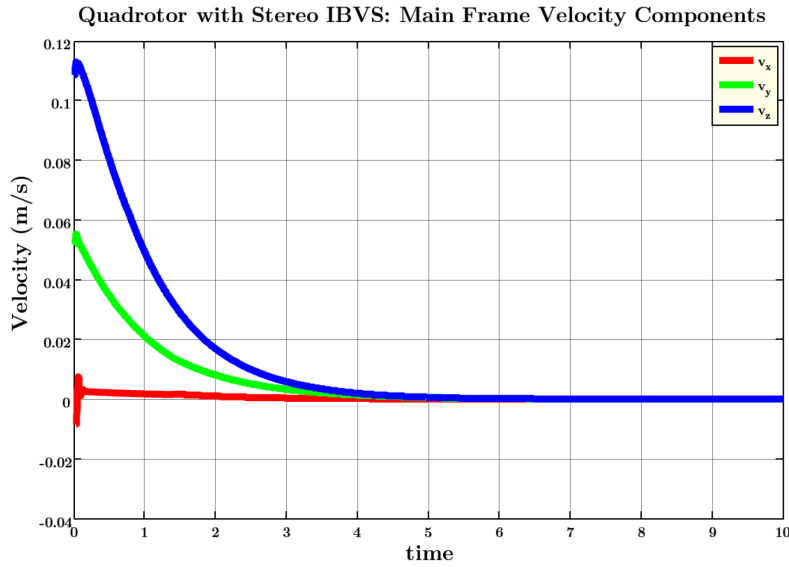


(d)

Figure 6-20: Image feature trajectories for the visual servoing system obtained from: (a, b) PSO optimization results with swarm size of  $n = 100$  with maximum iterations of  $T_{max} = 200$ , (c, d) PSO optimization results with swarm size of  $n = 500$  with maximum iterations of  $T_{max} = 1000$ .



(a)



(b)

Figure 6-21: Main frame translational velocity components during the object tracking process, obtained from: (a) PSO optimization results with swarm size of  $n = 100$  with maximum iterations of  $T_{max} = 200$ , (b) PSO optimization results with swarm size of  $n = 500$  with maximum iterations of  $T_{max} = 1000$ .

From the results listed in Tables 6-12:13 and also Figures 6-17:20, it can be inferred that the system performance with regards to most objective functions is improved by using the proposed detailed design algorithm. Moreover, using a larger swarm size and more iterations, the results are

mostly refined. The results demonstrate that we have better performance with regards to the flight control and visual servoing systems throughout the optimization process. From the step response graphs, we can observe that the rise time, settling time and maximum overshoot are all decreased throughout both optimization runs. The image feature tracking errors show less oscillations in the second attempt and the main frame translational velocity components start with relatively lower speeds during the visual tracking process. The visual servoing steady state error for both executions converges to zero, while it happens earlier for the second system. The results also demonstrate that the image feature trajectories are smoother with less unnecessary motions in the system with second optimization results. The smoothness of the trajectories can be seen in the image plane trajectories (Figure 6-19).

### 6.11 Conclusion

In this paper, a fuzzy-based particle swarm optimization (PSO) algorithm has been created, and integrated into a multiobjective design framework for mechatronic systems. Our proposed methodology is then applied to detailed design and optimization of a vision-guided quadrotor UAV system and the results are presented. Since the PSO is a gradient-free method and can solve discontinuous, multi-modal and non-convex problems, it is a suitable tool to be incorporated into engineering design frameworks. Using the proposed fuzzy-based method, all the design criteria and objectives from various disciplines and subsystems can be integrated in a single performance index while considering the interactions and correlations among the objectives. Furthermore, this design methodology offers an integrated, concurrent, and system-based viewpoint to mechatronic design, which deviates from the non-optimal sequential design methodologies. The detailed design results and related computer simulations, show the ability of the proposed method to find solutions for an optimal mechatronic design. In addition, using the proposed multi-level objective aggregation lightens up the possibility of distributing the objective function evaluations in multiple computers or even building upon a multi-agent platform, and thus will be the subject of further investigation.

## CHAPTER 7 GENERAL DISCUSSION

### 7.1 Research Contributions

During the course of present research, we mainly focused on development of concurrent, integrated, and optimal design methodologies to support the conceptual and detailed design of mechatronic systems. These developments can be summarized in a design roadmap for mechatronic systems as depicted in Figure 7-1. Moreover, the main research objective was divided into four sub-objectives as summarized in Figure 7-2.

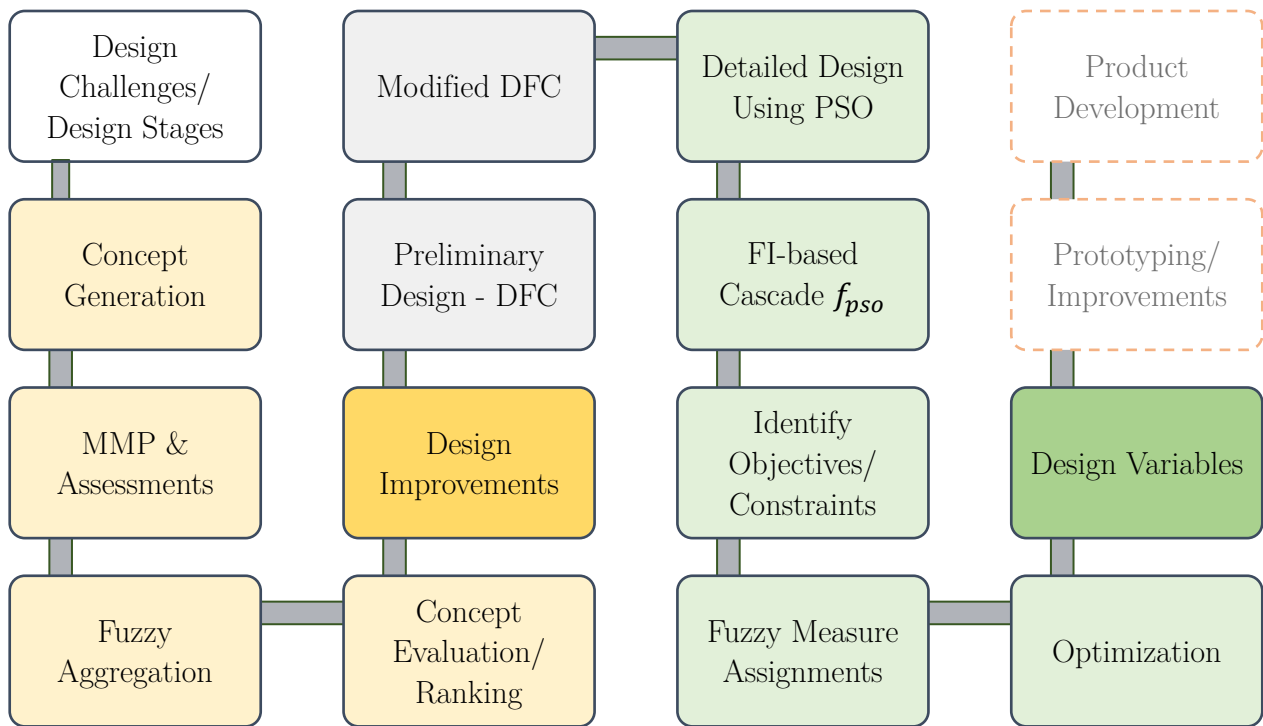


Figure 7-1: Proposed mechatronic design roadmap based on the research contributions and developments in various design phases

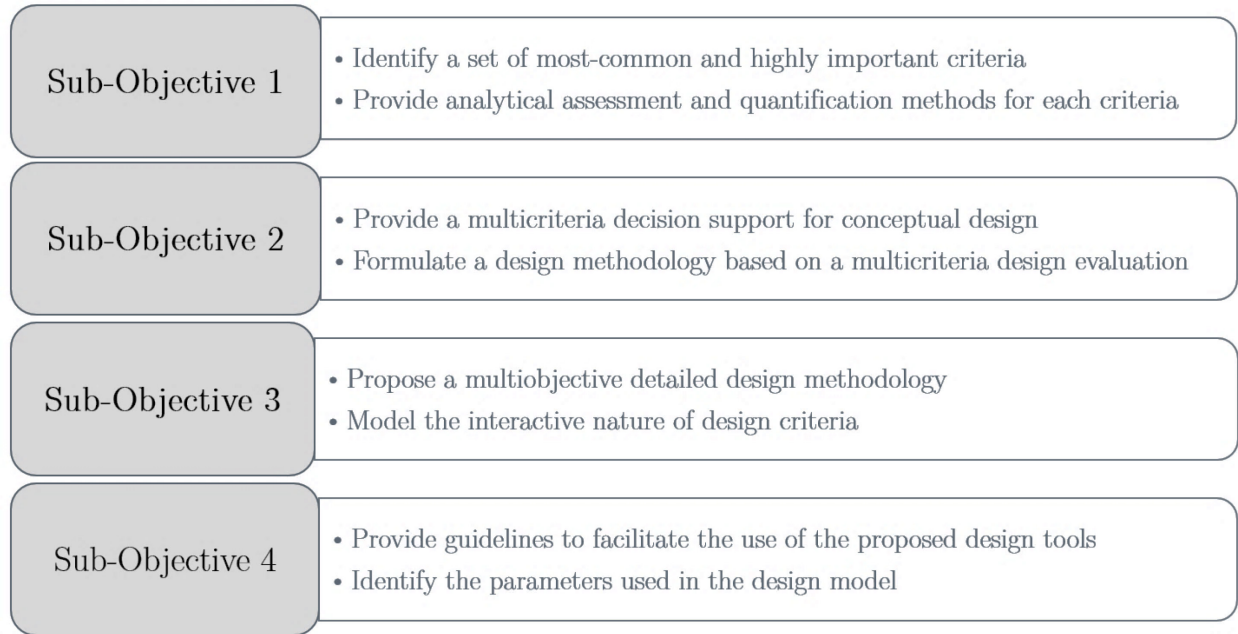


Figure 7-2: Research sub-objectives covered in this thesis

The outcomes of this research are published (or submitted for publication) in a number of journals and conference proceedings. Following is the list of author's contributions followed by the corresponding research sub-objectives (SO) and related publications;

1. A thorough Survey of current methodologies, and identification of main challenges in mechatronic system design;
  - A. Mohebbi, L. Baron, S. Achiche, "Trends in concurrent, multi-criteria and optimal design of mechatronic systems: A review," in Innovative Design and Manufacturing (ICIDM), Proceedings of the 2014 International Conference on, 2014, pp. 88-93.
2. Identification and optimization of the key objectives and criteria in designing a mechatronic product and forming an evaluation and measurement framework with regards to these requirements (**SO1**);
  - A. Mohebbi, S. Achiche, and L. Baron, "Multicriteria Decision Support for Conceptual Design of Mechatronic Systems; A Quadrotor Design Case Study", Submitted to the Springer Journal of Research in Engineering Design, 2015.
  - A. Mohebbi, S. Achiche, and L. Baron, "Mechatronic Multicriteria Profile (MMP) for Conceptual Design of a Robotic Visual Servoing System," in ASME 2014 12th

Biennial Conference on Engineering Systems Design and Analysis, 2014, pp. V003T15A015-V003T15A015.

3. Formulation of a fuzzy-based approach to model relative importance as well as interactions and correlations between the multi-domain criteria in mechatronic systems design (**SO2**);
  - A. Mohebbi, S. Achiche, L. Baron, and L. Birglen, “Fuzzy Decision Making for Conceptual Design of a Visual Servoing System Using Mechatronic Multi-Criteria Profile (MMP),” in ASME 2014 International Mechanical Engineering Congress and Exposition, 2014, pp. V011T14A055-V011T14A055.
  - A. Mohebbi, L. Baron, S. Achiche, and L. Birglen, “Neural network-based decision support for conceptual design of a mechatronic system using mechatronic multi-criteria profile (MMP),” in Innovative Design and Manufacturing (ICIDM), Proceedings of the 2014 International Conference on, 2014, pp. 105-110.
4. Application of the widely used “Design-for-Control” approach for preliminary design of mechatronic systems and providing analytical and comparative insights through a case study (**SO3**);
  - A. Mohebbi, S. Achiche, and L. Baron, “Design of a Vision Guided Mechatronic Quadrotor System Using Design for Control Methodology,” Transactions of the Canadian Society for Mechanical Engineering, vol. 40, pp. 201-219, 2016.
  - A. Mohebbi, S. Achiche, and L. Baron, “Integrated Design of a Vision-Guided Quadrotor UAV: A Mechatronics Approach”, Symposium of Mechanisms, Machines, and Mechatronics (M3), CCToMM 2015, Ottawa, Canada.
5. Proposition of a system-based multi-objective design optimization approach for detailed design of a complex mechatronic system (**SO3**);
  - A. Mohebbi, C. Gallacher, J. Willes, J. Harrison, S. Achiche, “Integrated Structure-Control Design Optimization of an Unmanned Quadrotor Helicopter (UQH) for Object Grasping and Manipulation”, Submitted to 21<sup>st</sup> international conference on Engineering Design, ICED 2017, Vancouver, Canada.
6. Formulating and application of a detailed design methodology by the means of fuzzy-based decision analysis tools embedded in a gradient-free optimization algorithm (**SO3**);



- A. Mohebbi, L. Baron and S. Achiche, “Integrated and Concurrent Detailed Design of a Mechatronic Quadrotor System Using a Fuzzy-based Particle Swarm Optimization”, Submitted to IEEE Transaction of Industrial Electronics, 2017.
7. Supporting the incorporation of multicriteria decision making tools into the design process, by proposing a framework to help the designers with assessment of criteria importance and interaction parameters (**SO4**);
    - A. Mohebbi, S. Achiche, and L. Baron, “A Fuzzy-based Framework to Support Concurrent and Multicriteria Design of Mechatronic Systems”, Submitted to the Elsevier Journal of Engineering Applications of Artificial Intelligence, 2017.
  8. Proposition of a novel fuzzy-based approach in accordance with the proposed multicriteria conceptual design methodology to suggest effective concept improvements (**SO4**);
    - A. Mohebbi, S. Achiche, and L. Baron, “A Fuzzy-based Approach Towards Conceptual Design Improvements for Mechatronic Systems”, Submitted to the Symposium of Mechanisms, Machines, and Mechatronics (M3), CCToMM 2017, Montreal, Canada.

## 7.2 Computer Implementations

In order to facilitate using the methodologies proposed in this work for researchers and practitioners, all the mathematical modelling and algorithms have been implemented using MATLAB and a collection of the functions, programs and scripts produced during the formulation of design methodologies has been created and organized as a Toolbox called “Fuzzy-based Mechatronic Multicriteria Design (FMMD)”. An alpha version of this toolbox is currently available and a more stable version will be available soon through MathWork’s file-exchange website under a free license agreement along with a user guide.

## CHAPTER 8 CONCLUSION AND FUTURE WORK

### 8.1 Summary of the Thesis

In this thesis, we have proposed novel approaches towards achieving our main goal which is providing a concurrent, integrated and multicriteria design framework for mechatronic systems. First, we performed a thorough literature survey on the challenges related to designing mechatronics and we also reported the research work and solutions available for tackling each of them. These challenges are faced towards design methodologies, design tools, design supports, human factors and control software. Searching for the research gaps aiming at providing effective solutions to these challenges, we chose a path towards formulating systematic methodologies and supporting various stages of design by the means of expert systems. To this end and to address the first research sub-objective (**SO1**), a set of five main criteria and corresponding sub-criteria for conceptual design have been identified through an extensive literature study and analysis of the available research work on mechatronic system design. Then, the assessment methods for each of the identified design criteria have been explained and in some cases adapted to the case of designing a complex mechatronic system.

To pursue our second sub-objective (**SO2**), we incorporated fuzzy-based multicriteria decision making tools into the conceptual design phase by formulating a design evaluation index and profile called multicriteria mechatronic profile (MMP). We examined and developed various aggregation functions to calculate scores for every design alternative while considering the interconnections between design objectives. We designed a process to benefit from this design evaluation approach and form a systematic conceptual design framework. We applied our proposed methods on designing two complex mechatronic systems.

After finalizing our contributions towards supporting conceptual design, and to address the third sub-objective (**SO3**), we evaluated various common tools and methods used for preliminary and detailed design phases. Among all, we were interested in analyzing the Design-for-Control (DFC) method. Hence, we used this method for preliminary design of a vision-guided quadrotor whose concept was previously created using our conceptual design methodology. This gave us valuable insights to formulate a detailed design methodology where we could concurrently design a complex mechatronic system with multiple design objectives stemming from various disciplines towards different subsystems. This methodology profits from the success we gained from our

conceptual design approach and that is the fuzzy aggregations embedded into an optimization algorithm. The results achieved from the case study, showed the ability and effectiveness of the proposed method to find solutions towards forming a near optimal mechatronic design.

While providing multicriteria supports for an optimal multidisciplinary design of mechatronic systems both for conceptual and detailed design phases, we realized that in order to use the fuzzy-based framework, numerous parameters should be determined based on the designer's (or analyst's) intuitions which jeopardizes the whole approach in terms of reliability. Thus, an effort to provide a number of solutions to facilitate this particular process was put forward as a solution to our fourth research sub-objective (**SO4**), in terms of developing fuzzy capacity identification methods tailored to mechatronic design problems. Furthermore, we developed an approach in accordance with the proposed multicriteria conceptual design methodology which can suggest the designers on which criteria for a selected concept an improvement should be done in order to get the maximal possible overall score. This development is described in Appendix A.

One possible limitation from our proposed methodologies specifically during the detailed design phase is that, even though very simple component models and system architecture have been utilized, the methodology is complicated in terms of specifying a large number of parameters. It will become even more complicated if it extends to cover more component types and physical phenomena. This immediately calls for a clear guideline for the designers to be able to use these approaches in their design activities. In order to get the practitioners to adopt this type of design method, it might be useful to implement it in a design tool with a relatively easy-to-use graphical user interface which is capable of efficiently interpret the design semantics into the right model parameters.

## 8.2 Future Work

Since the implemented design methodologies for both conceptual and detailed design phases are computationally extensive and numerous programming scripts are utilized, one can suggest to implement all of these functions into a unified software or a plugin for widely used commercial softwares with a user friendly graphical interface. Due to the data-oriented nature of some of these approaches, specifically for elicitation of decision making parameters, the possibility of implementing these approaches into a web-based platform can be an interesting subject to explore.

In order to process and survey the interdisciplinary design information and relations, and to facilitate the communication between the designers, one can suggest developing approaches based

on multi-agent systems (MAS). The basis on which a multi-agent system is able to make decisions concerning the cross-domain information and relations, can be used to form a mechatronic design methodology. Hence, a multi-agent modelling approach can be suggested to consider the interactions between design criteria and to generate design alternatives and solutions in conceptual and detailed design phases respectively, through negotiations between design agents. These agents can ideally handle the task of supervising the inter-relationships and interdependencies between components and knowledge-bases involved in a mechatronic system.

Lastly, we can suggest to use artificial intelligence (AI) tools and machine learning approaches to create a platform to simultaneously analyze and learn from the successful available product designs, and also to automatically perform design evolutions and ultimately create highly efficient and optimal products.

## BIBLIOGRAPHY

- [1] B. William, "Mechatronics, Electronic Control Systems in Mechanical and Electrical Engineering," ed: Addison Wesley Longman, 2001.
- [2] G. Rzevski, *Mechatronics: Designing Intelligent Machines Volume 1: Perception, Cognition and Execution*: Newnes, 2014.
- [3] S. Behbahani and C. W. de Silva, "Mechatronic Design Quotient as the Basis of a New Multicriteria Mechatronic Design Methodology," *Mechatronics, IEEE/ASME Transactions on*, vol. 12, pp. 227-232, 2007.
- [4] A. Mohebbi, S. Achiche, and L. Baron, "Mechatronic Multicriteria Profile (MMP) for Conceptual Design of a Robotic Visual Servoing System," in *ASME 2014 12th Biennial Conference on Engineering Systems Design and Analysis*, 2014, pp. V003T15A015-V003T15A015.
- [5] N. P. Suh, *The Principles of Design*: Oxford University Press on Demand, 1990.
- [6] Q. Li, W. J. Zhang, and L. Chen, "Design for control-a concurrent engineering approach for mechatronic systems design," *Mechatronics, IEEE/ASME Transactions on*, vol. 6, pp. 161-169, 2001.
- [7] L. T. M. Blessing and A. Chakrabarti, *DRM, a Design Research Methodology*: Springer London, Limited, 2009.
- [8] J. M. r. Torry-Smith, S. Achiche, N. H. Mortensen, A. Qamar, J. Wikander, and C. During, "Mechatronic Design-Still a Considerable Challenge," in *ASME 2011 International Design Engineering Technical Conferences and Computers and Information in Engineering Conference*, 2011, pp. 33-44.
- [9] J. N. Martin, *Systems Engineering Guidebook: A Process for Developing Systems and Products*: CRC PressINC, 1997.
- [10] Y. Umeda, M. Ishii, M. Yoshioka, Y. Shimomura, and T. Tomiyama, "Supporting conceptual design based on the function-behavior-state modeler," *Artificial Intelligence for Engineering Design, Analysis and Manufacturing: AIEDAM*, vol. 10, pp. 275-288, 1996.
- [11] R. H. Bracewell and J. E. E. Sharpe, "Functional descriptions used in computer support for qualitative scheme generation—"Schemebuilder"," *AI EDAM*, vol. 10, pp. 333-345, 1996.
- [12] J. Hunt, "MACE: A system for the construction of functional models using case-based reasoning," *Expert Systems with Applications*, vol. 9, pp. 347-360, 1995.

- [13] R. B. Stone and K. L. Wood, "Development of a Functional Basis for Design," *Journal of Mechanical Design*, vol. 122, pp. 359-370, 1999.
- [14] L. Wang, W. Shen, H. Xie, J. Neelamkavil, and A. Pardasani, "Collaborative conceptual design—state of the art and future trends," *Computer-Aided Design*, vol. 34, pp. 981-996, 2002.
- [15] J. Wikander, M. Torngren, and M. Hanson, "The science and education of mechatronics engineering," *Robotics & Automation Magazine, IEEE*, vol. 8, pp. 20-26, 2001.
- [16] W. H. Wood, H. U. I. Dong, and C. L. Dym, "Integrating functional synthesis," *AI EDAM*, vol. 19, pp. 183-200, 2005.
- [17] "Integration definition for function modeling (IDEF0)," *National Institute of Standards and Technology*, 1993.
- [18] B. Chandrasekaran, "Functional Representation: A Brief Historical Perspective," *Applied Artificial Intelligence*, vol. 8, pp. 173-197, 1994/04/01 1994.
- [19] "CATIA ", 6 ed: Dassault Systems, 2013.
- [20] M. R. Cutkosky, R. S. Engelmores, R. E. Fikes, M. R. Genesereth, T. R. Gruber, W. S. Mark, *et al.*, "PACT: an experiment in integrating concurrent engineering systems," *Computer*, vol. 26, pp. 28-37, 1993.
- [21] S. Citherlet, J. A. Clarke, and J. Hand, "Integration in building physics simulation," *Energy and Buildings*, vol. 33, pp. 451-461, 2001.
- [22] "Modelica," ed: Modelica Association, 2008.
- [23] B. P. A. ZEIGLER, H. Prähofer, and T. G. Kim, *Theory of Modeling [ Modelling ] and Simulation: Integrating Discrete Event and Continuous Complex Dynamic Systems*. Academic Press, 2000.
- [24] Q. Institute, "QFD Institute home page," ed.
- [25] D. Karnopp, D. L. Margolis, and R. C. Rosenberg, *System dynamics: modeling and simulation of mechatronic systems*. Wiley, 2000.
- [26] G. A. Hazelrigg, "A Framework for Decision-Based Engineering Design," *Journal of Mechanical Design*, vol. 120, pp. 653-658, 1998.
- [27] "National Institute of Standards and Technology. Integration definition for function modeling (IDEF0)," ed, 1993.
- [28] (2013). *Object management Group*. Available: <http://www.omg.org/>
- [29] (2013). *SysML*. Available: <http://www.sysml.org/>

- [30] P. Bentley, *Evolutionary design by computers*. Morgan Kaufmann Publishers, Incorporated, 1999.
- [31] P. F. Hingston, L. C. Barone, and Z. Michalewicz, *Design by Evolution: Advances in Evolutionary Design*. Springer Berlin Heidelberg, 2008.
- [32] A. L. Hale, W. E. Dahl, and J. Lisowski, "Optimal simultaneous structural and control design of maneuvering flexible spacecraft," *Journal of Guidance, Control, and Dynamics*, vol. 8, pp. 86-93, 1985/01/01 1985.
- [33] M. P. Bendsee, N. Olhoff, and J. E. Taylor, "On the Design of Structure and Controls for Optimal Performance of Actively Controlled Flexible Structures," *Mechanics of Structures and Machines*, vol. 15, pp. 265-295, 1987/01/01 1987.
- [34] N. Pagaldipti, J. N. Rajadas, and A. Chattopadhyay, "Multidisciplinary Optimization Procedure For High Speed Aircraft Using A Semi-Analytical Sensitivity Analysis Procedure And Multilevel Decomposition," *Engineering Optimization*, vol. 31, pp. 25-51, 1998/10/01 1998.
- [35] O. Chocron and P. Bidaud, "Evolutionary algorithm for global design of locomotion systems," in *Intelligent Robots and Systems, 1999. IROS '99. Proceedings. 1999 IEEE/RSJ International Conference on*, 1999, pp. 1573-1578 vol.3.
- [36] K. Seo, Z. Fan, J. Hu, E. D. Goodman, and R. C. Rosenberg, "Toward a unified and automated design methodology for multi-domain dynamic systems using bond graphs and genetic programming," *Mechatronics*, vol. 13, pp. 851-885, 10// 2003.
- [37] E. Cramer, J. Dennis, J., P. Frank, R. Lewis, and G. Shubin, "Problem Formulation for Multidisciplinary Optimization," *SIAM Journal on Optimization*, vol. 4, pp. 754-776, 1994.
- [38] D. Harel, "From play-in scenarios to code: an achievable dream," *Computer*, vol. 34, pp. 53-60, 2001.
- [39] G. Rzevski, "On conceptual design of intelligent mechatronic systems," *Mechatronics*, vol. 13, pp. 1029-1044, 2003.
- [40] M. Boucher and D. Houlihan, "System design: new product development for mechatronics," Aberdeen Group, Boston, MA2008.
- [41] I. SolidWorks, "Solidworks corporation," *Concord, MA*, 2002.
- [42] M. H. Rashid, *Introduction to PSpice using OrCAD for circuits and electronics*. Prentice-Hall, Inc., 2003.
- [43] T. MathWorks, "Matlab and Simulink," ed: The MathWorks, 2013.

- [44] V. C. Moulianitis, N. A. Aspragathos, and A. J. Dentsoras, "A model for concept evaluation in design—an application to mechatronics design of robot grippers," *Mechatronics*, vol. 14, pp. 599-622, 2004.
- [45] K. Geddes, G. Labahn, and M. Monagan, "Maple 12 advanced programming guide," *Maplesoft*, 2008.
- [46] G. W. Johnson, *LabVIEW graphical programming*: Tata McGraw-Hill Education, 1997.
- [47] UML, "Unified modeling language (UML)," ed: Object Management Group, 2012.
- [48] W. J. Zhang, Q. Li, and L. S. Guo, "Integrated design of mechanical structure and control algorithm for a programmable four-bar linkage," *Mechatronics, IEEE/ASME Transactions on*, vol. 4, pp. 354-362, 1999.
- [49] C. W. De Silva, "Sensory Information Acquisition For Monitoring And Control Of Intelligent Mechatronic Systems," *International Journal of Information Acquisition*, vol. 01, pp. 89-99, 2004/03/01 2004.
- [50] S. Behbahani, "Practical and analytical studies on the development of formal evaluation and design methodologies for mechatronic systems," 2007.
- [51] I. M. L. Ferreira and P. J. S. Gil, "Application and performance analysis of neural networks for decision support in conceptual design," *Expert Systems with Applications*, vol. 39, pp. 7701-7708, 7// 2012.
- [52] M. Hammadi, J. Y. Choley, O. Penas, A. Riviere, J. Louati, and M. Haddar, "A new multi-criteria indicator for mechatronic system performance evaluation in preliminary design level," in *Mechatronics (MECATRONICS) , 2012 9th France-Japan & 7th Europe-Asia Congress on and Research and Education in Mechatronics (REM), 2012 13th Int'l Workshop on*, 2012, pp. 409-416.
- [53] M. G. Villarreal-Cervantes, C. A. Cruz-Villar, and J. Alvarez-Gallegos, "Structure-control mechatronic design of the planar 5r 2dof parallel robot," in *Mechatronics, 2009. ICM 2009. IEEE International Conference on*, 2009, pp. 1-6.
- [54] Q. L. Xu, S. K. Ong, and A. Y. C. Nee, "Function-based design synthesis approach to design reuse," *Research in Engineering Design*, vol. 17, pp. 27-44, 2006/06/01 2006.
- [55] C. W. De Silva, *Mechatronics: A Foundation Course*: Taylor & Francis Group, 2010.
- [56] C. W. de Silva, *Mechatronic Systems: Devices, Design, Control, Operation and Monitoring*: Taylor & Francis, 2007.



- [57] H. Jianjun, E. Goodman, and R. Rosenberg, "Topological search in automated mechatronic system synthesis using bond graphs and genetic programming," in *American Control Conference, 2004. Proceedings of the 2004*, 2004, pp. 5628-5634 vol.6.
- [58] G. M. Bonnema, "Funkey architecting : an integrated approach to system architecting using functions, key drivers and system budgets," Enschede, 2008.
- [59] V. Moulianitis, N. Aspragathos, and A. Dentsoras, "A model for concept evaluation in design—an application to mechatronics design of robot grippers," *Mechatronics*, vol. 14, pp. 599-622, 2004.
- [60] L. Ferrarini and E. Carpanzano, "A structured methodology for the design and implementation of control and supervision systems for robotic applications," *Control Systems Technology, IEEE Transactions on*, vol. 10, pp. 272-279, 2002.
- [61] C. W. de Silva and S. Behbahani, "A design paradigm for mechatronic systems," *Mechatronics*.
- [62] J. H. Park and H. Asada, "Concurrent design optimization of mechanical structure and control for high speed robots," *ASME Transaction Journal on Dynamic Systems, Measurements and Control*, vol. 116, pp. 344-356, 1994.
- [63] W. Zhang, Q. Li, and L. Guo, "Integrated design of mechanical structure and control algorithm for a programmable four-bar linkage," *Mechatronics, IEEE/ASME Transactions on*, vol. 4, pp. 354-362, 1999.
- [64] "SysML," ed: OMG Group, 2013.
- [65] C. J. J. Paredis, R. B. Y. Bernard, H. P. de Koning, S. Friedenthal , P. Fritzson, N. Rouquette, *et al.*, "An Overview of the SysML-Modelica Transformation Specification," presented at the INCOSE International Symposium, 2010.
- [66] G. D. Wood and D. C. Kennedy, "Simulating mechanical systems in Simulink with SimMechanics," *The Mathworks Report*, 2003.
- [67] "SimScape," ed: Mathworks, 2013.
- [68] V. corporation, "CORE software," ed: Vitech corporation.
- [69] G. La Rocca and M. J. L. Van Tooren, "Enabling distributed multi-disciplinary design of complex products: a knowledge based engineering approach," *Journal of Design Research*, vol. 5, pp. 333-352, 2007.
- [70] J. Berends, M. Van Tooren, and E. Schut, "Design and implementation of a new generation multi-agent task environment framework," presented at the 49th AIAA/ASME/ASCE/AHS/ASC structures, structural dynamics, and materials

- conference, 4th AIAA multidisciplinary design optimization specialist conference, Schaumburg, IL, USA, 2008.
- [71] F. Roos, "Towards a methodology for integrated design of mechatronic servo systems," KTH, Stockholm, 2007.
  - [72] J. Sobieszczanski-Sobieski and R. T. Haftka, "Multidisciplinary aerospace design optimization: survey of recent developments," *Structural optimization*, vol. 14, pp. 1-23, 1997/08/01 1997.
  - [73] J. Martins and A. B. Lambe, "Multidisciplinary design optimization: Survey of architectures," *AIAA Journal*, 2012.
  - [74] G. Pahl, K. Wallace, and L. T. M. Blessing, *Engineering Design: A Systematic Approach*. Springer, 2007.
  - [75] J. Rash, M. Hinchey, C. Rouff, D. Gračanin, and J. Erickson, "A requirements-based programming approach to developing a NASA autonomous ground control system," *Artificial Intelligence Review*, vol. 25, pp. 285-297, 2006/06/01 2006.
  - [76] J. Mørkeberg Torry-Smith, A. Qamar, S. Achiche, J. Wikander, N. Henrik Mortensen, and C. During, "Challenges in Designing Mechatronic Systems," *Journal of Mechanical Design*, vol. 135, pp. 011005-011005, 2012.
  - [77] A. Mohebbi, L. Baron, S. Achiche, and L. Birglen, "Trends in concurrent, multi-criteria and optimal design of mechatronic systems: A review," in *Innovative Design and Manufacturing (ICIDM), Proceedings of the 2014 International Conference on*, 2014, pp. 88-93.
  - [78] A. Ziv-Av and Y. Reich, "SOS—Subjective objective system for generating optimal product concepts," *Design Studies*, vol. 26, pp. 509-533, 2005.
  - [79] Y. Reich and A. Ziv Av, "Robust product concept generation," in *ICED 05: 15th International Conference on Engineering Design: Engineering Design and the Global Economy*, 2005, p. 2726.
  - [80] E. Coelingh, T. J. A. De Vries, and R. Koster, "Assessment of mechatronic system performance at an early design stage," *Mechatronics, IEEE/ASME Transactions on*, vol. 7, pp. 269-279, 2002.
  - [81] G. Avigad and A. Moshaiiov, "Set-based concept selection in multi-objective problems: optimality versus variability approach," *Journal of Engineering Design*, vol. 20, pp. 217-242, 2009.
  - [82] E. P. Klement, R. Mesiar, and E. Pap, *Triangular Norms*. Springer Netherlands, 2000.

- [83] J-H Byun and EA Elsayed, "A producibility index with process capability and manufacturing cost," in *5th Industrial Engineering Research Conference Proceedings*, 1996, pp. 381-6.
- [84] S. Behbahani and C. W. de Silva, "System-Based and Concurrent Design of a Smart Mechatronic System Using the Concept of Mechatronic Design Quotient (MDQ)," *Mechatronics, IEEE/ASME Transactions on*, vol. 13, pp. 14-21, 2008.
- [85] K. Janschek, *Mechatronic Systems Design*: Springer, 2012.
- [86] D. G. Ullman, *The mechanical design process*: McGraw-Hill Higher Education, 2003.
- [87] Z. Bien, W.-C. Bang, D.-Y. Kim, and J.-S. Han, "Machine intelligence quotient: its measurements and applications," *Fuzzy Sets and Systems*, vol. 127, pp. 3-16, 4/1/ 2002.
- [88] S. W. Kim; and B. K. Kim;, "MIQ (Machine Intelligence Quotient) for process control system," in *World Automation Congress in, Anchorage, AK*, 1998.
- [89] H.-J. Park;, B.-K. Kim;, and K. Y. Lim;, "Measuring the machine intelligence quotient (MIQ) of human-machine cooperative systems," *Systems, Man and Cybernetics, Part A: Systems and Humans, IEEE Transactions on*, vol. 31, pp. 89-96, 2001.
- [90] A. Anthony and T. C. Jannett, "Measuring machine intelligence of an agent-based distributed sensor network system," in *Advances and Innovations in Systems, Computing Sciences and Software Engineering*, ed: Springer, 2007, pp. 531-535.
- [91] C. de Silva, "Sensory information acquisition for monitoring and control of intelligent mechatronic systems," *International Journal of Information Acquisition*, vol. 1, pp. 89-99, 2004.
- [92] X. Zhong, M. Ichchou, and A. Saidi, "Reliability assessment of complex mechatronic systems using a modified nonparametric belief propagation algorithm," *Reliability Engineering & System Safety*, vol. 95, pp. 1174-1185, 11// 2010.
- [93] T. R. Browning, "Applying the design structure matrix to system decomposition and integration problems: a review and new directions," *Engineering Management, IEEE Transactions on*, vol. 48, pp. 292-306, 2001.
- [94] A. Yassine and D. Braha, "Complex concurrent engineering and the design structure matrix method," *Concurrent Engineering*, vol. 11, pp. 165-176, 2003.
- [95] N. P. Suh, *The principles of design* vol. 990: Oxford University Press New York, 1990.
- [96] H. A. Bashir and V. Thomson, "Estimating design complexity," *Journal of Engineering Design*, vol. 10, pp. 247-257, 1999.

- [97] J. Corbett and J. Crookall, "Design for economic manufacture," *CIRP Annals-Manufacturing Technology*, vol. 35, pp. 93-97, 1986.
- [98] A. Mileham, G. Currie, A. Miles, and D. Bradford, "A parametric approach to cost estimating at the conceptual stage of design," *Journal of engineering design*, vol. 4, pp. 117-125, 1993.
- [99] R. Roy, "Cost engineering: why, what and how?," 2003.
- [100] T. Hegazy and A. Ayed, "Neural network model for parametric cost estimation of highway projects," *Journal of Construction Engineering and Management*, vol. 124, pp. 210-218, 1998.
- [101] G. Kim, D. Seo, and K. Kang, "Hybrid models of neural networks and genetic algorithms for predicting preliminary cost estimates," *Journal of Computing in Civil Engineering*, vol. 19, pp. 208-211, 2005.
- [102] M. Grabisch, "The application of fuzzy integrals in multicriteria decision making," *European journal of operational research*, vol. 89, pp. 445-456, 1996.
- [103] J.-L. Marichal and M. Roubens, "Dependence between criteria and multiple criteria decision aid," in *Proc. 2nd Int. Workshop on Preferences and Decision (TRENTO'98)*, 1998.
- [104] J.-L. Marichal, "Aggregation of interacting criteria by means of the discrete Choquet integral," in *Aggregation operators*, ed: Springer, 2002, pp. 224-244.
- [105] J. L. Marichal, "An axiomatic approach of the discrete Choquet integral as a tool to aggregate interacting criteria," *Fuzzy Systems, IEEE Transactions on*, vol. 8, pp. 800-807, 2000.
- [106] R. Krishnapuram and J. Lee, "Fuzzy-connective-based hierarchical aggregation networks for decision making," *Fuzzy sets and systems*, vol. 46, pp. 11-27, 1992.
- [107] D. Golmohammadi, "Neural network application for fuzzy multi-criteria decision making problems," *International Journal of Production Economics*, vol. 131, pp. 490-504, 2011.
- [108] C. Jung-Hsien, "Choquet fuzzy integral-based hierarchical networks for decision analysis," *Fuzzy Systems, IEEE Transactions on*, vol. 7, pp. 63-71, 1999.
- [109] C. Jian and L. Song, "A neural network approach-decision neural network (DNN) for preference assessment," *Systems, Man, and Cybernetics, Part C: Applications and Reviews, IEEE Transactions on*, vol. 34, pp. 219-225, 2004.
- [110] R. Hecht-Nielsen, "Theory of the backpropagation neural network," in *Neural Networks, 1989. IJCNN., International Joint Conference on*, 1989, pp. 593-605 vol.1.

- [111] J. A. Freeman and D. M. Skapura, *Neural Networks: Algorithms, Applications, and Programming Techniques*. Addison-Wesley, 1991.
- [112] K. J. Hunt, D. Sbarbaro, R. Żbikowski, and P. J. Gawthrop, "Neural networks for control systems—A survey," *Automatica*, vol. 28, pp. 1083-1112, 11// 1992.
- [113] P. I. Corke, "Visual control of robot manipulators-a review," *Visual servoing*, vol. 7, pp. 1-31, 1993.
- [114] A. Mohebbi, M. Keshmiri, and W. F. Xie, "An eye-in-hand stereo visual servoing for tracking and catching moving objects," in *Control Conference (CCC), 2014 33rd Chinese*, 2014, pp. 8570-8577.
- [115] T. L. Jones, *Handbook of Reliability Prediction Procedures for Mechanical Equipment*. West Bethesda, Maryland: Naval Surface Warfare Center, Carderock Division, 2011.
- [116] S. A. Nasar, *Schaum's outline of theory and problems of electric machines and electromechanics*. McGraw-Hill Ryerson, Limited, 1981.
- [117] (2014). *Lifetime of DC Vibration Motors (MTTF & FIT)*. Available: <http://www.precisionmicrodrives.com/application-notes-technical-guides/application-bulletins/ab-019-lifetime-of-vibration-motors>
- [118] J. M. Torry-Smith, A. Qamar, S. Achiche, J. Wikander, N. H. Mortensen, and C. During, "Challenges in designing mechatronic systems," *Journal of Mechanical Design*, vol. 135, p. 011005, 2013.
- [119] A. Mohebbi, S. Achiche, L. Baron, and L. Birglen, "Fuzzy Decision Making for Conceptual Design of a Visual Servoing System Using Mechatronic Multi-Criteria Profile (MMP)," in *ASME 2014 International Mechanical Engineering Congress and Exposition*, 2014, pp. V011T14A055-V011T14A055.
- [120] J. van Amerongen, "Mechatronic design," *Mechatronics*, vol. 13, pp. 1045-1066, 2003.
- [121] T. Tomiyama, P. Gu, Y. Jin, D. Lutters, C. Kind, and F. Kimura, "Design methodologies: Industrial and educational applications," *CIRP Annals-Manufacturing Technology*, vol. 58, pp. 543-565, 2009.
- [122] D. G. Ullman, *The mechanical design process* vol. 2: McGraw-Hill New York, 1992.
- [123] S. Behbahani and C. W. de Silva, "Mechatronic design quotient as the basis of a new multicriteria mechatronic design methodology," *IEEE/ASME Transactions on mechatronics*, vol. 12, pp. 227-232, 2007.

- [124] S. Behbahani and C. W. de Silva, "System-based and concurrent design of a smart mechatronic system using the concept of mechatronic design quotient (MDQ)," *IEEE/ASME Transactions on mechatronics*, vol. 13, pp. 14-21, 2008.
- [125] A. Mohebbi, L. Baron, S. Achiche, and L. Birglen, "Neural network-based decision support for conceptual design of a mechatronic system using mechatronic multi-criteria profile (MMP)," in *Innovative Design and Manufacturing (ICIDM), Proceedings of the 2014 International Conference on*, 2014, pp. 105-110.
- [126] M. Grabisch, "K-order additive discrete fuzzy measures and their representation," *Fuzzy sets and systems*, vol. 92, pp. 167-189, 1997.
- [127] J.-L. Marichal and M. Roubens, "Determination of weights of interacting criteria from a reference set," *European journal of operational Research*, vol. 124, pp. 641-650, 2000.
- [128] P. Meyer and M. Roubens, "On the use of the Choquet integral with fuzzy numbers in multiple criteria decision support," *Fuzzy Sets and Systems*, vol. 157, pp. 927-938, 2006.
- [129] M. Grabisch, "A new algorithm for identifying fuzzy measures and its application to pattern recognition," in *Int. Joint Conf. of the 4th IEEE Int. Conf. on Fuzzy Systems and the 2nd Int. Fuzzy Engineering Symposium*, 1995, pp. 145-150.
- [130] J.-L. Marichal and M. Roubens, "Dependence between criteria and multiple criteria decision aid," in *Proc. 2nd Int. Workshop on Preferences and Decision (TRENTO'98)*, 1998, pp. 69-75.
- [131] M. Timonin, "Robust optimization of the Choquet integral," *Fuzzy Sets and Systems*, vol. 213, pp. 27-46, 2013.
- [132] T. Mori and T. Murofushi, "An analysis of evaluation model using fuzzy measure and the Choquet integral," in *5th Fuzzy System Symposium*, 1989, pp. 207-212.
- [133] E. Coelingh, T. J. de Vries, and R. Koster, "Assessment of mechatronic system performance at an early design stage," *IEEE/ASME transactions on mechatronics*, vol. 7, pp. 269-279, 2002.
- [134] M. Sugeno, "Theory of fuzzy integrals and its applications," *Theory of Fuzzy Integrals and Its Applications*, 1975.
- [135] M. Grabisch, H. T. Nguyen, and E. A. Walker, *Fundamentals of uncertainty calculi with applications to fuzzy inference* vol. 30: Springer Science & Business Media, 2013.
- [136] A. Mohebbi, S. Achiche, and L. Baron, "Integrated Design of A Vision-Guided Quadrotor UAV: A Mechatronics Approach," in *2015 CCToMM Symposium on Mechanisms, Machines, and Mechatronics*, 2015, p. 185.

- [137] A. Mohebbi, M. Keshmiri, and W. Xie, "A Comparative Study of Eye-In-Hand Image-Based Visual Servoing: Stereo vs. Mono," *Journal of Integrated Design and Process Science*, vol. 19, pp. 25-54, 2016.
- [138] A. Mohebbi, S. Achiche, and L. Baron, "A Multicriteria Fuzzy Decision Support for Conceptual Evaluation in Design of Mechatronic Systems: A Quadrotor Design Case Study," *Springer Journal of Research in Engineering Design*, 2016.
- [139] H. Tahani and J. M. Keller, "Information fusion in computer vision using the fuzzy integral," *IEEE Transactions on systems, Man, and Cybernetics*, vol. 20, pp. 733-741, 1990.
- [140] K.-M. Lee and H. LeeKwang, "Identification of  $\lambda$ -fuzzy measure by genetic algorithms," *Fuzzy Sets and Systems*, vol. 75, pp. 301-309, 1995.
- [141] A. Mohebbi, S. Achiche, L. Baron, and L. Birglen, "Neural network-based decision support for conceptual design of a mechatronic system using mechatronic multi-criteria profile (MMP)," in *Innovative Design and Manufacturing (ICIDM), Proceedings of the 2014 International Conference on*, 2014, pp. 105-110.
- [142] C. W. de Silva and S. Behbahani, "A design paradigm for mechatronic systems," *Mechatronics*, vol. 23, pp. 960-966, 12// 2013.
- [143] J. A. Reyer and P. Y. Papalambros, "Combined optimal design and control with application to an electric DC motor," *Journal of Mechanical Design*, vol. 124, pp. 183-191, 2002.
- [144] J.-H. Park and H. Asada, "Concurrent design optimization of mechanical structure and control for high speed robots," *Journal of dynamic systems, measurement, and control*, vol. 116, pp. 344-356, 1994.
- [145] H.-S. Yan and G.-J. Yan, "Integrated control and mechanism design for the variable input-speed servo four-bar linkages," *Mechatronics*, vol. 19, pp. 274-285, 2009.
- [146] F. Wu, W. Zhang, Q. Li, and P. Ouyang, "Integrated design and PD control of high-speed closed-loop mechanisms," *Journal of dynamic systems, measurement, and control*, vol. 124, pp. 522-528, 2002.
- [147] M. G. Villarreal-Cervantes, C. A. Cruz-Villar, J. Alvarez-Gallegos, and E. A. Portilla-Flores, "Robust structure-control design approach for mechatronic systems," *Mechatronics, IEEE/ASME Transactions on*, vol. 18, pp. 1592-1601, 2013.
- [148] H. Van Brussel, "Mechatronics, a powerful concurrent engineering framework," *IEEE-ASME Transactions on Mechatronics*, vol. 1, pp. 127-136, 1996.
- [149] C. A. Cruz-Villar, J. Alvarez-Gallegos, and M. G. Villarreal-Cervantes, "Concurrent redesign of an underactuated robot manipulator," *Mechatronics*, vol. 19, pp. 178-183, 2009.

- [150] K. Youcef-Toumi and A. T. Y. Kuo, "High-speed trajectory control of a direct-drive manipulator," *Robotics and Automation, IEEE Transactions on*, vol. 9, pp. 102-108, 1993.
- [151] W. K. Belvin and K. Park, "Structural tailoring and feedback control synthesis-An interdisciplinary approach," *Journal of Guidance, Control, and Dynamics*, vol. 13, pp. 424-429, 1990.
- [152] H. Diken, "Trajectory control of mass balanced manipulators," *Mechanism and Machine Theory*, vol. 32, pp. 313-322, 4// 1997.
- [153] Q. Li, W. Zhang, and L. Chen, "Design for control-a concurrent engineering approach for mechatronic systems design," *Mechatronics, IEEE/ASME Transactions on*, vol. 6, pp. 161-169, 2001.
- [154] Q. Li and F. Wu, "Control performance improvement of a parallel robot via the design for control approach," *Mechatronics*, vol. 14, pp. 947-964, 2004.
- [155] L. Cheng, Y. Lin, Z.-G. Hou, M. Tan, J. Huang, and W. Zhang, "Integrated design of machine body and control algorithm for improving the robustness of a closed-chain five-bar machine," *Mechatronics, IEEE/ASME Transactions on*, vol. 17, pp. 587-591, 2012.
- [156] S. Bouabdallah, P. Murrieri, and R. Siegwart, "Design and control of an indoor micro quadrotor," in *Robotics and Automation, 2004. Proceedings. ICRA'04. 2004 IEEE International Conference on*, 2004, pp. 4393-4398.
- [157] S. Bouabdallah and R. Siegwart, "Full control of a quadrotor," in *Intelligent Robots and Systems, 2007. IROS 2007. IEEE/RSJ International Conference on*, 2007, pp. 153-158.
- [158] A. L. Salih, M. Moghavvemi, H. A. F. Mohamed, and K. S. Gaeid, "Modelling and PID controller design for a quadrotor unmanned air vehicle," in *Automation Quality and Testing Robotics (AQTR), 2010 IEEE International Conference on*, 2010, pp. 1-5.
- [159] A. A. Mian and D. Wang, "Nonlinear Flight Control Strategy for an Underactuated Quadrotor Aerial Robot," in *Networking, Sensing and Control, 2008. ICNSC 2008. IEEE International Conference on*, 2008, pp. 938-942.
- [160] S. Bouabdallah, A. Noth, and R. Siegwart, "PID vs LQ control techniques applied to an indoor micro quadrotor," in *Intelligent Robots and Systems, 2004. (IROS 2004). Proceedings. 2004 IEEE/RSJ International Conference on*, 2004, pp. 2451-2456 vol.3.
- [161] A. Mohebbi, "Real-Time Stereo Visual Servoing of a 6-DOF Robot for Tracking and Grasping Moving Objects," Concordia University, 2013.
- [162] M. Cutler, N. K. Ure, B. Michini, and J. P. How, "Comparison of fixed and variable pitch actuators for agile quadrotors," in *AIAA Guidance, Navigation, and Control Conference (GNC), Portland, OR*, 2011.



- [163] P. E. I. Pounds, "Design, construction and control of a large quadrotor micro air vehicle," Australian National University, 2007.
- [164] R. W. Prouty, *Helicopter performance, stability, and control*. PWS Engineering, 1986.
- [165] D. Shetty and R. A. Kolk, *Mechatronics system design, SI version*. Cengage Learning, 2010.
- [166] A. Mohebbi, S. Achiche, and L. Baron, "Design of a Vision Guided Mechatronic Quadrotor System Using Design For Control Methodology," *Transactions of the Canadian Society for Mechanical Engineering*, vol. 40, pp. 201-219, 2016.
- [167] Z. Affi, E. Badreddine, and L. Romdhane, "Advanced mechatronic design using a multi-objective genetic algorithm optimization of a motor-driven four-bar system," *Mechatronics*, vol. 17, pp. 489-500, 2007.
- [168] M. Hammadi, A. Kellner, J.-Y. Choley, and P. Hehenberger, "Mechatronic design optimization using multi-agent approach," in *Presente A the 14th Mechatronics Forum International Conference*, 2014, pp. 310-317.
- [169] R. C. Eberhart and J. Kennedy, "A new optimizer using particle swarm theory," in *Proceedings of the sixth international symposium on micro machine and human science*, 1995, pp. 39-43.
- [170] J. F. Schutte, J. A. Reinbolt, B. J. Fregly, R. T. Haftka, and A. D. George, "Parallel global optimization with the particle swarm algorithm," *International journal for numerical methods in engineering*, vol. 61, p. 2296, 2004.
- [171] E. F. Campana, G. Fasano, and A. Pinto, "Dynamic system analysis and initial particles position in particle swarm optimization," in *IEEE Swarm Intelligence Symposium*, 2006.
- [172] F. Van Den Bergh and A. P. Engelbrecht, "A study of particle swarm optimization particle trajectories," *Information sciences*, vol. 176, pp. 937-971, 2006.
- [173] G. Venter and J. Sobieszczanski-Sobieski, "Multidisciplinary optimization of a transport aircraft wing using particle swarm optimization," in *9th AIAA/ISSMO Symposium on Multidisciplinary Analysis and Optimization*, 2002, p. 5644.
- [174] J. Kennedy, J. F. Kennedy, R. C. Eberhart, and Y. Shi, *Swarm intelligence*. Morgan Kaufmann, 2001.
- [175] A. P. Engelbrecht, *Fundamentals of computational swarm intelligence*. John Wiley & Sons, 2006.
- [176] R. C. Eberhart and Y. Shi, "Comparison between genetic algorithms and particle swarm optimization," in *International Conference on Evolutionary Programming*, 1998, pp. 611-616.

- [177] A. J. R. Medina, G. T. Pulido, and J. G. Ramírez-Torres, "A Comparative Study of Neighborhood Topologies for Particle Swarm Optimizers," in *IJCCI*, 2009, pp. 152-159.
- [178] C. A. C. Coello, "Theoretical and numerical constraint-handling techniques used with evolutionary algorithms: a survey of the state of the art," *Computer methods in applied mechanics and engineering*, vol. 191, pp. 1245-1287, 2002.
- [179] X. Hu, Y. Shi, and R. Eberhart, "Recent advances in particle swarm," in *Evolutionary Computation, 2004. CEC2004. Congress on*, 2004, pp. 90-97.
- [180] Y. Shi, "Particle swarm optimization: developments, applications and resources," in *evolutionary computation, 2001. Proceedings of the 2001 Congress on*, 2001, pp. 81-86.
- [181] H. Fan and Y. Shi, "Study on Vmax of particle swarm optimization," in *Proc. Workshop on Particle Swarm Optimization, Purdue School of Engineering and Technology*, 2001.
- [182] E. Ozcan and C. K. Mohan, "Particle swarm optimization: surfing the waves," in *Evolutionary Computation, 1999. CEC 99. Proceedings of the 1999 Congress on*, 1999, pp. 1939-1944.
- [183] Y. Shi and R. C. Eberhart, "Parameter selection in particle swarm optimization," in *International Conference on Evolutionary Programming*, 1998, pp. 591-600.
- [184] M. Grabisch, "A new algorithm for identifying fuzzy measures and its application to pattern recognition," in *Fuzzy Systems, 1995. International Joint Conference of the Fourth IEEE International Conference on Fuzzy Systems and The Second International Fuzzy Engineering Symposium., Proceedings of 1995 IEEE Int*, 1995, pp. 145-150.
- [185] S. Bouabdallah, A. Noth, and R. Siegwart, "PID vs LQ control techniques applied to an indoor micro quadrotor," in *Intelligent Robots and Systems, 2004.(IROS 2004). Proceedings. 2004 IEEE/RSJ International Conference on*, 2004, pp. 2451-2456.
- [186] G. Fay, "Derivation of the aerodynamic forces for the mesicopter simulation," *Standord University. Stanford, CA*, 2001.
- [187] G. J. Leishman, *Principles of helicopter aerodynamics with CD extra*: Cambridge university press, 2006.
- [188] A. Zulu and S. John, "A review of control algorithms for autonomous quadrotors," *arXiv preprint arXiv:1602.02622*, 2016.
- [189] G. Szafranski and R. Czyba, "Different approaches of PID control UAV type quadrotor," 2011.
- [190] P. Pounds, R. Mahony, and P. Corke, "Modelling and control of a large quadrotor robot," *Control Engineering Practice*, vol. 18, pp. 691-699, 7// 2010.

- [191] R. F. Gibson, *Principles of composite material mechanics*: CRC press, 2016.
- [192] R. W. Prouty, *Helicopter performance, stability, and control*, 1995.
- [193] P. Pounds, R. Mahony, and P. Corke, "Modelling and control of a quad-rotor robot," in *Proceedings Australasian Conference on Robotics and Automation 2006*, 2006.
- [194] Q. Li, "Grey-box system identification of a quadrotor unmanned aerial vehicle," Citeseer, 2014.
- [195] T. Krajník, V. Vonásek, D. Fišer, and J. Faigl, "AR-drone as a platform for robotic research and education," in *International Conference on Research and Education in Robotics*, 2011, pp. 172-186.
- [196] J. P. Puerta, J. L. S. López, I. M. Bataller, C. Fu, and P. C. Cervera, "AR drone identification and navigation control at CVG-UPM," 2012.
- [197] C. A. C. Coello, G. T. Pulido, and M. S. Lechuga, "Handling multiple objectives with particle swarm optimization," *IEEE Transactions on evolutionary computation*, vol. 8, pp. 256-279, 2004.
- [198] C. Labreuche, "Argumentation of the results of a multi-criteria evaluation model in individual and group decision aiding."
- [199] A. Mohebbi, M. Keshmiri, and W. Xie, "A Comparative Study of Eye-In-Hand Image-Based Visual Servoing: Stereo vs. Mono," *Journal of Integrated Design and Process Science*, vol. 19, pp. 25-54, 2015.

## APPENDIX A IMPROVEMENTS ON CONCEPTUAL DESIGN OF MECHATRONIC SYSTEMS USING A FUZZY-BASED APPROACH

In the presence of multiple interacting criteria, designing an integrated multidisciplinary product such as mechatronic systems, is not a trivial task and requires a systematic and concurrent methodology to achieve optimal design. Thus, there is an urgent need for a comprehensive tool to facilitate decision-making in the design process. During the conceptual design phase and after a careful assessment of design objectives for each alternative, a nonlinear fuzzy integral can be used for aggregation of different criteria and providing a global score reflecting the sense of design satisfaction. The goal of concept evaluation is to compare the generated alternatives against the design criteria and to select the best one for further developments into a product. In this Chapter, we introduce a fuzzy-based approach in accordance with the proposed multicriteria conceptual design to know on which criteria for a selected concept an improvement should be done in order to get the maximal possible overall score. As an application, the mechatronics design of a robotic visual servoing system is analyzed.

### A.1 Concept Improvement Methodology

It is quite usual in a conceptual design process that the design alternatives which are evaluated are not fixed and the designer wishes to obtain recommendations on how to improve a concept. More precisely, the designer is eager to know on which criterion or criteria an improvement should be done in order to get the maximal possible improvement of the overall global score. The concept is selected based on the process explained in Chapter 3 and can be described by a profile  $F = MMP(f) = [f_1, f_2, \dots, f_n] \in \mathbb{R}^n$  which based on the MMP, here  $n = 5$ . Most of the time the designer wants to know how to improve a profile  $F$  into a new profile  $\hat{F}$  such that the overall evaluation  $S(f_1, \dots, f_n)$  reaches a given expectation level. This can be mathematically formulated as an optimization problem as follows;

$$\begin{aligned} & \min c(F, F') \\ & \left\{ \begin{array}{l} F' \in \mathbb{R}^n \\ \forall i \in N, F' \geq F \\ C_\mu(F') = \eta \end{array} \right. \end{aligned} \quad (1)$$

where  $C_\mu(\cdot)$  is the Choquet aggregation function,  $\eta$  is the expectation level, and  $c(F, \hat{F})$  quantifies the cost to improve option  $F$  into a new profile  $\hat{F}$ . The above optimization problem provides the new profile  $\hat{F}$  that should be reached. The main drawback of this approach is that the designer is not always able to easily construct a new option corresponding to the profile  $\hat{F}$ . She/he will thus proceed iteratively by transforming  $F$  into a better profile  $F_1$ , then  $F_1$  into  $F_2$ , and so on, until the expectation level  $\eta$  is reached. The recommendation the designer is willing to have is a priority indication of a criterion in  $F$  that should be improved. Thus, there will not be a semantic about the intensity of the improvement that the overall score will gain. To tackle this problem, we can use a worth index proposed by Labreuche [198] and denoted by  $w_A^\psi(F)$  which quantifies the improvement worth of a set of criteria  $A \subseteq N$  from the profile  $F$ , subject to the evaluation function  $\psi(\cdot)$ . This index can be calculated as follows:

$$w_A^\psi(F) = \int_0^1 \left[ \psi\left((1-\tau)F_A + \tau 1_A, F_{N \setminus A}\right) - \psi(F) \right] d\tau. \quad (2)$$

Above equation gives the mean impact of uniformly improving all of criteria in subset  $A$  at the same time, where one assumes that all possible levels of improvement (from sticking to  $F_A$  up to reaching the ideal profile  $1_A$ ) have the same probability to occur. It is important to note that the subset  $A$  should not be restricted in singletons  $\{1\}, \{2\}, \dots, \{n\}$  and any coalition of criteria  $\{i, j, k, \dots\}$  should be considered in the process. Moreover, if the evaluation function  $\psi(\cdot)$  is constant over criteria set  $A$ , then  $w_A^\psi(F) = 0$ . As an example, let's say we would like to calculate the worth index for a coalition  $A = \{1, 3\}$  among criteria where  $n = 5$ . Then we get  $F_A = [f_1, f_3]$  and  $F_{N/A} = [f_2, f_4, f_5]$ . Consequently, we can rewrite Equation (12) for the coalition  $A = \{1, 3\}$  as follows:

$$w_{\{1,3\}}^\psi(F) = \int_0^1 [\psi([(1-\tau)f_1 + \tau], f_2, [(1-\tau)f_3 + \tau], f_4, f_5) - \psi(F)] d\tau. \quad (3)$$

We continue calculating the worth index for all the coalitions- from singletons to the largest coalition, and choose the largest value as an index of the worth for improving the criteria subset which is most beneficial towards the global score. For a profile consisting of  $n$  criteria we would get  $(2^n - 2)$  subsets which will not include the null set  $\emptyset$  and  $N$ . Thus, for  $n = 5$ , we need to calculate  $(2^5 - 2) = 30$  indices. The general proposed process of concept improvement is depicted in Figure A-1.

Equation (3) can be extended as follows, so as to take into account the improvement cost  $c$  from Equation (1) which can be arbitrarily defined by the designer;

$$\hat{w}_A^\psi(F) = \int_0^1 \frac{\left[ \psi \left( (1-\tau)F_A + \tau 1_A, F_{N \setminus A} \right) - \psi(F) \right]}{c \left( F, \left( (1-\tau)F_A + \tau, F_{N \setminus A} \right) \right)} d\tau. \quad (4)$$

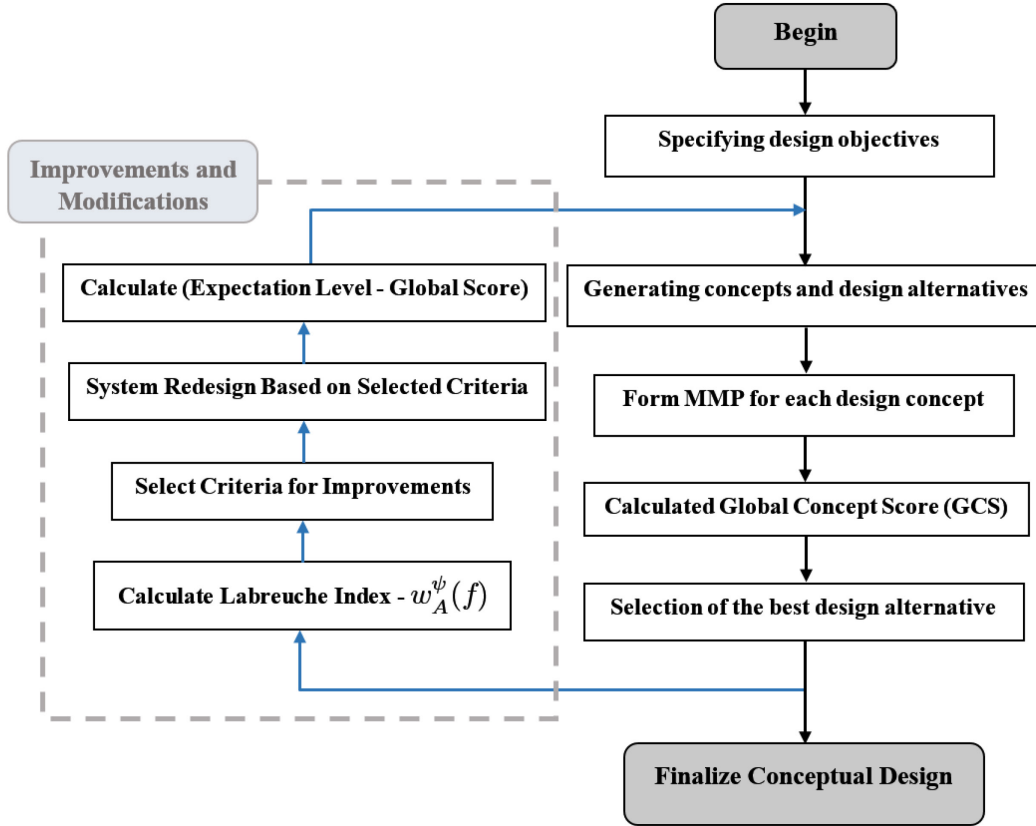


Figure A-1: The process of concept improvement using fuzzy integrals and worth index

## A.2 Application: Design Improvement of a Robotic Visual Servoing System

During last decades, using robotic systems and automation machineries is considerably increased in various industrial, urban and exploratory applications. However, robotic systems are generally limited to operate in highly structured environments. Thus, integration of vision sensors and generally “visual servoing” control systems helped solve this problem by digitally reconstructing the environment and producing non-contact measurements of the working area for the machine [199]. In this section, a case study of concept improvement for a 6 DOF manipulator equipped with robotic visual servoing system is presented. Figure A-2 shows a schematic of the proposed robotic visual servoing system and its components.

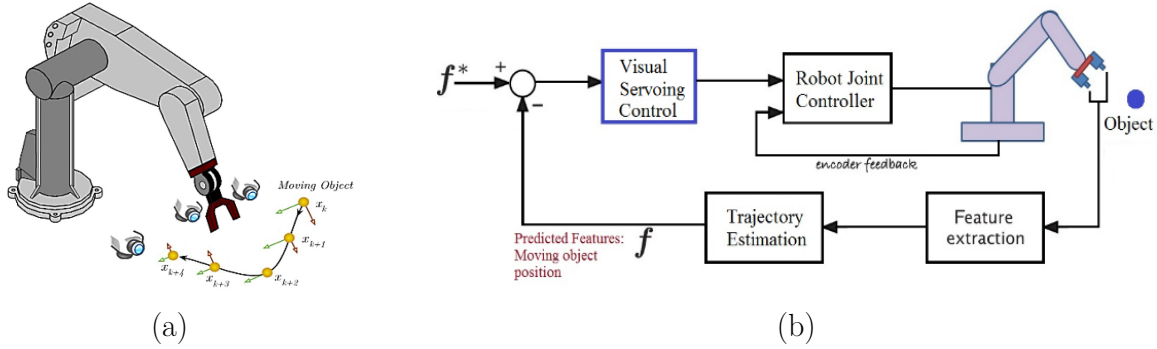


Figure A-2: A robotic visual servoing system and its components, (a) 6-DOF robot manipulator and the moving object, (b) Visual servoing control system

The conceptual design of the above system has been previously carried out and described in [4]. The objective was to design a robotic visual servoing system capable of tracking and catching a moving object with the maximum mass of 1 kg and maximum velocity of 1 m/s within 3 seconds after the object enters the vision system's field of view, and also within the area of motion with dimensions of 500mm×500mm×500mm. For the selected design alternative, we have the following assessments for the elements of MMP sorting in ascending order:

$$F = [0.8, 0.905, 0.964, 1, 1]^T = [CT, CX, FX, RS, MIQ]^T, \quad (5)$$

for which the resulting global score using Choquet integral is  $C_\mu(F) = 0.9462$ . Table A.1 shows the identified fuzzy measures used in the proposed multicriteria conceptual design process.

Table A-1: Fuzzy measures used for the conceptual design process using MMP methodology

$\mu_1$ = 0.3105	$\mu_{12}$ = 0.4537	$\mu_{13}$ = 0.5989	$\mu_{14}$ = 0.2892	$\mu_{15}$ = 0.6244
$\mu_{123}$ = 0.7893	$\mu_2$ = 0.2450	$\mu_{23}$ = 0.4724	$\mu_{24}$ = 0.5381	$\mu_{25}$ = 0.4863
$\mu_{124}$ = 0.4537	$\mu_{135}$ = 0.7105	$\mu_3$ = 0.1802	$\mu_{34}$ = 0.4708	$\mu_{35}$ = 0.1797
$\mu_{125}$ = 0.8070	$\mu_{145}$ = 0.6507	$\mu_{245}$ = 0.8269	$\mu_4$ = 0.2717	$\mu_{45}$ = 0.5212
$\mu_{134}$ = 0.5965	$\mu_{234}$ = 0.7844	$\mu_{345}$ = 0.5180	$\mu_{235}$ = 0.5113	$\mu_5$ = 0.2018
$\mu_{1234}$ = 0.8082	$\mu_{1235}$ = 0.9403	$\mu_{1345}$ = 0.8082	$\mu_{2345}$ = 0.8082	$\mu_{1245}$ = 0.8546

Moreover, using the values from Table A-1, the importance and interaction indices can be also calculated which result in the following values.

$$I = [I(i, j)] = \begin{bmatrix} 0.2232 & -0.1018 & 0.1082 & -0.2931 & 0.1121 \\ -0.1018 & 0.2481 & 0.0472 & 0.0213 & 0.0394 \\ 0.1082 & 0.0472 & 0.1662 & 0.0189 & -0.2023 \\ -0.2931 & 0.0213 & 0.0189 & 0.1691 & 0.0476 \\ 0.1121 & 0.0394 & -0.2023 & 0.0476 & 0.2002 \end{bmatrix} \quad (6)$$

$$\Phi = [\phi_1, \phi_2, \phi_3, \phi_4, \phi_5]^T = [0.2232, 0.2481, 0.1662, 0.1691, 0.2002]^T. \quad (7)$$

Now by using an algorithm incorporating the discrete form of the Equation (12) with an interval number of  $m = 20$ , we can calculate the worth index for all the criteria coalitions in  $F$ . The coalition on which the worth index is the largest is  $\{CT, CX\}$  for which  $w_{\{1,2\}}^\psi(F) = 3.481\text{E} - 4$ . This result is completely natural as these two criteria have the worst evaluation scores  $[0.8, 0.905]$ , and also the greatest importance indices  $[\phi_1, \phi_2] = [0.2232, 0.2481]$ . Moreover, there is a strong correlation (negative interaction index) among them. Hence, it is more rewarding to improve both cost (CT) and complexity (CX) rather than any of them individually as  $w_{\{1\}}^\psi(F) = 0.539\text{E} - 4$ , and  $w_{\{2\}}^\psi(F) = 0.785\text{E} - 4$ . Table A-2 shows the calculated worth index for some coalitions in  $F$ .

Table A-2: Worth index  $w_A^\psi(F)$  for several coalitions in MMP

A	$w_A^\psi(F)$
$\{CT, CX\}$	$3.481\text{E} - 4$
$\{FX, RS\}$	$1.181\text{E} - 4$
$\{CT, MIQ\}$	$1.994\text{E} - 4$
$\{CT, CX, MIQ\}$	$3.091\text{E} - 4$
$\{CT\}$	$0.539\text{E} - 4$
$\{CX\}$	$0.785\text{E} - 4$

After finding the intended criteria coalition, we can proceed with the case specific design improvements and try to redo the process in an iterative manner as described in Figure A-1 until we reach a desirable global score threshold.